SUPERCRITICAL WATER GASIFICATION OF BIOMASS

by

Fernando L. Pacheco de Resende

A dissertation submitted in partial fulfillment
of the requirements for the degree of
Doctor of Philosophy
(Chemical Engineering)
in The University of Michigan
2009

Doctoral Committee:

Professor Phillip E. Savage, Chair
Professor Johannes W. Schwank
Professor Gary S. Was
Assistant Professor Suljo Linic

To my wife, Waldea Resende

ACKNOWLEDGEMENTS

My journey to become a Ph.D. student in Michigan started about six years ago. At the time, I was finishing my M.Sc. degree in Brazil and was looking for an opportunity to start a PhD at a top university overseas. I was looking for an opportunity to learn more about research and teaching. I was looking for a good research project with chances of obtaining a fellowship to support my studies. And all the opportunities I was looking for started to show up at the moment I sent an email to Professor Phillip Savage.

This is not to say that anything was easy. It was a tough road that included, among other things: admission documents getting lost, pneumonia during my first week in the U.S., the ceiling in our office falling not far from my head, and all my experimental data disappeared from my computer a few months prior to the defense. But none of the drawbacks I experienced prevented me from completing my plans of graduating, because fortunately for me they were also God's plans. And I am glad he put in my life all the people that I mention here.

Professor Phillip Savage surpassed all my expectations as mentor. His constant availability, attention to detail and willingness to engage in productive discussions made this thesis the result of a collaborative effort. Every trip to his office still gives me the feeling I have just learned something new, even though I have been doing this on a daily basis for the last four years and a half. His endless questions, comments and suggestions for every oral presentation, every version of a manuscript and every chapter of this thesis drastically improved my understanding of the topic and made an enormous positive impact on this thesis. His genuine interest for the development and interests of his students is something I will take with me for my entire career. Even during his sabbatical leave, the interactions were constant and I never had to wait much to be able to discuss anything. I will never forget sending a chapter of my thesis by e-mail during the afternoon of December 31st, and receiving a reply with detailed comments before the New Year arrived. I also have been fortunate enough to win a teaching award (2007

Outstanding Student Instructor Award) and a research award (2008 Walter J. Weber Jr. Student Award in Environmental and Energy Sustainability) under his guidance, and I can say with no hesitation that neither of these awards would be possible without the lessons I learned from him.

I was also very fortunate in the choice of my thesis committee: Professor Johannes Schwank, Professor Suljo Linic and Professor Gary Was. Professors Schwank and Linic had been in my committee since the Doctoral Qualifying Exam (DQE), and I was always impressed with their ability to make quick suggestions that would end up making a major impact in my work. Professor Was has made suggestions that will influence my work even after the final version of this thesis is complete.

This research would not have even started without the fellowship provided by the Brazilian Government, through the CNPq (National Council for Research and Development). They fully supported my graduate studies during four years, and I am very grateful to them.

I have received substantial support for my experimental work from Harald Eberhart. His expertise in handling quartz and willingness to teach was a key to all experiments I have made. I had a lot of fun preparing, sealing, and working with the quartz reactors (and a few minor injuries as well), and I am thankful to Harald for his guidance on this fundamental part of my experimental work. Pablo Lavalle has also provided substantial help in our lab. There were a number of situations in which we needed his help to keep the lab working properly, and his intelligent suggestions were the solutions to several problems we had. Christine Moellering, Shelley Fellers, Leslie Cypert and Susan Hamlin were some of the members of the chemical engineering staff that were always kind and willing to help.

The Savage group members were possibly the people I spent most of my time with during my stay in Michigan. They were good friends and provided many ideas through discussion of topics related to my research, either during group meetings or regular conversations. Jeff Henrickson and Jennifer Dunn gave me a warm welcome and helped me during my first steps as a graduate student. Jianli Yu was the first person I would go to every time I had a problem in the lab. I was always amazed on how he could fix anything in about five seconds, after I had spent two hours attempting it. Shawn

Hunter taught me many details about the Swagelock reactors, and became a great friend with whom I shared an intense passion for basketball and the Portuguese language. Watching any Pistons game with him was guaranteed fun. I am so glad he chose me as one of his groomsman for his wedding. Craig Comisar was a constant source of help and ideas in the lab. During the worst moments of my homesickness, he made me feel at home with his great enthusiasm about soccer, even though he never learned to appreciate the beauty of the best soccer in the world (Brazilian). I miss the great friendship he provided, as well as beating him on “Winning Eleven” during the weekends. Greg DiLeo has worked on a similar research project, which made him one of the best sources of information and a great option to discuss ideas. I really enjoyed the interactions with him. I also thank Juandria Williams for being part of our group. Tanawan Pinnarat was one of the new students I took for a tour in our lab, and it immediately became evident that she was a great fit for our group. I am glad she joined us to make positive contributions. I am also glad I was chosen to be the first one to try the cookies she often made at home, except in the cases those contained dark chocolate. Nathalie Rebacz, with her chemistry background, was able to provide a different perspective to many of my questions. She was also my “unofficial mentor” when I thought CHE 360 (Chemical Engineering Lab). I have learned a great deal from her about research and teaching, and have enjoyed her company. I also had the opportunity to work with many undergraduate student researchers. Their effort was very important to perform a number of experiments that I would not be able to do by myself, and many of their suggestions made important contributions for this research: Matthew Neff, Stephanie Fraley, Michael Berguer, Jacob Gruesbeck, Kathryn Jorgenson, Shawn Mayfield, Soo Kim, and Joe Yonkoski.

During my stay in Michigan, I met Waldea Gomes. She was kind, patient, helpful, caring, and lovely. She stayed with me and offered me unconditional support and love since the first day we met, even when I had nothing to offer myself. She changed my life and taught me things that go much beyond this thesis and research work. Her constant support and help allowed me to focus on my research when I most needed, and I do not know how I would have made it this far without her. I am so glad she is now Waldea Resende, my wife, and I am looking forward to continue our life together.

My parents, Fernando A. Resende and Graca Resende, are the two people who have been supporting me, suffering with me during the tough times and rejoicing with my accomplishments since before I can remember. I was far from them in Michigan, for almost five years, but there is no distance and there is no time that could change that. I needed them in many opportunities, and they were always there for me. The same can be said of my siblings: Carlos Resende, Fernanda Resende and Graca M. Resende. Despite the distance, I always felt their support and love. I also thank my uncle Marcos Pacheco, who was the first person to suggest me to do the PhD in a foreign country.

I also would like to thank the friends that made my stay in Ann Arbor so pleasant: Laura, Blake and Sue Lancaster, Caroline and Joan Brewer, Paul Nkansah, Daniel Burlingame, Alysson Roberto, Matt and Michelle Kreke, Stephan Braum, Karen Balzer, Jill Burghardt, Edward Kim, Sue Ressler.

TABLE OF CONTENTS

DEDICATION……..……..ii

ACKNOWLEDGMENTS……..……..iii

LIST OF FIGURES……...x

LIST OF TABLES……...…xv

ABSTRACT…….xvi

CHAPTER

1 INTRODUCTION 1

1.1 MOTIVATION FOR THE USE OF BIOMASS AS AN ENERGY SOURCE 1
1.2 CHEMICAL COMPOSITION OF BIOMASS 2
1.3 TECHNOLOGIES TO PROCESS BIOMASS 6
1.4 SUPERCRITICAL WATER (SCW): DEFINITION AND PROPERTIES 7
1.5 SUPERCRITICAL WATER GASIFICATION (SCWG): INTRODUCTION 10

2 LITERATURE REVIEW 16

2.1 REACTION MECHANISMS AND KINETICS FOR SCWG 16
2.1.1 Methanol 17
2.1.2 Ethanol 18
2.1.3 Glucose 19
2.1.4 Cellulose 19
2.1.5 Hemicellulose 22
2.1.6 Lignin 22
2.1.7 Interactions among model compounds 23
2.1.8 Other materials 26
2.2 CATALYSIS IN SCWG 26
2.2.1 Alkali Catalysts 28
2.2.2 Nickel Catalyst 28
2.2.3 Zirconia Catalyst 29
2.2.4 Ruthenium Catalyst 30
2.2.5 Other Catalysts 30
2.2.6 Catalyst Supports 31
2.2.7 Catalysis at Reactor Walls 31
2.3 EFFECT OF REACTION CONDITIONS ON PRODUCTS 32
2.3.1 Concentration 32
2.3.2 Temperature 33
2.3.3 Water Density 33

2.3.4 Heating Rate 34
2.3.5 Partial Oxidation 34
2.4 Operational Issues in SCWG 34
2.4.1 Reactor Plugging 34
2.4.2 Feeding/Pumping 35
2.4.3 Corrosion 36
2.4.4 Catalyst Deactivation 36
2.4.5 Other issues 37
2.5 Separation of Components 37
2.6 Units in Operation 38
2.7 Summary of Relevant Gaps in the Literature 38

3 EXPERIMENTAL METHODS 44

3.1 Reactor Preparation 44
3.2 Carrying Out SCWG 46
3.3 Experimental Conditions 48
3.4 Gas Sample Analysis 49
3.5 Calculations 49
3.6 Problems with Gas Analysis 52
3.7 Effect of the Heating Rate 54
3.8 Effect of Oxygen 54

4 NON-CATALYTIC GASIFICATION OF CELLULOSE IN SUPERCRITICAL WATER 59

4.1 Introduction 59
4.2 Results and Discussion 60
4.2.1 Base Case Results 61
4.2.2 Effect of Temperature 67
4.2.3 Effect of Cellulose Loading 68
4.2.4 Effect of Water Density 76
4.2.5 Comparison with Previous Results 81
4.3 Conclusions 82

5 NONCATALYTIC GASIFICATION OF LIGNIN IN SUPERCRITICAL WATER ……86

5.1 Introduction 86
5.2 Results and Discussion 87
5.2.1 Base Case Results 89
5.2.2 Effect of Temperature 94
5.2.3 Effect of Lignin Loading 96
5.2.4 Effect of Water Density 102
5.2.5 Comparison with Stainless Steel 107
5.2.6 Comparison with Cellulose 108
5.3 Conclusions 113

6 A KINETIC MODEL FOR SUPERCRITICAL WATER GASIFICATION OF BIOMASS 117

6.1 INTRODUCTION 117
6.2 REACTION ENGINEERING. 121
6.3 METHOD 123
6.4 RESULTS 125
6.5 CONCLUSIONS 152
7 GASIFICATION OF CELLULOSE AND LIGNIN IN THE PRESENCE OF ADDED METALS 154
7.1 INTRODUCTION 154
7.2 METHOD 155
7.3 RESULTS 156
7.3.1 Effect of Temperature 156
7.3.2 Effect of Water Density 159
7.3.3 Effect of Biomass Loading 159
7.4 CONCLUSIONS 188
CONCLUSIONS AND FUTURE WORK 192

LIST OF FIGURES

Figure

Figure 1.1. Chemical Structure of Glucose 3

Figure 1.2. Chemical Structures of the main components of hemicelluloses 4

Figure 1.3. Chemical Structure of the main components of lignin 5

Figure 1.4. Phase diagram for a pure component 9

Figure 2.1. Reaction Pathway for SCWG of Cellulose. 24

Figure 2.2. Pathway for lignin decomposition in SCWG. 25

Figure 3.1. Temperature profile for the quartz reactors 47

Figure 3.2. Consecutive analysis of the same sample (lignin, 600°C, 0.08 g/ml, 9.0 wt %, 10 min). 53

Figure 3.3. Comparison between Sand Bath and Tube Furnace (600°C, 0.08 g/ml, 9.0 wt %, 10 min). 56

Figure 3.4. Effect of O_2 on the gasification of lignin (600°C, 0.08 g/ml, 9.0 wt %, 10 min). 57

Figure 4.1. Temporal variation of gas composition (base case). 63

Figure 4.2. Temporal variation of yields (mmol/g) of CO, CO_2, H_2, and CH_4 (base case). 64

Figure 4.3. Temporal variation of C, H, O and total gas yields (base case). 66

Figure 4.4. Gas composition at 5 minutes as function of temperature (9.0 wt % loading, 0.08 g/ml water density). 69

Figure 4.5. C, H, O and total gas yields at 5 minutes as a function of temperature (9.0 wt % loading, 0.08 g/ml water density). 70

Figure 4.6. Gas yields at 5 minutes as function of temperature (9.0 wt % loading, 0.08 g/ml water density). 71

Figure 4.7. Gas composition at 10 min as function of cellulose loading (500°C, 0.08 g/ml water density). 72

Figure 4.8. C, H and O yields at 10 min as function of cellulose loading (500°C, 0.08 g/ml water density). 74

Figure 4.9. Gas yields at 10 minutes as function of cellulose loading (500°C, 0.08 g/ml water density). 75

Figure 4.10. Gas composition at 7.5 min as function of water density (500°C, 9.0 wt % cellulose loading). 77

Figure 4.11. C, H, O and total gas yields at 7.5 min as function of water density (500°C, 9.0 wt % cellulose loading). 78

Figure 4.12. Gas yields at 7.5 minutes as function of water density (500°C, 0.08 g/ml water density). 80

Figure 5.1. Temporal variation of gas composition (base case). 90

Figure 5.2. Temporal variation of yields (mmol/g) of CO, CO_2, H_2, and CH_4 (base case). 91

Figure 5.3. Temporal variation of C, H, O and total gas yields (base case). 93

Figure 5.4. Gas composition as function of temperature (45 minutes, 9.0 wt % lignin loading, 0.08 g/ml). 95

Figure 5.5. C, H, O and total gas yields as a function of temperature (45 minutes, 9.0 wt % lignin loading, 0.08 g/ml). 97

Figure 5.6. Gas yields as function of temperature (45 minutes, 9.0 wt % lignin loading, 0.08 g/ml). 98

Figure 5.7. Gas composition as function of lignin loading (75 minutes, 600°C, 0.08 g/ml). 99

Figure 5.8. C, H, O, and total gas yields as function of lignin loading (75 minutes, 600°C, 0.08 g/ml). 100

Figure 5.9. Gas yields as function of lignin loading (75 minutes, 600°C, 0.08 g/ml). ... 101

Figure 5.10. Gas composition as function of water density (60 minutes, 600°C, 9.0 lignin loading). 103

Figure 5.11. C, H, O, and total gas yields as function of water density (60 minutes, 600°C, 9.0 lignin loading)..... 105

Figure 5.12. Gas yields as function of water density (60 minutes, 600°C, 9.0 % lignin loading). 106

Figure 5.13. Gas yields for cellulose and lignin at 600°C, 10 minutes, 0.08 g/cm^3 and 9.0 wt % loading. 110

Figure 5.14. C, H, O, and total gas yields for cellulose and lignin at 600°C, 10 minutes, 0.08 g/cm^3 and 9.0 wt % loading. 111

Figure 5.15. CH_4/H_2 molar ratio as function of biomass loading for cellulose and lignin (500°C/10 min for cellulose and 600 °C/75 min for lignin). 112

Figure 6.1. Base case fitting for cellulose SCWG (500°C, 0.08 g/ml, 9.0 wt %)..... 127

Figure 6.2. Base case fitting for lignin SCWG (600°C, 0.08 g/ml, 9.0 wt %). 128

Figure 6.3. Model Predictions for Cellulose (10 min for wt %, 7.5 min for g/ml)..... 129

Figure 6.4. Model Predictions for Lignin (75 min for wt %, 60 min for g/ml). 130

Figure 6.5. Effect of lignin loading (75 min). 132

Figure 6.6. Effect of water density for cellulose (7.5 min). 133

Figure 6.7. Effect of water density for lignin (60 min). 134

Figure 6.8. Equilibrium Composition for Lignin, Base Case. 136

Figure 6.9. Effect of Lignin Loading on Equilibrium Composition. 138

Figure 6.10. Effect of Water Density on Equilibrium Composition (Lignin). 139

Figure 6.11. Rates of formation / consumption for H_2 (cellulose, 500°C, 9.0 wt % loading, 0.08 g/ml). 142

Figure 6.12. Rates of formation / consumption for CH_4 (cellulose, 500°C, 9.0 wt % loading, 0.08 g/ml). 143

Figure 6.13. Rates of formation / consumption for CO (cellulose, 500°C, 9.0 wt % loading, 0.08 g/ml). 144

Figure 6.14. Rates of formation / consumption for CO_2 (cellulose, 500°C, 9.0 wt % loading, 0.08 g/ml). 145

Figure 6.15. Rates of formation / consumption for H_2 (lignin, 600°C, 9.0 wt % loading, 0.08 g/ml). 146

Figure 6.16. Rates of formation / consumption for CH_4 (lignin, 600°C, 9.0 wt % loading, 0.08 g/ml). 147

Figure 6.17. Rates of formation / consumption for CO (lignin, 600°C, 9.0 wt % loading, 0.08 g/ml). 148

Figure 6.18. Rates of formation / consumption for CO_2 (lignin, 600°C, 9.0 wt % loading, 0.08 g/ml). 149

Figure 7.1. Effect of metals presence as a function of temperature (Cellulose), at 10 min. 157

Figure 7.2. Effect of metals presence as a function of temperature (Lignin), at 15 min. 158

Figure 7.3. Effect of metals presence as a function of water density (cellulose), at 7.5 min. 160

Figure 7.4. Effect of metals presence as a function of water density (lignin), at 15 minutes. 161

Figure 7.5. Effect of metals presence as a function of cellulose loading, 10 min. 162

Figure 7.6. Effect of metals presence as a function of lignin loading, 15 min. 163

Figure 7.7. Catalysts comparison at 5.0 wt % (cellulose), 10 min. 166

Figure 7.8. Catalysts comparison at 5.0 wt % (Lignin), 15 min. 167

Figure 7.9. Model predictions for 5000 min at 5.0 wt % (lignin, 9.0 wt %, 0.08 g/cm^3). 168

Figure 7.10. Comparison of Efficiencies at 5.0 wt % (cellulose), 10 min. 169

Figure 7.11. Comparison of Efficiencies at 5.0 wt % (Lignin), 15 min. 170

Figure 7.12. Catalysts comparison at 1.0 wt % (cellulose), 10 min. 173

Figure 7.13. Catalysts comparison at 1.0 wt % (lignin), 15 min. 174

Figure 7.14. Comparison of efficiencies at 1.0 wt % (cellulose), 10 min. 175

Figure 7.15. Comparison of efficiencies at 1.0 wt % (lignin), 10 min. 176

Figure 7.16. Yields of gases with only water and metal (10 min, 500°C, 0.08 g/ml). ... 178

Figure 7.17. Yields of gases with only water and metal (15 min, 600°C, 0.08 g/ml). ... 179

Figure 7.18. Effect of multiple Nickel wires (cellulose, 500°C, 10 min, 1.0 wt %, 0.08 g/ml). 182

Figure 7.19. Effect of multiple Nickel wires (lignin, 600°C, 15 min, 1.0 wt %, 0.08 g/ml). 183

Figure 7.20. Efficiencies for multiple Nickel wires (cellulose, 500°C, 10 min, 1.0 wt %, 0.08 g/ml). 184

Figure 7.21. Efficiencies for multiple Nickel wires (lignin, 600°C, 15 min, 1.0 wt %, 0.08 g/ml). 185

Figure 7.22. Effect of Nickel Exposure to SCW for 2 hours (cellulose, 500°C, 10 min, 1.0 wt %, 0.08 g/ml)..... 186

Figure 7.23. Effect of Nickel Exposure to SCW for 2 hours (lignin, 600°C, 15 min, 1.0 wt %, 0.08 g/ml)..... 187

LIST OF TABLES

Table

1.1. Experimental Conditions. 48

3.1. Henry's Constants at 25°C……..……....51

4. 1. Summary of Previous Research on SCWG of Cellulose (all in stainless steel reactors). (NR = Not Reported) 60

4.2. Gas Yields (mmol/g) from SCWG of Cellulose with no added catalyst (500 °C, 20 min, 0.07 g/ml, 9.1 wt % cellulose). 81

4.3. Gas Yields (mmol/g) from SCWG of Cellulose with no added catalyst (400 °C, 15 min)……...……...……..82

5.1. Summary of Previous Research on SCWG of Lignin with no added catalyst..... 87

5.2. Gas yields (mmol/g) from SCWG of lignin with no added catalyst (400°C, 60 min, 0.35 g/cm^3, 12.6 wt %)..... 107

5.3. Molar % from lignin SCWG with no catalyst added (400°C, 15 min, 0.33 g/cm^3, 5.0 wt %). 108

6.1. Input and output Gas Concentrations (mol/L) in ASPEN. 125

6.2. Rate Constants at 500°C (Cellulose) and 600°C (Lignin). 125

6.3. Rate constants for water-gas shift in SCW. 140

6.4. Rate constants for water-gas shift and methanation. 140

6.5. Sensitivity coefficients for cellulose (1 min). 150

6.6. Sensitivity coefficients for cellulose (30 min). 151

6.7. Sensitivity coefficients for lignin (1 min). 151

6.8. Sensitivity coefficients for lignin (75 min). 151

7.1. Summary of Catalysts used in SCWG. 155

ABSTRACT

SUPERCRITICAL WATER GASIFICATION OF BIOMASS

by

Fernando L. Pacheco de Resende

Chair: Phillip E. Savage

We performed Supercritical Water Gasification (SCWG) for cellulose and lignin for the first time in the absence of catalytic effects from metallic walls, by using quartz reactors. We quantified the catalytic effect of metals by adding metal wires to the reactors. We also performed the first systematic study of the effect of variables on gas yields. We varied time (2.5 to 75 minutes), temperature (365-725°C), water density (0.00-0.18 g/cm^3), and biomass loading (1.0 wt %-33.3 wt %).

In the absence of metals, high temperatures and water densities provide the highest gas yields. Up to 3.3 mmol/g of H_2 were obtained from cellulose (at 0.18 g/cm^3) and up to 7.5 mmol/g (at 725°C) from lignin. Up to 2.6 mmol/g of CH_4 were obtained from cellulose (at 600°C), and up to 9.0 mmol/g from lignin (at 725°C). The highest

energetic content (LHV gas/LHV biomass) was 20.0 % from cellulose (at 600°C), and 37.4 % from lignin (at 725°C).

The presence of metals increases gas yields to a significant extent if the catalyst surface area/biomass weight ratio is at least 15.4 mm^2/mg (5.0 wt % biomass loading). Nickel and copper provide high yields at 5.0 wt % loading, and nickel provides the highest yields at 1.0 wt % loading. Nickel at 240 mm^2/mg provides 23.5 mmol/g of H_2 from cellulose and 21.1 mmol/g of H_2 from lignin, which is close to equilibrium yields. CH_4 yields are not strongly influenced by the presence of metals. With nickel, it is possible to generate a gas with almost 50 % energetic content from cellulose, and 45 % from lignin.

The non-catalytic results were used to fit the first kinetic model describing gas formation in SCWG. The proposed 11 reactions and the concept of a generic intermediate led to a model that can successfully fit the base case experimental data for cellulose and lignin. We verified that the model can predict yields at different biomass loadings and water densities. Its equilibrium predictions agree with thermodynamic calculations, and the rate constants obtained for the water-gas shift are in the range reported by previous authors.

CHAPTER 1
INTRODUCTION

1.1 Motivation for the Use of Biomass as an Energy Source

Worldwide concerns about the depletion of fossil fuel reserves and the pollution caused by combustion of petroleum-based fuels make renewable sources of energy an attractive alternative to address environmental issues and reduce countries' dependence on imported oil. Among the renewable sources of energy, substantial focus of research is currently on the use of biomass. The term biomass identifies all non-fossilized organic matter, from living and dead plant material to human waste, which is available on a renewable basis, including dedicated energy crops and trees, agricultural food and feed crops, agricultural crop wastes and residues, aquatic plants, and other waste materials. Many of these wastes, such as agricultural residues and sewage sludge, have been employed in thermo chemical conversion processes to produce fuels (gases and liquids) from biomass, and simultaneously eliminate residues.

Besides being a renewable source of energy, there are many other advantages associated to the use of biomass. It is available abundantly in the world. Its use does not increase the net amount of CO_2 in the atmosphere. The CO_2 released from processing biomass originally came from the atmosphere itself, and was captured by the vegetation during the photosynthesis process, so that by thermally processing biomass we are simply promoting the CO_2 cycle.

An important question that arises in this discussion is whether the growth of biomass is sufficient to substitute main energy sources such as crude oil. Lieth and Whittaker [1] claim that the annual biomass growth on the continents amounts to 118 X 10^9 tons, when calculated as dry matter. The energy equivalent of oil fuel on a weight basis is 2.5 times higher than that of dry plant biomass. The present crude oil production of 3 X 10^9 tons per year is therefore equivalent to 7.5 X 10^9 tons of biomass, which is just

6.4 % of the annual growth. This large amount of biomass is distributed on the earth's surface with a greater degree of evenness than crude oil [2].

1.2 Chemical Composition of Biomass

Biomass is typically composed of cellulose, hemicellulose, lignin, and small percentages of other substances, including minerals and organic molecules [2, 3]. Cellulose is a linear biopolymer composed of glucose units connected by ether bonds, with polymerization degree among 7,000 and 10,000 [3, 4]. Cellulose chains gather to form a structure where crystalline and amorphous zones can be found [3]. The chemical structure of glucose is shown in Figure 1.1.

The hemicelluloses are a group of ramified and amorphous polymers made up of hexoses, pentoses and glicuronic acid. They have low polymerization degrees (50-300). The main components of hemicelluloses are shown in Figure 1.2.

The lignins are crossed-linked and amorphous phenolic polymers. Its aromatic structure in a three-dimensional macromolecular network provides high chemical stability [2, 5]. The chemical structures of the main components of lignin are shown in Figure 1.3.

Although cellulose, hemicellulose and lignin may add to up to more than 90 % of the global plant mass, there are additional plant components. Grain, potatoes, cassava, etc. have in their organic compounds approximately 50 % starch and 10 % protein. Ripe, sugar cane and sugar beet contain large amounts of sugar. Certain vegetables, such as beans, have an exceptionally high protein content [2].

Some of these additional plant components can be particularly useful when processing biomass if their elements can be recovered in useful form. For instance, many biomass feedstocks contain large amounts of nitrogen, phosphorus and potassium. These elements have a high commercial and environmental value if recovered in biologically available forms for use as fertilizer. The major components of fertilizers are chemical compounds of nitrogen, phosphorus, and potassium [6].

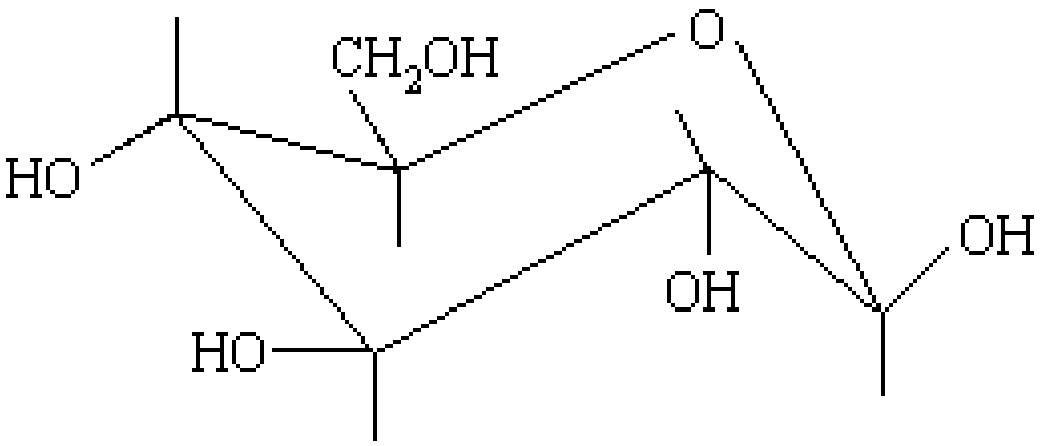

Figure 1.1.Chemical Structure of Glucose [5].

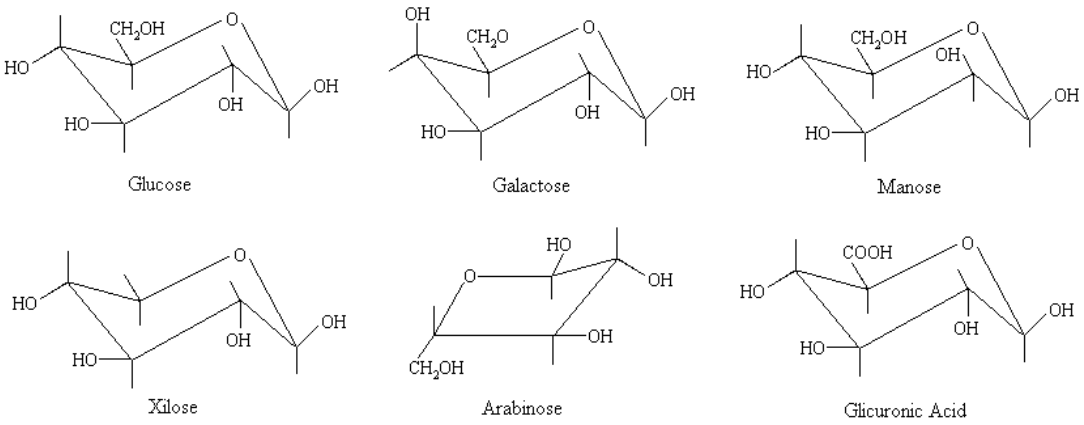

Figure 1.2. Chemical Structures of the main components of hemicelluloses [5].

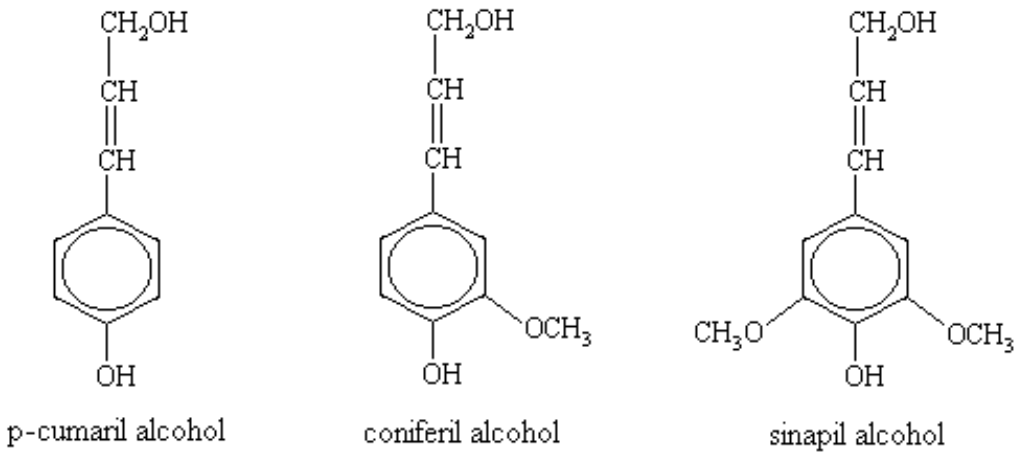

Figure 1.3. Chemical Structure of the main components of lignin [5].

Perhaps the most important difference between biomass and fossil fuels, in terms of composition, is the oxygen content. Biomass feedstocks often contain 40-60 wt % oxygen and conventional fuels are mostly hydrocarbons [6]. There are advantages and disadvantages for the use of biomass related to this topic.

For fossil fuels, the reforming reactions between hydrocarbons and water to generate H_2 are endothermic. Conventional steam reforming of petroleum depends on heat provided by the combustion of additional hydrocarbons. In contrast, oxygenated compounds such as the biomass components are able to form alkanes through exothermic reaction pathways, meaning that the energy required for the aqueous-phase reforming may be produced internally [7]. In this respect, the formation of a mixture of H_2 and alkanes from aqueous-phase reforming of glucose is essentially neutral energetically, and little additional energy is required to drive the reaction [7].

On the other side, hydrocarbons are usually better quality fuels. For instance, for oils, high oxygen content can impart a number of undesirable qualities to the oil product, such as lower energy content, poor thermal stability, lower volatility, higher corrosivity, and a tendency to polymerize. For this reason, generally speaking, in producing fuels from biomass, one overall objective is to remove oxygen and create fuels with as high of a H:C ratio as possible [6].

1.3 Technologies to Process Biomass

There are a number of technologies used to obtain fuel/energy out of biomass. Normally they differ on the % of O_2 present in the reactor. For instance, for combustion there is an excess of O_2 relative to the amount necessary for stoichiometric oxidation of the feedstock. In this case the energy (heat) is obtained directly in one step, but if there are plans of using biomass as a source of energy for the transportation sector, the fuel needs to be in a form suitable for use in engines or fuel cells.

In pyrolysis, a non-reactive gas is used in the reactor (absence of O_2) to avoid oxidation and allow the heat to break the large molecules into smaller ones. Pyrolysis can produce oils and fuel gases as well. It usually employs high heating rates.

Gasification is a technology that employs a reaction medium with O_2 content below the stoichiometric one required for combustion. O_2 (or air) causes partial

combustion and maintains the high reaction temperatures (> 973 K) [8], so that the biomass feedstock decomposes by pyrolysis reactions into lighter compounds such as H_2, CH_4, CO_2 and CO [4, 9, 10]. Once produced, process applications for the obtained gas are very wide, for example, use in gas turbines, in fuel cells and for the synthesis of chemicals [11]. The present work focuses on gasification.

Biomass gasification has been facing several technical difficulties that prevent its utilization in large scale. Much of the biomass resource is composed of material with higher levels of moisture, more typically 50 wt % and some even consists of wet biomass or biomass in water slurries at 85 % moisture or higher [12]. Examples are sewage sludge, cattle manure and food industry waste. For water contents above 40 %, the thermal efficiency of a conventional gasification plant decreases dramatically [13], because of the energy required to dry the feedstock.

The conventional methods for thermal treatment of biomass, such as gasification, also have the inconvenient effect of producing significant amounts of char and tar (higher hydrocarbons) in addition to the desired light gases [10]. Any production of char represents an effective loss of gas. The formation of pyrolytic char and tar during gasification sets limits on the efficient production of H_2 from biomass conversion under atmospheric pressure [14]. Furthermore, char and tar are difficult to gasify and to separate from the main stream [8, 13], compromising its use in further applications.

For wet biomass, biomethanation has been the most common method used [15]. This is a cheap process that produces CH_4 from biomass as well as fermentation sludge for fertilizer. Thirty days are required for fermentation and 10 h for active sludge treatment. [11]. So, biomethanation is a slow reaction and the treatment of fermentation sludge and wastewater from the reactors is now a large problem in Japan [15].

1.4 Supercritical Water (SCW): Definition and Properties

The properties of SCW as a reaction medium have been shown to affect thermal degradation of organic wastes, and this is one reason SCW has been widely proposed as a solvent to carry out organic reactions. A pure substance is referred to as supercritical when temperature and pressure are both above those of the critical point (which for water is 374 ºC and 22.1 MPa) [16]. The critical point represents the highest temperature and

pressure at which the substance can exist as a gas and liquid in equilibrium. The phenomenon can be clearly explained with reference to the phase diagram shown in Figure 1.4.

At the supercritical region, the high pressure keeps the density of the fluid close to those of liquids, increasing thermal conductivity [9]. The high temperature keeps viscosity close to those observed in gases, increasing diffusion rates [18]. These combined properties of gases and liquids make SCW a good option as a solvent for many reactions.

When water is at supercritical conditions, the hydrogen bonds of water are weakened, causing its dielectric constant to decrease from about 78 at 298 K to the range 2 to 20 near the critical point, which is similar to that of polar organic solvents at room temperature [19, 20]. This causes SCW to be able to dissolve many organic compounds completely, resulting in a single homogeneous phase [3, 8, 17, 21], and making rapid reactions of organic compounds possible [11, 22].

Other interesting properties can be mentioned as well. The ion product (K_W) of water goes through a maximum with temperature around the critical point. It first increases from 10^{-14} to 10^{-11} just below 350°C and then decreases by five orders of magnitude or more above 500°C [6]. In other words, at near-critical conditions there is large availability of H^+ and OH^- ions. This way, many acid-catalyzed or base-catalyzed reactions have their rates enhanced in the presence of water. Above the critical temperature, the ion product of water decreases dramatically, favoring radical-based reactions, which is necessary to form gases [8, 18]. As we will see later, this shift from ionic-based to radical-based is one of the reasons SCW can be used as a solvent for gasification reactions [8, 14, 23].

The advantage of using SCW as a solvent rather than common organic solvents is its environmentally benign nature and feasibility in the adjustment of solvent characteristics [24]. At supercritical conditions, water is compressible, and properties such as density and dielectric constant depend strongly on the pressure [25-27].

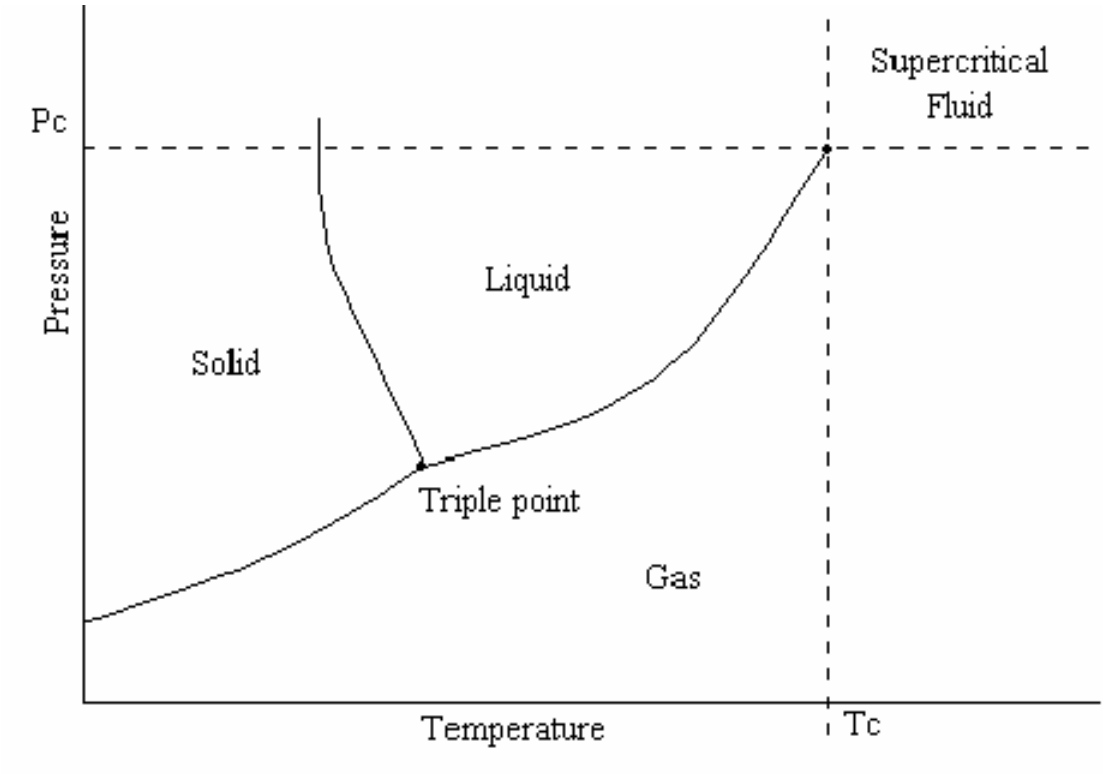

Figure 1.4. Phase diagram for a pure component [17].

1.5 Supercritical Water Gasification (SCWG): Introduction

SCW is completely miscible with O_2. For this reason, SCW has been employed for oxidation of hazardous organic compounds in the process called Supercritical Water Oxidation (SCWO). The homogeneous conditions in SCWO eliminate the rate-determining step of mass-transfer [4], leading to high destruction efficiencies with low residence times. Also because the supercritical process is fully contained, there are no vapor emissions or stack releases of products of incomplete combustion [6].

This ability to degrade organic compounds in a clean and efficient way has led to the idea of supercritical water gasification (SCWG), also called hydrothermal gasification, in which the organic waste is intended to generate fuel gases when eliminated. In SCWG, there is a large excess of water relative to the biomass. In the present work, the water-carbon ratio is typically 15-20 kg/kg. For comparison, the steam-carbon ratio in conventional steam-gasification is typically 3 kg/kg [28].

Hydrothermal gasification has emerged in 1985, initiated by the pioneering work of Modell at the Massachusetts Institute of Technology (MIT) [29]. Modell described experiments involving the immersion of maple wood sawdust in SCW, where it quickly decomposed to tars and some gas without the formation of char. Since then, many applications for thermal conversion of biomass have been proposed to use properties of SCW, such as gasification of glucose, cellulose, sewage sludge and organic wastes, with or without the use of catalysts, that usually decrease the temperature required for decomposition of theses materials [16].

There are several applications for the gases produced: compressed H_2/CH_4 could be used to substitute natural gas, compressed H_2, if alone, can be used in fuel cells, and CO_2 can be reused in other processes. The gas produced can be used as syngas to produce chemicals.

Compared to the traditional gasification process, the following advantages can be expected for a wet biomass/organic waste feedstock in SCWG:

- The water contained in the biomass is used as solvent in SCWG, and therefore the drying procedure is not required [14, 30];
- A H_2-rich gas with low CO yield can be produced by driving the water gas-shift reaction ($CO + H_2O \rightarrow CO_2 + H_2$) [13, 14];

- The presence of water as reaction medium leads to hydrolysis reactions, for instance, hydrolysis of cellulose to glucose and oligomers, rapidly degrading the polymeric structure of biomass. This depolymerization via hydrolysis instead of pyrolysis is one important difference with thermal gasification. The intermediates formed via hydrolysis and consecutive reactions show a high solubility in hot compressed water, undergoing an extraordinary variety of isomeration, dehydration, fragmentation, and condensation reactions in homogeneous phase, ultimately forming gas and tars [10, 25, 31]. The homogeneous media depresses formation of char and increases the reactivity [3, 16, 31];
- Formation of tars (which are mainly composed of furfural and phenols) [31],which is the chief obstacle to complete gasification of biomass, can be inhibited. Strategies to achieve this may include increasing temperature: above 700 °C most (but not all) of the tar effectively is converted to gas [14, 32]. Catalysts may also be used for this purpose: when wood is gasified using a Raney nickel catalyst, it leads to a colorless aqueous phase with low DOC (dissolved organic carbon) content [29];
- The heteroatoms (S, N and halogens) leave the process with the aqueous effluent avoiding expensive gas cleaning [13];
- Products of SCWG will be available at high pressure, which is practically always needed for any further use [9, 14];
- The water in SCWG is not only a solvent, but also a reactant which provides H atoms to form H_2 [10, 33]. Evidences of this are data for glucose gasification that have achieved H yields (mass H in gas/mass H in glucose) higher than 100 % [3]. Direct evidence supporting this fact has been obtained by gasifying naphthalene in a RuO_2-supercritical deuterium oxide (D_2O) system [34]. In fact, it is believed that up to half of the H_2 formed in SCWG originates from water rather than the biomass [25].

One of the questions that originates from the use of SCW as a solvent is concerning the energy required to reach supercritical conditions, as opposed to the energy necessary in other more conventional methods. Yoshida [11] compared several technologies from the perspective of energy conversion, and concluded that for electricity generation, SCWG is the most efficient process when the biomass moisture content is above 40 %. Also, one important difference to conventional methods is the possibility of

avoiding a phase change to steam during the heating-up process. This avoids large energy penalties [6].

On top of this, the heat can be largely recovered from the reaction effluent for temperatures up to 600°C [4, 11, 14]. The efficiency of a heat exchanger has a strong effect on the overall energy efficiency [25]. High efficiency of heat recovery and quick heating of the feedstock to avoid char and tar formation should be considered in designing the heating-up section [14].

A large variety of biomass feedstocks could be used in SCWG. A cyclic biomass gasification process has been proposed. It is based on cultivating microalgae that are further gasified hydrothermally. The effluent from the gasification containing nutrients could be recycled to the algae [6].

It is also possible to use water in subcritical conditions (temperature and pressure slightly below the critical point of water) to degrade biomass, in which case the use of alkali catalysts may become necessary, and liquid products are more likely to be formed, depending on the reaction conditions (liquefaction). Gases are also produced in lesser amounts, consisting of CO_2, H_2, CH_4 and CO [16]. The advantage of gasifying biomass at lower temperatures is to decrease the input thermal energy needed to carry out the process, and the role of catalysts becomes important to prevent the reaction from being slow [8]. If instead of the gases the purpose is to generate liquid fuels, then the overall objective is to remove oxygen; most readily by dehydration, which removes oxygen in the form of water, and by decarboxylation, which removes oxygen in the form of carbon dioxide. Since both water and carbon dioxide are fully oxidized and have no residual heating value, they are ideal compounds to remove oxygen without losing heating value [6].

SCWG opens a door to the effective thermochemical gasification of wet biomass. It is a novel process, under development since the late seventies. Large-scale commercial installations do not yet exist [14].

REFERENCES

[1] H. Lieth and R. H. Whittaker, *Primary Productivity of the Biosphere. Ecologica Studies.* , vol. 14, New York: Springer-Verlag, 1975, pp. 339.

[2] O. Bobleter, "Hydrothermal degradation of polymers derived from plants." *Progress in Polymer Science,* vol. 19, pp. 797-841, 1994.

[3] I. Lee, M. Kim and S. Ihm, "Gasification of Glucose in Supercritical Water." *Ind Eng Chem Res,* vol. 41, pp. 1182-1188, 2002.

[4] Y. Matsumura, M. Sasaki, K. Okuda, S. Takami, S. Ohara, M. Umetsu and T. Adschiri, "Supercritical water treatment of biomass for energy and material recovery." *Combustion Sci. Technol.,* vol. 178, pp. 509-536, 2006.

[5] S. Alves and J. Figueiredo, "Pyrolysis Kinetics of Lignocellulosic Materials by Multistage Isothermal Thermogravimetry," *J. Anal. Appl. Pyrolysis,* pp. 123-134, 1998.

[6] A. A. Peterson, F. Vogel, R. P. Lachance, M. Froling, M. J. Antal Jr. and J. W. Tester, "Thermochemical biofuel production in hydrothermal media: a review of sub- and supercritical water technologies." *Energy & Environmental Science,* vol. 1, pp. 32-65, 2008.

[7] R. D. Cortright, R. R. Davda and J. A. Dumesic, "Hydrogen from catalytic reforming of biomass-derived hydrocarbons in liquid water," *Nature,* vol. 418, pp. 964-967, 2002.

[8] M. Osada, O. Sato, M. Watanabe, K. Arai and M. Shirai, "Water Density Effect on Lignin Gasification over Supported Noble Metal Catalysts in Supercritical Water." *Energy Fuels,* vol. 20, pp. 930-935, 2006.

[9] N. Boukis, V. Diem, W. Habicht and E. Dinjus, "Methanol Reforming in Supercritical Water." *Ind Eng Chem Res,* vol. 42, pp. 728-735, 2003.

[10] M. J. Antal Jr., S. G. Allen, D. Schulman, X. Xu and R. J. Divilio, "Biomass Gasification in Supercritical Water." *Ind Eng Chem Res,* vol. 39, pp. 4040-4053, 2000.

[11] Y. Yoshida, K. Dowaki, Y. Matsumura, R. Matsuhashi, D. Li, H. Ishitani and H. Komiyama, "Comprehensive comparison of efficiency and CO2 emissions between biomass energy conversion technologies-position of supercritical water gasification in biomass technologies." *Biomass Bioenergy,* vol. 25, pp. 257-272, 2003.

[12] D. C. Elliott, "Catalytic hydrothermal gasification of biomass." *Biofuels, Bioproducts & Biorefining,* vol. 2, pp. 254-265, 2008.

[13] H. Schmieder, J. Abeln, N. Boukis, E. Dinjus, A. Kruse, M. Kluth, G. Petrich, E. Sadri and M. Schacht, "Hydrothermal gasification of biomass and organic wastes." *Journal of Supercritical Fluids,* vol. 17, pp. 145-153, 2000.

[14] Y. Matsumura, T. Minowa, B. Potic, S. R. A. Kersten, W. Prins, W. P. M. van Swaaij, B. van de Beld, D. C. Elliott, G. G. Neuenschwander, A. Kruse and M. J. Antal Jr, "Biomass gasification in near- and supercritical water: Status and prospects." *Biomass Bioenergy,* vol. 29, pp. 269-292, 2005.

[15] Y. Matsumura and T. Minowa, "Fundamental design of a continuous biomass gasification process using a supercritical water fluidized bed." *Int J Hydrogen Energy,* vol. 29, pp. 701-707, 2004.

[16] Z. Fang, T. Minowa, R. L. Smith Jr., T. Ogi and J. A. Kozinski, "Liquefaction and Gasification of Cellulose with Na2CO3 and Ni in Subcritical Water at 350 DegC." *Ind Eng Chem Res,* vol. 43, pp. 2454-2463, 2004.

[17] M. A. McHugh and V. J. Krukonis, "Supercritical Fluid Extraction: Principles and Practice." pp. 512, 1986.

[18] A. Loppinet-Serani, C. Aymonier and F. Cansell, "Current and foreseeable applications of supercritical water for energy and the environment." *ChemSusChem,* vol. 1, pp. 486-503, 2008.

[19] P. E. Savage, "Organic Chemical Reactions in Supercritical Water." *Chemical Reviews (Washington, D.C.),* vol. 99, pp. 603-621, 1999.

[20] N. Akiya and P. E. Savage, "Roles of water for chemical reactions in high-temperature water," *Chem. Rev.,* vol. 102, pp. 2725-2750, 2002.

[21] C. J. Martino, P. E. Savage and J. Kasiborski, "Kinetics and Products from o-Cresol Oxidation in Supercritical Water." *Ind Eng Chem Res,* vol. 34, pp. 1941-1951, 1995.

[22] Y. Matsumura, "Evaluation of supercritical water gasification and biomethanation for wet biomass utilization in Japan." *Energy Conversion and Management,* vol. 43, pp. 1301-1310, 2002.

[23] M. Watanabe, H. Inomata and K. Arai, "Catalytic hydrogen generation from biomass (glucose and cellulose) with ZrO2 in supercritical water." *Biomass Bioenergy,* vol. 22, pp. 405-410, 2002.

[24] T. Arita, K. Nakahara, K. Nagami and O. Kajimoto, "Hydrogen generation from ethanol in supercritical water without catalyst." *Tetrahedron Lett.,* vol. 44, pp. 1083-1086, 2003.

[25] A. Kruse and A. Gawlik, "Biomass conversion in water at 330-410 DegC and 30-50 MPa. Identification of Key Compounds for Indicating Different Chemical Reaction Pathways." *Ind Eng Chem Res,* vol. 42, pp. 267-279, 2003.

[26] T. Sato, M. Osada, M. Watanabe, M. Shirai and K. Arai, "Gasification of Alkylphenols with Supported Noble Metal Catalysts in Supercritical Water." *Ind Eng Chem Res,* vol. 42, pp. 4277-4282, 2003.

[27] M. Watanabe, H. Inomata, M. Osada, T. Sato, T. Adschiri and K. Arai, "Catalytic effects of NaOH and ZrO2 for partial oxidative gasification of n-hexadecane and lignin in supercritical water." *Fuel,* vol. 82, pp. 545-552, 2003.

[28] M. Baratieri, P. Baggio, L. Fiori and M. Grigiante, "Biomass as an energy source: Thermodynamic constraints on the performance of the conversion process." *Bioresour. Technol.,* vol. 99, pp. 7063-7073, 2008.

[29] M. H. Waldner and F. Vogel, "Renewable Production of Methane from Woody Biomass by Catalytic Hydrothermal Gasification." *Ind Eng Chem Res,* vol. 44, pp. 4543-4551, 2005.

[30] M. Lanzetta and C. Di Blasi, "Pyrolysis kinetics of wheat and corn straw." *J. Anal. Appl. Pyrolysis,* vol. 44, pp. 181-192, 1998.

[31] A. Kruse, T. Henningsen, A. Sinag and J. Pfeiffer, "Biomass gasification in supercritical water: influence of the dry matter content and the formation of phenols." *Ind Eng Chem Res,* vol. 42, pp. 3711-3717, 2003.

[32] J. Herguido, J. Corella and J. Gonzalez-Saiz, "Steam gasification of lignocellulosic residues in a fluidized bed at a small pilot scale. Effect of the type of feedstock." *Ind Eng Chem Res,* vol. 31, pp. 1274-1282, 1992.

[33] T. Minowa and T. Ogi, "Hydrogen production from cellulose using a reduced nickel catalyst." *Catalysis Today,* vol. 45, pp. 411-416, 1998.

[34] K. C. Park and H. Tomiyasu, "Gasification reaction of organic compounds catalyzed by RuO2 in supercritical water." *Chemical Communications (Cambridge, United Kingdom),* pp. 694-695, 2003.

CHAPTER 2
LITERATURE REVIEW

SCWG is currently receiving a great deal of attention from researchers, and several reviews have been published recently to summarize the current knowledge in the area [1-4]. These reviews cover a wide variety of topics, including SCWG with and without added catalysts, and also report research which is currently being performed to overcome technical problems.

2.1 Reaction Mechanisms and Kinetics for SCWG

Research concerning SCWG of biomass is recent and has intensified over the last years, but only recently relevant findings about the mechanisms and kinetics of gasification for the components of biomass have been published. The reason for this arises from the complex structure and chemistry of ligno-cellulosic materials, which makes it difficult to describe gasification by detailed chemical reaction pathways with well-defined single reaction steps, imposing a difficult challenge to overcome in this area [5].

For this reason, the most common approach that has been employed is the use of simpler model compounds, which can provide information about fundamental aspects of gasification. Mainly methanol [6-8], ethanol [9], and glucose [10-14], have been employed to this purpose. The components of biomass: cellulose, hemicellulose and lignin have also been studied [15-20]. Some authors have performed research with real biomass, but in these cases the reaction mechanism is normally not addressed [21-24].

The fundamental research carried out with model compounds has revealed some features and trends of SCWG. Organic wastes decompose in homogeneous phase, but it is believed that smaller model compounds (such as methanol and ethanol), if formed, follow heterogeneous catalyzed mechanisms on the reactor surface. Some studies have been reported to evaluate catalytic effects of reactor walls such as those composed of the

nickel based Inconel 625 catalyzing methanol [6, 7] and glucose gasification, and Hastelloy C-276, which also catalyzes glucose gasification [10].

Despite the importance of a rate law and global kinetic parameters for the design of reactors, estimation of product distribution and energetic efficiency, not many results have been published concerning the kinetics of SCWG. Kinetic models were proposed for glucose [10, 13] and cellulose [18, 25]. These models focus solely on feedstock conversion, without capturing the chemistry leading to formation of gas species. The complexity of biomass feedstocks has been a major obstacle to advances in this area.

Intermediates of biomass degradation often have double bonds and are able to polymerize. On the other hand, these compounds are dissolved in SCW. Coke formation is reduced if the molecules that may polymerize have a lower probability to meet. And solvation of the intermediate supports reactions with water or catalyzed by OH^- or H_3O^+ ions, which are bond-fission reactions in most cases [2].

For kinetics and mechanism studies, there is a new application with transparent quartz capillaries (1 mm ID and 150 mm length) as batch micro-reactors. It allows high speed and inexpensive testing, with the additional advantage of possible visual observations. The capillaries are heated rapidly (within 5 s) in a fluidized sand bath to the desired reaction temperature. A drawback however is that the pressure inside the capillary cannot be measured, rather it is derived indirectly. Quartz has no or hardly any effect on the reaction kinetics, and some of the reaction products are visible (tar, char) [26]. The following sections describe the most relevant findings about mechanisms for each model compound and biomass components in SCWG.

2.1.1 Methanol

The simplest model compound for these studies is methanol, a liquid miscible with water. Methanol gasification performed in continuous systems results in a H_2-rich product stream with low concentrations of CO and CO_2 [8]. It is possible to reach up to 99 % methanol conversion without addition of a catalyst (25-45 MPa, 400-600°C, 3-100 s, 5- 64 wt% methanol). Conversion increases sharply at 500 °C or higher temperatures, and also increases with higher residence time and lower concentrations. Soot and tar formation are usually negligible [6].

The following scheme of reactions is assumed for the reforming of methanol:

(1) $CH_3OH \leftrightarrow CO + 2\ H_2$

(2) $CO + H_2O \leftrightarrow CO_2 + H_2$

(3) $CO + 3\ H_2 \leftrightarrow CH_4 + H_2O$

(4) $CO_2 + 4\ H_2 \leftrightarrow CH_4 + 2\ H_2O$

H_2 yield as a function of the residence time reaches a maximum due to increase in the rates of methanol decomposition and water-gas shift reaction (1 and 2), and after that, decreases because the rate for methanation reactions increase (3 and 4). [6]. The high concentration of CO observed is likely due to the fact that the water-gas shift reaction is much slower at lower temperatures, indicating a higher activation barrier than the methanol decomposition step. DiLeo and Savage [27] suggested a scheme including steam-reforming of the methanol:

(1) $CH_3OH + H_2O \rightarrow 3\ H_2 + CO_2$

(2) $CH_3OH \rightarrow 2\ H_2 + CO$

(3) $CO + H_2O \leftrightarrow CO_2 + H_2$

To confirm that these are actually the main reactions taking place, they calculated the "H/C" ratio as in Equation 2.1:

$$\frac{H}{C} = \frac{Y_{H_2} + Y_{CO}}{Y_{CO} + Y_{CO2}} \qquad (2.1)$$

Where Y_i is the gas composition. Stoichiometry indicates that H/C should be three if the reactions taking place are the main ones. Experimentally, they found that the H/C ratio is indeed close to three, confirming the reactions suggested as the main ones in methanol SCWG.

2.1.2 Ethanol

Ethanol as a model compound in SCW produces H_2 and acetaldehyde at 400-500 °C and water density 0.20 g/cm^3 [9]. Acetaldehyde is the only detectable component in the liquid phase, while H_2, CH_4, CO, CO_2 and small amounts of ethylene and ethane are present in the gas phase. According to the authors, the initial step would be the dehydrogenation of ethanol, which is followed by the decomposition of acetaldehyde into CH_4 and CO, and finally CO is converted into CO_2 by the water-gas shift reaction,

according to the following scheme. All these processes can proceed without any catalyst [9].

(1) $CH_3CH_2OH \rightarrow CH_3CHO$ (acetaldehyde) + H_2

(2) $CH_3CHO \rightarrow CH_4 + CO$

(3) $CO + H_2O \rightarrow CO_2 + H_2$

The presence of ethylene among the products suggests an additional reaction pathway, i.e., the elimination of a water molecule from ethanol. This process occurred with a smaller branching ratio relative to the dehydrogenation. A part of resulting ethylene could be converted to ethane by H_2 addition. This is shown in the following scheme:

(4) $CH_3CH_2OH \rightarrow CH_2=CH_2 + H_2O$

(5) $CH_2=CH_2 + H_2 \rightarrow CH_3CH_3$

2.1.3 Glucose

Glucose is the monomer for cellulose and one of the monomers for hemicellulose. It is therefore an important model compound and many studies have been performed regarding its decomposition in SCW. As reported by Kruse [2], conversion of glucose leads to almost the same product distribution of gas, oil, and coke as that of cellulose at the different temperatures. The pathway for decomposition for glucose is practically the same as cellulose, so the mechanism for glucose decomposition will be described in the cellulose section.

2.1.4 Cellulose

As one of the main components of biomass, cellulose has been extensively used as a model compound, and its decomposition has been carried out at both subcritical and supercritical conditions [10]. Most researchers seem to agree in the reaction mechanism proposed for its decomposition, with small differences.

In SCW, the first step is the dissolution of cellulose. After cellulose molecules are solvated by water, hydrolysis reactions take place, breaking the polymeric structure into glucose and oligomers [28]. There are very important differences in what concerns the

hydrolysis step in supercritical compared to subcritical conditions, and these are highlighted next.

Around the critical point of water, there is a change in reaction mechanism for cellulose hydrolysis, from heterogeneous to homogeneous [29]. In other words, at sub-critical conditions, the dissolution of cellulose does not take place to the same extent, and hydrolysis takes place on the cellulose crystal surface rather than a homogeneous medium [29].

Researchers believe this is one of the reasons why there is a discontinuity in reaction rates close to the critical point of water [5, 20]. At low temperatures, glucose and oligomers react much faster than cellulose hydrolyzes. Thus, even if cellulose hydrolyzes to glucose and oligomers, these further react rapidly and no hydrolysis products are left. Above the critical point, dissolution leads to a hydrolysis rate jump to more than an order of magnitude higher and it becomes faster than the glucose decomposition rate, leading to many hydrolysis products in the liquid phase [20]. Evidence of this is the observation made with a diamond-anvil cell, showing that in subcritical water, the hydrolysis of cellulose takes place nearly at the same time as its dissolution [3].

Furthermore, as mentioned previously, it is believed that around the critical point, the main reaction mechanism changes from ionic in subcritical to free radical in the supercritical region, favoring formation of gases [26, 30]. At subcritical conditions, the relatively high ion product of water leads to the formation of five-atom-ring species (furfurals) and to a smaller extent aromatic compounds via water elimination. These ionic reactions can be dominant because of the liquid like properties of subcritical water. Free-radical reactions, which are necessary to form gases, are less pronounced [30].

Next we discuss what takes place following hydrolysis. The hydrolysis reaction breaks ether bonds to form oligomers: cellobiose, cellotriose, cellotetraose, cellopentose and cellohexaose, and the oligomers further hydrolyze to single units of glucose [18, 20, 26, 31], which can isomerize to fructose [13]. Glucose undergoes fast decomposition reactions [28]. The complete conversion of cellulose to glucose/fructose and its oligomers can be achieved at temperatures as high as 400 °C in 0.05 s [10, 19].

Glucose and fructose undergo a variety of reactions:

- dehydration, leading to either 1,6 anhydroglucose or 5-HMF (5-hydroxymethyl furfural)

- retro-aldol condensation, leading to erythrose and glycolaldehyde
- hydrolysis, to form levoglucosan
- generation of dihydroxyacetone [5, 30].

If recovered, erythrose can be used as a raw material for erythritol, a low calorie sweetener, and glycolaldehyde can be used to produce biodegradable plastics [29]. When erythrose, glycolaldehyde and 5-HMF decompose, they can form a variety of low-molecular weight alcohols, carboxylic acids, aldehydes and ketones. The dihydroxyacetone (formed from fructose) isomerizes to glyceraldehyde and also decomposes to phenols. The phenols further lead to alcohols, carboxylic acids, aldehydes and ketones, which could also be formed directly from fructose decomposition. Note that, in biomass decomposition, aromatic compounds are normally assumed to originate from lignin, but as this mechanism shows, they can originate from cellulose as well [4].

The steps leading to gas formation are the decomposition reactions of the low-molecular weight alcohols, carboxylic acids, aldehydes and ketones via decarbonylation and decarboxylation to form CO_2, CO, CH_4 and H_2. Tars can be formed when 5-HMF reacts to form polyphenols. The reactions described compete with the formation of furfurals and phenols, which are preferred at ionic conditions ($T < 374$ °C). This free-radical mechanism dominates at high-temperature and low-density regions. [30].

In order to avoid tar formation, either the 5-HMF has to decompose rapidly, or polyphenols formed from it must decompose to low-molecular-weight compounds. The excellent solvation properties of SCW are probably enhancing the reforming of the polyphenols. Polyphenols tend to form dark and oily oligomeric compounds when heated and/or exposed to O_2. In a low-pressure vapor phase, these compounds would not be solubilized and would, therefore, be difficult to gasify. Care must be taken not to enter the vapor region during heat-up to avoid tar formation. High pressure should be kept during reactor heat up to always keep a dense, liquid phase in the reactor [32].

The gas formed consists mainly of CO_2, H_2 and CH_4 and CO [33]. Once the gas species are formed, they can be converted one into the other by water-gas shift, methanation, and hydrogenation.

Above the critical point of water, there is a drastic increase in the yields of H_2 and CH_4 and decrease in CO [28]. One of the reasons for this is the conversion of CO and

water to CO_2 and H_2 via the water-gas shift reaction. The rate of CO formation is faster than that of water-gas shift reaction at low temperatures. It is well known that the water-gas shift reaction rate is slow at low temperatures and that its equilibrium constant decreases with increasing temperature in gas phase [34]. However, the water gas-shift reaction becomes very fast at temperatures as high as 700 °C [10], increasing H_2 rapidly. Therefore, in the absence of catalysts, high temperatures are necessary to increase high H_2 yields from gasification of cellulose/glucose in SCW.

The mechanism for SCWG of cellulose is shown in Figure 2.1. Figure 2.1 is based on information collected from literature and previously discussed.

2.1.5 Hemicellulose

The most important fact about hemicelluloses is that all possess side chains and pendant groups, such as glucuronic acid and acetic acid, which inhibit the formation of H-bridges. This makes hemicellulose much more accessible to hydrolytic attack, and therefore much more soluble in water and/or alkali than cellulose (xylans are hydrolyzed 60-80 times more quickly than cellulose). Hydrothermolysis dissolves approximately all hemicellulose in the 180 - 200°C temperature region [35]. This is only true, though, if hemicellulose is separated from plant matter. Within the plant, hemicelluloses are mostly connected to lignin by covalent links and are thus fixed in the fiber structure [35]. Hemicellulose breaks down to form a number of monosaccharides, the most prevalent being the 5-carbon sugar xylose [4, 28].

2.1.6 Lignin

When isolated lignin is used as a starting material for SCWG, it must first be remembered that it undergoes modification during the separation procedure used to extract it from the plant material. In most cases, it can be assumed that lignin isolation leads to more highly condensed, cross-linked materials. The degradation of lignin contained in plant materials is therefore usually more readily achieved than for the case of pre-isolated lignin samples [35].

Lignin decomposition in SCW also starts by hydrolysis, forming phenolics. Although its aromatic structure provides lignin high thermal stability, much of the connections among their monomeric components are ether bridges, and hydrolysis leads

to cleavage of ether and ester bonds by the addition of one molecule of water for every broken linkage. In addition, the low activation energies suggest that lignin degradation could be achieved at temperatures below 200 °C. These facts suggest that lignin macromolecular structure could be easily dissolved under hydrothermal conditions [35]. In reality, this is not observed, and the main reason is the high chemical activity of the low molecular weight lignin fragments such as formaldehyde, syringols, guaiacols, and catechols. Recondensation of dissolved products by cross-linking reactions between these fragments can take place. This leads to heavier molecular weight compounds which correspond to the solid residues [29, 30], with low yield of gases [29].

Differences are observed for different types of lignins. Softwood lignin (based on conyferyl alcohol linkages) is highly resistant to degradation because of its cross-linked structure, and it gains H atoms when decomposed (it consumes H atoms if they are available). Hardwood lignin (termed guayaciyl-syringil lignin, composed of conyferyl alcohol and sinapyl alcohol) eliminates H and O atoms from the side-chain [36]. The mechanism for lignin decomposition as proposed is shown in Figure 2.2.

2.1.7 Interactions among model compounds

Once the main reaction pathways for the three main components of biomass are known, it is essential to understand the interactions among them [37]. Gasification of a mixture of cellulose, xylan and lignin does not behave as a sum of the degradation for the individual components, because interactions among them change the product distribution [37].

If there were no interaction between the components, data for the mixture should fall on a weighted-average for contributions for each compound. For cellulose and hemicellulose mixtures, this is observed, indicating the behavior of these two components is summative and no significant interaction exists. On the other hand, a large deviation from this average is observed for lignin-cellulose mixtures and lignin-hemicellulose mixtures. It is observed that when lignin is present, production of H_2 is suppressed [26].

It is believed that cellulose and xylan donate H atoms to lignin. This hydrogenation uses atoms that otherwise would turn out to generate H_2, and thus interactions among cellulose and xylan with lignin tend to decrease H_2 production.

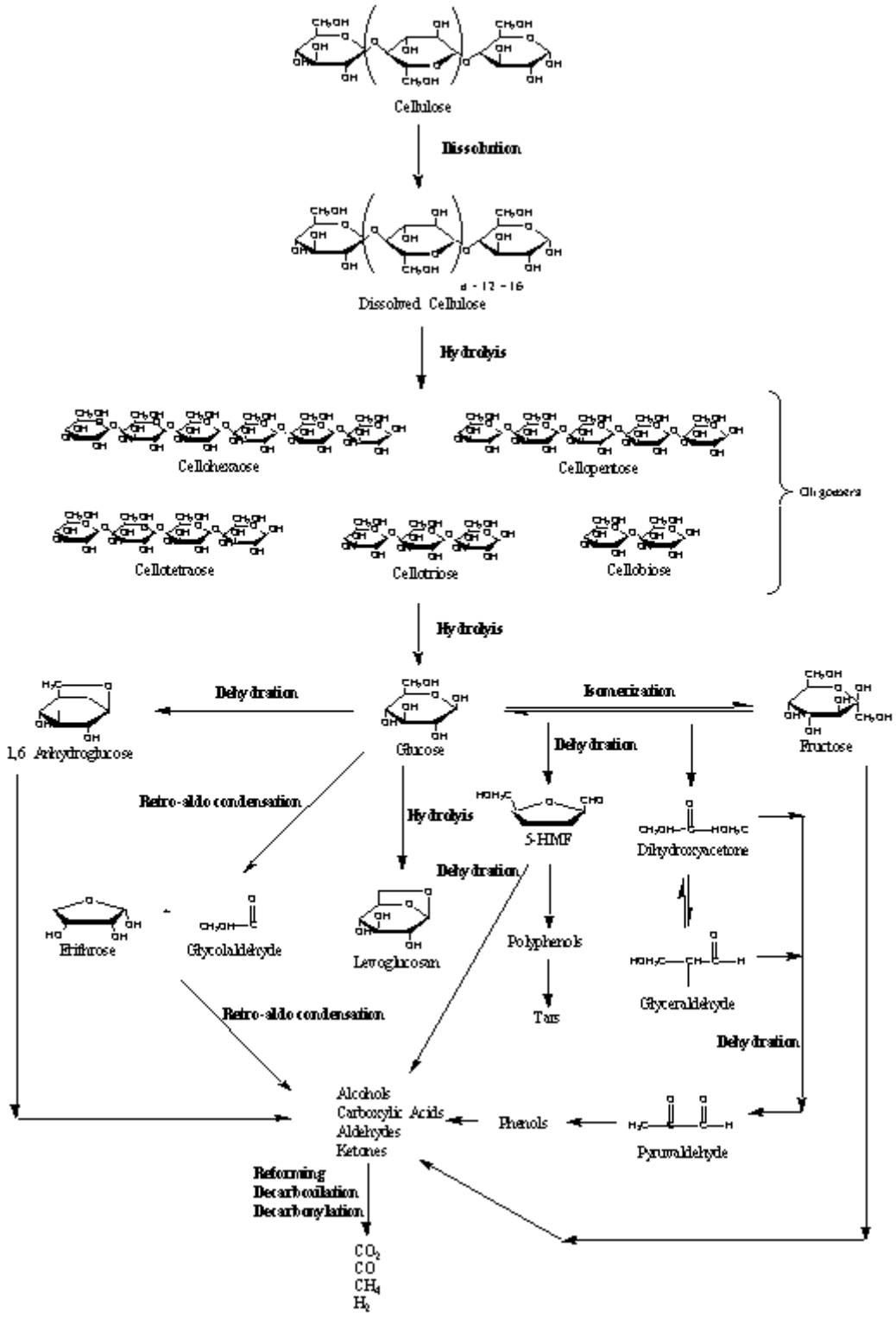

Figure 2.1. Reaction Pathway for SCWG of Cellulose.

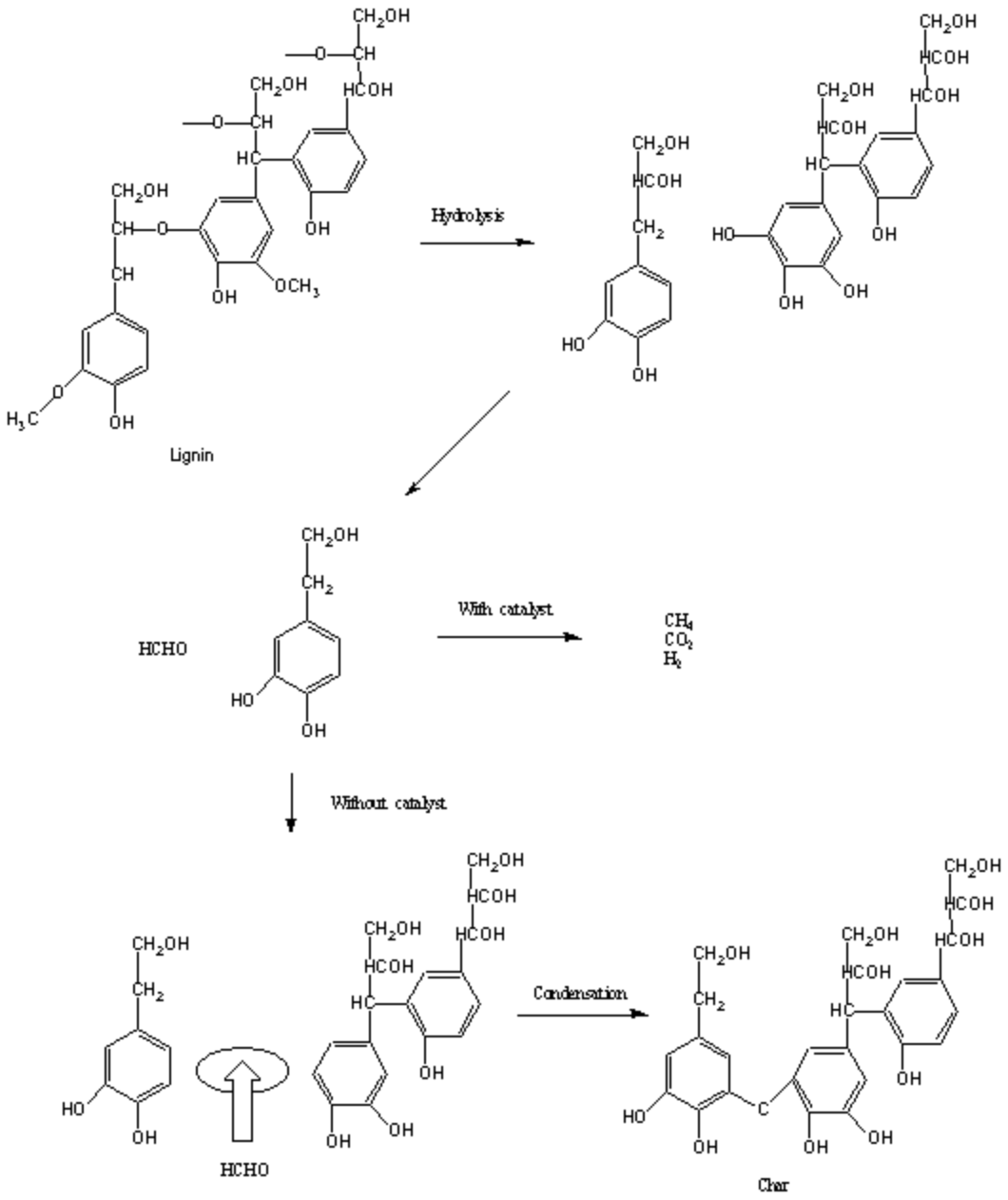

Figure 2.2. Pathway for lignin decomposition in SCWG [30].

Yoshida and Matsumura [37] fitted a model to predict how interactions affect production of H_2, CH_4 and CO_2.

It has been suggested that added phenol supports lignin SCWG. Apparently, the presence of phenol can prevent polymerization because it avoids recombination of intermediate species, which would lead to heavier fragments. This increases the yield of smaller phenolic compounds and decreases char yields at these conditions [3, 5].

2.1.8 Other materials

Organic materials other than cellulose, hemicellulose and lignin may also affect the yield and composition of gas products. Gasification of amino acids is important for gasification of animal matter, because proteins may be contained in biomass feedstocks. Studies with glycine as a model compound showed that it is rather resistant to gasification [2]. DiLeo reported that a significant portion of the carbon in glycine remained in aqueous phase even after reaction times of up to 1 h at 600°C [38]. It has been suggested that glycine forms a heterocyclic, free radical scavenger inhibiting further gasification reactions. A free radical scavenger is a stable free radical that is not reactive enough to start a free radical chain reaction, but interacts with the reactive free radicals, reducing their number and inhibiting the free radical reaction chain. The other possible explanation for this behavior is oligomerization [2]. Also, the presence of minerals in biomass has a significant effect on the gasification properties [26].

2.2 Catalysis in SCWG

Reducing energy inputs for SCWG is an important accomplishment in order to make the process feasible. Catalysts can be used to reduce temperature and pressure necessary for the production of fuel gases. Many catalysts have been tested for model compounds and real biomass.

The general agreement on how catalysts achieve complete conversion of biomass feed is centered on the catalyst's ability to gasify reactive intermediates that are rapidly formed from the feed molecules by hydrolysis and dehydration. The gasification of intermediates must be fast enough to avoid the formation of polymeric materials and

eventually char. Reactive intermediates that are water-soluble have been identified to be mainly phenols and furfurals [4].

A good catalyst should be able to help break C-C bonds, especially for opening aromatic rings (phenols), and it should also dissociate H_2O to yield reactive O and OH adsorbed intermediates on the catalyst surface. These radicals will then combine with the adsorbed $C_xH_yO_z$ fragments, and finally release CO and CO_2. The adsorbed hydrogen atoms from water splitting and from the cleaved $C_xH_yO_z$ fragments will combine to form H_2. These are some of the mechanistic features that a good gasification catalyst must exhibit. Others features are a fast equilibration of the water-gas shift reaction, and the hydrogenation of CO and CO_2 to CH_4 and H_2O [4, 39].

Catalysts are used not only to increase the rate of a desired chemical reaction (activity), but also to steer the product distribution toward the desired one (selectivity). Therefore, a catalyst may still be useful in the case of unfavorable thermodynamics, if reaching chemical equilibrium is not the goal [4].

It must be kept in mind that performing a truly non-catalytic experiment in supercritical water media is complicated by a number of factors:

- Reactor walls may act as heterogeneous catalysts;
- Alkali salts present in real biomass may act as homogeneous catalysts;
- Corrosion products from the reactor (transition metal ions such as Ni, Fe, and Cr) may act as catalysts [4].

Metals are typical catalysts for SCWG, because they promote a high level of carbon conversion to gas at relatively low temperature [26]. But, as mentioned, they are also typical components of the reactor walls, interfering with reaction rates even when no catalyst is added to the system. To our knowledge, the only studies of SCWG in the absence of metals are the ones performed by Potic [40] and DiLeo [38], using capillary quartz reactors. Potic gasified glucose, and DiLeo gasified methanol, glycine, and phenol. Data for non-catalytic SCWG of more complex model compounds, such as cellulose and lignin, are not available. This adds an obstacle to the understanding and quantification of the true effects of catalysts added to SCWG systems.

Also, when catalyst metals are added to SCWG reactors, a common result is the oxidation of the metal in the hydrothermal system. In Elliott's study, nickel and copper

were the only base metals found to remain reduced in the metallic form after the test [1]. The next sections describe results reported for the most common catalysts used in SCWG.

2.2.1 Alkali Catalysts

Basic conditions promoted by alkali catalysts increase the rates of several gasification reactions. With $NaCO_3$, the degradation of cellulose starts at 180 °C, accelerating formation of liquid products from cellulose [15, 17]. Alkali catalysts lower the onset temperature of the cellulose degradation [26].

Alkali salts usually support the splitting of C-C bonds [28] and have the ability to prevent tarry material formation thus enhancing gasification efficiency [29]. NaOH, K_2CO_3, $KHCO_3$ and KOH severely attack monomeric and dimeric carbohydrates, such as glucose, fructose or cellobiose, even below 100 °C [26, 35]. When gas products are finally formed, the alkali also influences composition since they effectively promote the water-gas shift reaction, increasing H_2 and CO_2 yields, and decreasing CO [5, 28, 33, 41]. Lignin also has its macromolecular structure decomposed by hydrolysis enhanced by alkali (mostly NaOH) [35].

The use of alkali catalysts to gasify real biomass has been reported. Straw is completely gasified using alkali catalysts with a batch-type reactor at 773 K, 35 MPa during 120 min, obtaining mainly H_2 and CO_2 [30]. However, the use of homogeneous alkali catalysts has the inconvenience of difficult recovery from the effluent stream, which could make the process expensive [42].

2.2.2 Nickel Catalyst

Nickel has been found to greatly improve gasification yields, even at subcritical conditions. Gasification of cellulose in near-critical water at 350 °C and 16.5 MPa with a reduced nickel catalyst prevented the formation of char and led to 70 % carbon gasification [3].

Extensive use of nickel has been reported for SCWG. Nickel catalyst is known to largely suppress tar formation by cracking it, and is also known to promote water-gas shift reaction, methanation, and hydrogenation reactions, leading to a higher yield of gas product, especially H_2, CO_2 and CH_4 [1, 26, 36, 43]. Nickel catalyst causes cellulose to

start decomposing between 260 and 320 °C, strongly promoting formation of gases [15]. Nickel can also lead to complete gasification of lignin at a temperature as low as 470 K. A large amount of catalyst (1.2 g catalyst/g biomass) is needed for effective gasification of lignin to take place [36].

The main problem associated with nickel is its rapid deactivation [36]. Elliott's studies suggested that only nickel in a reduced form had any significant amount of activity. In his work, nickel sintered and deactivated rapidly, but could be stabilized by doping with another metal [4]. Vogel's group also reported that nickel sinters rapidly at 400 °C [1]. Stable nickel metal catalysts were developed by Elliott's group by impregnating promoting metals onto the most stable nickel catalyst formulation. The most useful promoter metals were copper, silver, and tin, impregnated at 1 wt %. This stabilization method was attempted by Vogel, and although stability was improved over their earlier results, deactivation was still evident over 100 h of operation [1].

Raney nickel catalysts are porous nickel frameworks covered by hydrated alumina particles [39]. With Raney nickel as a catalyst, high CH_4 yields are achieved in the gasification of wood from 370°C to 420°C. Also, the water resulting is nearly tar-free. Continuous-flow reactor experiments showed that Raney nickel is deactivated over time in a 50-h experiment [1]. It has been found that addition of Sn to Raney-Ni catalysts significantly decreases the rate of CH_4 formation without inhibiting the rate of H_2 formation [39]. The beneficial effect of Sn on the selectivity for production of H_2 may be caused by the presence of Sn at Ni-defect sites and by the formation of Ni-Sn alloy surfaces. The decoration of defect sites by Sn may thereby suppress methanation reactions. It is also possible that methanation reactions are suppressed by the presence of Sn on Ni_3Sn alloy surfaces [39]. Raney nickel with Sn leads to gas products which are 50 to 70 mole % H_2, 30 to 40 % CO_2, and 2 to 11 % alkanes. A slight increase of carbon deposits on the used Raney nickel surface can be observed after the reaction. Also, according to the manufacturer, aging is an issue to the Raney type catalysts and storage should not be prolonged to more than one year [32, 39].

2.2.3 Zirconia Catalyst

Recently it was found that zirconia (ZrO_2), which is a solid acid-base catalyst and stable in SCW, is an effective catalyst for the decomposition of carbonyl compounds such

as carboxylic acid in SCW. Since decomposition of biomass such as glucose and cellulose in SCW produces aldehydes and ketones intermediates, the yield of H_2, as well as CO_2, could be promoted by using zirconia as a catalyst in SCWG, although in smaller extent than NaOH and Na_2CO_3 [41, 42].

For glucose and cellulose the gasification efficiency with zirconia is twice as much as that without catalyst [42]. For lignin, the yields of H_2 with ZrO_2 are almost twice as much as that without catalyst [41].

2.2.4 Ruthenium Catalyst

Ruthenium catalyzes the gasification of cellulose, lignin, formaldehyde and real biomass [24] with better performance than other catalysts such as NaOH and Ni/AlO_3 [26]. In fact, ruthenium on carbon support has been shown to be more active than nickel [1], and other metals such as rhodium, palladium and platinum [30]. This effectiveness is probably a result of the high activity of ruthenium in breaking C-C bonds [30]. By breaking these bonds, ruthenium gasifies reactive intermediates such as formaldehyde, which otherwise participate in cross-linking reactions to form solids [33, 44]. It has been suggested that Ru^{II} exists as an intermediate in the catalytic mechanism, and that the catalytic effect of ruthenium oxide results from a redox couple of Ru^{IV}/Ru^{II}[44]. Tests made by Elliott et al. [1] showed that for phenolic model compounds, ruthenium has useful levels of activity. Ruthenium showed long-term stability when used in gasification of phenol as a model compound, especially with a carbon-supported form.

2.2.5 Other Catalysts

The majority of the published research concentrates on the catalysts previously mentioned, but some groups have tested less common catalysts in SCWG. Yanik et al. [45] report that iron can be an effective catalyst for the gasification of red-mud (a by-product of the electrochemical process of aluminum production). Arita [9] has reported that the addition of copper wires accelerates gasification of ethanol considerably. Since nickel and many other metals that have been shown to be active catalysts for tar gasification are subject to severe corrosion by SCW at the temperatures needed to secure high yields of H_2, carbon catalyst has been used and is particularly effective because it is stable in supercritical water, especially in the presence of H_2 [8, 26, 46]. Activated

carbon catalysts are effective for inhibiting formation of char [30]. The main issue with activated carbon is the rapid drop in carbon gasification efficiency below 823 K [29].

2.2.6 Catalyst Supports

The effectiveness of catalysts in hydrothermal gasification can be greatly improved by the use of support materials with long-term stability in hot liquid water. Many alumina and silica based materials commonly used for catalyst formulations in the petroleum and gas processing industries are less useful for hydrothermal gasification. The better supports for SCWG include activated carbon, mono-clinic zirconia, titania, and α-alumina [1].

Nickel, for instance, has high activity and generates more CH_4 with a magnesia support than without the support [17, 28]. Ruthenium has been evaluated on many supports [39, 47]. Ruthenium on rutile titania extrudate is particularly effective in this process. It is easily reduced to its active form and maintains its activity for long periods of operation [26]. Osada [30] obtained high carbon gasification yields with ruthenium on titania for repetitive uses. In general, γ-alumina as a support leads to higher gas yields than carbon [47]. But it is not a useful catalyst support for more than a few hours in aqueous systems because it does not survive in long-term processing [47, 48].

2.2.7 Catalysis at Reactor Walls

Nickel/chromium super alloys such as Inconel and Hastelloy, which are excellent materials of construction for high-pressure and high-temperature steam process, have been shown to have catalytic effects in hydrocarbon-reforming systems [7]. The nickel-based Inconel 625 is believed to catalyze the water-gas shift reaction and suppress CH_4 formation when gasifying glucose, acetic acid and formic acid, resulting in a H_2-rich product stream [14]. Previous oxidation of Inconel 625 with H_2O_2 in water (3 wt %) catalyzes methanol gasification to achieve up to 99 % conversion (600 °C and 25 MPa). This treatment dissolves Cr and Mo from the reactor walls, increasing the concentration of nickel oxides in the surface. The oxides can be formed during the treatment with H_2O_2, and are later reduced to Ni during gasification. This reduction accelerates methanol decomposition and the water-gas shift reaction, decreasing CO yields [6]. The

alloy Hastelloy C-276 influences gasification of glucose [46], especially after treatment with aqueous salts such as NaCl solution [14, 26].

To evaluate the effect of added catalysts, it is desirable to eliminate catalysis from the reactor walls. Different reactor types can be used for this purpose:

- Quartz reactors
- "Seasoned" or "aged" reactors. The reactor is exposed to reaction conditions in the presence of the feedstock for one or two weeks until the planned experiment starts. New reactors show a significant catalytic effect that vanishes with operation time. These reactors have a lower and constant catalytic effect
- Metal reactor with ceramic liner: Use in supercritical water total oxidation [2].

2.3 Effect of Reaction Conditions on Products

Effects of parameters such as concentration of biomass and temperature on products have been evaluated [46]. The next sections describe the main findings on how reaction conditions affect gas yields.

2.3.1 Concentration

Concentration is an important variable, as observed for methanol gasification. Gasification yields decrease at high feed concentrations, which can be explained by saturation of the active sites in the reactor wall with adsorbed methanol [26, 48]. Glucose in tubular reactors is completely gasified only in small concentrations: 0.001 M and 0.1 M (600 °C and 24.6 MPa) [26, 29]. Concentrations lower than 0.6 M, as well as residence times of at least 60 s, avoid formation of soot and tar [17]. Concentrations higher than 5-10 % lead to significant drop of the H_2 yield [26]. However, higher concentrations of biomass must be handled to commercially use SCWG [11], since low concentrations would not be economically practical [48].

Concentration can be also important for selectivity. Higher methanol concentration (less water present) decreases the rate of water-gas shift reaction, increasing CO and decreasing CO_2 [7]. The selectivity for production of H_2 also decreases as concentration increases [39].

Antal et al. pointed out that the feed concentration was a reason for the formation of soot and tar during supercritical water gasification [3]. Lu et al. [49] found that high concentrations of biomass have a negative effect on the gas yield and lead to the plugging of the reactor.

2.3.2 Temperature

Temperature has a strong effect on product distribution. As temperature increases, solid product is consumed, liquid and oil formation go through a maximum, and gas formation increases [15, 17, 28]. This suggests the pathway solids $\rightarrow$ liquids $\rightarrow$ gases, which proceeds further as temperature increases.

At high temperatures, the CH_4 steam reforming reaction is driven to increase H_2 yields at the expense of CH_4 [46]. From 873 to 973 K and 25-30 MPa, glucose and vanillin can be completely gasified to H_2 and CO_2 within 140 s [30]. Packed carbon gasification in SCW of granular coconut shell activated carbon using a packed bed reactor at 600-650 °C, 25.5-34.5 MPa obtained H_2 (64 %), CO_2 (33 %), CH_4 (2 %) and CO (1%), by mole. By increasing the reaction temperature above 650 °C, the yields of H_2 and CO_2 sharply increase, while the yield of CO decreases because there is stronger water gas-shift activity above 650 °C. The CH_4 yield is not affected [26].

2.3.3 Water Density

The water density affects the interaction between catalysts and reactants. It is believed that rates and equilibrium of the reaction can be controlled by changing water density. High water densities increase the breakdown of lignin for the production of oil and gases, presumably by enhanced hydrolysis [4]. It has been shown, for alkyl phenols, cellulose and lignin gasification, that the yield of liquid products has a maximum, and yields of gases such as CH_4 and CO_2 increase with water density up to 0.2 g/cm^3, remaining then constant. It is suggested that a larger number of water molecules in space promotes formation of CH_4 and CO_2 from alkyl phenol or alkyl benzene [33, 47, 50]. Gasification of these fragments occurs over metal catalysts and condensation between fragments can be suppressed, which means that char formation can be reduced [30]. Sato et al. [47] found gasification efficiency to decrease when the density increased beyond

0.4 g/cm^3, and explained it using the Le Chatelier's principle (the increasing pressure inhibits gas formation) [4].

2.3.4 Heating Rate

The heating rate in SCWG strongly influences phase behavior, since lower heating rates cause the biomass to spend more time at lower temperatures, leading to heterogeneous conditions for hydrolysis. Higher heating rates take the biomass above the critical point of water promptly, being rapidly dissolved achieving homogeneous conditions. Therefore, increase in the heating rate leads to higher yields of gas [3, 15]. It has been observed that slower heating rates favor the formation of refractory compounds when gasifying wood, as well as coke/char, tarry materials, resulting in more CH_4 (rather than H_2) production [26, 29, 32].

2.3.5 Partial Oxidation

It was observed that introduction of O_2 to perform partial oxidation enhances H_2 and CO_2 yields at all times [41]. When H_2O_2 is added to the biomass-SCW mixture, carbon gasification efficiency improves. But if the concentration of H_2O_2 is too high, oxidation of the product gas into water and carbon dioxide takes place [29], decreasing the energetic value of the product.

2.4 Operational Issues in SCWG

This section describes the main challenges researchers working with SCWG have been facing, and some of the solutions that have been employed.

2.4.1 Reactor Plugging

One of the main issues with SCWG is reactor plugging, which usually leads to system shut downs in tubular reactors [7, 23]. The plugging is generally caused by precipitation of feedstock inorganic impurities [12, 29]. Plugging by salts is mainly a problem of gasification with solid bed catalysts [2]. Other causes for plugging are the small size of the bench-scale demonstrations used, the robustness of tubing structures in enduring high-pressures, formation of char at the heating section and the buildup of ash inside the reactor [51]. Reactors can plug after only 2-3 hours on stream [46].

To avoid plugging by precipitation, some possible solutions have been tested. One of them is to treat the biomass prior to delivering the feedstock into the reactor. Attempts to pretreat biomass to allow extended use of catalysts, by removing certain components like alkaline earths [22] and biomass slurry preparation in a temperature range 150-200°C have been documented. Careful monitoring and control of feedstock trace components (e.g., calcium, magnesium, sulfur, and phosphorus) are critical for maintaining long-term operability and catalyst activity [22].

Another possibility is the use of multiple reactors. Having one reactor with a system for residues removal is described as an attempt to prevent reactor plugging. It requires a cleaning procedure with water, air and a soft metal brush, after some time of operation. Cleaning with H_2O_2 is also cited [46].

Penninger and co-workers flash pyrolyze their feed, which consists of beechwood sawdust. In this way, the minerals are concentrated in the char produced and not fed to their reactor. They use the condensate of this reaction, which is now a liquid and easier to pump, to feed their supercritical reactor, operated at 600-650°C and 28 MPa. Problems were encountered in their runs associated with tar build-up in their preheater exit [4].

2.4.2 Feeding/Pumping

It is not easy to feed biomass against high pressures [35]. Feeding a mixture of solids into a reactor operating at 22 MPa is challenging especially at smaller scales [4]. A reliable high pressure feeding system is needed for slurries [12].

Groups have solved this problem by a number of means, including using starch gels with cement pumps, pre-hydrolyzed feeds, solid-free feeds, or by pumping water against a piston containing the biomass slurry [4]. Antal's group succeeded in feeding sawdust continuously by suspending it in a starch gel. Also, a successful device to feeding slurries with a coaxial reciprocating feeder has been suggested [26].

Limitations of conventional high-pressure pumps also have to be considered for continuous SCWG systems. In general, there is a limit of dry-matter content which these pumps can still work with biomass/water slurries, which is usually 20 wt % or less, depending on the type of biomass and its pretreatment. For example, sewage sludge can be pumped up to 40 wt % dry-matter content [2]. The use of wastewater and pyrolysis

condensates has the advantage of pumping to high pressure being very easy and homogeneous solutions being used instead of slurries or suspensions [2].

2.4.3 Corrosion

A major drawback of applications in SCW is the corrosion of reactor materials. Water is an aggressive reaction medium: under certain reaction conditions, corrosion can be extremely high, especially when chlorine, sulfur, or phosphorous-containing compounds are oxidized and the corresponding acids are formed [52]. Still, as expected, corrosion is much less of a problem than in supercritical water oxidation [2].

There is evidence of corrosion in several SCWG experiments with alkali salts. For example, Kruse et al. [2] support a theory that this alkali environment may be dissolving the protective metal oxide layer on the reactor walls. If the outer metal oxide layer dissolves, it exposes fresh, temporarily reduced metal to SCW. The metal can quickly oxidize in SCW, producing hydrogen. As a consequence, change in material properties (ductility, tensile strength) and a subsequent embrittlement take place.

Severe corrosion is observed for high-nickel alloys such as Hastelloy and Inconel, meaning these might not be proper for use in SCWG [46]. Boukis et al. [6] and Habicht et al. [53] observed no corrosion and severe ductility loss for a Ni-based alloy 625 (which is the widest applied alloy for SCW applications) exposed to methanol-SCW (reactor was previously treated with 3 wt % H_2O_2), at 25 MPa and 600 °C, at 5 wt % methanol. It has been suggested [53], based on results with the alloys C-22 (superior in resistance at various environments) and 625, that subcritical conditions force a partial dissolution of the major and minor alloying elements and therefore, cause maximum corrosion [52, 53]. In the supercritical region, the previously dissolved alloying elements and the appropriate anions precipitate. Corrosion products dissolved at subcritical conditions can precipitate at supercritical conditions and plug the reactor [52].

2.4.4 Catalyst Deactivation

When using nickel, catalyst deactivation in SCWG takes place primarily by deposition of tarry intermediates on the catalyst [1]. Ash and carbon buildup on the wall of the reactor can also reduce access of the reactant to the catalytic metal, causing changes in gas composition with time [46].

For nickel, Elliott [1] attributed the deactivation to decomposition of the nickel and poisoning by mineral content in the feedstocks. He attempted to solve this problem by liquifying the biomass solids prior to entering the catalyst bed. However, mineral precipitates from the biomass remained a significant problem leading to plugging at the front end of the catalyst bed.

2.4.5 Other issues

Besides the problems already mentioned, Peterson [4] listed other challenges involved in SCWG:

- capital cost;
- pumping expenses for moving all of that water through the plant;
- heat transfer and recovery: hydrothermal technologies operate at high temperatures, and have severe heating requirements to reach these temperatures, although these are lower than the heating requirements if the system were unpressurized (which would result in water vaporization). This emphasizes the importance of heat integration; that is, recovering the heat from the hot effluent stream to heat the incoming cold stream.
- Recovery of homogeneous catalysts;
- It is difficult to separate the wall effects of catalysts from the effects of the intended catalyst. This may ultimately lead to scale-up issues if not properly understood.

2.5 Separation of Components

Separation of components might be desired depending on the application of the gas produced. For instance, if the H_2 produced is intended to be used in fuel cells, it is necessary to separate the H_2 from the main gas stream. For use in PEM fuels cells, a concentration of CO as low as 10 ppm has an unacceptable effect on the performance [54]. The gaseous effluents separated from the main product H_2 could be combusted to generate the energy necessary for the reactor [48].

After complete gasification, cooling down and depressurization of the effluent stream will separate gas and water automatically [25]. All tarry materials and char, if any, remain in the liquid phase, and a completely tar free product gas is available. This is an advantage of SCWG over conventional gasification processes. Thus, it is expected that

the product gas may be fed to gas engines or gas turbines without any treatment [26]. The problem then becomes only separation of components in the gas phase.

Usually, an easy separation of CO_2 is possible, because CO_2 is much more soluble in water at high pressure and ambient temperature than CH_4 and H_2 [2]. If the amount of CO_2 to be removed is large, additional water may be used to absorb the CO_2 [26].

There are a couple different ways to separate H_2 from the gas mixture. Lee et al. [10] suggested the use of a pressure swing adsorption and a palladium-alloy membrane. Although CO can poison palladium-alloy membranes at low to moderate temperatures, its ability to block H_2 permanent sites is reduced at temperatures greater than 300 °C. Taylor et al. [7] suggested the recovery of the H_2 cooled using a polymer membrane separator. This would avoid the use of precious metals. This separation method is aided by the high pressure at which the gases are available.

2.6 Units in Operation

In Germany, the VERENA test facility was built to process 100 kg/h, becoming the largest SCWG test facility existing so far. It consists of components suitable for further scale-up. It operates up to 700°C and 35 MPa, and has hot-components made of a nickel-based alloy. Biomass is crushed, the water content is adjusted to the desired dry matter content, subjected to pressure using membrane pumps, and heated up by a tube-in-tube heat exchanger, The pre-heater and reactor are fired by hot flue gas from a propane burner. The gas-phase is separated from the liquid phase still under pressure. In this way, a large part of CO_2 remains dissolved in the aqueous phase. Afterwards, the H_2-rich gas phase is CO_2 depleted in a scrubber [2]. VERENA has achieved gasification yields as high as 90-98% with feedstocks of 9-25% ethanol, pyroligneous acid and corn silage [4].

2.7 Summary of Relevant Gaps in the Literature

There are three major aspects which are missing in the literature, which we would like to point out. The present work makes contributions which address these three aspects. First, as mentioned by Peterson [4] and Kruse [2], when catalysts are added to

SCWG, it is difficult to separate the wall effects of catalysts from the effects of the intended catalyst. This may lead to scale-up issues if not properly understood. The lack of information on reactions in the absence of metals makes it difficult to quantify the true effect of metals when these are added to the reactors. For this purpose, some studies in quartz reactors were reported for glucose and ethanol. This work is the first one to report SCWG for cellulose and lignin in the absence of metals.

Second, there is no systematic study on the effects of experimental conditions. The information available in the literature for effects of variables in SCWG deals with a large variety of model compounds at different experimental conditions, many of them in the presence of different catalysts. In this work we perform a systematic study of the effects of time, temperature, water density, and biomass loading for cellulose and lignin. We performed this study in the absence of metals and also in the presence of added nickel, iron and copper. Most previous studies with cellulose and lignin focus on one time, temperature, water density and biomass loading.

Third, there are no kinetic models dealing with gas yields for SCWG. The few attempts to fit kinetic models to biomass decomposing in hot compressed water focus solely on feedstock conversion [13, 20], without capturing the chemistry leading to formation of gas species. Despite the knowledge available on the reaction pathways for SCWG, especially for cellulose, not much is known at the moment about the rates at which these reactions occur, and the main routes of gas formation are unclear. For instance, it is known that the methanation reaction takes place in SCWG systems, but it is not known if most of the CH_4 formed actually originates from methanation or possibly from other gasification routes, such as direct pyrolysis of methyl groups present in lignin. If most of the CH_4 originates from methanation, how close to equilibrium are we at typical SCWG conditions? Can we substantially improve CH_4 yields by adding a catalyst that promotes methanation? These are some of the questions we aim to answer with the aid of the kinetic model we developed in the present work. This information is useful in designing SCWG systems.

REFERENCES

[1] D. C. Elliott, "Catalytic hydrothermal gasification of biomass." *Biofuels, Bioproducts & Biorefining,* vol. 2, pp. 254-265, 2008.

[2] A. Kruse, "Supercritical water gasification." *Biofuels, Bioproducts & Biorefining,* vol. 2, pp. 415-437, 2008.

[3] A. Loppinet-Serani, C. Aymonier and F. Cansell, "Current and foreseeable applications of supercritical water for energy and the environment." *ChemSusChem,* vol. 1, pp. 486-503, 2008.

[4] A. A. Peterson, F. Vogel, R. P. Lachance, M. Froling, M. J. Antal Jr. and J. W. Tester, "Thermochemical biofuel production in hydrothermal media: a review of sub- and supercritical water technologies." *Energy & Environmental Science,* vol. 1, pp. 32-65, 2008.

[5] A. Kruse, T. Henningsen, A. Sinag and J. Pfeiffer, "Biomass gasification in supercritical water: influence of the dry matter content and the formation of phenols." *Ind Eng Chem Res,* vol. 42, pp. 3711-3717, 2003.

[6] N. Boukis, V. Diem, W. Habicht and E. Dinjus, "Methanol Reforming in Supercritical Water." *Ind Eng Chem Res,* vol. 42, pp. 728-735, 2003.

[7] J. D. Taylor, C. M. Herdman, B. C. Wu, K. Wally and S. F. Rice, "Hydrogen production in a compact supercritical water reformer." *Int J Hydrogen Energy,* vol. 28, pp. 1171-1178, 2003.

[8] X. Xu, Y. Matsumura, J. Stenberg and M. J. Antal Jr, "Carbon-Catalyzed Gasification of Organic Feedstocks in Supercritical Water." *Ind Eng Chem Res,* vol. 35, pp. 2522-2530, 1996.

[9] T. Arita, K. Nakahara, K. Nagami and O. Kajimoto, "Hydrogen generation from ethanol in supercritical water without catalyst." *Tetrahedron Lett.,* vol. 44, pp. 1083-1086, 2003.

[10] I. Lee, M. Kim and S. Ihm, "Gasification of Glucose in Supercritical Water." *Ind Eng Chem Res,* vol. 41, pp. 1182-1188, 2002.

[11] H. R. Holgate, J. C. Meyer and J. W. Tester, "Glucose hydrolysis and oxidation in supercritical water." *AICHE J.*, vol. 41, pp. 637-648, 1995.

[12] H. Schmieder, J. Abeln, N. Boukis, E. Dinjus, A. Kruse, M. Kluth, G. Petrich, E. Sadri and M. Schacht, "Hydrothermal gasification of biomass and organic wastes." *Journal of Supercritical Fluids,* vol. 17, pp. 145-153, 2000.

[13] B. M. Kabyemela, T. Adschiri, R. M. Malaluan and K. Arai, "Kinetics of Glucose Epimerization and Decomposition in Subcritical and Supercritical Water." *Ind Eng Chem Res,* vol. 36, pp. 1552-1558, 1997.

[14] D. Yu, M. Aihara and M. J. Antal Jr, "Hydrogen production by steam reforming glucose in supercritical water." *Energy Fuels,* vol. 7, pp. 574-577, 1993.

[15] Z. Fang, T. Minowa, R. L. Smith Jr., T. Ogi and J. A. Kozinski, "Liquefaction and Gasification of Cellulose with Na2CO3 and Ni in Subcritical Water at 350 DegC." *Ind Eng Chem Res,* vol. 43, pp. 2454-2463, 2004.

[16] T. Minowa, T. Ogi, Y. Dote and S. Yokoyama, "Methane production from cellulose by catalytic gasification." *Renewable Energy,* vol. 5, pp. 813-815, 1994.

[17] T. Minowa and T. Ogi, "Hydrogen production from cellulose using a reduced nickel catalyst." *Catalysis Today,* vol. 45, pp. 411-416, 1998.
[18] W. Schwald and O. Bobleter, "Hydrothermolysis of cellulose under static and dynamic conditions at high temperatures." *J. Carbohydr. Chem.,* vol. 8, pp. 565-578, 1989.
[19] T. Sakaki, M. Shibata, T. Miki, H. Hirosue and N. Hayashi, "Decomposition of Cellulose in Near-Critical Water and Fermentability of the Products." *Energy Fuels,* vol. 10, pp. 684-688, 1996.
[20] M. Sasaki, B. Kabyemela, R. Malaluan, S. Hirose, N. Takeda, T. Adschiri and K. Arai, "Cellulose hydrolysis in subcritical and supercritical water." *Journal of Supercritical Fluids,* vol. 13, pp. 261-268, 1998.
[21] D. C. Elliott and L. J. Sealock Jr, "Chemical processing in high-pressure aqueous environments: low-temperature catalytic gasification." *Chem. Eng. Res. Design,* vol. 74, pp. 563-566, 1996.
[22] D. C. Elliott and L. J. Sealock Jr, "Chemical processing in high-pressure aqueous environments: low-temperature catalytic gasification." *Chem. Eng. Res. Design,* vol. 74, pp. 563-566, 1996.
[23] D. C. Elliott, E. G. Baker, R. S. Butner and L. J. Sealock Jr, "Bench-scale reactor tests of low temperature, catalytic gasification of wet industrial wastes." *Journal of Solar Energy Engineering,* vol. 115, pp. 52-56, 1993.
[24] D. C. Elliott, G. G. Neuenschwander, T. R. Hart, R. S. Butner, A. H. Zacher, M. H. Engelhard, J. S. Young and D. E. McCready, "Chemical Processing in High-Pressure Aqueous Environments. 7. Process Development for Catalytic Gasification of Wet Biomass Feedstocks." *Ind Eng Chem Res,* vol. 43, pp. 1999-2004, 2004.
[25] Y. Matsumura, "Evaluation of supercritical water gasification and biomethanation for wet biomass utilization in Japan." *Energy Conversion and Management,* vol. 43, pp. 1301-1310, 2002.
[26] Y. Matsumura, T. Minowa, B. Potic, S. R. A. Kersten, W. Prins, W. P. M. van Swaaij, B. van de Beld, D. C. Elliott, G. G. Neuenschwander, A. Kruse and M. J. Antal Jr, "Biomass gasification in near- and supercritical water: Status and prospects." *Biomass Bioenergy,* vol. 29, pp. 269-292, 2005.
[27] G. J. DiLeo and P. E. Savage, "Catalysis during methanol gasification in supercritical water." *Journal of Supercritical Fluids,* vol. 39, pp. 228-232, 2006.
[28] A. Kruse and A. Gawlik, "Biomass conversion in water at 330-410 DegC and 30-50 MPa. Identification of Key Compounds for Indicating Different Chemical Reaction Pathways." *Ind Eng Chem Res,* vol. 42, pp. 267-279, 2003.
[29] Y. Matsumura, M. Sasaki, K. Okuda, S. Takami, S. Ohara, M. Umetsu and T. Adschiri, "Supercritical water treatment of biomass for energy and material recovery." *Combustion Sci. Technol.,* vol. 178, pp. 509-536, 2006.
[30] M. Osada, O. Sato, M. Watanabe, K. Arai and M. Shirai, "Water Density Effect on Lignin Gasification over Supported Noble Metal Catalysts in Supercritical Water." *Energy Fuels,* vol. 20, pp. 930-935, 2006.
[31] Y. Matsumura, H. Nonaka, H. Yokura, A. Tsutsumi and K. Yoshida, "Co-liquefaction of coal and cellulose in supercritical water." *Fuel,* vol. 78, pp. 1049-1056, 1999.

[32] M. H. Waldner and F. Vogel, "Renewable Production of Methane from Woody Biomass by Catalytic Hydrothermal Gasification." *Ind Eng Chem Res,* vol. 44, pp. 4543-4551, 2005.
[33] M. Osada, T. Sato, M. Watanabe, T. Adschiri and K. Arai, "Low-Temperature Catalytic Gasification of Lignin and Cellulose with a Ruthenium Catalyst in Supercritical Water." *Energy Fuels,* vol. 18, pp. 327-333, 2004.
[34] C. N. Satterfield, "Heterogeneous Catalysis in Industrial Practice. 2nd Ed." pp. 554, 1991.
[35] O. Bobleter, "Hydrothermal degradation of polymers derived from plants." *Progress in Polymer Science,* vol. 19, pp. 797-841, 1994.
[36] T. Yoshida, Y. Oshima and Y. Matsumura, "Gasification of biomass model compounds and real biomass in supercritical water," *Biomass and Bioenergy,* pp. 71-78, 2004.
[37] T. Yoshida and Y. Matsumura, "Gasification of cellulose, xylan, and lignin mixtures in supercritical water." *Ind Eng Chem Res,* vol. 40, pp. 5469-5474, 2001.
[38] G. J. DiLeo, M. E. Neff, S. Kim and P. E. Savage, "Supercritical Water Gasification of Phenol and Glycine as Models for Plant and Protein Biomass." *Energy Fuels,* vol. 22, pp. 871-877, 2008.
[39] G. W. Huber, J. W. Shabaker and J. A. Dumesic, "Raney Ni-Sn Catalyst for H2 Production from Biomass-Derived Hydrocarbons." *Science (Washington, DC, United States),* vol. 300, pp. 2075-2078, 2003.
[40] B. Potic, S. R. A. Kersten, W. Prins and W. P. M. van Swaaij, "A High-Throughput Screening Technique for Conversion in Hot Compressed Water." *Ind Eng Chem Res,* vol. 43, pp. 4580-4584, 2004.
[41] M. Watanabe, H. Inomata, M. Osada, T. Sato, T. Adschiri and K. Arai, "Catalytic effects of NaOH and ZrO2 for partial oxidative gasification of n-hexadecane and lignin in supercritical water." *Fuel,* vol. 82, pp. 545-552, 2003.
[42] M. Watanabe, H. Inomata and K. Arai, "Catalytic hydrogen generation from biomass (glucose and cellulose) with ZrO2 in supercritical water." *Biomass Bioenergy,* vol. 22, pp. 405-410, 2002.
[43] T. Yoshida and Y. Oshima, "Partial Oxidative and Catalytic Biomass Gasification in Supercritical Water: A Promising Flow Reactor System." *Ind Eng Chem Res,* vol. 43, pp. 4097-4104, 2004.
[44] K. C. Park and H. Tomiyasu, "Gasification reaction of organic compounds catalyzed by RuO2 in supercritical water." *Chemical Communications (Cambridge, United Kingdom),* pp. 694-695, 2003.
[45] J. Yanik, S. Ebale, A. Kruse, M. Saglam and M. Yueksel, "Biomass gasification in supercritical water: II. Effect of catalyst." *Int J Hydrogen Energy,* vol. 33, pp. 4520-4526, 2008.
[46] M. J. Antal Jr., S. G. Allen, D. Schulman, X. Xu and R. J. Divilio, "Biomass Gasification in Supercritical Water." *Ind Eng Chem Res,* vol. 39, pp. 4040-4053, 2000.
[47] T. Sato, M. Osada, M. Watanabe, M. Shirai and K. Arai, "Gasification of Alkylphenols with Supported Noble Metal Catalysts in Supercritical Water." *Ind Eng Chem Res,* vol. 42, pp. 4277-4282, 2003.

[48] R. D. Cortright, R. R. Davda and J. A. Dumesic, "Hydrogen from catalytic reforming of biomass-derived hydrocarbons in liquid water," *Nature*, vol. 418, pp. 964-967, 2002.
[49] Y. J. Lu, L. J. Guo, C. M. Ji, X. M. Zhang, X. H. Hao and Q. H. Yan, "Hydrogen production by biomass gasification in supercritical water: A parametric study." *Int J Hydrogen Energy*, vol. 31, pp. 822-831, 2006.
[50] M. Osada, K. Toyoshima, T. Mizutani, K. Minami, M. Watanabe, T. Adschiri and K. Arai, "Estimation of the degree of hydrogen bonding between quinoline and water by ultraviolet-visible absorbance spectroscopy in sub- and supercritical water." *J. Chem. Phys.*, vol. 118, pp. 4573-4577, 2003.
[51] Y. Matsumura and T. Minowa, "Fundamental design of a continuous biomass gasification process using a supercritical water fluidized bed." *Int J Hydrogen Energy*, vol. 29, pp. 701-707, 2004.
[52] P. Kritzer, N. Boukis and E. Dinjus, "The corrosion of nickel-base alloy 625 in sub- and supercritical aqueous solutions of oxygen: a long time study." *J. Mater. Sci. Lett.*, vol. 18, pp. 1845-1847, 1999.
[53] W. Habicht, N. Boukis, G. Franz and E. Dinjus, "Investigation of nickel-based alloys exposed to supercritical water environments." *Microchimica Acta*, vol. 145, pp. 57-62, 2004.
[54] P. T. Moseley, "Fuel cell systems explained, edited by James Larminie, Andrew Dicks." *J. Power Sources*, vol. 93, pp. 285, 2001.

CHAPTER 3
EXPERIMENTAL METHODS

This chapter describes the procedure developed to obtain experimental data in the present work. The experiments were performed in quartz batch reactors. A fluidized sand bath is used for temperature control, and gas samples are analyzed in a gas chromatograph (GC).

3.1 Reactor Preparation

For each experiment, the solid biomass model compound was either cellulose or lignin. Microcrystalline cellulose powder (0.6 g/cm^3, particle size 0.1 wt. % +60 mesh, 70 wt. % +325 mesh*)* and organosolv lignin (0.5 g/cm^3, particle size 5.5 % +40 mesh, 92.4 % +100 mesh) were purchased from Sigma-Aldrich and used as received. Quartz capillary tubes (2 mm ID, 6 mm OD, 18.0 cm length) served as mini-batch reactors. The internal reactor volume was 0.58 cm^3 (calculated from the dimensions given). Deionized water was obtained from Professor Burn's laboratory (3005 Dow). The water is deionized by passing city water through an ion exchange water softener, reverse osmosis, and high capacity ion exchange units. The purified water is then continuously circulated through a system that contains ultra pure ion exchange, UV sterilization, and submicron filtration units [1].

The water was loaded into the reactor before the cellulose/lignin, so its expansion during heating would favor mixing. The water was loaded with 50 μL or 150 μL gas-tight syringes from Fisher Scientific. We used needles 20 cm long to load the water directly at the bottom of the reactors. The biomass was weighed with an analytical balance (American Scientific, B1240-1) and loaded with the aid of a glass funnel. For the non-catalytic experiments, only water and biomass were loaded. For the catalytic experiments, we typically added a metal wire (16 cm long, 0.25 mm diameter). The total surface area

of the catalyst wire was 40 mm^2 (or 125 mm^2/g). Using a catalyst in wire form is appropriate for the geometry of the reactor, because the maximum distance between any particle reacting and the catalyst is the internal diameter. The wire metals tested were copper, iron, nickel, zinc, and zirconium. The wires were purchased from Alfa-Aesar and Sigma-Aldrich, wiped with 320 grit sand paper (3M Imperial Wetordry 413Q sandpaper 9x11 02004) to reduce the amount of oxides on the wire surface, and loaded into the reactors.

The exceptions to this were the ruthenium (purchased from Alfa Aesar) and Raney nickel (Raney 2800 nickel, slurry in water, active catalyst purchased from Sigma Aldrich) catalysts. Ruthenium was a powder (~325 mesh) and Raney-nickel a 50 wt % slurry in water. We calculated the amount of ruthenium needed to be 3.6 mg (for 40 mm2). The idea of using Raney nickel is to verify the effect of a high surface area nickel catalyst that has been reported as an effective catalyst for SCWG. When working with Raney nickel, loading only 40 mm^2 of active nickel is not even possible considering its high surface area. Instead, we based our loading on the amount of water needed for the experiment (43 μl). Therefore, 86 μl of the Raney-nickel slurry were loaded to each reactor. This corresponds to 148 mg of catalyst, with total surface area 1.34x107 mm^2.

The amounts of cellulose and water loaded varied with the reaction conditions to be used. Setting the reaction temperature and pressure fixed the water density. All water densities were obtained from the steam tables. The desired water density and the reactor volume then set the mass of water to be loaded. Finally, the desired biomass loading (wt %) was used to calculate the mass of biomass that should be loaded into the reactor. The water loadings used in these experiments ranged from 0 μl (water density 0.00 g/ cm^3) to 103 μl (0.18 g/cm^3), and the biomass loadings ranged from 0.5 mg (1 wt % loading) to 26.0 mg (33.3 wt.% loading). After being loaded, the reactors were flame sealed. The length and external volume of sealed reactor were measured for the purpose of calculating the yields. The reactor external volume was measured by inserting it into a pipette containing water and measuring water displacement.

3.2 Carrying Out SCWG

SCWG was performed by placing the sealed capillary either in a preheated, isothermal fluidized sand bath (Techne model SBL-2) or in a tube furnace (Type F21100 Tube Furnace from Barnstead Thermolyne). For the sand bath, a Techne model TC-8D temperature controller keeps the temperature constant to within ± 1°C. After the reaction time had elapsed, the reactors were removed from the sand bath/tube furnace and placed in front of a fan for cooling. Reactions were performed for batch hold times ranging from 2.5 to 75 minutes (2.5; 5.0; 10.0; 15.0; 30.0; 45.0; 60.0; and 75.0 minutes). Experiments at 10 minutes were repeated four times to determine representative standard deviations. At other times, 2 replicates were made, unless standard deviations were high, in which case additional replicates were performed. In all cases, mean values are reported.

The heat-up time of the quartz reactors was measured by DiLeo [2]. DiLeo measured the temperature profile with a thermocouple in an open quartz reactor placed in a fluidized sand bath at 600°C, as shown in Figure 3.1. In Figure 3.1, the pressure is a function of temperature and is estimated with steam tables, assuming the water density to be 0.08 g/cm^3. Even though the reactor had no water, DiLeo calculated the heat absorbed by the water during heat up to be less than 4% of the heat absorbed by the quartz itself, being therefore negligible. The heat-up time is about 30 seconds at 600°C. It should be kept in mind, therefore, especially for the shorter experiments (2.5 minutes), that part of the experiment is carried out at non-isothermal conditions.

Quartz is slightly soluble in supercritical water, but at 600°C, only about 0.04 % of the reactor material would be leached out at equilibrium [3]. Dissolution of quartz, if occurring, did not compromise the structural integrity of the reactors. Di Leo [1] showed that SCWG of formic acid at 600°C for several hours led to experimental gas yields that agreed well with yields expected at equilibrium. This agreement indicates that the reactors maintained their structural integrity (no microcracks or gas leaks).

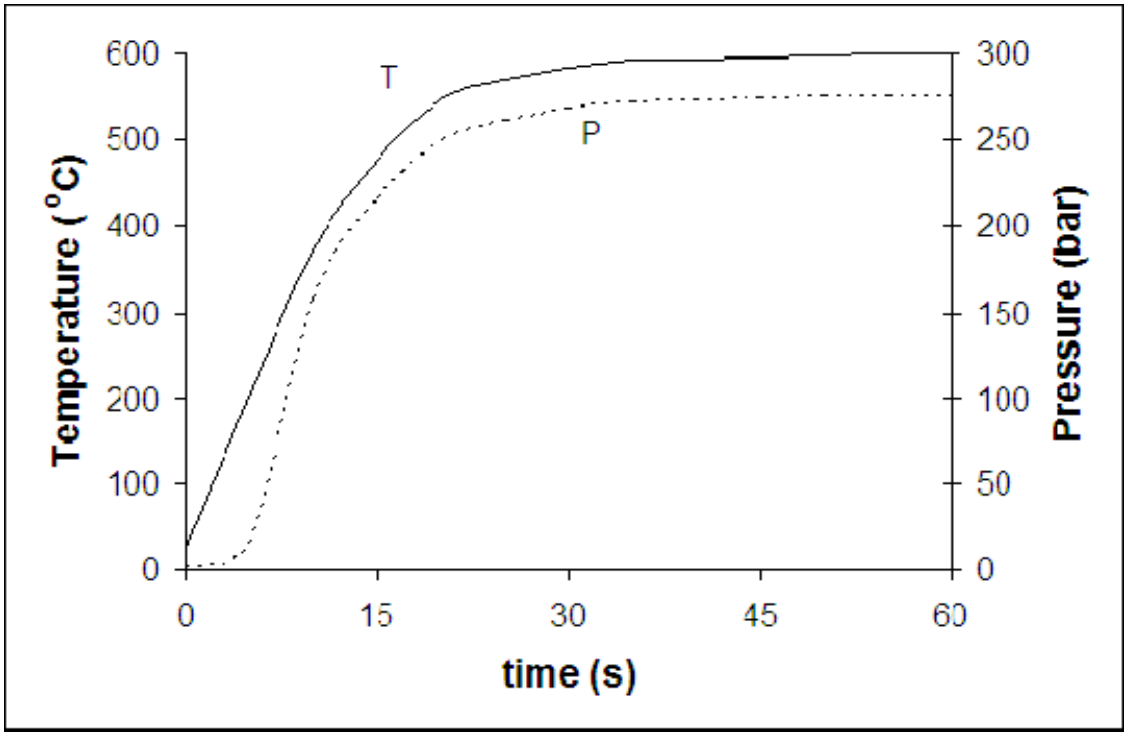

Figure 3.1. Temperature profile for the quartz reactors [1].

3.3 Experimental Conditions

For cellulose, we arbitrarily designate SCWG at 500°C, 9.0 wt. % biomass, and 0.08 g/cm^3 water density (22 MPa) as the base case. From this starting point, we varied one parameter at a time to evaluate its effect on the gas yields and composition. We considered temperatures of 365 °C (to evaluate yields at subcritical conditions), 400, 500, and 600°C, biomass loadings of 1.0, 5.0, 9.0 and 33.3 wt %, and water densities of 0.00 (no water), 0.05, 0.08 and 0.18 g/cm^3. For lignin, all conditions except temperature are identical. We observed very low gas yields at the lowest temperature (400°C), and for this reason the base case temperature was switched to 600°C (27 MPa water partial pressure). The other temperatures used for lignin were 500°C and 725°C.

At some of the high-temperature, high-density, and high biomass loading conditions evaluated, reactors consistently burst at the longer reaction times. For these conditions, results could be obtained only for the shorter times (for instance, for cellulose, data could only be obtained up to 30 min). In general, we attempted to perform experiments for residence times as long as possible. Table 1.1 summarizes the experimental conditions used.

Table 1.1. Experimental Conditions.

	T (°C)	**biomass wt. %**	**Water Density (g/ml)**
Base Case	500 (cellulose) / 600 (lignin)	9.0	0.08
Low Temperature	400 (cellulose) / 500 (lignin)	9.0	0.08
High Temperature	600 (cellulose) / 725 (lignin)	9.0	0.08
Subcritical Temperature	365	9.0	0.08
Lowest Biomass Loading	500 (cellulose) / 600 (lignin)	1.0	0.08
Low Biomass Loading	500 (cellulose) / 600 (lignin)	5.0	0.08
High Biomass Loading	500 (cellulose) / 600 (lignin)	33.3	0.08
Low Water Density	500 (cellulose) / 600 (lignin)	9.0	0.05
High Water Density	500 (cellulose) / 600 (lignin)	9.0	0.18
Pyrolysis	500 (cellulose) / 600 (lignin)	100.0	0.00

3.4 Gas Sample Analysis

To collect the gases formed during SCWG, the cooled quartz reactor was first inserted into a 1/2-in x 20 cm long metal tube, which is sealed with a 1/2-in cap at one end and has a valve at the other. The tube was then connected to a helium cylinder, pressurized to 10 psi, and removed from the cylinder. The helium provides the driving force needed to push the gas sample out of the tube for GC analysis. Next the metal tube was struck sharply to shatter the quartz reactor within and release the product gases into the helium-filled metal tube.

The metal tube was then connected to a gas sampling valve on a 5890 Series II Hewlett Packard gas chromatograph (GC) with a thermal conductivity detector (TCD) equipped with a HP model 3394A integrator. The employed column was a 10-ft x 1/8-in O.D. stainless steel tube packed with 100/200 mesh Supelco Carboseive S-II. We used argon as the carrier gas, because helium was used to pressurize the metal tube. This way we could quantify the helium used to pressurize the metal tube. Also, argon gives positive peaks for H_2 on the TCD. The GC was operated with a temperature program of 35°C for 5 minutes, then increased to 225°C at a rate of 20°C/min, and held at 225°C for 5 minutes. The GC separates and detects H_2, O_2, N_2, CO, CO_2 and CH_4. Prior to the analysis of reaction products, the GC was calibrated with ten commercial gas standards containing the components of interest in the range of concentrations observed during experiments. N_2 (present from the residual air in the reactor and metal tube) served as a standard during the gas analysis. Knowing the amount of N_2 present and then determining its mole fraction from the GC allowed us to calculate the number of moles of all other gases present. More details will be provided later in this chapter.

3.5 Calculations

The first step in our calculations was to verify whether the results obtained experimentally were within the expected bounds based on the theoretical calculations. We defined a range of possible molar % of N_2 that should originate from air in the samples. For example, if we have no gas formation in the reactor, based on the amount of helium used to pressurize the metal tube, the N_2 molar % should be 76 %. This is the maximum possible molar % of N_2. Any formation of gas from SCWG should decrease

this percentage. The minimum molar % of N_2 should be observed when there is maximum yield of gases formed from SCWG. To calculate this amount, we assumed the biomass reacts completely with water via a typical steam-reforming reaction, producing CO_2 and H_2. The resulting mole % depends on the specific experimental condition. For instance, for cellulose at the base case, the minimum molar % of N_2 obtained should be 44 %. In other words, we expected these reactors to show a N_2 molar % in the range 44 – 76.0 %. The vast majority of the reactors showed N_2 molar % within the acceptable range. In few cases this was not observed, and these experiments were neglected.

The next step is actually calculating the gas yields. The GC analysis provides only the gas composition. The absolute amount of each component present in the gas phase was calculated using N_2 (from air initially in the reactor, the metal tube and cylinder connections) as an internal standard. Since the amount of N_2 from air is known (and it does not react during gasification), and the molar ratio of any gas to N_2 is determined experimentally from the GC analysis, the yields in mmol gas/g of biomass for each gas species can be calculated. The volume of air in the tube is the sum of the air initially inside the reactor and the air between the external wall of the reactor and internal wall of the metal tube. Each of these is given as follows:

volume of air inside quartz reactor = internal volume of reactor – water volume – biomass volume – wire volume (when added)

volume of air outside reactor = volume of metal tube – external volume of reactor

Besides these two components, there is also air coming from the connections that go from the metal tube to the regulator of the helium gas cylinder during pressurization, and this has to be taken into account. The internal volume of the metal tubing is 15.1 ml, and the internal volume of the connections mentioned is 6.0 ml (total volume 21.1 ml). Given the experimental setup, one could wonder if, during consecutive runs, the lines will be completely filled with air, or if helium can remain in the line and contaminate the following sample. The total length of the connections is 28.4 cm (1/4-in ID), and the diffusivity coefficient of He in air is 7.20×10^{-5} m^2/s [4]. Using Fick's Law, we estimate that all the helium diffuses out of the line in 12.5 minutes. Since the minimum interval between consecutive gas analyses is 45 minutes, we are assuming the line to be completely filled with air for every analysis. As experimental confirmation of this

finding, we performed a series of GC analysis using the metal tube without a glass reactor inside. The metal tube, initially filled only with air, was connected to the helium cylinder and pressurized with 10 psi. 45 minutes later, the mixture was analyzed in the GC. The procedure was then repeated, to verify if potential helium contamination of the line changed results. Based on the dimensions of the tubing/connections, we estimated the composition of this gas to be 65.7 % N_2, 17.5 % O_2, and 16.8 % He in a molar basis. Experimentally, we obtained 70.2 ± 0.0 % N_2, 18.3 ± 0.1 % O_2, and 11.4 ± 0.1 % He. The agreement between the calculated and experimental compositions suggests that our volume estimates are close to the real values. Also, the very small standard deviations for consecutive analysis of the gas sample suggest no contamination of the line with helium from the previous sample.

The product gases from SCWG, especially CO_2, are partially soluble in water. To account for this, we applied Henry's Law to the reactor (equation 3.1) :

$$k_H = \frac{c_a}{P_g} \tag{3.1}$$

Where k_H is Henry's constant at temperature T (M/atm), P_g is the partial pressure of the gas species (atm) and c_a is the concentration of the gas species dissolved in water (M). P_g is known for each gas species from GC information and assumption of ideal gas behavior. k_H for each species is shown in Table 3.1. Table 3.1 shows data collected from the literature [5] for this purpose.

Table 3.1. Henry's Constants at 25°C.

Species	**k_H (M/atm)**
O_2	1.3×10^{-3}
H_2	7.8×10^{-4}
N_2	6.5×10^{-4}
He	3.8×10^{-4}
Ar	1.4×10^{-3}
CH_4	1.4×10^{-3}
CO	9.5×10^{-4}
CO_2	3.4×10^{-2}

k_h for each gas can be used to calculate c_a with Henry's Law, leading to information about the number of moles of each gas dissolved in water. Results indicated, though, that the amount of gas dissolved in water was negligible relative to the amount in the gas phase, even for CO_2.

3.6 Problems with Gas Analysis

Figure 3.2 shows typical results when analyzing the same gas sample (lignin, base case, 10 min) from the metal tube for 3 consecutive times. The first sample is injected immediately after breaking the glass reactor tube. The second sample is injected when the GC is ready for the next run, 45 min later. The third and last sample is injected 90 minutes after breaking the reactor.

The pattern shown here is observed with every other sample we ran multiple times. The yields from the sample injected immediately after breaking the glass reactor are always lower, because of poor mixing of the gases within the metal tube. Based on these results, we decided to wait 45 minutes after shattering the reactor before the injection of each sample.

Another possible problem for gas analysis was the contamination of the metal tube with traces from previous samples, when analyzing multiple samples on a day. To avoid this contamination, we always flushed the metal tube with air for five minutes before placing another reactor in it. We tested this cleaning method by analyzing gas samples without reactors (only air and 10 psi of helium), and observing no contamination.

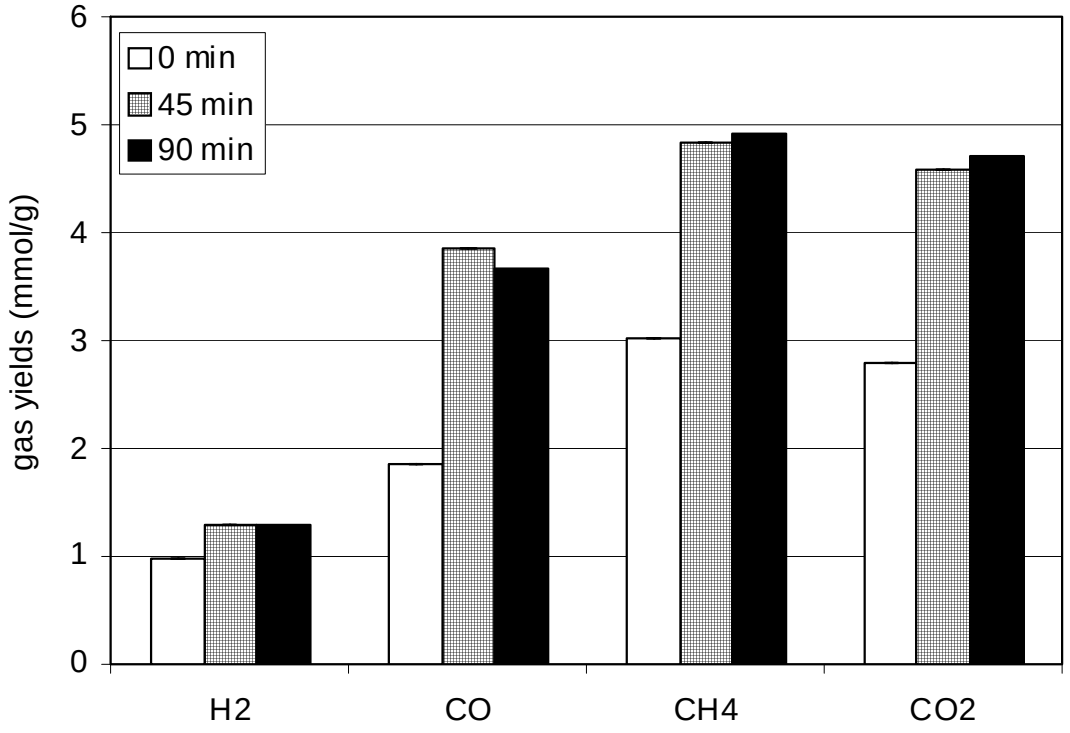

Figure 3.2. Consecutive analysis of the same sample (lignin, 600°C, 0.08 g/ml, 9.0 wt %, 10 min).

3.7 Effect of the Heating Rate

For most of the experiments performed in this work, the fluidized sand bath was used to control temperature. The sand bath provides uniform conditions for temperatures that can be as high as 600°C. However, for lignin experiments we had to go to 725°C, which the sand bath cannot reach. For these experiments, we used a F2100 type Tube Furnace from Barnstead International. Heating rates in fluidized systems like a sand bath could be higher than in systems like a tube furnace. To determine what influence this difference has on gas yields, we performed base case experiments for lignin (10 min) in both the sand bath and the tube furnace. Figure 3.3 shows a comparison of results for the two heaters.

There is little difference between the yields obtained in the tube furnace and the ones from the sand bath. If it was possible to go as high as 725°C with the sand bath, we would expect differences in heating rates between the two devices to be even smaller. For these reasons, we believe results from the sand bath and the tube furnace can be directly compared.

3.8 Effect of Oxygen

The presence of air inside the quartz rectors raised the question of whether the O_2 from air can influence gas yields by promoting combustion reactions. To evaluate the effect of O_2, we conducted a set of experiments where we purged the air from the reactors with a different gas, immediately before sealing. We injected the purge gas at the bottom of the reactor with a gas-tight syringe. The volume injected was 5 ml, 10 times the volume of the reactor. The purge gas to be injected was collected from a glass tube (through a septum) connected to a gas cylinder. In one of the cases, the purge gas was pre-purified argon, so that no residual O_2 is left inside the reactor. In the other case, the purge gas was O_2, so that the gas phase would be enriched in oxygen. The results are shown in Figure 3.4.

There is no clear difference between the experiments regardless of the % of O_2 left in the reactor. The results agree with expectations, since even when the entire reactor

is filled with O_2, only 8.3 % of the stoichiometric amount is available for combustion. When air is present, this percentage drops to 1.7 %. Also, if all the O_2 present in the reactor is consumed for combustion, 1.0 mmol/g of CO_2 would be formed as a result. In conventional gasification, for instance, typically 25 % of the stoichiometric amount required for complete combustion is present [6, 7]. We are therefore neglecting the effect of O_2 in our experiments.

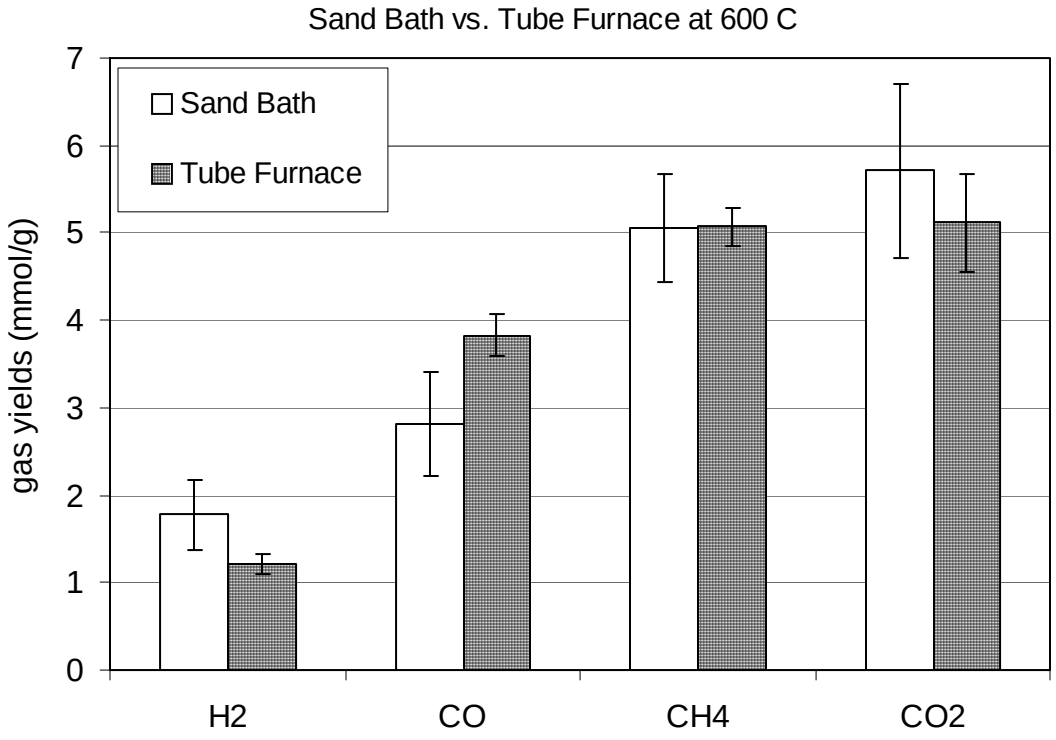

Figure 3.3. Comparison between Sand Bath and Tube Furnace (600°C, 0.08 g/ml, 9.0 wt %, 10 min).

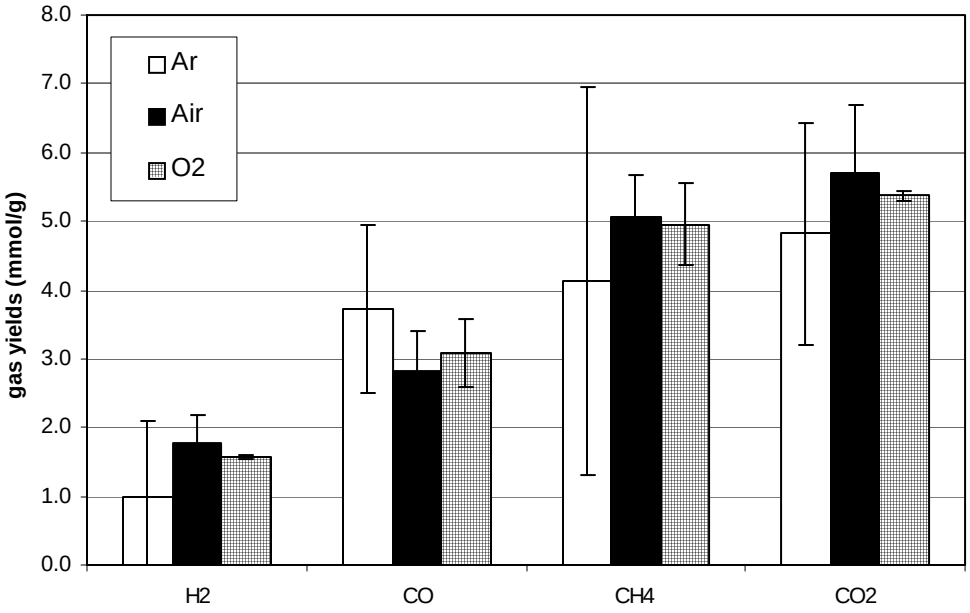

Figure 3.4. Effect of O_2 on the gasification of lignin (600°C, 0.08 g/ml, 9.0 wt %, 10 min).

REFERENCES

[1] S.E. Hunter, “Acid-Catalyzed Organic Synthesis in Carbon Dioxide-Enriched High Temperature Water”, 292 pp., 2005.

[2] G. J. Dileo, "Gasification of biomass model compounds in supercritical water." pp.114, 2007, PhD Thesis, University of Michigan, Ann Arbor.

[3] R. O. Fournier, "An equation correlating the solubility of quartz in water from 25.degree. to 900.degree.C at pressures up to 10,000 bars." *Geochim. Cosmochim. Acta*, vol. 46, pp. 1969-1973, 1982.

[4] Y. A. Cengel, “Heat Transfer. A practical approach”, 2nd ed., McGraw-Hill, New York (1998).

[5] R. Sandler, "Compilation of Henry's Law Constants for Inorganic and Organic Species of Potential Importance in Environmental Chemistry (Version 3)," 1999.

[6] Dutch Gasification Site, “Gasification, a substitute of ECN”, http://www.vergassing.nl/main.html, 01/09/08.

[7] DESI Power Technologies, “Biomass Gasification”, http://www.desipower.com/technology/biomass.htm, 01/09/08.

CHAPTER 4
NON-CATALYTIC GASIFICATION OF CELLULOSE IN SUPERCRITICAL WATER

This chapter presents the results of experimental work for the gasification of cellulose powder in quartz reactors. This is the first study involving SCWG of cellulose in non-metal reactors, in such a way that catalysis from metal reactor walls is avoided. We start by presenting results obtained at the base case conditions (500°C, 0.08 g/ml water density and 9.0 wt %) until 30 minutes of gasification. We then discuss the effects of experimental conditions on SCWG. We varied temperature, biomass loading and water density. Lastly, we compare experimental data in quartz reactors to experiments performed at the same conditions in stainless steel reactors, in order to gain insight on the effects from the reactor material of construction.

4.1 Introduction

Table 4.1 summarizes previous work on cellulose SCWG in the absence of an added catalyst. Most previous work considered a single temperature, water density, biomass loading, and reaction time. The focus in these earlier studies was often on the effect of different catalysts on SCWG. These previous studies make it difficult to learn the effects of the process variables. This chapter provides results for the first systematic study of the effects of temperature, biomass concentration, water density, and reaction time on cellulose SCWG.

The work presented here is also unique because it is the first to report SCWG of cellulose in a metal-free reactor. We used quartz capillary tubes as mini batch reactors. Previous studies with no added catalyst have been performed in stainless steel reactors. The internal walls of these reactors catalyze some of the reactions in SCWG, so at this moment it is not clear how much influence the metal catalyzed reactions have on the product yields. DiLeo and Savage [9] and Kersten et al. [10] report on SCWG of simple

compounds in quartz reactors, and the two studies show that gas yields are strongly influenced when a metal catalyst is added to the system. One of our motivations for the present work was to obtain results for cellulose gasification in SCW that would be attributable exclusively to non-catalytic reactions. This information would be very useful for subsequent evaluation of different catalysts, because the non-catalytic contribution could be subtracted out and the effect of the catalyst alone can be more clearly seen.

Table 4. 1. Summary of Previous Research on SCWG of Cellulose (all in stainless steel reactors). (NR = Not Reported)

Reference	Temp	Water Dens. (g/cm^3)	Cellulose	Time (min)
Yoshida, Matsumura[1]	400	0.166	NR	20
Watanabe et al.[2]	400, 440	0.2, 0.35	4.8	10, 15
Williams, Onwudilli [3]	380	0.2	5	up to 120
Osada et al.[4]	400	0.33	5	up to 180
Minowa et al.[5, 6]	400	0.05	20, 40	60
Hao et al.[7]	up to 650	up to 0.094	10	20
Lu et al.[8]	500	0.071	9	20

We arbitrarily designate SCWG at 500°C, 9.0 wt. % biomass, and 0.08 g/cm^3 water density (22 MPa) as the base case. From this starting point, we varied one parameter at a time to evaluate its effect on the gas yields and composition. We considered temperatures of 365 (to evaluate yields at subcritical conditions), 400, 500, and 600°C, biomass loadings of 5.0, 9.0 and 33.3 wt %, and water densities of 0.00 (no water), 0.05, 0.08 and 0.18 g/cm^3.

4.2 Results and Discussion

Sasaki et al. [11] showed that cellulose is completely converted in water at 350 °C and 25 MPa after only 4 s. We are interested in gas formation, however, and not only the disappearance of the reactant. Once the cellulose is quickly consumed, it forms intermediates that take longer to decompose and form gases. These gases can also react further among themselves, changing the product distribution.

Visual observation of the quartz reactors after SCWG experiments indicates the presence of char (a black residue adhering to the reactor internal walls) in all cases. The

char strongly adhered to the quartz, making it impossible to collect samples in enough quantity for analysis.

As a reference for our discussion and results, we suggest a reaction scheme, based on literature information [2, 4, 6, 12-14] that accounts for the main solid and liquid-phase reactions and focuses on the main routes for gas formation. We use the following scheme to describe cellulose SCWG. $C_xH_yO_z$ indicates generic intermediate species resulting from glucose decomposition.

Cellulose Hydrolysis: $(C_6H_{10}O_5)_n + n\ H_2O \rightarrow n\ C_6H_{12}O_6$

Glucose Decomposition: $C_6H_{12}O_6 \rightarrow C_xH_yO_z$

Steam-reforming I: $C_xH_yO_z + (x\text{-}z)\ H_2O \rightarrow x\ CO + \left(x - z + \frac{y}{2}\right) H_2$

Steam Reforming II: $C_xH_yO_z + (2x\text{-}z)\ H_2O \rightarrow x\ CO_2 + \left(2x - z + \frac{y}{2}\right) H_2$

Intermediate Pyrolysis (to form CO): $C_xH_yO_z \rightarrow CO + C_xH_yO_z$

Intermediate Pyrolysis (to form CO_2): $C_xH_yO_z \rightarrow CO_2 + C_xH_yO_z$

Intermediate Pyrolysis (to form CH_4): $C_xH_yO_z \rightarrow CH_4 + C_xH_yO_z$

Intermediate Pyrolysis (to form H_2): $C_xH_yO_z \rightarrow H_2 + C_xH_yO_z$

Char formation through intermediates: $C_xH_yO_z \rightarrow w\ C + C_{x\text{-}w}H_yO_z$

Water-Gas Shift: $CO + H_2O \leftrightarrow CO_2 + H_2$

Methanation: $CO + 3\ H_2 \leftrightarrow CH_4 + H_2O$

Chapter 6 deals with this model in greater detail when using it to fit the rate constants to base case results. The reaction scheme does not include combustion via residual air in the reactor because as shown in Chapter 3 (Experimental Methods), this amount of oxygen is not enough to play a significant role on the gasification yields.

4.2.1 Base Case Results

We first present results for the base case conditions (500 °C, 0.08 g/cm^3, 9.0 wt% cellulose), and then proceed to analyze how changes in reaction parameters affect the results. Figure 4.1 shows the temporal variation of the molar composition (dry basis) of the gases formed for the base case. The error bars in all the figures represent the standard

deviation. The lines in the graphs connecting experimental data points are intended only to help the reader see the trends. CO_2 and CO are the major products initially, with CO_2 constituting about 50 % of the gas, and CO 35 %. CO_2 remains the major product at all times and its mole % remains stable at all times examined. The mole % of CO, which is a highly undesirable component for some applications (e.g., PEM fuel cells), appears to decrease after the initial 2.5 minutes. The mole % of H_2 appears to slightly increase with time, as does the mole % of CH_4. Figure 4.1 also shows equilibrium compositions, calculated by ASPEN Plus. We used the RGibbs reactor block in ASPEN. This block calculates equilibrium concentrations without requiring knowledge of reaction stoichiometry, by minimizing the Gibbs free energy. For properties calculation, the UNIQUAC method was used. Our starting material for the calculation is glucose. The feed contains cellulose and water in the same initial compositions as the base case. The product can contain glucose, water, CO, H_2, CO_2 and CH_4. The pressure was set to 22 MPa.

The equilibrium H_2 molar % (29.5 %) and CH_4 molar % (27.8 %) are twice as high as the experimental molar % of these species at 30 minutes. The CO_2 molar % in equilibrium (42.4 %) is smaller than the experimental value, and the equilibrium CO molar % is much smaller than the experimental one. Considering the slow change in molar % as function of time for all gases, it seems the system is far from reaching equilibrium.

Figure 4.2 shows the yields of CO, CO_2, CH_4, and H_2 as a function of time for cellulose SCWG at the base case conditions. The yield of CO_2 appears to increase during the first five minutes, and then its yield is relatively stable at about 6.0 mmol/g, until it increases again to 8.4 mmol/g at 30 minutes. CO_2 can be formed from steam-reforming, pyrolysis of intermediate compounds, and from water-gas shift. During the first minutes, the rate of CO formation is high. Therefore water-gas shift does not appear to be a dominant reaction at this point. Instead, pyrolysis of intermediates could be taking place, forming both CO and CO_2.

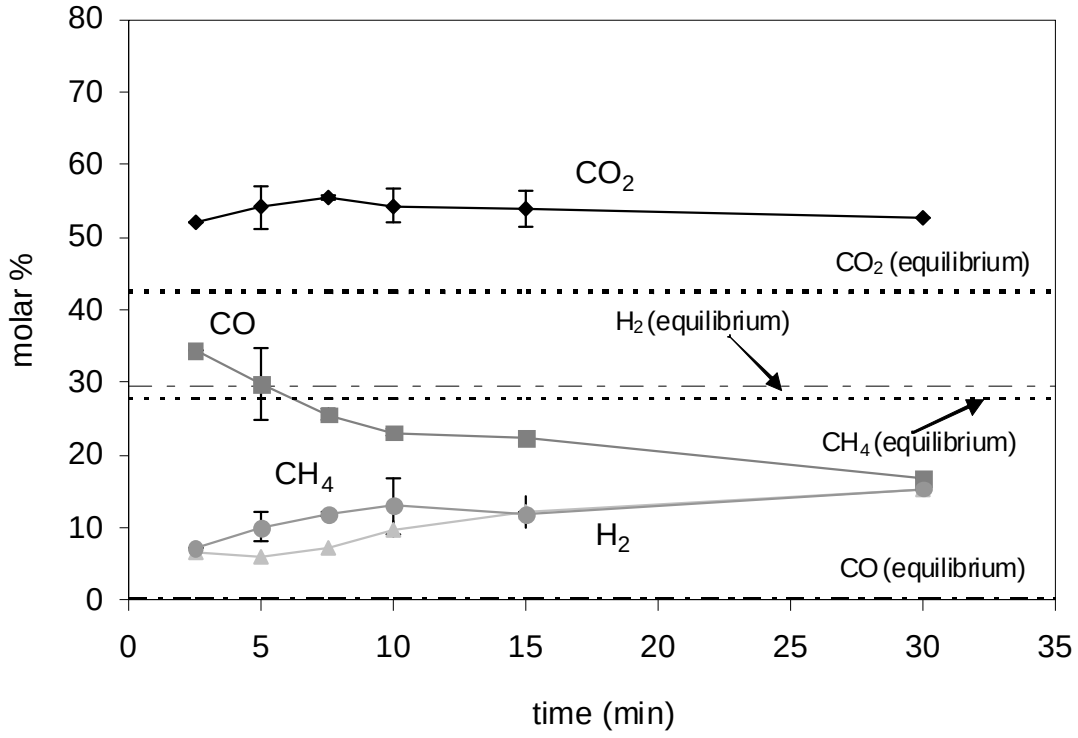

Figure 4.1. Temporal variation of gas composition (base case).

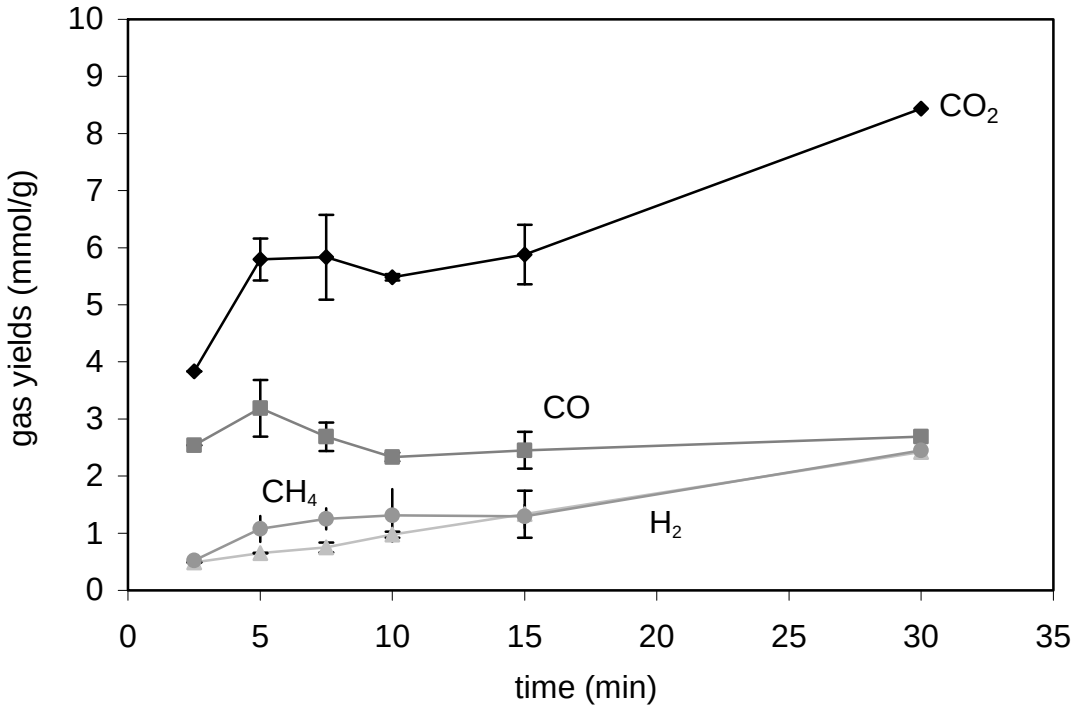

Figure 4.2. Temporal variation of yields (mmol/g) of CO, CO_2, H_2, and CH_4 (base case).

The yield of CO remains stable at about 2.5 mmol/g after 5 minutes. In our reaction scheme, CO is formed by steam reforming and decomposition of intermediate, and later consumed by water-gas shift and methanation. The CO initially formed drives the rate of these reactions.

Small amounts of H_2 and CH_4 are detected at 2.5 minutes. H_2 can be formed from steam-reforming, intermediates and water-gas shift. CH_4 formation can be a result of methanation and decomposition of the intermediate.

In gasification systems, several quantities are normally used to provide an assessment of the overall gasification efficiency. The total gas yield is defined as the sum of the masses of all the gas products (CH_4, H_2, CO, and CO_2 in our case) divided by the mass of cellulose loaded into the reactor. This quantity measures how much of the cellulose was converted into gases. Similarly, the H, C, and O yields are the percentages of the total mass of H, C, or O atoms from the initial cellulose that appear in the product gases. This information is important for estimating the potential to make certain products via further processing of the gases. For instance, if the main goal is to produce H_2, and the H_2 yields are relatively low but the H yield is high (because of a high CH_4 content), this goal can still be achieved by converting the H atoms in CH_4 to H_2.

Another important definition is the energy content of the gas (%). This can be defined as the Lower Heating Value of the product gas (the mole fraction weighted averages of the LHVs for CH_4, H_2 and CO) relative to the LHV of the original feedstock (cellulose in our case). The energy content of the gas is largely influenced by the yields of CH_4 obtained (0.80 MJ/mol). H_2 (0.24 MJ/mol) and CO (0.28 MJ/mol) influence the energy content the LHV to a much smaller extent than CH_4.

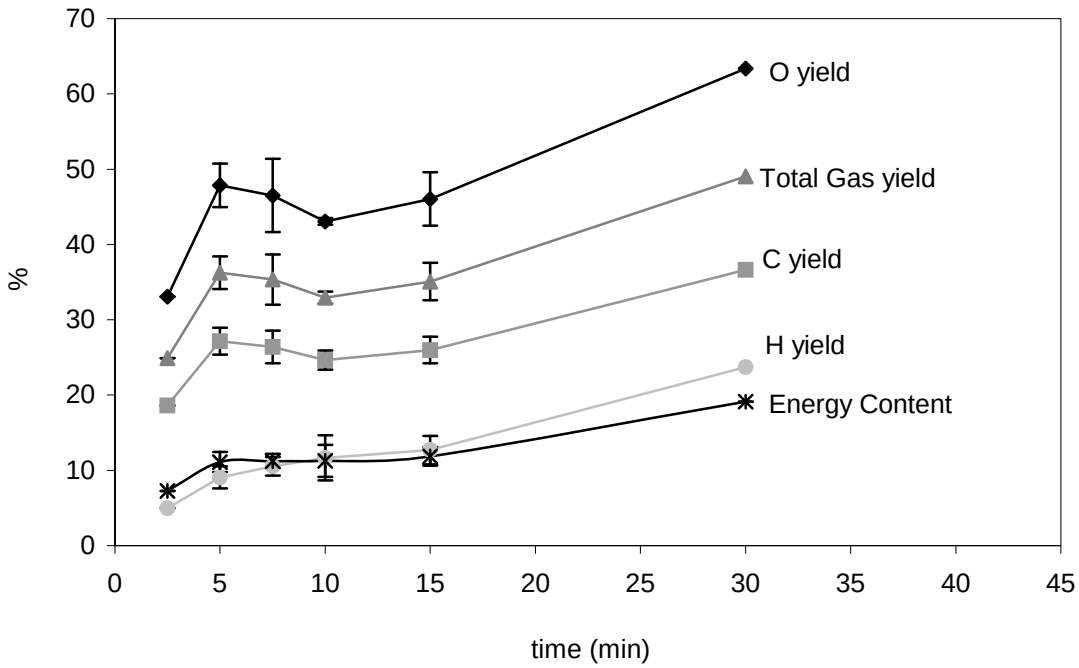

Figure 4.3. Temporal variation of C, H, O and total gas yields (base case).

Figure 4.3 shows the total gas yield, the energetic content and the H, C, and O yields for the base case conditions. 25.0 wt % of the cellulose is converted into gases in the first 2.5 minutes. This conversion increases in the first 5 minutes to about 35 %, after which the yield remains approximately stable, only increasing again at 30 minutes to 49.0 %. Since the most abundant product gas is CO_2, the C yield follows a trend similar to that species. The O and H yields also increase with time. The O yield is 63.4 % after 30 minutes, and the H yield is 23.7 %. The energy content of the gas remains almost constant at 11 % until 30 minutes, when it increases to 19.1 %. For comparison, if we assume cellulose completely undergoes steam-reforming producing H_2 and CO_2, the energetic content would be 103.4 %. For steam-reforming producing H_2 and CO, the energetic content would be 112.3 %.

4.2.2 Effect of Temperature

The effect of temperature was evaluated by keeping the cellulose loading and water density fixed at the base case values (9.0 wt% and 0.08 g/cm^3) and running experiments at 365, 400, 500, and 600 °C.

Figure 4.4 shows the effect of temperature on the composition of the product gas at 5 minutes. As temperature increases, the mole fractions of H_2 and CH_4 increase, the mole fraction of CO goes through a maximum, and the mole fraction of CO_2 decreases. H_2, CO and CH_4 are gases we wish to produce because of their economic importance, while lower mole fractions of CO_2 are interesting from an environmental point of view. The H_2 mole % at 600°C is about 5 times larger than it is at 365 °C, and a similar increase is observed for CH_4.

Figure 4.5 shows the effect of temperature on the C, H, O and total gas yield. In general, the yields increase with temperature, and there is a particularly large jump from 400°C to 500°C. The reactions that consume solids and liquids (such as pyrolysis and steam-reforming) must have their rates increased to provide the results we observe. The increase in H and O yields is impressive at 600°C, especially considering the short reaction time (5 minutes). The results in Figure 4.5 clearly show that temperature can be used to increase gas yields from SCWG of cellulose.

Figure 4.6 shows how the molar yields of individual gases are affected by changes in temperature. The effect of temperature is similar for all species. Yields for all gases are lowest at 365°C. The major effect of temperature is to accelerate the rates of steam-reforming and decomposition of intermediates into gases. This effect is very important above 500 °C. A large increase in yield occurs when going from 500 to 600 °C. The CO_2 yield at 600°C and 5 minutes (7.3 mmol/g) is twice as big as the ones at the lower temperatures. After 5 minutes, the yield of H_2 is more than 4 times higher at 600 °C than at 500°C, reaching 2.9 mmol/g. CH_4, which is barely produced at 400 °C, reaches 2.8 mmol/g at 600 °C.

4.2.3 Effect of Cellulose Loading

The second parameter we varied to determine its effect on gas production was the loading of cellulose. From an engineering perspective, one desires to process biomass/water mixtures with as high a biomass content as possible. Doing so would reduce the capital and operating costs for a SCWG process. For cellulose, a stoichiometric mixture with water would be 56.25 wt% (if the final products were CO_2 and H_2). We used 5.0 wt % and 33.3 wt % cellulose mixtures in addition to the 9.0 wt % loading used in the base case, therefore water was always present in excess. The temperature (500 °C) and water density (0.08 g/cm^3) remained at their base case values.

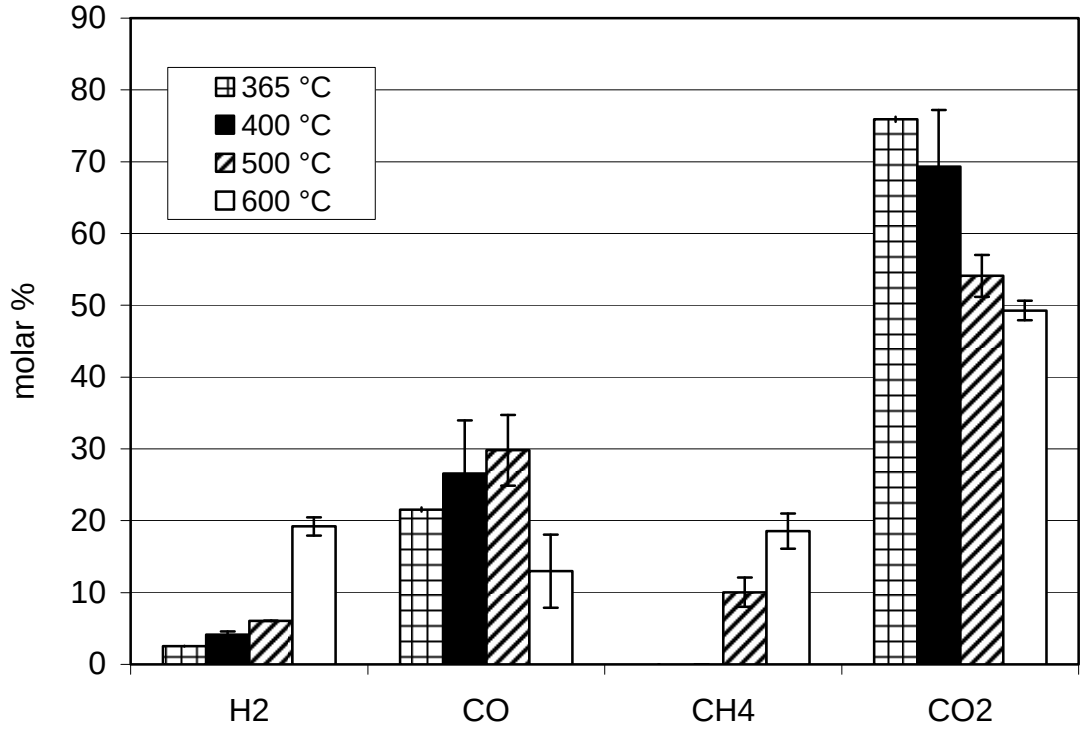

Figure 4.4. Gas composition at 5 minutes as function of temperature (9.0 wt % loading, 0.08 g/ml water density).

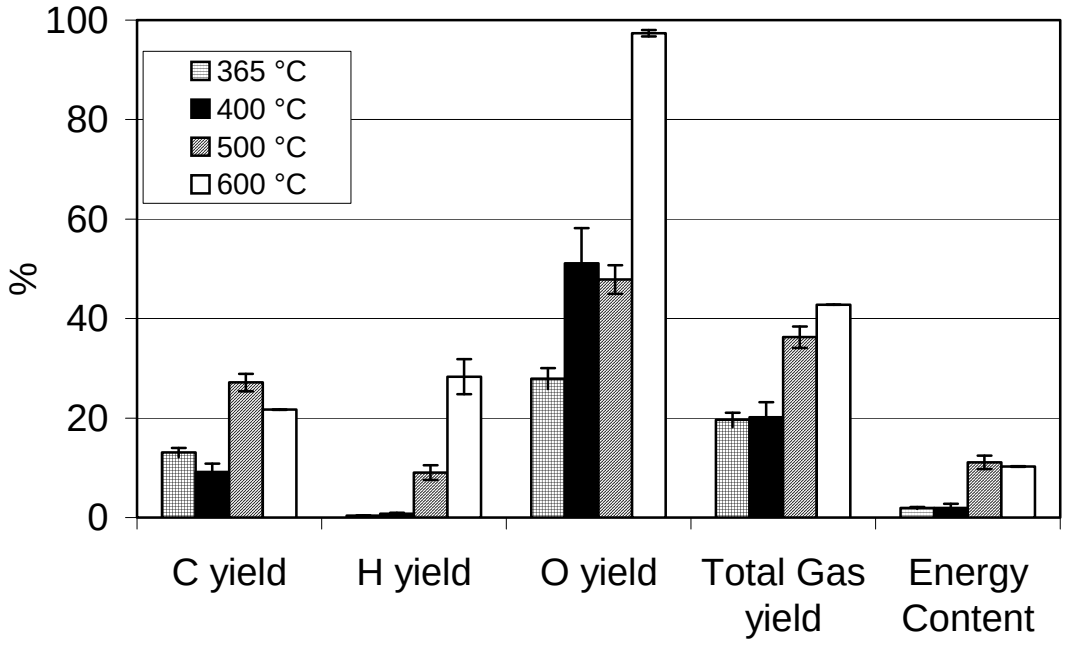

Figure 4.5. C, H, O and total gas yields at 5 minutes as a function of temperature (9.0 wt % loading, 0.08 g/ml water density).

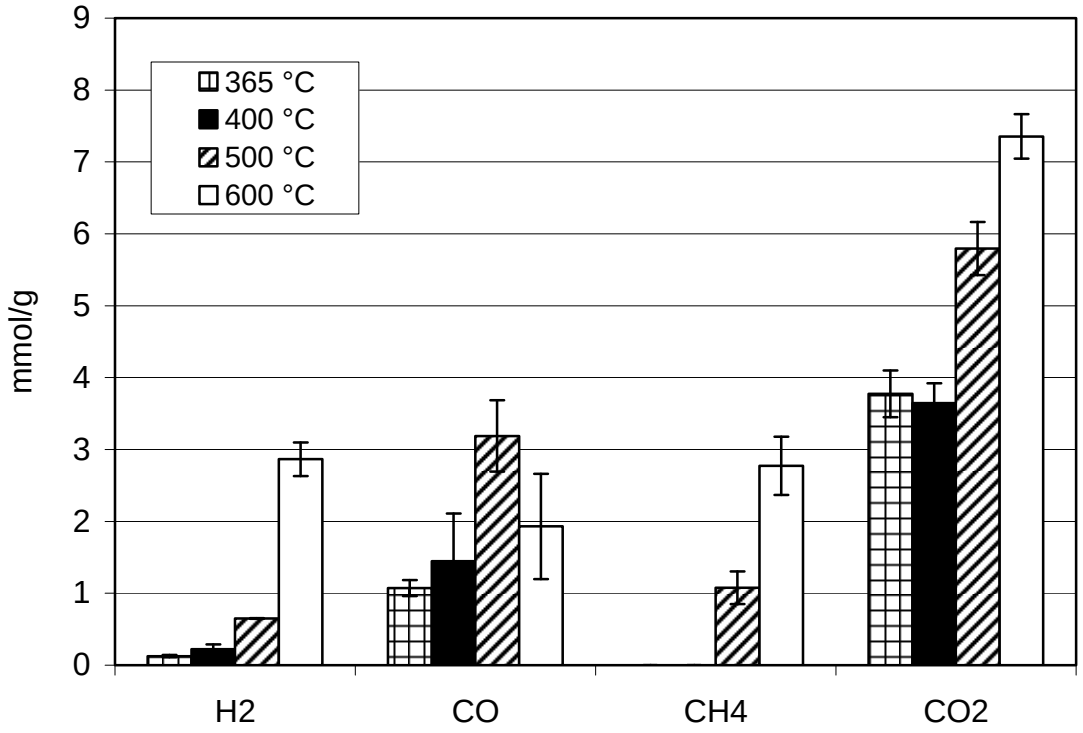

Figure 4.6. Gas yields at 5 minutes as function of temperature (9.0 wt % loading, 0.08 g/ml water density).

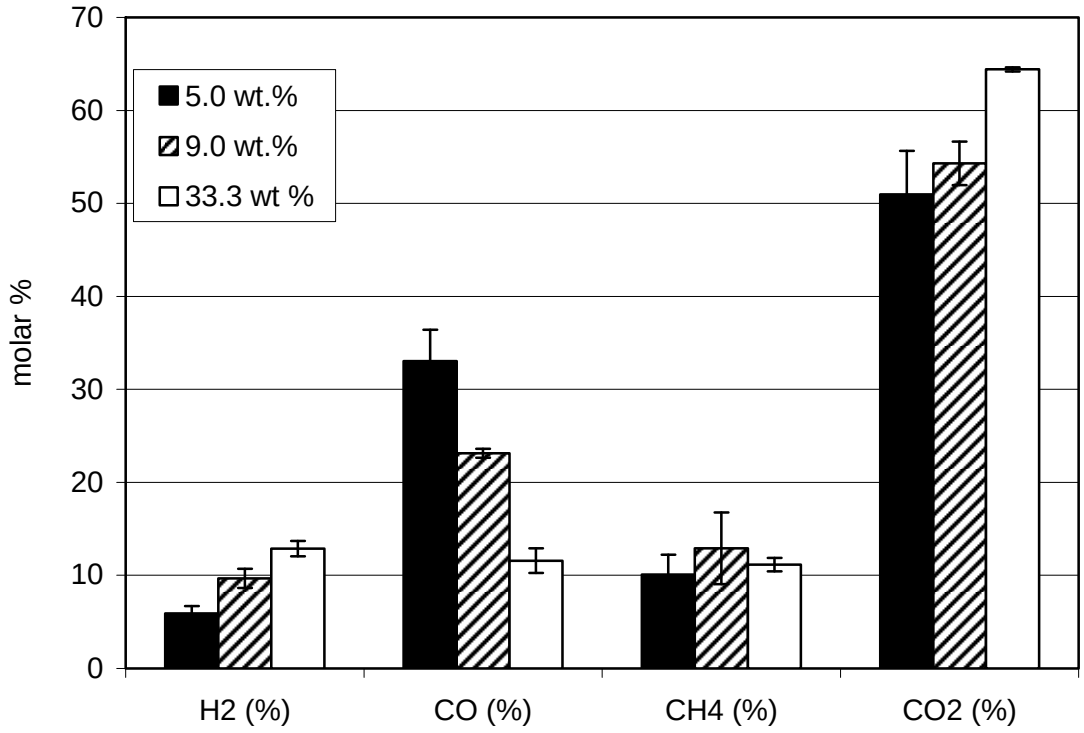

Figure 4.7. Gas composition at 10 min as function of cellulose loading (500°C, 0.08 g/ml water density).

Figure 4.7 shows how the composition of the gas is affected by the cellulose loading. Experiments at low loadings (5.0 wt %) seem to strongly favor the formation of CO. Increasing the loading to 9.0 wt.% and to 33.3 wt % significantly reduces the mole fraction of CO. The CO_2 mole fraction increases with cellulose loading at 33.3 wt %. The H_2 mole fraction also increases with concentration. This is important information because higher loadings are an important aspect for the commercial viability of SCWG.

Figure 4.8 shows the effect of cellulose loading on the yields of C, H, O, energetic content, and total gas at 10 minutes. The data show that the yields are largely independent of the cellulose loading. At all loadings, the C yield is about 25 %, the H yield about 10 %, the O yield about 42 % and the total gas yield about 33 %. The energy content of the gas remains at about 10 %.

Figure 4.9 shows the molar yields of all gases as a function of cellulose loading. The cellulose loading is not a powerful variable to increase gas yields, as was the case for temperature. While CH_4 and CO_2 remain nearly constant at the range of cellulose loading studied, the most noticeable effects are a slight increase in H_2 yield and the decrease in CO yield from about 3.0 mmol/g at 5.0 wt % to about 1.0 mmol/g at 33.3 wt %. Given that changes in the cellulose loading affect only H_2 and CO, the cellulose loading can be used to change the selectivity to the different products. Higher loading will shift the selectivity towards H_2 at the expense of CO.

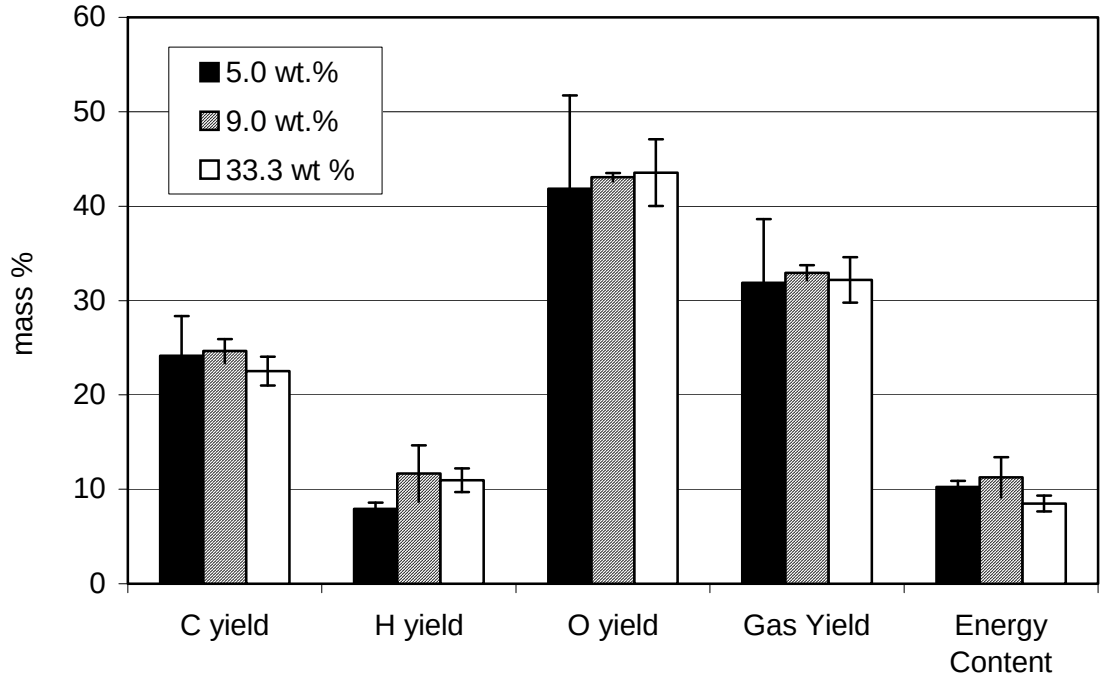

Figure 4.8. C, H and O yields at 10 min as function of cellulose loading (500°C, 0.08 g/ml water density).

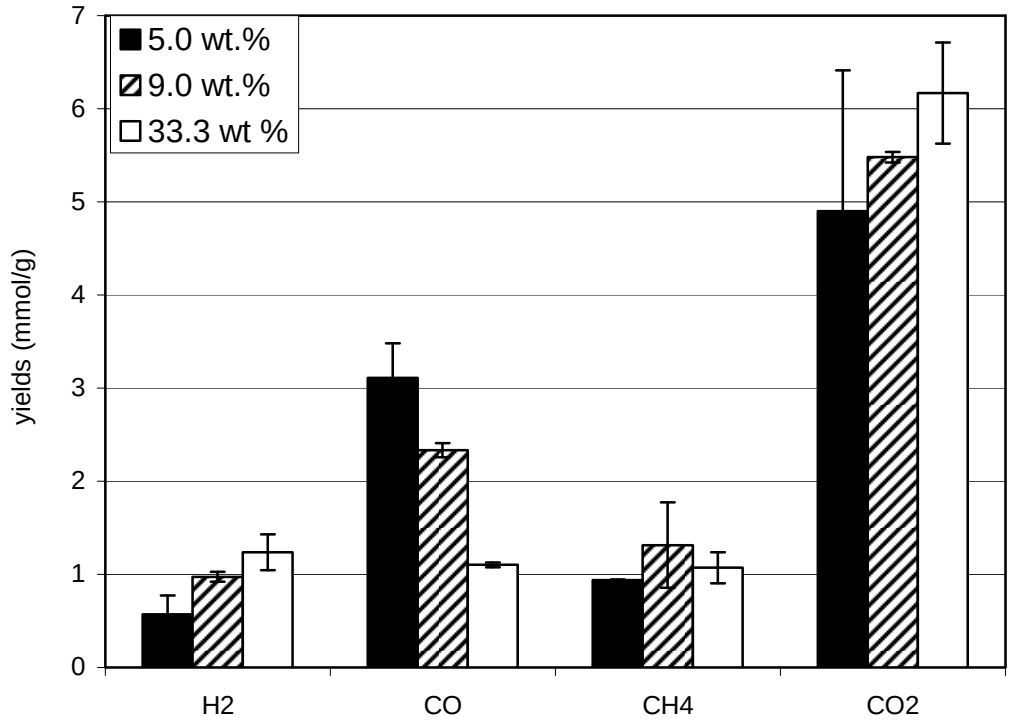

Figure 4.9. Gas yields at 10 minutes as function of cellulose loading (500°C, 0.08 g/ml water density).

4.2.4 Effect of Water Density

The effect of water density on cellulose SCWG was evaluated by examining one density lower than the base case (0.05 g/cm^3) and one higher (0.18 g/cm^3). We also performed experiments without addition of water (0.00 g/cm^3). The base case temperature (500 °C) and the biomass loading (9.0 wt %) were retained.

Figure 4.10 shows the effect of water density on the gas product composition at 7.5 minutes. The H_2 mole fraction, which was only 1.0 % without water added, increases with water density from 4.5 % at 0.05 g/cm^3 to 25.8 % at 0.18 g/cm^3. CO is nearly absent at 0.18 g/cm^3. The CO_2 mole fraction remains high at all densities, and only increases at 0.18 g/cm^3 to 65 %. The CH_4 mole fraction is not affected by water density, and it is not even affected by the presence of water.

Figure 4.11 shows the effect of water density on the C, H, O and total gas yields. The yields were lowest when no water was present. As expected, the major effect of adding water is the increase in H and O yields. This experimental evidence suggests the participation of water as a reactant in the system. The C yield increases from 19.2 to 26.9 % when water is added, and remains nearly constant for all water densities. The H yield gradually increases with water density, going from 5.9 % with no water to 18.3 % at 0.18 g/cm^3. The O yield increases from 32.4 % with no water to 47.3 % when water is added. The total gas yield increases from 24.9 % without water to 35.8 % in the presence of water. The energy content of the gas is nearly constant at 10 %. The water density of 0.18 g/cm^3 was the most severe condition used in this work. No reactors lasted longer than 7.5 minutes, and we estimate the pressure here to be about 510 atm, and the mixture density to be about 0.7 mmol/ml.

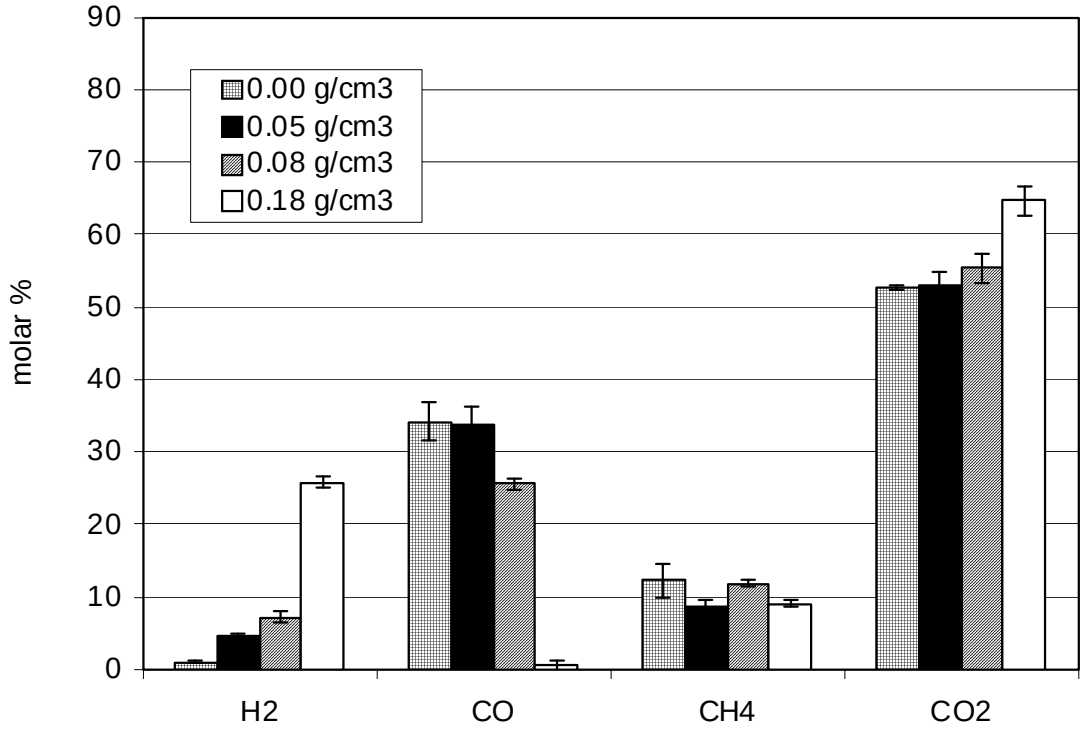

Figure 4.10. Gas composition at 7.5 min as function of water density (500°C, 9.0 wt % cellulose loading).

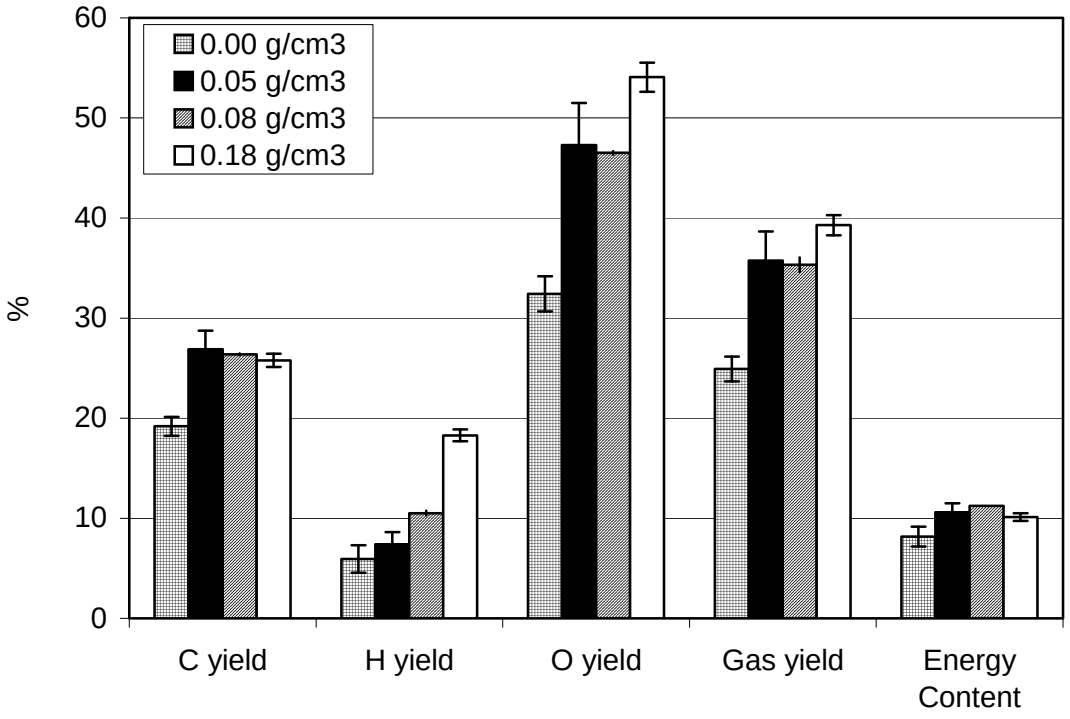

Figure 4.11. C, H, O and total gas yields at 7.5 min as function of water density (500°C, 9.0 wt % cellulose loading).

Figure 4.12 shows how water density affects gas yields. The major effect of increasing the water density is the increase of the H_2 and CO_2 yields and decrease in CO at the high density (0.18 g/cm^3). The CO_2 yield at 0.18 g/cm^3 is more than twice as much as the yield with no water. When the density increases from 0.08 g/cm^3 to 0.18 g/cm^3, the CO_2 yield increases from 5.8 to 8.3 mmol/g (increase of 2.5 mmol/g). Accordingly, the H_2 yield increases from 0.7 mmol/g at 0.08 g/cm^3 to 3.3 mmol/g at 0.18 g/cm^3 (increase of 2.6 mmol/g). The CO yield decreases from 2.7 mmol/g at 0.08 g/cm^3 to 0.1 mmol/g (decrease of 2.6 mmol/g). The H_2 and CO_2 yields increase by the same amount as the CO decrease, which is consistent with the water-gas shift reaction being the reason for the effects of water density from 0.08 g/cm^3 to 0.18 g/cm^3. For smaller water densities, H_2 and CO_2 also increase but by smaller amounts, and CO does not seem to be affected. In these cases, steam-reforming rather than water-gas shift could be the reason for water density effects. There is also the possibility of the rates of H_2 and CO_2 formation from intermediates affecting these yields. The yield of CH_4 remains unchanged for all water densities, including the situation where no water is present.

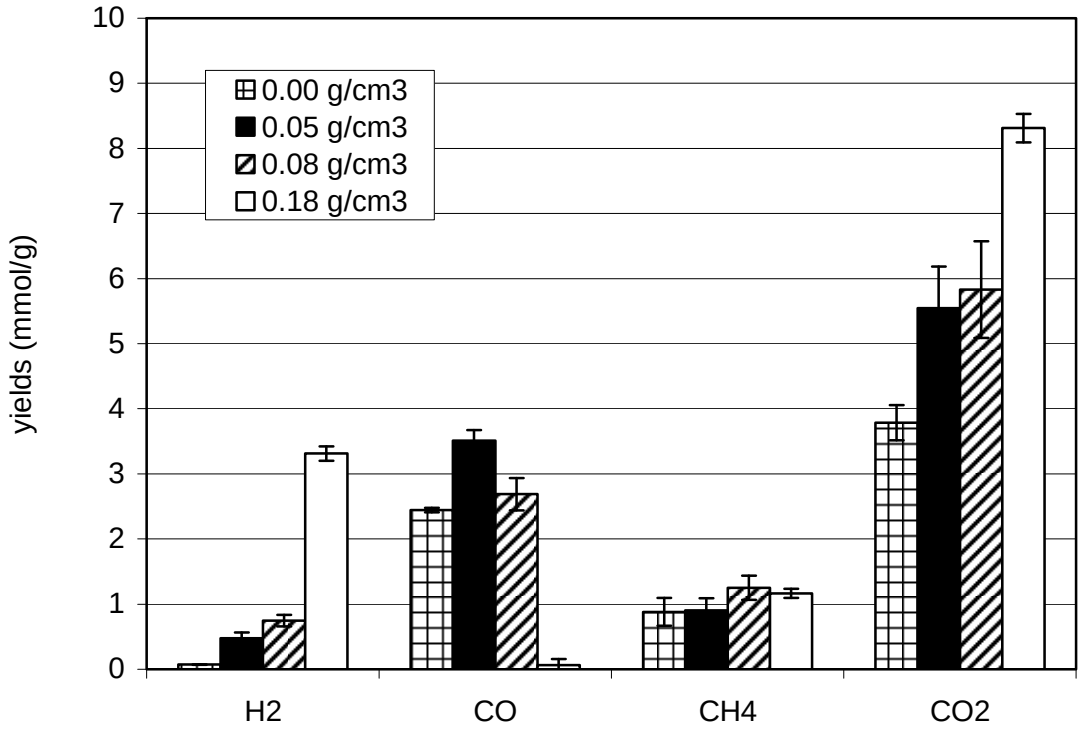

Figure 4.12. Gas yields at 7.5 minutes as function of water density (500°C, 0.08 g/ml water density).

4.2.5 Comparison with Previous Results

Having just presented the first published results for cellulose gasification in supercritical water in a metal-free reactor, we now compare some of these results with previous work on SCWG of cellulose with no added catalyst. This previous work was done in metal reactors (stainless steel), so this comparison may provide some insight into the contribution of catalytic reactions from the metal reactor wall during nominally uncatalyzed SCWG.

Table 4.2 compares some of our results with those of Hao et al. [7]. We replicated exactly the conditions used by Hao, which happen to be very close to what we used as our base case scenario. Hao also used microcrystalline cellulose. From information provided in the article, we estimate the reactor surface area/biomass weight to be about 18 mm^2/mg. Table 4.2 shows that the yields of H_2, CH_4, CO and CO_2 reported by Hao et al. for SCWG in a stainless steel autoclave with no added catalyst are all higher than the yields we obtained from SCWG in quartz with no added catalyst. While the increase in CO_2 is relatively small, the CO and CH_4 yields were more than twice as high in stainless steel than they were in quartz, and the H_2 yield was more than three times higher. As a consequence, the total gas yield was also higher in their experiment. Thus it appears that a significant portion of the gas yields observed by Hao et al. may be attributable to heterogeneous reactions catalyzed by the reactor wall.

Table 4.2. Gas Yields (mmol/g) from SCWG of Cellulose with no added catalyst (500 °C, 20 min, 0.07 g/ml, 9.1 wt % cellulose).

	This work	**Hao et al.** [7]
Reactor Material	**Quartz**	**316 stainless**
CO_2	5.1 ± 0.5	6
CO	2.4 ± 0.3	5.5
H_2	1.2 ± 0.2	4
CH_4	1.3 ± 0.2	3
Sum	10.0 ± 0.6	18.5

We now look at a different situation in terms of experimental conditions. Table 4.3 compares other results in quartz with previous results obtained in stainless steel reactors with no added catalyst. In this case, the experimental conditions used by

Watanabe [2] and Osada [4] are very high water densities (0.33 g/cm^3) and low cellulose loading (about 5.0 wt %). From information provided in the articles, we estimate the reactor surface area/biomass ratio in both cases to be about 19 mm^2/mg. The outcome now suggests a different trend, with H_2 and CO_2 yields higher in quartz than in stainless steel, and CO yields in quartz being lower. CH_4 is nearly absent in all cases. This trend is very similar to the one we observed for effects of water density, but here we would not expect the water-gas shift to play a significant role because of the temperature (400°C). The conditions presented here (low cellulose loading and high water density) strongly favor SCWG reactions. The reason why the yields in quartz are higher in comparison to stainless steel is unclear, though. Perhaps the relative importance of catalysis by metal walls depends upon the water density and biomass loading. We will consider this possibility later in the chapter on SCWG with added metals.

Table 4.3. Gas Yields (mmol/g) from SCWG of Cellulose with no added catalyst (400 °C, 15 min). *Yields in mmol/g were calculated from data provided in the article.

	This Work	**Watanabe et al.** [2]	**Osada et al.** [4]
W Dens. (g/cm^3)	0.33	0.35	0.33
Wt % cellulose	5.0	4.8 %	5 %
Reactor	quartz	316 stainless	316 stainless
CO_2	5.9 ± 0.4	4.1	2.6
CO	0.4 ± 0.1	1.8	1.4
H_2	1.4 ± 0.2	0.6	0.8
CH_4	0.1 ± 0.0	n.d.	0.1
Sum	7.3 ± 0.4	6.5	4.9

4.3 Conclusions

1.) In this chapter we reported the first study of SCWG in the absence of catalytic effects from metal walls. In Chapter 7, these results will be used to evaluate the real effect of added catalysts in SCWG. We also performed the first systematic study of the effects of experimental conditions on gas yields, and showed that gas composition in SCWG can be controlled by manipulating process variables.

2.) In some cases, results from SCWG of cellulose in quartz reactors differ from those obtained from nominally “uncatalyzed” SCWG in stainless steel reactors. In quartz at

mild water densities, the total gas yields are lower and the H_2 mole fraction in the gas is also lower. These comparisons indicate that the reactor surface influences both the rate of gas formation and the composition of the gas. At high water densities and low cellulose loadings, however, H_2 and CO_2 are higher in quartz then they were in stainless steel reactors. These comparisons indicate that the relative influence of metal surfaces is likely a function of the precise reaction conditions employed.

3.) Based on the observed trends, one should use high temperatures (600°C) and high water densities (0.18 g/cm^3) in order to maximize H_2 production. In short, as the severity of the reaction conditions increased, the H_2 yield increased. The highest H_2 yield in this study was 3.3 mmol/g, obtained at the high water density (0.18 g/cm^3).

4.) If the product gas is to be used as a fuel, the LHV is maximized by the use of higher temperatures (to increase H_2 and CH_4 yields), high water density (to increase H_2 yield), and low biomass loading (to increase CO) yield. The highest energy content was 20.0 %, obtained at the highest temperature (600°C). In general, conditions that favor CH_4 formation greatly increase the energetic content, because of its high LHV. The highest CH_4 yield was 2.6 mmol/g, obtained at the high temperature (600°C).

5.) If there is interest in producing CO, low biomass loadings and short residence times are recommended, since CO yields decrease with loading and time. At 33.3 wt %, it is possible to obtain a 1:1 CO/H_2 ratio. At the base case conditions (500°C, 9.0 wt % loading, 0.08 g/cm^3, 5 min), a gas with 1:2 CO/H_2 ratio is produced. This ratio is proper for use of the product as syngas to produce methanol.

6.) Manipulating the cellulose loading (wt %) and water density provides a means to control the selectivity to H-containing gases. The relative amounts of H_2 and CH_4 were strongly influenced by these two process variables. The molar ratio of CH_4 to H_2 decreased from 1.6 to 0.9 as the cellulose loading increased from 5.0 to 33.3 wt %, at 500°C and 0.08 water density. Likewise, this ratio decreased from 1.9 to 0.4 as the water density increased from 0.05 to 0.18 g/cm^3, at 500 °C and 9.0 wt % cellulose.

7.) CO_2 was the major product at all experimental conditions in this work.

8.) There is slow formation of H_2, CO_2 and CH_4 with time, and slow CO consumption. The results indicate that after 30 minutes at 500 °C, the system might not yet be at equilibrium. This opens the possibility of the use of catalysts to achieve higher yields.

REFERENCES

[1] T. Yoshida and Y. Matsumura, "Gasification of cellulose, xylan, and lignin mixtures in supercritical water." *Ind Eng Chem Res,* vol. 40, pp. 5469-5474, 2001.

[2] M. Watanabe, H. Inomata and K. Arai, "Catalytic hydrogen generation from biomass (glucose and cellulose) with ZrO2 in supercritical water." *Biomass & Bioenergy,* vol. 22, pp. 405-410, 2002.

[3] P. T. Williams and J. Onwudili, "Subcritical and Supercritical Water Gasification of Cellulose, Starch, Glucose, and Biomass Waste." *Energy & Fuels,* vol. 20, pp. 1259-1265, 2006.

[4] M. Osada, T. Sato, M. Watanabe, T. Adschiri and K. Arai, "Low-Temperature Catalytic Gasification of Lignin and Cellulose with a Ruthenium Catalyst in Supercritical Water." *Energy & Fuels,* vol. 18, pp. 327-333, 2004.

[5] T. Minowa, T. Ogi, Y. Dote and S. Yokoyama, "Methane production from cellulose by catalytic gasification." *Renewable Energy,* vol. 5, pp. 813-815, 1994.

[6] T. Minowa and T. Ogi, "Hydrogen production from cellulose using a reduced nickel catalyst." *Catalysis Today,* vol. 45, pp. 411-416, 1998.

[7] X. Hao, L. Guo, X. Zhang and Y. Guan, "Hydrogen production from catalytic gasification of cellulose in supercritical water." *Chemical Engineering Journal (Amsterdam, Netherlands),* vol. 110, pp. 57-65, 2005.

[8] Y. J. Lu, L. J. Guo, C. M. Ji, X. M. Zhang, X. H. Hao and Q. H. Yan, "Hydrogen production by biomass gasification in supercritical water: A parametric study." *Int J Hydrogen Energy,* vol. 31, pp. 822-831, 2006.

[9] G. J. DiLeo, M. E. Neff and P. E. Savage, “Gasification of guaiacol and phenol in supercritical water”. *Energy & Fuels*, vol. 21, pp. 2340-2345, 2007.

[10] S. R. A. Kersten, B. Potic, W. Prins and W. P. M. Van Swaaij, "Gasification of Model Compounds and Wood in Hot Compressed Water." *Ind Eng Chem Res,* vol. 45, pp. 4169-4177, 2006.

[11] M. Sasaki, B. Kabyemela, R. Malaluan, S. Hirose, N. Takeda, T. Adschiri and K. Arai, "Cellulose hydrolysis in subcritical and supercritical water." *Journal of Supercritical Fluids,* vol. 13, pp. 261-268, 1998.

[12] M. J. Antal Jr., S. G. Allen, D. Schulman, X. Xu and R. J. Divilio, "Biomass Gasification in Supercritical Water." *Ind Eng Chem Res,* vol. 39, pp. 4040-4053, 2000.

[13] D. C. Elliott and L. J. Sealock Jr, "Chemical processing in high-pressure aqueous environments: low-temperature catalytic gasification." *Chem. Eng. Res. Design*, vol. 74, pp. 563-566, 1996.

[14] Q. Yan, L. Guo and Y. Lu, "Thermodynamic analysis of hydrogen production from biomass gasification in supercritical water." *Energy Conversion and Management*, vol. 47, pp. 1515-1528, 2006.

[15] J. Figueiredo and S. Alves, "Waste wood pyrolysis," in *Encyclopedia of Environmental Control Technology* , vol. 1, Anonymous Houston: Gulf, 1989, pp. 282-286.

[16] C. A. Bernardo and D. L. Trimm, "The kinetics of gasification of carbon deposited on nickel catalysts." *Carbon*, vol. 17, pp. 115-120, 1979.

[17] N. Jand, V. Brandani and P. U. Foscolo, "Thermodynamic Limits and Actual Product Yields and Compositions in Biomass Gasification Processes." *Ind Eng Chem Res*, vol. 45, pp. 834-843, 2006.

CHAPTER 5
NONCATALYTIC GASIFICATION OF LIGNIN IN SUPERCRITICAL WATER

This chapter presents results for the non-catalytic gasification of lignin in supercritical water, in a similar fashion to what was presented for cellulose. Gasification of lignin in supercritical water in the absence of metals was performed for the first time by using quartz reactors. We also performed the first systematic study of the effects of experimental conditions on gas yields. Temperature, water density, lignin loading and time were evaluated. The aromatic structure of lignin and the possibility of recombination of the reactive intermediates that originate from lignin make it a difficult feedstock for gasification. For this reason, the base case temperature was switched to 600°C instead of the 500°C used for cellulose.

5.1 Introduction

Table 5.1 summarizes previous work on lignin SCWG in the absence of added catalysts. It is interesting to observe that none of the previous work was performed above 400 °C. At this temperature and without a catalyst added to the reactor, though, total gas yields are usually low, (5 to 10 mmol/g at most) according to Watanabe [1]. In the present research we use temperatures as high as 725 °C. The articles in Table 5.1 generally consider only one temperature, water density, lignin loading, and reaction time. This chapter provides results for the first systematic study of the effects of temperature, biomass loading, water density, and reaction time on lignin SCWG.

The work presented here is also unique because it is the first to report lignin SCWG in a metal-free reactor. We used quartz capillary tubes as mini batch reactors. We sought results for lignin gasification in SCW that would be attributable exclusively to non-catalytic reactions. This information would be very useful for subsequent evaluation

of different catalysts, because the non-catalytic contribution could be subtracted out and the effect of the catalyst alone can then be clearly seen.

Table 5.1. Summary of Previous Research on SCWG of Lignin with no added catalyst.

Reference	Temp (°C)	Water Dens. (g/cm^3)	Lignin wt. %	Time (min)
Watanabe [1]	400	0.35	12.6	15-60
Osada [2]	400	0.33	5	15
Sato [3]	400	0.3	up to 16	120
Osada [4]	400	0.33	5	15

Results obtained from methods other than SCWG to generate fuels from lignin have been previously reported. Font et al. [5] performed direct combustion and pyrolysis of Kraft lignin under a variety of N_2/air flows and temperatures. Ferdous et al. [6] performed gasification using steam and a commercial catalyst at 750°C. Hanaoka et al. [7] gasified lignin using air and steam simultaneously at 900°C. Some studies using supercritical water in partial oxidative environments have also been reported. Watanabe et al. [1] performed partial oxidation of lignin in supercritical water, evaluating NaOH and ZrO_2 as catalysts. General Atomics [8] has developed a pilot plant facility that performed Supercritical Water Partial Oxidation (SCWPO) of several biomass feedstocks (corn starch, coal, wood, etc.). We cannot compare our results with those from these technologies because the experimental conditions used are vastly different (the sole exception is the work from Font et al., to which we later compare our results from experiments with no water added).

5.2 Results and Discussion

We arbitrarily designate SCWG at 600°C, 9.0 wt. % biomass, and 0.08 g/cm^3 water density (31 MPa water partial pressure) as the base case. From this starting point, we varied one parameter at a time to evaluate its effect on the gas yields and composition. We considered temperatures of 365 (to evaluate yields at subcritical conditions), 500, 600, and 725°C, lignin loadings of 5.0, 9.0 and 33.3 wt %, and water densities of 0.00,

0.05, 0.08 and 0.18 g/cm^3. Reactions were performed for batch hold times ranging from 2.5 to 75 minutes (2.5; 5.0; 10.0; 15.0; 30.0; 45.0; 60.0; 75.0).

Visual observation of the quartz reactors after SCWG experiments indicates the presence of char (a black residue adhering to the reactor internal walls) in all cases. The char strongly adhered to the quartz, making it impossible to collect samples in enough quantity for analysis. Char was found along the entire length of the reactors, which suggests good mixing and reasonably uniform distribution of lignin in the reactor.

At the longer reaction times and higher temperatures, the reactors showed a thin white layer in their walls, indicating that SCW might be attacking the reactor walls. Quartz is slightly soluble in supercritical water, but at 725°C, only about 0.24 % of the reactor material would be leached out at equilibrium [9].

To provide a basis for our discussion of results, we suggest a reaction scheme for lignin SCWG, based largely on literature information [2, 10-17] which accounts for the main solid- and liquid-phase reactions and focuses on the main routes for gas formation. Although the complex structure of lignin and variety of monomeric structures makes the elaboration of a simplified reaction scheme a difficult task, we can start by defining a molecular formula for a typical lignin monomer. Elemental analysis of organosolv lignin [1, 3, 18] leads to $C_{10}H_{10}O_3$ as the appropriate formula for the hypothetical monomer for lignin. This formula will be used for the monomer in our reaction scheme, which follows below. $C_xH_yO_z$ indicates generic intermediate species resulting from the monomer decomposition.

Lignin Hydrolysis: $(C_{10}H_{10}O_3)_n + n\ H_2O \rightarrow n\ C_{10}H_{12}O_4$

Monomer Oligomerization: $n\ C_{10}H_{12}O_4 \rightarrow (C_{10}H_{12}O_4)_2 + (C_{10}H_{12}O_4)_3 + \ldots$

Monomer Decomposition: $C_{10}H_{12}O_4 \rightarrow C_xH_yO_z$

Steam-reforming I: $C_xH_yO_z + (x\text{-}z)\ H_2O \rightarrow x\ CO + \left(x - z + \frac{y}{2}\right) H_2$

Steam Reforming II: $C_xH_yO_z + (2x\text{-}z)\ H_2O \rightarrow x\ CO_2 + \left(2x - z + \frac{y}{2}\right) H_2$

Intermediate Pyrolysis: (to form CO): $C_xH_yO_z \rightarrow CO + C_xH_yO_z$

Intermediate Pyrolysis (to form CO_2): $C_xH_yO_z \rightarrow CO_2 + C_xH_yO_z$

Intermediate Pyrolysis (to form CH_4): $C_xH_yO_z \rightarrow CH_4 + C_xH_yO_z$

Intermediate Pyrolysis (to form H_2): $C_xH_yO_z \rightarrow H_2 + C_xH_yO_z$

Char formation through intermediates: $C_xH_yO_z \rightarrow w\ C + C_{x-w}H_yO_z$

Water-Gas Shift: $CO + H_2O \leftrightarrow CO_2 + H_2$

Methanation: $CO + 3\ H_2 \leftrightarrow CH_4 + H_2O$

5.2.1 Base Case Results

We first present results for the base case conditions (600 °C, 0.08 g/cm^3, 9.0 wt% lignin), and then proceed to analyze how changes in reaction parameters affect the results. The error bars in all the figures represent the standard deviation. The line segments connecting experimental data points are provided only to guide the reader.

Figure 5.1 shows the temporal variation of the molar composition (dry basis) of the gases formed for the base case. The gas is composed mostly of CO_2 and CH_4 at all times. The CO_2 molar % remains relatively stable around 35-40 %. Likewise, the CH_4 mole % is relatively stable and between 30-35 %. The CO mole % decreases from about 22 % at 2.5 minutes to 10 % after 75 minutes, and H_2 rises from about 10 % in the first minutes to about 15 % after 60 minutes. The base case conditions, therefore, strongly favor the formation of CH_4 and CO_2. Although the CO mole % decreases with time, it appears that a long reaction time would be necessary to completely eliminate CO.

Figure 5.1 also shows equilibrium compositions. ASPEN Plus was used for the calculations. We used the RGibbs reactor block in ASPEN. This block calculates equilibrium concentrations without requiring knowledge of reaction stoichiometry, by minimizing the Gibbs free energy. For properties calculation, the UNIQUAC method was used. Our starting monomer from lignin is $C_{10}H_{12}O_4$. The feed contains the monomer and water in the same initial compositions as the corresponding situations in the experiment. The product can contain the monomer, water, CO, H_2, CO_2 and CH_4. The pressure was 28 MPa. Figure 5.1 shows that the H_2 equilibrium molar % (35.8 %) is much higher than the experimental H_2 molar % at 75 minutes (17.0 %). The CH_4 and CO equilibrium molar % (26.1 and 0.9 % respectively) are both lower than the experimental values. The equilibrium CO_2 molar % (37.2%), though, is very close to the experimental value at 75 minutes (40.1 %). It seems, therefore, that the system is far from equilibrium at 75 minutes.

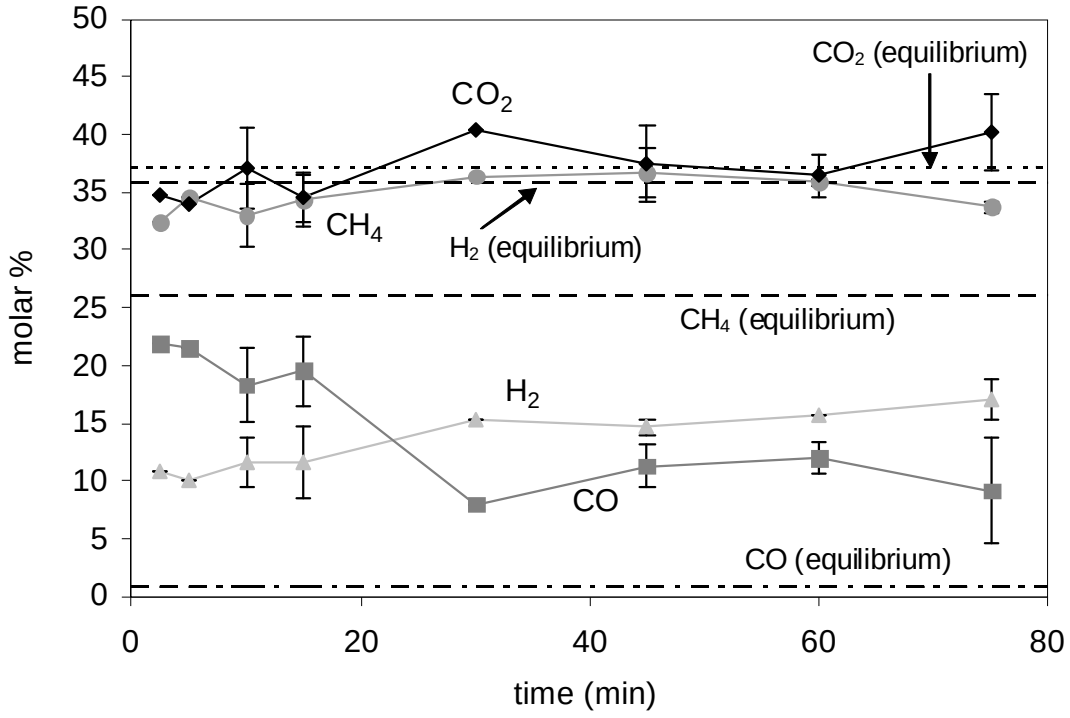

Figure 5.1. Temporal variation of gas composition (base case).

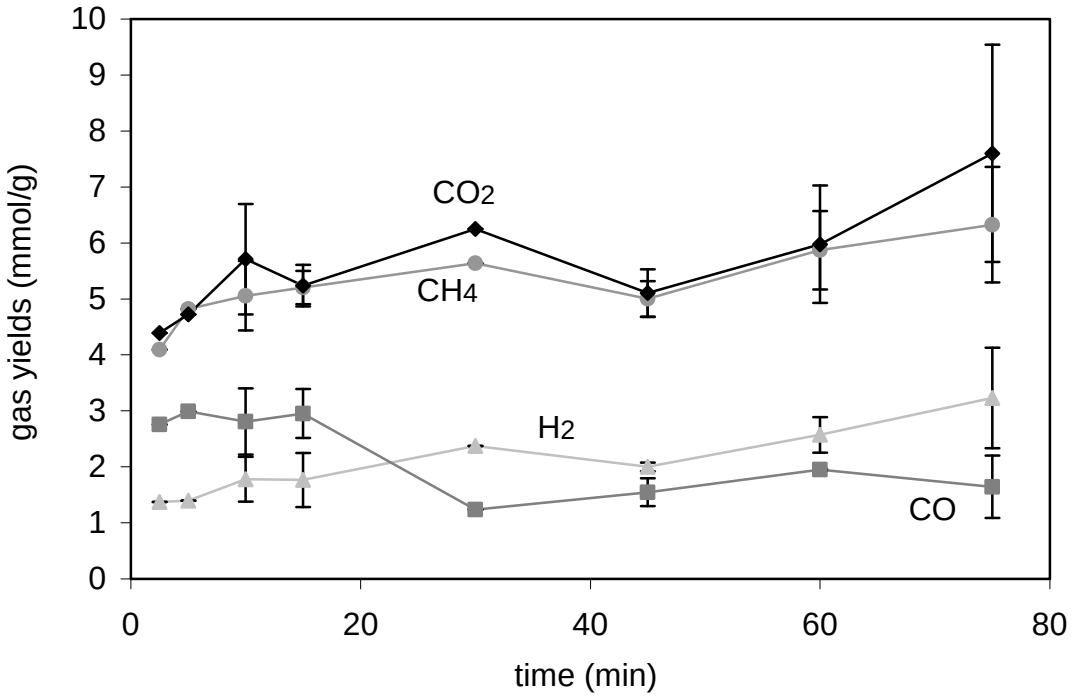

Figure 5.2. Temporal variation of yields (mmol/g) of CO, CO_2, H_2, and CH_4 (base case).

Figure 5.2 shows the temporal variation of the molar yields of the gaseous products. During the first 2.5 minutes, 4.4 mmol/g of CO_2 and 4.1 mmol/g of CH_4 are formed. Recalling our reaction scheme, we can infer the reactions that possibly lead to formation of CO_2 during these early minutes of gasification. CO_2 is a product of steam reforming of the intermediate species, intermediate pyrolysis, and water-gas shift. The relatively large amount of CO and small amount of H_2 present at 2.5 minutes suggest that water-gas shift is not a dominant reaction during the early minutes. It appears, therefore, that the large amount of CO_2 is a direct result of intermediate and steam-reforming. For the longer reaction times, the CO_2 contribution from water-gas shift could be greater. It is interesting to note how the molar yields of CO, CO_2 and H_2 change from 2.5 minutes to 75 minutes. The H_2 yield increases from 1.4 to 3.2 mmol/g (plus 1.8 mmol/g), the CO yield decreases from 2.7 to 1.6 mmol/g (minus 1.1 mmol/g), and the CO_2 yield increases from 4.4 mmol/g to 7.6 mmol/g (plus 3.2 mmol/g). This means that, during this period of time, H_2 and CO_2 must originate from at least one source other than the water-gas shift reaction.

CH_4 can result either from reactions of other gas species (CO and H_2) via methanation, or from reactions of the organic material in the reactor. The large CO content in the first minutes suggests methanation is not a dominant reaction, so the intermediates could be the main precursors of the CH_4 initially formed.

Figure 5.3 shows the total gas yield, the energetic content, and the H, C, and O yields for the base case condition. The total gas yield is 34 % at 2.5 minutes and increases only slightly with time, reaching 49 % after 75 minutes. It appears that the reactions that convert lignin and intermediate species into gases take place mostly during the first 2.5 minutes. After that time reactions among gas species and water, such as water-gas shift and methanation, dominate. This conclusion is further supported by the individual yields of C, H and O. The C yield stays relatively stable at about 20-25 %, but the H yield increases from 32 to 53 % with increasing time. This behavior suggests that H atoms in water are converted into gases, which again is consistent with water-gas shift being the dominant reaction after the initial minutes. The energetic content of the gas stays stable at 20-25 % for all times.

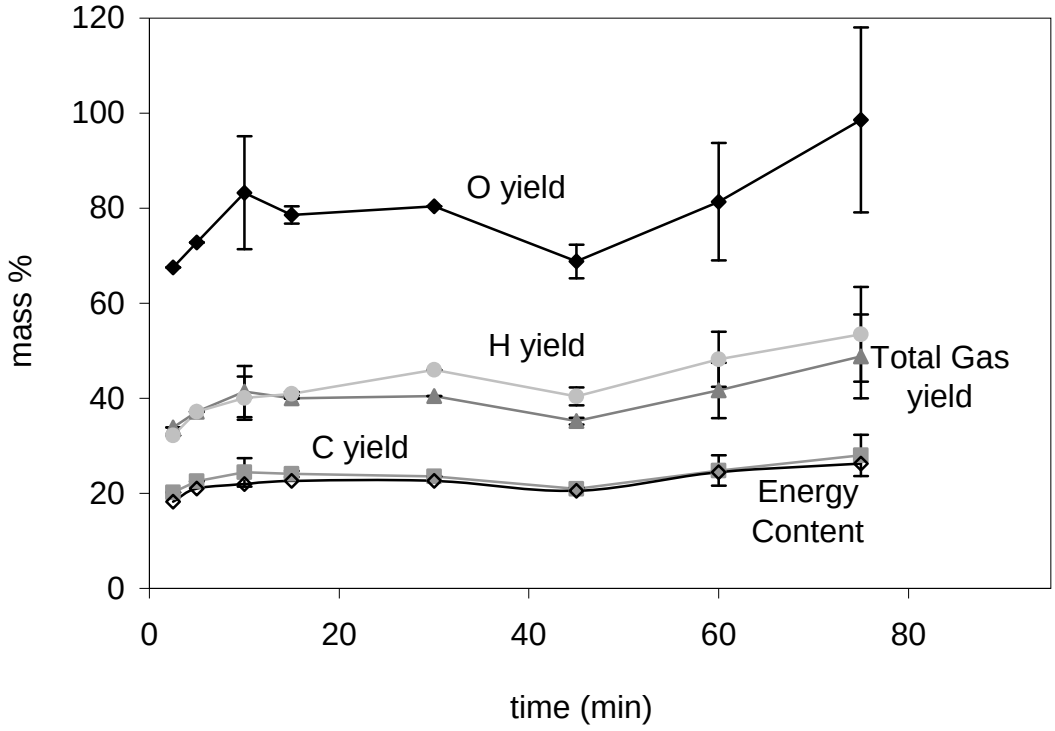

Figure 5.3. Temporal variation of C, H, O and total gas yields (base case).

5.2.2 Effect of Temperature

The effect of temperature was evaluated by keeping the lignin loading and water density fixed at the base case values (9.0 wt% and 0.08 g/cm^3) and running experiments at 365, 500, 600 and 725°C. The experiments at 365°C (below the critical point of water, 374°C) were performed to determine the extent of gasification at subcritical conditions, which are encountered during the 30 seconds heat-up time in the SCWG experiment. Figure 5.4 shows the effect of temperature on the composition of the product gas at 45 minutes. Results at other reaction times showed similar trends.

Below the critical point of water, the gas formed is mostly CO_2 (70 %), with lesser amounts of CO and CH_4 (16 and 12 % respectively). H_2 is less than 2 % of the gas formed at 365 °C. As the temperature exceeds the critical value, the H_2 and CH_4 mole fractions substantially increase, the CO_2 molar % decreases and the CO molar % remains unchanged.

In the supercritical region (500°C and above), temperature does not seem to affect strongly the molar percentages of CH_4 and CO_2. CH_4 is about 30-35 % of the gas produced, and CO_2 is about 35-40 %. The main effect of temperature is on the molar % of H_2 and CO. The H_2 mole % is about four times greater at 725°C than it was at 500°C. The CO mole % is about 13 times smaller at 725°C than at 500°C. Temperature is therefore an important tool to accomplish a nearly CO-free product when gasifying lignin in supercritical water.

Figure 5.5 shows the effect of temperature on the C, H, O and total gas yield. All of the yields generally increase with temperature. At 725°C, the H yield is about 20 times higher, the O yield is about 3 times higher, and the C yield is about 4 times higher than at 365°C. There is a particularly large jump from 600°C to 725°C for the H and O yields, suggesting more gas formation from water through the water-gas shift reaction at 725°C. The total mass of gases relative to the initial mass of lignin increases from 19 % to 64 % when the temperature increases from 365°C to 725°C. The energy content of the gas also increases with temperature. It increases from 3 % at 365°C to 38 % at 725°C.

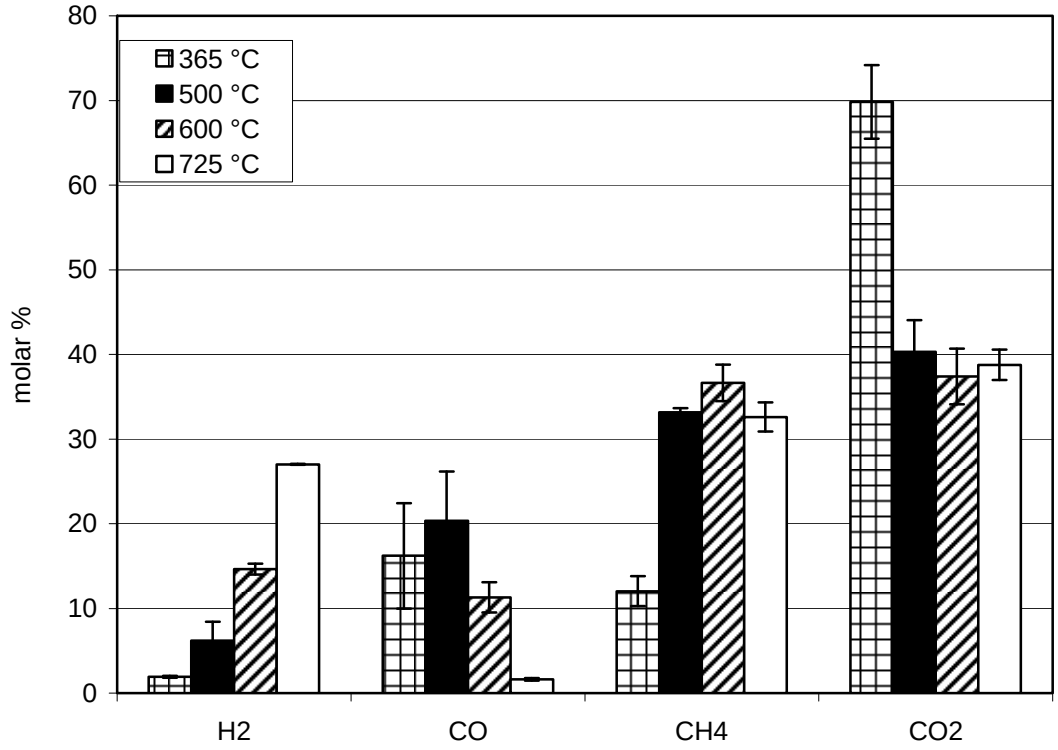

Figure 5.4. Gas composition as function of temperature (45 minutes, 9.0 wt % lignin loading, 0.08 g/ml).

Higher temperatures are therefore extremely important to obtain higher gas yields for uncatalyzed lignin SCWG.

Figure 5.6 shows how the molar yields of gases are affected by changes in temperature. The effect of temperature is similar for all species except CO. The molar yields of H_2, CH_4 and CO_2 increase with temperature, and there is a large jump from 600°C to 725°C. The species most strongly affected by temperature is H_2. It is barely produced at 365°C (only 0.1 mmol/g), but it is produced in amounts 75 times larger at 725°C (7.5 mmol/g). It is interesting to note that the absolute increase in H_2 yield (5.5 mmol/g) from 600°C to 725°C is very close to the absolute increase in CO_2 yield (5.6 mmol/g). This trend is consistent with both H_2 and CO_2 formation being accelerated mainly by an increase in the rate of water-gas shift and steam reforming. The change in the CO yields is smaller, though, which suggest that the CO yields are influenced by reactions in addition to water-gas shift. The CH_4 yield is also strongly affected by temperature, most likely because of intermediates pyrolysis. CH_4 yields increase from 0.6 mmol/g to 8.9 mmol/g as the temperature increases from 365°C to 725°C. The results also show that part of the CO_2 yields might be attributable to reactions taking place at the subcritical region, during the heat-up time.

5.2.3 Effect of Lignin Loading

The second parameter we varied to determine its effect on gas production was the loading of lignin in water. From an engineering perspective, one desires to process biomass/water mixtures with as high a biomass content as possible. Doing so would reduce the capital and operating costs for a SCWG process. For lignin, a stoichiometric mixture with water would be 36.8 wt% (if the final products were CO_2 and H_2). We used 5.0 wt % and 33.3 wt % lignin mixtures in addition to the 9.0 wt % loading used in the base case, therefore water was always present in excess. The temperature (600 °C) and water density (0.08 g/cm^3) remained at their base case values.

Figure 5.7 shows how the composition of the gas at 75 minutes is affected by the lignin loading. Results at other reaction times were similar. The CO_2 molar % is the one that was least influenced. It was consistently around 40 mole %.

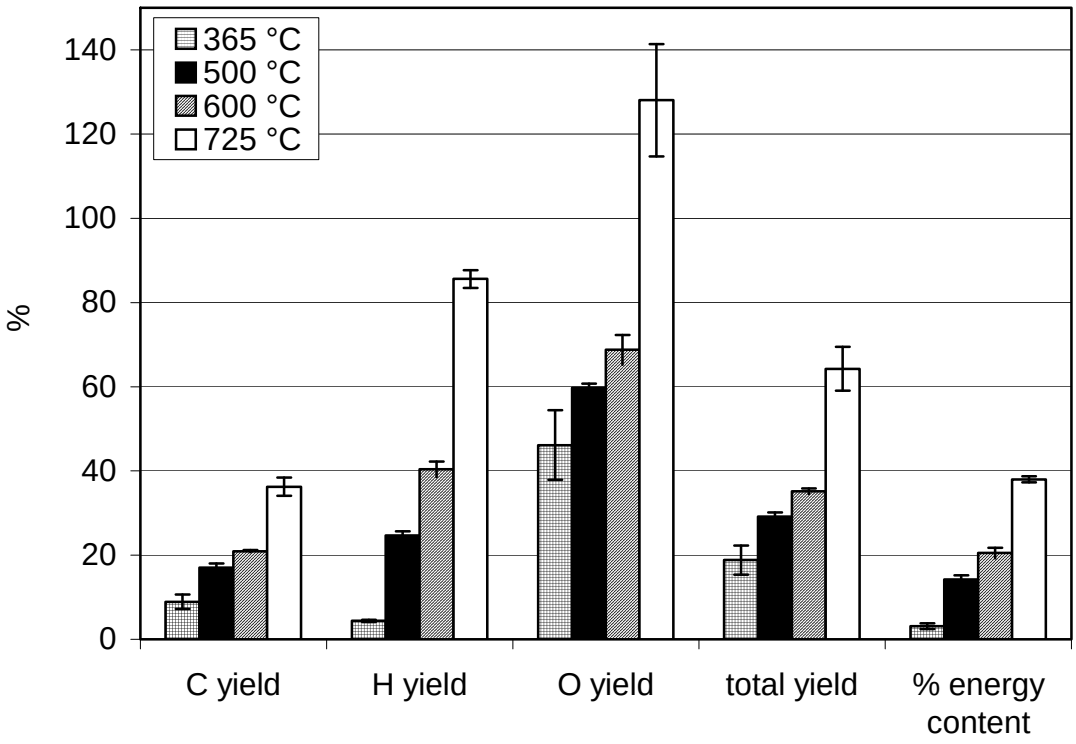

Figure 5.5. C, H, O and total gas yields as a function of temperature (45 minutes, 9.0 wt % lignin loading, 0.08 g/ml).

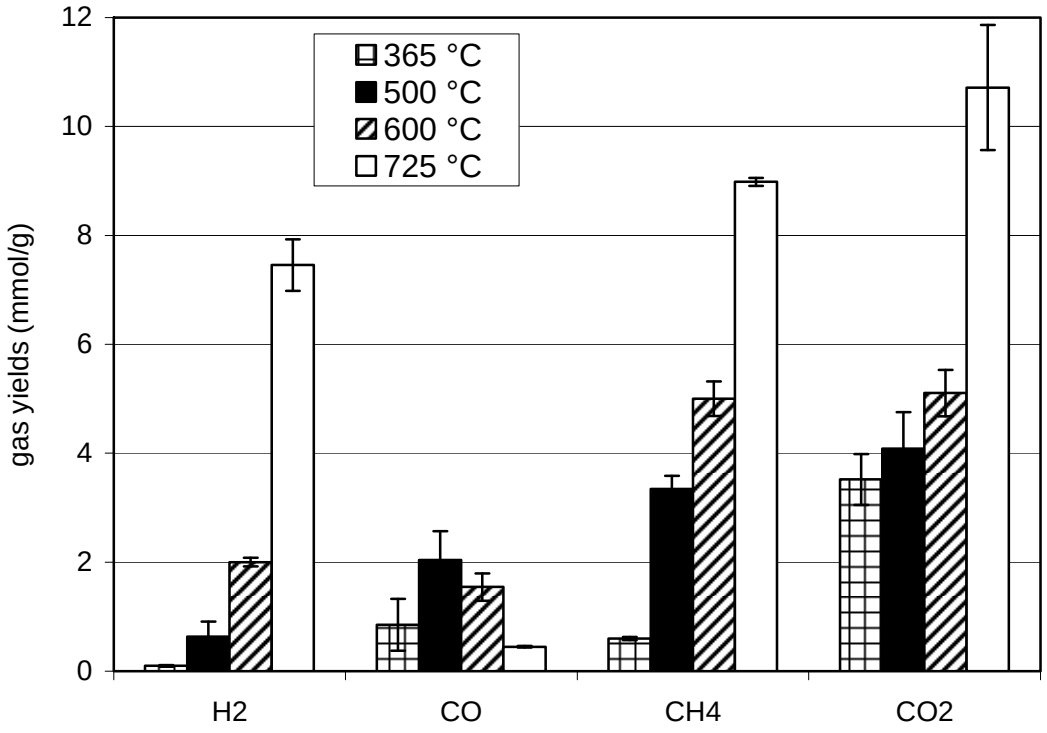

Figure 5.6. Gas yields as function of temperature (45 minutes, 9.0 wt % lignin loading, 0.08 g/ml).

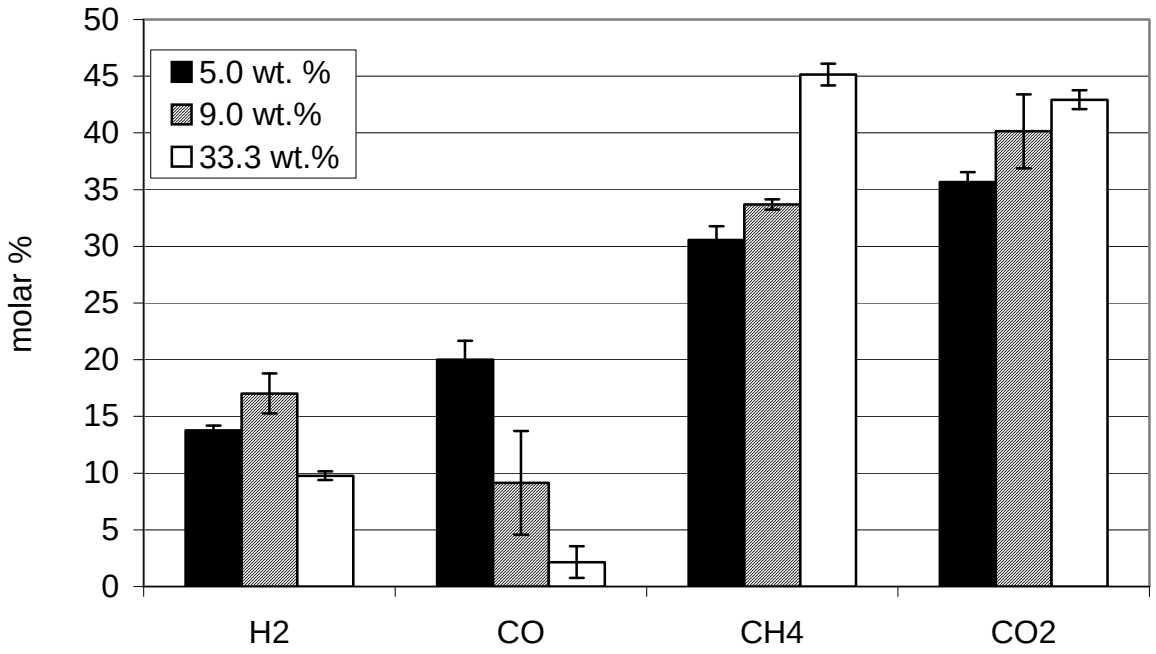

Figure 5.7. Gas composition as function of lignin loading (75 minutes, 600°C, 0.08 g/ml).

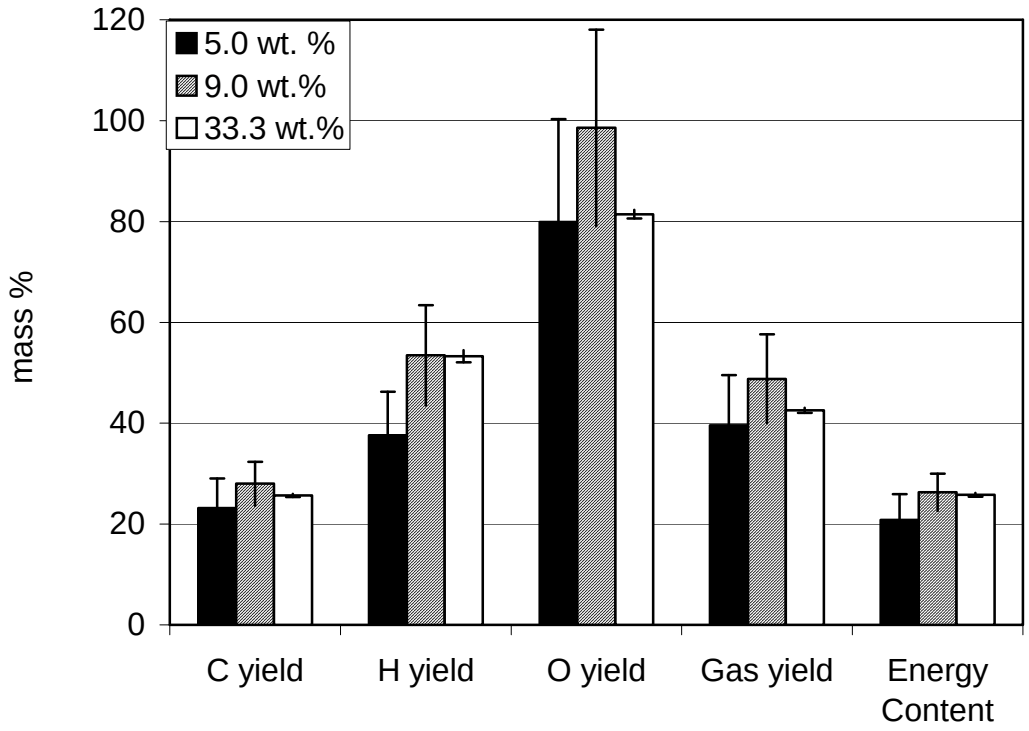

Figure 5.8. C, H, O, and total gas yields as function of lignin loading (75 minutes, 600°C, 0.08 g/ml).

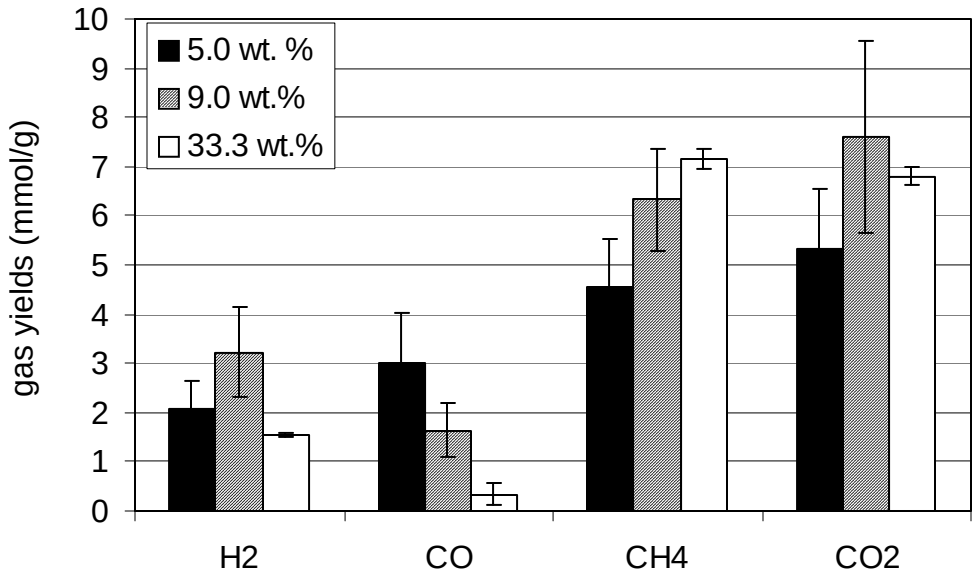

Figure 5.9. Gas yields as function of lignin loading (75 minutes, 600°C, 0.08 g/ml).

CH_4 formation appears to be favored by higher lignin loadings, especially at 33.3 wt %, where it becomes the major product. On the other hand, higher lignin loadings reduce the H_2 molar %, which decreases from 14 % at 5.0 wt% to 10 % at 33.3 wt %. Therefore, the CH_4/H_2 ratio is strongly affected by the lignin loading. The CO mole fraction decreases substantially at 33.0 wt %.

Figure 5.8 shows the effect of lignin loading on the C, H, O, and total gas yields at 75 minutes. All of the yields are largely independent of the lignin loading. The C yield stays around 25 %, the H yield around 50 %, the O yield around 80 %, the total gas yield about 40 %, and the energy content about 25 %. Based on these results, the highest biomass loading (33.3 %) would be recommended, since there is no advantage in lowering the concentration in terms of changing the yields.

Figure 5.9 shows the molar yields of the individual gases as a function of the lignin loading. In general, the lignin loading is not a powerful variable to change the gas yields. The most noticeable effects is on CO. The CO molar yield decreases from 3.0 mmol/g at 5.0 wt % to only 0.3 mmol/g at 33.3 wt %.

5.2.4 Effect of Water Density

The effect of water density on lignin SCWG was evaluated by examining one density lower than the base case (0.05 g/cm^3) and one higher (0.18 g/cm^3). We also performed experiments with no water added (0.00 g/cm^3) to establish a basis for comparison with pyrolysis. The base case temperature (600 °C) and biomass loading (9.0 wt %) were retained.

Figure 5.10 shows the effect of water density on the gas product composition at 60 minutes. Results at other times were similar. The CH_4 mole fraction is largely insensitive to changes in the water density. Even the absence of water does not affect its molar fraction. The H_2 molar % is about 15 % at all water densities, as long as water is present. In the absence of water, it drops to 9 %. The CO and CO_2 mole fractions are about the same at the two intermediate water densities. SCWG at the highest water density, however, reduced CO to only 1 %, and increases CO_2 to 44 %. In the absence of water, the CO molar % increases to 28 %, and the CO_2 molar % decreases to 27 %.

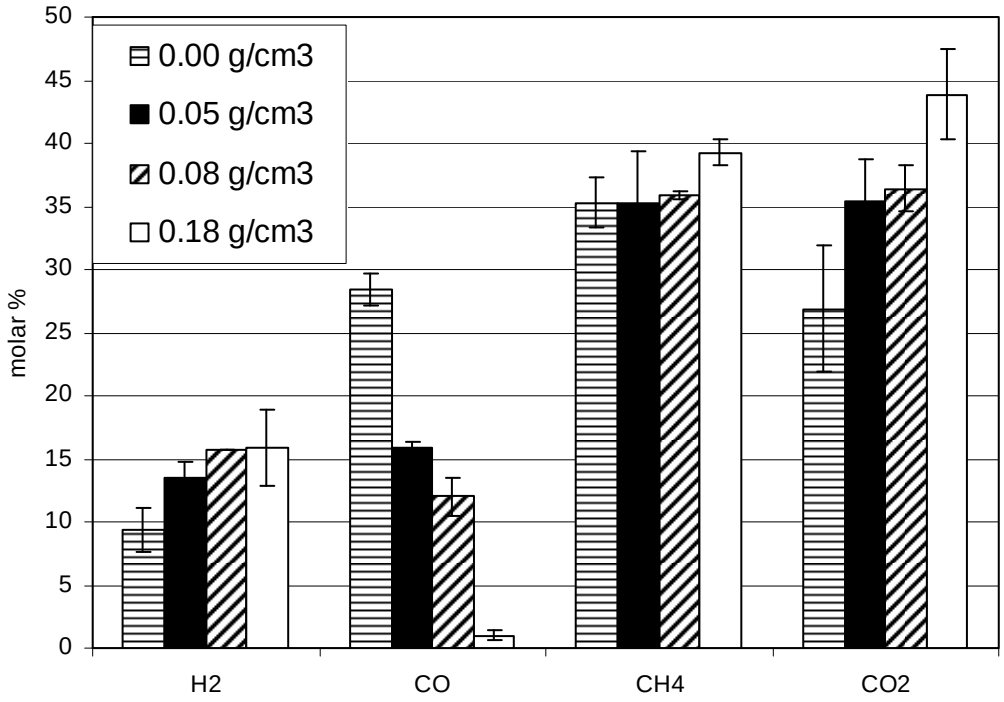

Figure 5.10. Gas composition as function of water density (60 minutes, 600°C, 9.0 lignin loading).

Therefore, the main effect of water density on molar compositions at 60 minutes is the increase in CO_2 and decrease in CO at 0.18 g/cm^3.

Figure 5.11 shows the effect of water density on the C, H, O, total gas yields and energetic content. For pyrolysis, the yields are generally lower than for SCWG at any water density. With water present, H and O yields substantially increase (as expected).

The influence of water density is small as long as water is present. The C yield stays at about 20-25 %, the H yield stays at about 50-55 %, and the O yield stays at about 90 %. The results suggest the use of low water densities would be preferred, since the use of higher water densities requires higher pressures, and it does not seem higher densities generate any advantage in terms of increasing yields.

Figure 5.12 shows how water density affects the yields of individual gases at 60 minutes. For pyrolysis, the yields of H_2, CH_4 and CO_2 are lower than for SCWG. For SCWG, the H_2, CH_4, and CO_2 yields are nearly the same at all densities. In contrast, the CO yield keeps decreasing as the water density increases. Almost all the CO formed at 0.18 g/cm^3 had reacted away at 60 minutes. In a previous work, Font et al. [5] pyrolyzed Kraft lignin at 850°C in a N_2 atmosphere and obtained 3.8 mmol/g of CH_4, 1.7 mmol/g of CO_2 and 9.4 mmol/g of CO. These yields (except for CO) were similar to the ones we found with no water present. This agreement with previously published pyrolysis results suggests that pyrolysis is the dominant reaction in our system when no water is present. This result is consistent with our findings about O_2 effect in Chapter 3: even though there is O_2 from air in the quartz reactor, combustion is not a major reaction in determining gas yields.

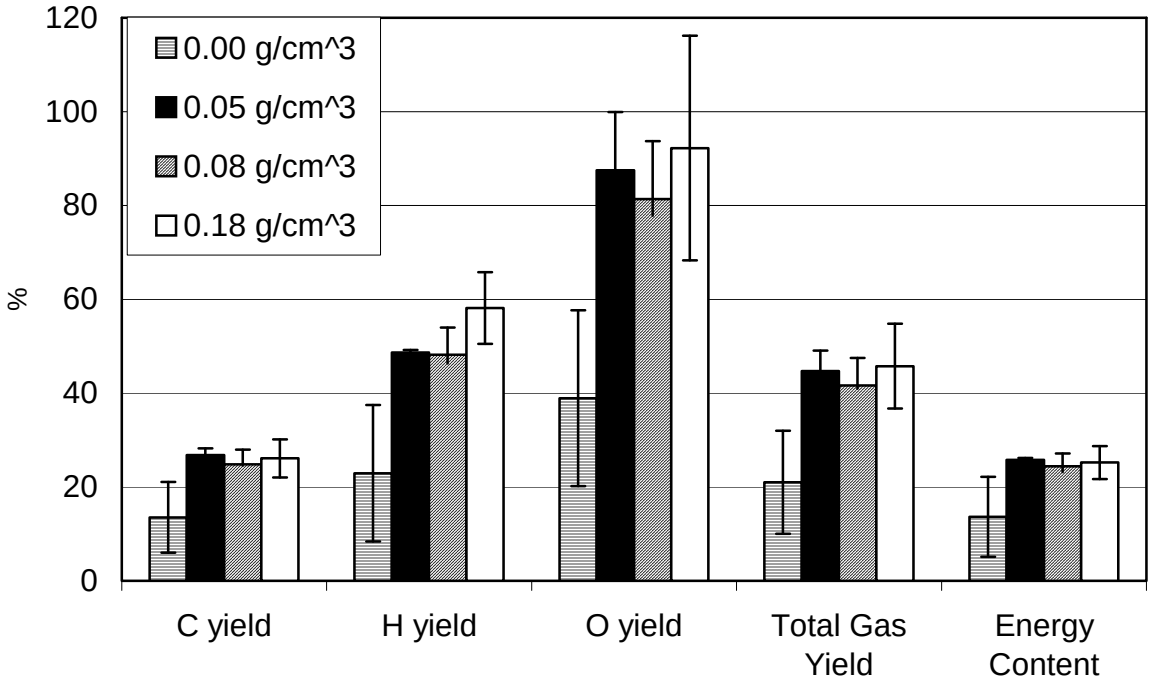

Figure 5.11. C, H, O, and total gas yields as function of water density (60 minutes, 600°C, 9.0 lignin loading).

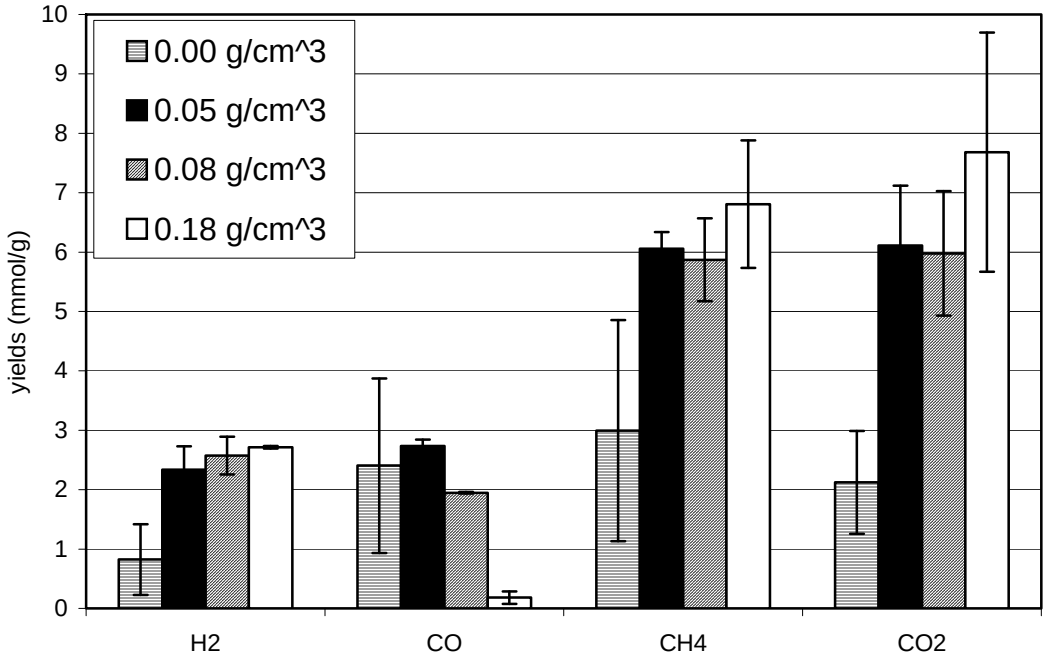

Figure 5.12. Gas yields as function of water density (60 minutes, 600°C, 9.0 % lignin loading).

5.2.5 Comparison with Stainless Steel

In Chapter 4, we found that the gas yields from cellulose SCWG can be higher than yields in stainless steel reactors in some cases. In others cases, such as high water density and low biomass loading situations, the yields from quartz reactors can be higher than the ones from stainless steel at the same conditions. In this section we present results from experiments in quartz reactors that were performed at the same conditions as the ones previously reported in the literature for stainless steel, in order to establish the same comparison for lignin SCWG.

Table 5. 2 makes a comparison with the work of Watanabe [1] in stainless steel, at 400°C, 60 min, 0.35 g/cm^3, and 12.6 wt %. From information in the article, we calculate the reactor surface area/biomass weight ratio to be about 6 mm^2/mg. The CO_2 yield is the same in quartz and stainless steel. All the other yields are higher in stainless steel than in quartz. The CO yield is 85 % higher, the H_2 yield is 52 % higher, and the CH_4 yield is 99 % higher in stainless steel. As a result, the sum of the yields is 33 % higher in stainless steel. These results suggest that catalysis from the stainless steel walls can significantly increase gas yields in lignin SCWG at these conditions.

Table 5. 2. Gas yields (mmol/g) from SCWG of lignin with no added catalyst (400°C, 60 min, 0.35 g/cm^3, 12.6 wt %).

	This Work	**Watanabe [1]**
Reactor Material	**Quartz**	**316 Stainless Steel**
CO_2	3.3	3.33
CO	0.3	0.56
H_2	0.5	0.76
CH_4	1.4	2.78
Sum	5.6	7.42

Table 5.3 shows a comparison of results in quartz reactors with results obtained in stainless steel from Osada [2, 4], at 400°C, 15 min, 0.33 g/cm^3, 5.0 wt %. From information in the articles, we estimate the reactor surface area/biomass ratio to be about

19 mm^2/mg for both studies. The two studies reported by Osada, even though at the same conditions, are inconsistent in places. The range of molar % reported for CO and H_2 are close to the ones we obtained in quartz reactors. It seems, though, that CO_2 is present in higher % in quartz, and CH_4 is present in higher % in stainless steel. The C, H and O yields are all higher in quartz reactors. The C yield is 83 % higher, the H yield is 31 % and the O yield is 118 % higher in quartz than in stainless steel. It is interesting to note that Osada's experiments were performed at high water densities and low biomass loadings. These conditions provided a similar outcome for cellulose as well, with yields in quartz being higher than the ones in stainless steel. The results suggest that the water density and biomass loading affect the relative importance of catalytic effects from reactors walls for SCWG of both cellulose and lignin.

Table 5.3. Molar % from lignin SCWG with no catalyst added (400°C, 15 min, 0.33 g/cm^3, 5.0 wt %).

	This Work	Osada [2]	Osada [4]
Reactor Material	Quartz	316 Stainless Steel	316 Stainless Steel
CO_2 (%)	53.2 ± 0.9	42	19
CO (%)	17.8 ± 0.1	16	7.4
H_2 (%)	4.5 ± 0.0	7	3.4
CH_4 (%)	24.5 ± 0.1	33	69.5
C yield (%)	6.8 ± 0.3	3.7	3.7
H yield (%)	7.6 ± 0.5	5.8	-
O yield (%)	29.4 ± 1.4	13.5	-

5.2.6 Comparison with Cellulose

In Chapter 4, we presented results for the gasification of cellulose in supercritical water. Having just described a similar work for lignin, we are now in a position to compare the gasification of the main components of biomass in supercritical water in the absence of catalytic effects.

Figure 5.13 shows the yields of each of the individual gases from SCWG of both cellulose and lignin at 600°C. Lignin provides substantially more CH_4 than cellulose,

which is reasonable given the potential direct formation of CH_4 from cleavage of methyl groups in lignin. Cellulose lacks these methyl substituents. Cellulose formed 2.6 mmol/g of H_2 after 10 minutes, and lignin only formed 1.8 mmol/g. Perhaps lignin produces less H_2 than cellulose because a larger quantity of H atoms is taken from lignin during formation of CH_4. While the CO yields are larger for lignin, cellulose provided a much higher yield of CO_2. This result could be related to cellulose containing 49 wt % O whereas lignin contains only 27 wt % O.

Figure 5.14 shows the C, H, O, and total gas yields for cellulose and lignin at 600°C and 10 minutes. The total gas yields (slightly over 40 %) are about the same for cellulose and lignin. Cellulose gasification produces a higher C yield than lignin (33.0 compared to 24.2 %), but H and O yields are higher for lignin. The H yield for lignin is 42.3 % (compared to 25.4 % for cellulose), and the O yield is 84.4 % (compared to 56.6 % for cellulose). The energy content is similar (about 20 % for cellulose and lignin). It seems, therefore, that lignin SCWG consumes more water than cellulose, leading to higher H and O yields, even though a larger fraction of the carbon is gasified in the case of cellulose. In most instances, the gas yields from cellulose and lignin respond similarly to changes in temperature, water density, and biomass loading. A few differences in the responses to changes in process variables can be highlighted, however. CH_4 responds differently for cellulose and lignin as the biomass loading changes. For cellulose, the CH_4 yield is not affected by increasing the loading, but it slightly increases for lignin. Actually, the biomass loading is an important tool to control CH_4/H_2 for SCWG of lignin and cellulose.

Figure 5.15 shows the CH_4/H_2 molar ratio as a function of the biomass loading for cellulose and lignin. Increasing the biomass loading decreases the CH_4/H_2 ratio from cellulose, but it increases the ratio from lignin. Therefore, the loading of cellulose and lignin can be adjusted to control the CH_4/H_2 ratio. For real biomass the optimum loading will depend on its cellulose/lignin ratio, as well as the intended use of the gas produced.

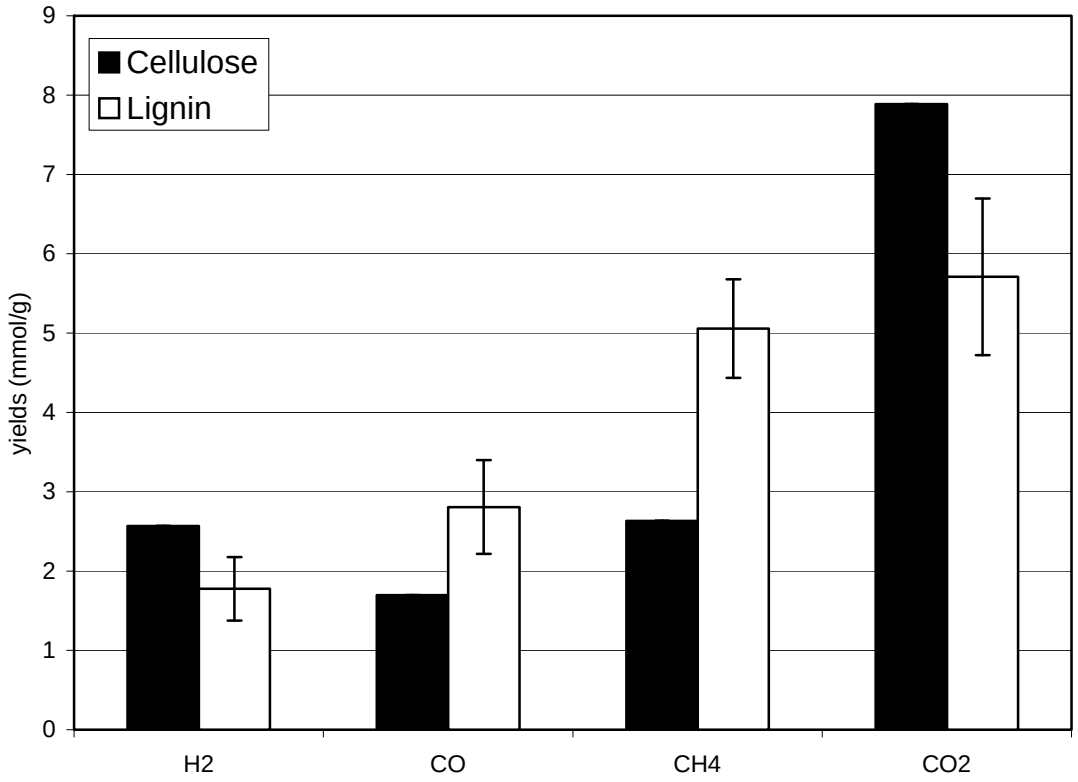

Figure 5.13. Gas yields for cellulose and lignin at 600°C, 10 minutes, 0.08 g/cm^3 and 9.0 wt % loading.

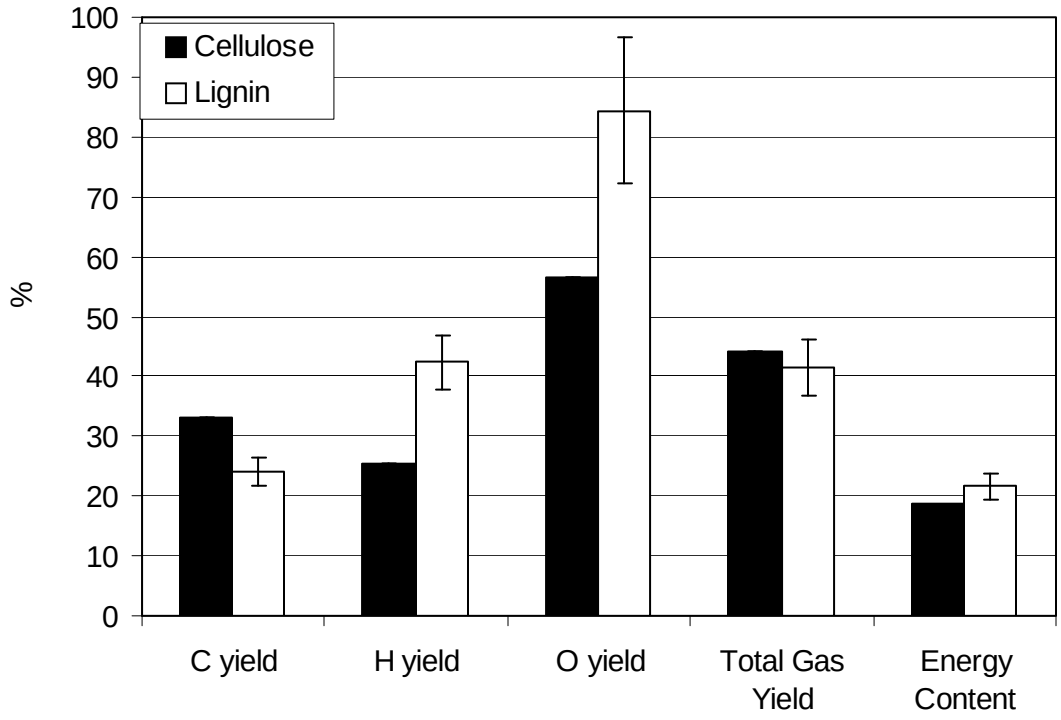

Figure 5.14. C, H, O, and total gas yields for cellulose and lignin at 600°C, 10 minutes, 0.08 g/cm^3 and 9.0 wt % loading.

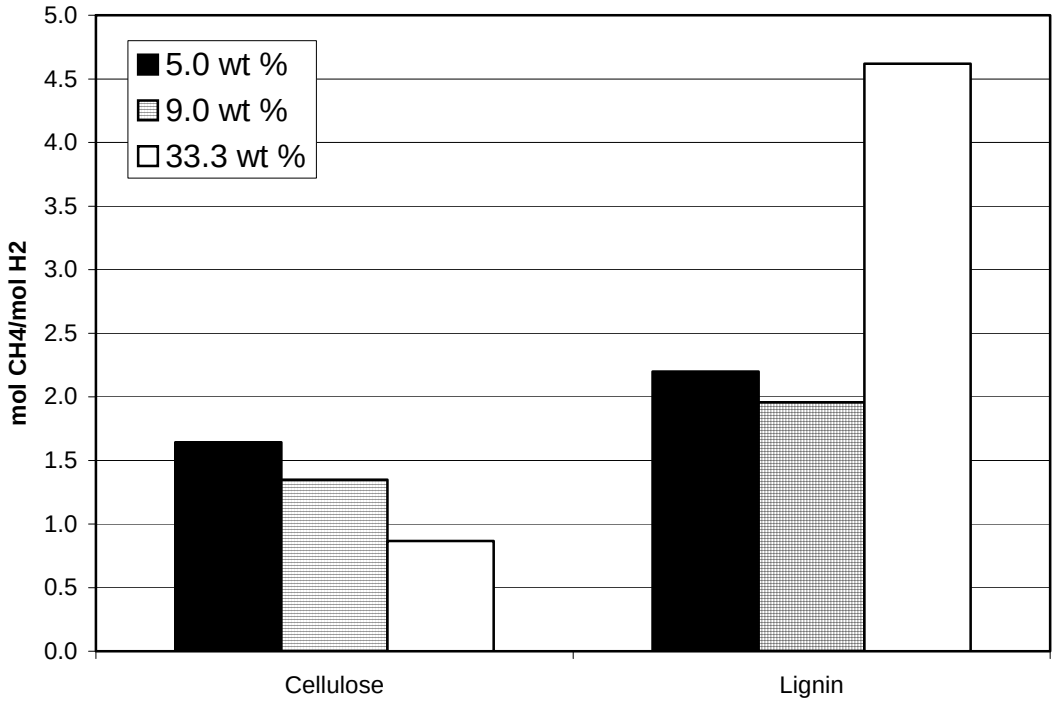

Figure 5.15. CH_4/H_2 molar ratio as function of biomass loading for cellulose and lignin (500°C/10 min for cellulose and 600 °C/75 min for lignin).

5.3 Conclusions

1.) This chapter presented the first results for lignin SCWG in the absence of catalytic effects from metal walls. These results will be helpful to evaluate effects of added metals in Chapter 7. We also presented the first systematic study of variables influencing gas yields from lignin SCWG.

2.) Yields in quartz reactors can be higher than the yields in stainless steel in some situations. At situations with low biomass loading (5.0 wt %) and high water density (0.33 g/cm^3), yields in quartz reactors can be higher. It seems that water density and biomass loading strongly affect the relative importance of catalysis from reactor walls in SCWG.

3.) The temperature is the most important variable controlling yields on lignin SCWG. Manipulating the lignin loading (wt %) provides a means to control the selectivity to H-containing gases.

4.) Unless a product gas with low CO yield is required, it is recommended to perform lignin SCWG always at low density (0.05 g/cm^3). The water density has little effect on yields (except for CO, that decreases with increasing water density). It is advantageous, therefore, to use low water densities to minimize energy consumption.

5.) To maximize H_2 and CH_4 production, high temperatures should be used. The highest H_2 yield (7.5 mmol/g) and the highest CH_4 yield (9.0 mmol/g) were obtained at the highest temperature (725°C). As a consequence, the highest energy content of the gas (37.4 %) was also obtained at this condition. If lignin SCWG goes to completion and forms exclusively CO and H_2, the product gas could contain 134 % of the original chemical energy. These higher gas yields can likely be obtained via catalyzed SCWG.

6.) CO yields decrease with increasing lignin loading and water density. At low water density (0.05 g/ml), a 1:1 CO/H_2 ratio is obtained. At the base case (600°C, 9.0 wt % loading, 0.08 g/ml), a 1:2 CO/H_2 ratio is obtained after 75 minutes.

7.) In the absence of catalysts, CH_4 and CO_2 are always the major products from SCWG of lignin. In the absence of SCW, CH_4 replaced CO_2 as a major product, the yields of H_2 and CO_2 are smaller, and the yield of CO is higher.

8.) SCWG of lignin appears to take place in two stages. During the first stage, gases are formed from solid and liquid species. During the second stage, the total gas yield remains roughly constant, but the product distribution changes because gas species react between themselves. The water-gas shift is a predominant reaction during the second stage. For lignin SCWG at the base case conditions, the first stage occurs during the initial 2.5 minutes, and the second stage occurs at longer times.

REFERENCES

[1] M. Watanabe, H. Inomata, M. Osada, T. Sato, T. Adschiri and K. Arai, "Catalytic effects of NaOH and ZrO2 for partial oxidative gasification of n-hexadecane and lignin in supercritical water." *Fuel,* vol. 82, pp. 545-552, 2003.

[2] M. Osada, T. Sato, M. Watanabe, T. Adschiri and K. Arai, "Low-Temperature Catalytic Gasification of Lignin and Cellulose with a Ruthenium Catalyst in Supercritical Water." *Energy & Fuels,* vol. 18, pp. 327-333, 2004.

[3] T. Sato, T. Furusawa, Y. Ishiyama, H. Sugito, Y. Miura, M. Sato, N. Suzuki, N. Itoh, "Effect of Water Density on the Gasification of Lignin with Magnesium Oxide Supported Nickel Catalysts in Supercritical Water" *Ind Eng Chem Res,* vol. 2, 615-622, 2006.

[4] M. Osada, O. Sato, M. Watanabe, K. Arai and M. Shirai, "Water Density Effect on Lignin Gasification over Supported Noble Metal Catalysts in Supercritical Water." *Energy & Fuels,* vol. 20, pp. 930-935, 2006.

[5] R. Font, M. Esperanza, A. Nuria Garcia, "Toxic by-products from the combustion of Kraft lignin", *Chemosphere,* vol. 6, 1047-1058, 2003.

[6] D. Ferdous, A.K. Dalai, A.K. Bej, S.K. Thring, "Production of H_2 and medium heating value gas via steam gasification of lignins in fixed-bed reactors", *Can. J. Chem. Eng.*, vol. 6, 913-922, 2001.

[7] T. Hanaoka, S. Inoue, S. Uno, T. Ogi, T. Minowa, "Effect of woody biomass components on air-steam gasification", *Biomass & Bioenergy*, v. 1, 69-76, 2004.

[8] N.W. Johanson, M.H. Spritzer, G.T. Hong, W.S. Rickman, *Proceedings of the 2001 U.S. DOE Hydrogen Program Review*, Baltimore, MD, U.S., National Renewable Energy Laboratory: Golden, CO, 2001; pp 197-212, Apr 17–19, 2001.

[9] R.O. Fournier, "An equation correlating the solubility of quartz in water from 25.degree. to 900.degree.C at pressures up to 10,000 bars", *Geochim. Cosmochim. Acta* vol. 10, 1969-1973, 1982.

[10] M. J. Antal Jr., S. G. Allen, D. Schulman, X. Xu and R. J. Divilio, "Biomass Gasification in Supercritical Water." *Ind Eng Chem Res,* vol. 39, pp. 4040-4053, 2000.

[11] D. C. Elliott and L. J. Sealock Jr, "Chemical processing in high-pressure aqueous environments: low-temperature catalytic gasification." *Chem. Eng. Res. Design,* vol. 74, pp. 563-566, 1996.

[12] G. J. DiLeo, M. E. Neff and P. E. Savage, "Gasification of guaiacol and phenol in supercritical water", *Energy & Fuel,* vol. *21*, pp. 2340-2345, 2007.

[13] Q. Yan, L. Guo, Y. Lu, “Thermodynamic analysis of hydrogen production from biomass gasification in supercritical water”, *Energy Conversion & Management*, vol. 27, pp. 1515-1528, 2006.

[14] M. Watanabe, H. Inomata and K. Arai, "Catalytic hydrogen generation from biomass (glucose and cellulose) with ZrO2 in supercritical water." *Biomass Bioenergy*, vol. 22, pp. 405-410, 2002.

[15] J. Figueiredo and S. Alves, "Waste wood pyrolysis," in *Encyclopedia of Environmental Control Technology* , vol. 1, Anonymous Houston: Gulf, 1989, pp. 282-286.

[16] C. A. Bernardo and D. L. Trimm, "The kinetics of gasification of carbon deposited on nickel catalysts." *Carbon*, vol. 17, pp. 115-120, 1979.

[17] N. Jand, V. Brandani and P. U. Foscolo, "Thermodynamic Limits and Actual Product Yields and Compositions in Biomass Gasification Processes." *Ind Eng Chem Res*, vol. 45, pp. 834-843, 2006.

[18] T. Yoshida, Y. Oshima and Y. Matsumura, "Gasification of biomass model compounds and real biomass in supercritical water," *Biomass and Bioenergy*, vol. 26, pp. 71-78, 2004.

[19] M.D. Mann, R.Z. Knutson, J. Erjavec, J.P. Jacobsen, “Modeling reaction kinetics of steam gasification for a transport gasifier”, *Fuel*, vol. 11-12, 1643-1650, 2004.

CHAPTER 6
A KINETIC MODEL FOR SUPERCRITICAL WATER GASIFICATION OF BIOMASS

Chapters 4 and 5 presented the first results for gasification of cellulose and lignin in supercritical water in the absence of potential metal catalysts. When describing the experimental results, we provided possible explanations for the observed trends in terms of chemical phenomena commonly reported in SCWG systems. In this chapter, we develop a kinetic model and fit our data to it in order to gain understanding of the chemical reactions taking place. In this fitting process, we used information on the temporal variation of the gas yields (H_2, CO_2, CO and CH_4) at the base case conditions for cellulose and lignin. The objective of the model is to identify the reaction pathways leading to the formation of gases and quantify rates of formation. This information is useful to identify potential catalysts for SCWG. The first part of this chapter is devoted to explaining the concepts involved in the elaboration of the model. The second part shows rate constants, quality of fittings and predictions, and comparisons to equilibrium calculations. In the last part, we use the model to identify the most important reactions forming the gases.

6.1 Introduction

Kinetic models dealing with gas yields for SCWG are non-existent. The few attempts to fit kinetic models to biomass decomposing in hot compressed water focus solely on feedstock conversion [1, 2], without capturing the chemistry leading to formation of gas species. The complexity of biomass feedstocks has been a major obstacle to advances in this area. Chapter 2 provides a description of the currently accepted reaction pathways for SCWG, especially for cellulose, but not much is known at the moment about the rates at which these reactions occur, and the main routes of gas formation are unclear. For instance, it is known that the methanation reaction takes place

in SCWG systems, but it is not known if most of the CH_4 formed actually originates from methanation or possibly from other gasification routes, such as direct pyrolysis of methyl groups present in lignin. If most of the CH_4 originates from methanation, how close to equilibrium are we at typical SCWG conditions? Can we substantially improve CH_4 yields by adding a catalyst that promotes methanation? These are some of the questions we aim to answer with the aid of our kinetic model. This information is useful in designing SCWG systems.

The model is largely based on the pathways currently accepted in the literature for SCWG. It focuses on reactions involving gas species and simplifies reactions involving intermediates, by defining a generic intermediate species. Following, we define the reactions involved in the model.

Reaction 1. Hydrolysis

For Cellulose: $(C_6H_{10}O_5)_n + n\ H_2O \xrightarrow{k_1} n\ C_6H_{12}O_6$

For Lignin: $(C_{10}H_{10}O_3)_n + n\ H_2O \xrightarrow{k_1} n\ C_{10}H_{12}O_4$

When cellulose (or lignin) is placed in water at supercritical conditions, the first step, as reported by Matsumura [3], is the physical process of solvation of the organic polymer molecules by water. This physical process takes place simultaneously with the hydrolytic attack of the polymeric structures by the water surrounding it. Water hydrolyzes cellulose and lignin by attacking ether bonds connecting its monomers. This step often leads to the formation of oligomers, such as cellobiose and cellotriose originating from cellulose. These oligomers can be further hydrolyzed, forming the monomer glucose. For the purpose of this model, we will assume hydrolysis leads directly to the monomers. While the monomer for cellulose is glucose, the monomer for lignin is simply based on the average composition of organosolv lignin, which is decomposed into monomers by the addition of one molecule of water. It is known that the hydrolysis step is very fast. Sasaki [1] showed that cellulose is completely converted in water at 350 °C and 25 MPa after only 4 s. Bobleter [4] reported that over 90 % of lignin disappears after only 0.4 min at 365°C. For this reason, we assume that the initial reactant

is the monomer instead of the polymer itself. Therefore, for the gasification of cellulose, our initial reactant is glucose. Calculation of the amount of monomer initially present is based on the amount of carbon present in the cellulose/lignin.

Reaction 2. Intermediate Formation.

For cellulose: $C_6H_{12}O_6 \xrightarrow{k_2} C_xH_yO_z$

For lignin. $C_{10}H_{12}O_4 \xrightarrow{k_2} C_xH_yO_z$

Once the monomer is formed, it can undergo a variety of reactions leading to a great number of decomposition products. Glucose, for instance, can undergo isomerization forming fructose, dehydration, retro-aldol condensation, and hydrolysis [5, 6]. A key concept in the present model is the treatment of all the different intermediate compounds as a single pseudo-component. It is not practical to monitor and explicitly account for every possible intermediate compound, so we adopted this lumping scheme for the intermediates. We define the intermediate species as $C_xH_yO_z$, which represents any reactive intermediate originating from glucose or the lignin monomer. These intermediates ultimately lead to the formation of gases.

Reactions 3 and 4. Steam-Reforming.

Steam-Reforming I $C_xH_yO_z + (x\text{-}z)\ H_2O \xrightarrow{k_3} x\ CO + (x\text{-}z + y/2)\ H_2$

Steam-Reforming II $C_xH_yO_z + (2x\text{-}z)\ H_2O \xrightarrow{k_4} x\ CO_2 + (2x\text{-}z + y/2)\ H_2$

One of the ways organic compounds decompose in the presence of water to form gases is via steam-reforming. The intermediate $C_xH_yO_z$ reacts with the water in excess leading to CO and H_2 (Steam-reforming I), or CO_2 and H_2 (Steam-Reforming II). For the purposes of our steam reforming calculations, we assume that the intermediate species is chemically similar to the original monomer, just as fructose is similar to glucose. So, for cellulose, x = 6, y = 12 and z = 6. For lignin, x = 10, y = 12 and z = 4.

Reactions 5 to 8. Intermediate Decomposition

CO from Intermediate $C_xH_yO_z \xrightarrow{k_5} CO + C_xH_yO_z$

CO_2 from intermediate $C_xH_yO_z \xrightarrow{k_6} CO_2 + C_xH_yO_z$

CH_4 from intermediate $C_xH_yO_z \xrightarrow{k_7} CH_4 + C_xH_yO_z$

H_2 from intermediate $C_xH_yO_z \xrightarrow{k_8} H_2 + C_xH_yO_z$

Steam-reforming by itself cannot accurately describe the way gases are formed in SCWG. There are multiple ways the intermediates can decompose forming gases. For instance, in the case of lignin decomposition, the methyl groups in the monomer structure can be pyrolyzed, directly leading to the formation of CH_4. To account for these phenomena, we introduced the possibility of direct formation of the gas species from the reactive intermediate. Also, each intermediate molecule can undergo decomposition reactions multiple times, releasing small molecules such as H_2 or CO in each step and creating a new intermediate molecule.

Reaction 9. Char Generation.

$$C_xH_yO_z \xrightarrow{k_9} wC + C_{x-w}H_yO_z$$

Intermediate species in SCWG can react forming char. In our model, the formation of char is also a termination reaction of the active intermediate $C_xH_yO_z$, forming a non-reactive intermediate $C_{x-w}H_yO_z$. Reaction 9 does not generate any products of interest, so ideally its rate should be as small as possible in order to maximize the production of H_2, CH_4, CO and CO_2 from the intermediate.

Reactions 10 and 11. Gas-phase reactions.

Water-Gas Shift $CO + H_2O \leftrightarrow CO_2 + H_2$

Methanation $CO + 3\,H_2 \leftrightarrow CH_4 + H_2O$

Once the gas species are formed, reactions 10 and 11 can change gas product composition. The water-gas shift reaction consumes CO and is usually believed to be one of the main reaction pathways for the production of H_2. Likewise, methanation is believed to be an important route for the formation of CH_4. In situations where H_2 is the target product, the forward methanation reaction should be avoided. Water-gas shift and

methanation are the only reversible reactions in this model. We considered the possibility of adding other typical gasification reactions such as hydrogenation and the Boudouard reaction, but equilibrium calculations done in ASPEN showed that these reactions do not take place to any appreciable extent in the conditions of this work. We used the REquil reactor block in ASPEN to perform the calculations. This block is designed to provide equilibrium concentrations for a given reaction or set of reactions defined by the user. For properties calculation, the UNIQUAC method was used. For the input concentrations, we used the base case experimental concentrations obtained at 2.5 minutes. We then calculated the equilibrium concentrations for the hydrogenation and Boudouard reaction at each temperature. To keep the water density at 0.08 g/ml (base case), the pressure was set to 25 MPa at 500°C and 31 MPa at 600°C.

6.2 Reaction Engineering.

We used constant-volume quartz batch reactors for all the experiments, so the reaction engineering analysis is relatively simple. Following are the main assumptions used in writing the rate equations:

- The initial reactant is the monomer instead of the polymer (hydrolysis is fast)
- The intermediate species is chemically identical to the monomer for steam reforming reactions
- The intermediate species is only consumed when it undergoes a termination reaction, forming char and a non-reactive intermediate.
- Only the water-gas shift and methanation reactions are reversible.

Following are the rate equations for each of the species involved.

CO:

Cellulose:

$$\frac{dC_{CO}}{dt} = xk_3C_I + k_5C_I - k_{10}C_{CO}C_W + k_{10i}C_{CO_2}C_{H2} - k_{11}C_{CO}C_{H2} + k_{11i}C_{CH4}C_W \quad (6.1)$$

Lignin: $\frac{dC_{CO}}{dt} = xk_3C_IC_W + k_5C_I - k_{10}C_{CO}C_W + k_{10i}C_{CO_2}C_{H2} - k_{11}C_{CO}C_{H2} + k_{11i}C_{CH4}C_W \quad (6.2)$

CO_2:

$$\frac{dC_{CO_2}}{dt} = xk_4C_IC_W + k_6C_I + k_{10}C_{CO}C_W - k_{10i}C_{CO2}C_{H2} \quad (6.3)$$

CH_4:

$$\frac{dC_{CH4}}{dt} = k_7C_I + k_{11}C_{CO}C_{H2} - k_{11i}C_{CH4}C_W \quad (6.4)$$

H_2:

Cellulose:

$$\frac{dC_{H2}}{dt} = (x - y + y/2)k_3C_I + (2x - z + y/2)k_4C_IC_w + k_8C_I + k_{10}C_{CO}C_W - k_{10i}C_{CO2}C_{H2} - 3k_{11}C_{CO}C_{H2} + 3k_{11i}C_{CH4}C_W \quad (6.5)$$

Lignin:

$$\frac{dC_{H2}}{dt} = (x - y + y/2)k_3C_IC_W + (2x - z + y/2)k_4C_IC_w + k_8C_I + k_{10}C_{CO}C_W - k_{10i}C_{CO2}C_{H2} - 3k_{11}C_{CO}C_{H2} + 3k_{11i}C_{CH4}C_W \quad (6.6)$$

Intermediate:

For cellulose:

$$\frac{dC_I}{dt} = k_2C_M - k_3C_I - k_4C_IC_W - k_9C_I \quad (6.7)$$

For lignin:

$$\frac{dC_I}{dt} = k_2C_M - k_3C_IC_w - k_4C_IC_W - k_9C_I \quad (6.8)$$

Monomer:

$$\frac{dC_M}{dt} = -k_2C_M \quad (6.9)$$

Water:

Cellulose:

$$\frac{dC_W}{dt} = -6k_3C_IC_W - 18k_4C_IC_W - k_{10}C_{CO}C_W + k_{10i}C_{CO2}C_{H2} + k_{11}C_{CO}C_{H2} - k_{11i}C_{CH4}C_W \quad (6.10)$$

Lignin:

$$\frac{dC_W}{dt} = -6k_4C_IC_W - k_{10}C_{CO}C_W + k_{10i}C_{CO2}C_{H2} + k_{11}C_{CO}C_{H2} - k_{11i}C_{CH4}C_W \quad (6.11)$$

Non-reactive species:

$$\frac{dC_{Non}}{dt} = k_9C_I \quad (6.12)$$

Equation 6.12 accounts for what we call a non-reactive species (Non). This is simply accounting for the char (C) and the non-reactive intermediate ($C_{x-w}H_yO_z$) from reaction 9 altogether. By using this definition it is possible to quantify the amount of material left unreacted after SCWG.

6.3 Method

The experimental data reported as the base case in Chapters 4 and 5 for non-catalytic SCWG of cellulose and lignin were used in fitting the model. The fitted variables were the concentrations of CH_4, CO_2, CO, and H_2 (mol/l) as functions of time, and the base case conditions are 500°C (cellulose), 600°C (lignin), 0.08 g/ml water density, and 9.0 wt % biomass loading. Experiments were performed from 2.5 to 30 minutes for cellulose, and from 2.5 to 75 minutes for lignin.

The average particle size for cellulose is 116 μm, and for lignin it is 289 μm. Simmons [7] has shown that pyrolysis of cellulose in the range 450-500°C is free from mass transfer limitations for particles as large as 200 μm. Vamvuka [8] performed TGA for several biomass feedstocks and was able to measure kinetics without mass-transfer limitations using particles of 250 μm at 10°C/min heating rate. In the present work, the use of SCW as solvent along with the high heating rates of our experimental setup should minimize mass transfer limitations in comparison to pyrolysis at low heating rates. For this reason, we believe that mass transfer limitations can be safely neglected in the present study.

The objective function minimized is the Sum of the Square of Prediction Errors (difference between calculated and measured gas concentrations). Scientist 3.0 from Micromath was used to fit experimental data. Initial guesses for the rate constants were found manually by trial-and-error method. Polymath 5.1 was used for the simulations after the rate constants were known.

The rate constants fitted were k_2, k_3, k_4, k_5, k_6, k_7, k_8, k_9, k_{10} and k_{11}. The rate constants for the reverse reactions (k_{10r} and k_{11r}) were related to the forward rate constants (k_{10} and k_{11}) by the equilibrium constant K:

$$k_r = \frac{k_f}{K} \tag{6.13}$$

The equilibrium constant for the water-gas shift and methanation reactions were obtained from the ASPEN Plus Software. We used the REquil reactor block in ASPEN to perform the calculations. This block is designed to provide equilibrium concentrations for a given reaction or set of reactions defined by the user. For properties calculation, the UNIQUAC method was used. For the input concentrations, we used the base case experimental concentrations obtained at 2.5 minutes. We then calculated the equilibrium constants using the equilibrium concentrations for the water-gas shift and methanation at each temperature. To keep the water density at 0.08 g/ml (base case), the pressure was set to 25 MPa at 500°C and 31 MPa at 600°C. shows the input concentrations and the resulting output concentrations obtained from ASPEN. Using the output concentrations in Table 6.1, we calculated K_{10} (equilibrium constant for the water-gas shift) and K_{11} (equilibrium constant for methanation) using equations 6.14 and 6.15:

$$K_{10} = \frac{C_{H2}.C_{CO2}}{C_{CO}.C_{H2O}} \tag{6.14}$$

$$K_{11} = \frac{C_{CH4}.C_{H2O}}{C_{CO}.C_{H2}^{\ 3}} \tag{6.15}$$

For the water-gas shift reaction, we obtained the equilibrium constant 5.15 at 500°C and 2.68 at 600°C. For methanation, the equilibrium constant is 3.62×10^5 l^2/mol^2 at 500°C and 1.02×10^4 l^2/mol^2 at 600°C.

Table 6.1. Input and output Gas Concentrations (mol/L) in ASPEN.

Water-Gas Shift	Input (500° C)	Output (500° C)	Input (600° C)	Output (600° C)
CO	$2.22x10^{-2}$	$6.36x10^{-5}$	$2.22x10^{-2}$	$1.56x10^{-4}$
H_2O	$4.12x10^{0}$	$4.10x10^{0}$	$4.12x10^{0}$	$4.10x10^{0}$
CO_2	$2.97x10^{-2}$	$5.18x10^{-2}$	$2.97x10^{-2}$	$5.17x10^{-2}$
H_2	$3.71x10^{-3}$	$2.59x10^{-2}$	$1.11x10^{-2}$	$3.32x10^{-2}$
Methanation	Input (500° C)	Output (500° C)	Input (600° C)	Output (600° C)
CO	$2.22x10^{-2}$	$2.42x10^{-2}$	$2.22x10^{-2}$	$3.68x10^{-2}$
H_2	$3.71x10^{-3}$	$9.45x10^{-3}$	$1.11x10^{-2}$	$5.48x10^{-2}$
CH_4	$3.71x10^{-3}$	$1.79x10^{-3}$	$2.97x10^{-2}$	$1.51x10^{-2}$
H_2O	$4.12x10^{0}$	$4.12x10^{0}$	$4.12x10^{0}$	$4.10x10^{0}$

6.4 Results

The rate constants obtained are shown in Table 6.2.

Table 6.2. Rate Constants at 500°C (Cellulose) and 600°C (Lignin).

	Cellulose	**Lignin**
k_2 (min^{-1})	$2.00x10^{1}$	$1.67x10^{0}$
k_3 (min^{-1}) or ($L.mol^{-1}.min^{-1}$)	$5.15x10^{-3}$	$5.00x10^{-4}$
k_4 ($L.mol^{-1}.min^{-1}$)	$0.00x10^{0}$	$2.73x10^{-3}$
k_5 (min^{-1})	$2.44x10^{-1}$	$5.39x10^{-1}$
k_6 (min^{-1})	$4.22x10^{-1}$	$7.67x10^{-1}$
k_7 (min^{-1})	$1.11x10^{-1}$	$9.42x10^{-1}$
k_8 (min^{-1})	$5.56x10^{-4}$	$0.00x10^{0}$
k_9 (min^{-1})	$4.26x10^{-1}$	$9.38x10^{-1}$
k_{10} ($L.mol^{-1}.min^{-1}$)	$6.09x10^{-3}$	$2.80x10^{-3}$
k_{10i} ($L.mol^{-1}.min^{-1}$)	$1.18x10^{-3}$	$1.05x10^{-3}$
k_{11}($L.mol^{-1}.min^{-1}$)	$0.00x10^{0}$	$7.71x10^{-2}$
k_{11i} ($L.mol^{-1}.min^{-1}$)	$0.00x10^{0}$	$7.52x10^{-6}$

Figures 6.1 and 6.2 show the base case experimental data, along with the fitting, for cellulose and lignin. The model clearly identifies the trends and fits the base case data very well for both cases. CO is rapidly formed in the initial minutes, reaching a maximum and being consumed at longer times. CO_2 and CH_4 formation rates are also high in the first minutes, becoming much smaller at longer times. The yield of H_2 increases steadily for cellulose, while for lignin it increases rapidly during the initial minutes.

Once the rate constants are known, there are some questions we would like to address in order to verify how accurate the model is in capturing the chemistry taking place in SCWG. These questions are: 1) Can the model be used to predict experimental data that were not used in the fitting process? 2) If we use the model equations to simulate SCWG for long periods of time in an attempt to reach equilibrium, how well would these predictions match thermodynamic equilibrium calculations?

To answer the first question, we refer back to Chapters 4 and 5 where we presented results obtained at different temperatures, biomass loadings and water densities. We cannot use data at different temperatures to test the model, since for those data the rate constants are different than the ones we have from the fitting process. Therefore we chose to use the biomass loading and the water density as testing variables for our model. We simulated SCWG at different biomass loadings (5.0 wt % and 33.3 wt %), and different water densities (0.00 g/ml, 0.05 g/ml, 0.18 g/ml). In order to show how well the predictions worked in general, we gathered all the results in a single plot for each feedstock (Figures 6.3 and 6.4). The experimental yields are plotted as a function of the predicted yields, in such a way that perfect predictions would make the points fall in the diagonal line shown.

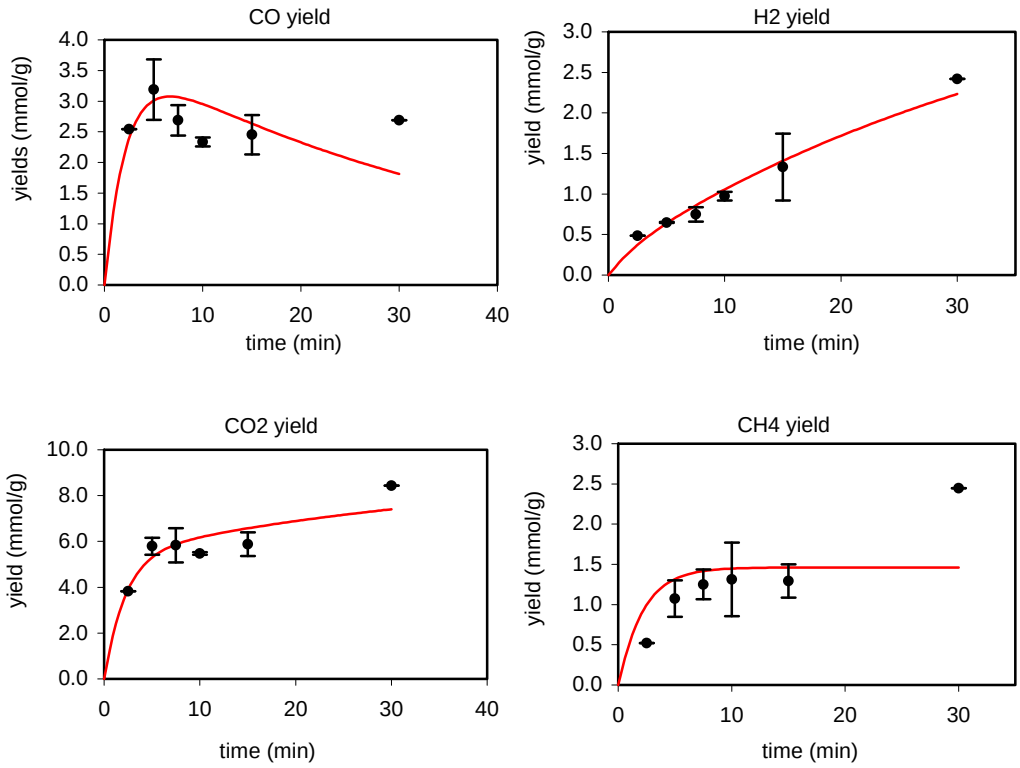

Figure 6.1. Base case fitting for cellulose SCWG (500°C, 0.08 g/ml, 9.0 wt %).

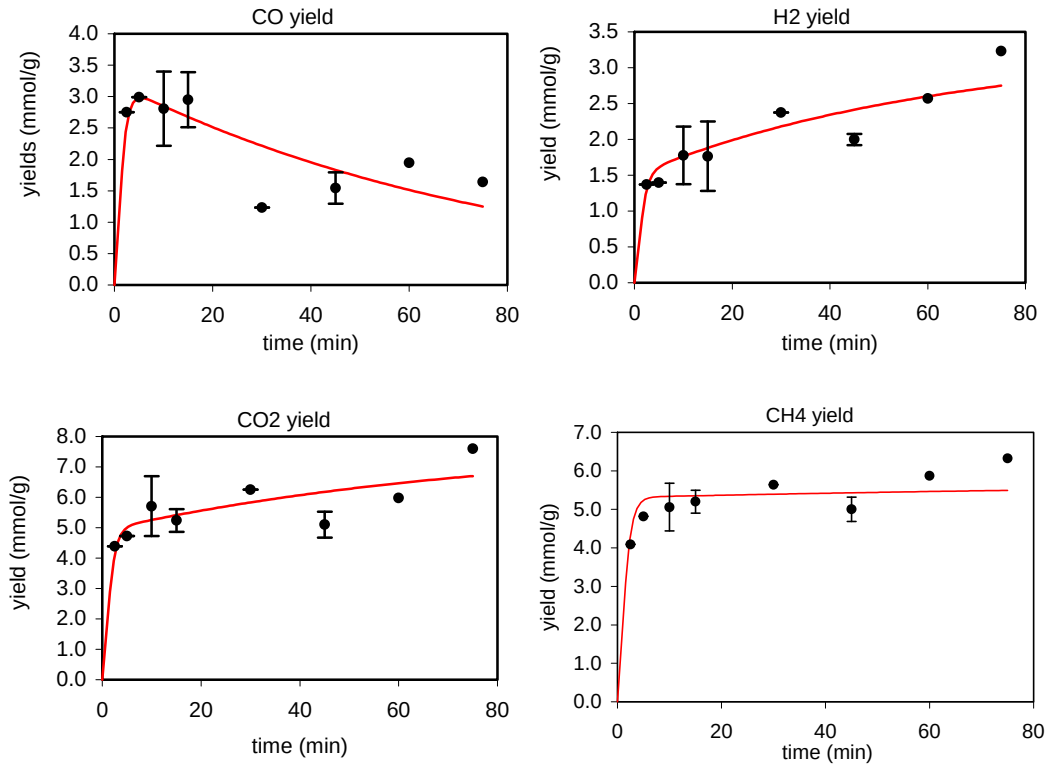

Figure 6.2. Base case fitting for lignin SCWG (600°C, 0.08 g/ml, 9.0 wt %).

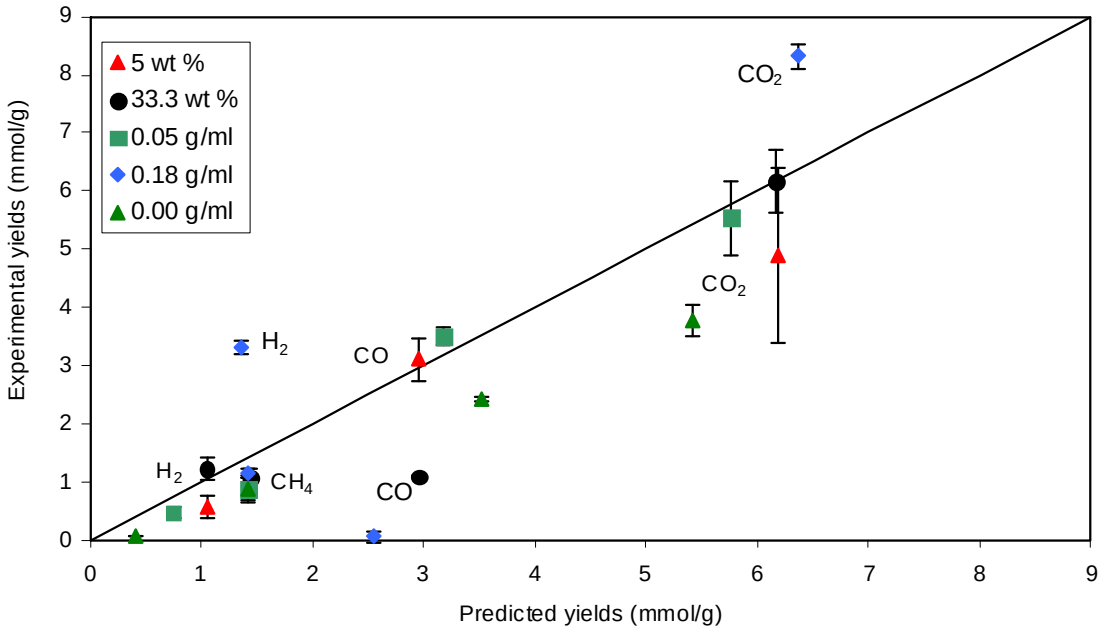

Figure 6.3. Model Predictions for Cellulose (10 min for wt %, 7.5 min for g/ml).

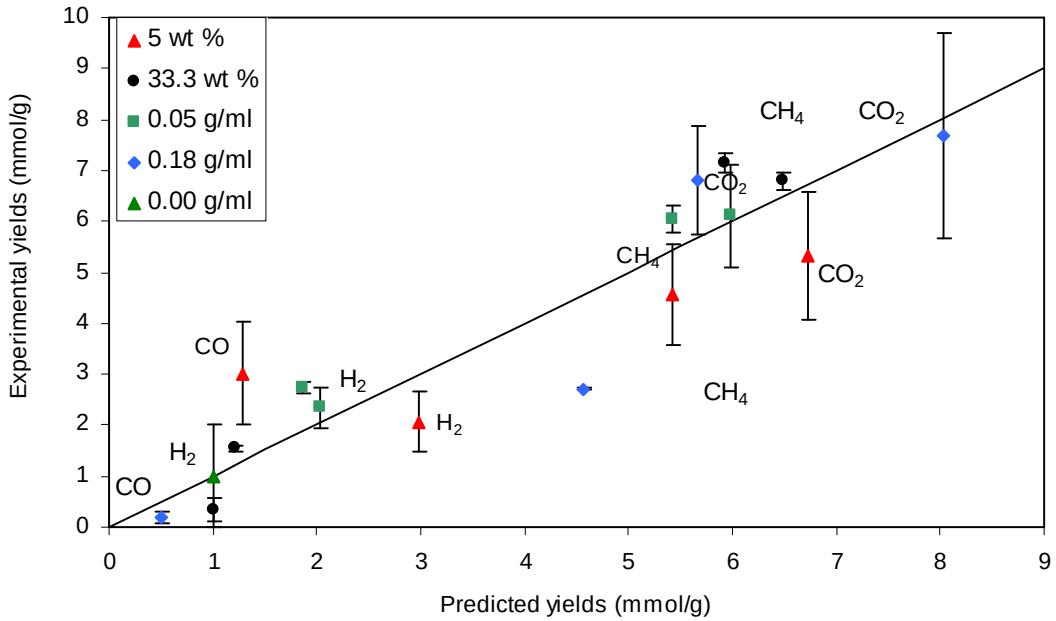

Figure 6.4. Model Predictions for Lignin (75 min for wt %, 60 min for g/ml).

Figures 6.3 and 6.4 show that the model can predict the results for most of the gas yields at the several biomass loadings for both cellulose and lignin with good proximity. We can also look at the same information in a different way to evaluate more specific situations. In Figures 6.5 – 6.7, we examine the trends of how the yields change with biomass loading and water density, comparing experimental results with model predictions. For cellulose, there was no effect of the biomass loading on yields. This finding is in good agreement to what was already reported on Chapter 4, where changes in cellulose loading have little effect on gas yields in the range 5.0 to 33.3 wt %. For lignin, the biomass loading has a larger effect on yields, and this effect is shown in Figure 6.5. The model captures the slight decreases in H_2 and CO yields as the lignin loading increases, as well as the slight increase in CH_4, while CO_2 appears to remain constant.

The effect of water density on gas yields in shown for cellulose in Figure 6.6 and for lignin in Figure 6.7. The model identifies the main trends for cellulose and lignin, matching the experimental results reasonably well in most cases. CO decreases with water density, while H_2 increases. The CO_2 yield slightly increases with water density, and CH_4 remains nearly unchanged. The largest disagreement between experimental data and model predictions seem to take place at the highest water density, 0.18 g/ml (especially for cellulose). These differences are possibly due to changes in the rates of the water-gas shift reaction as function of the water density. As has been reported by Rice et al [9] and Araki et al [10], the kinetics of the water-gas shift depends on water density.

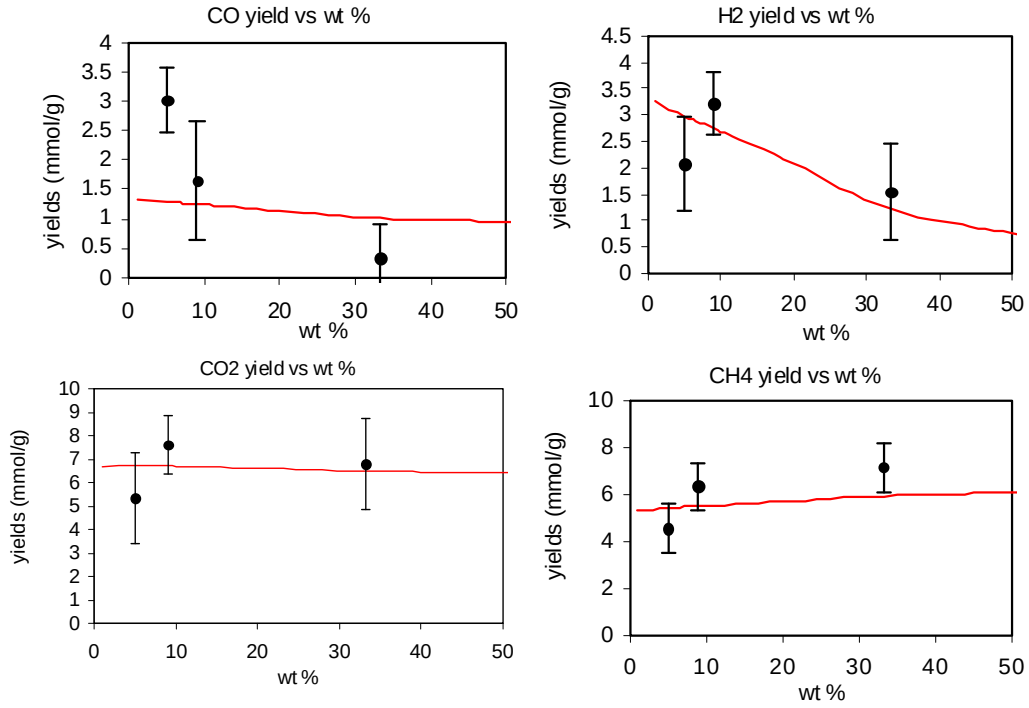

Figure 6.5. Effect of lignin loading (75 min).

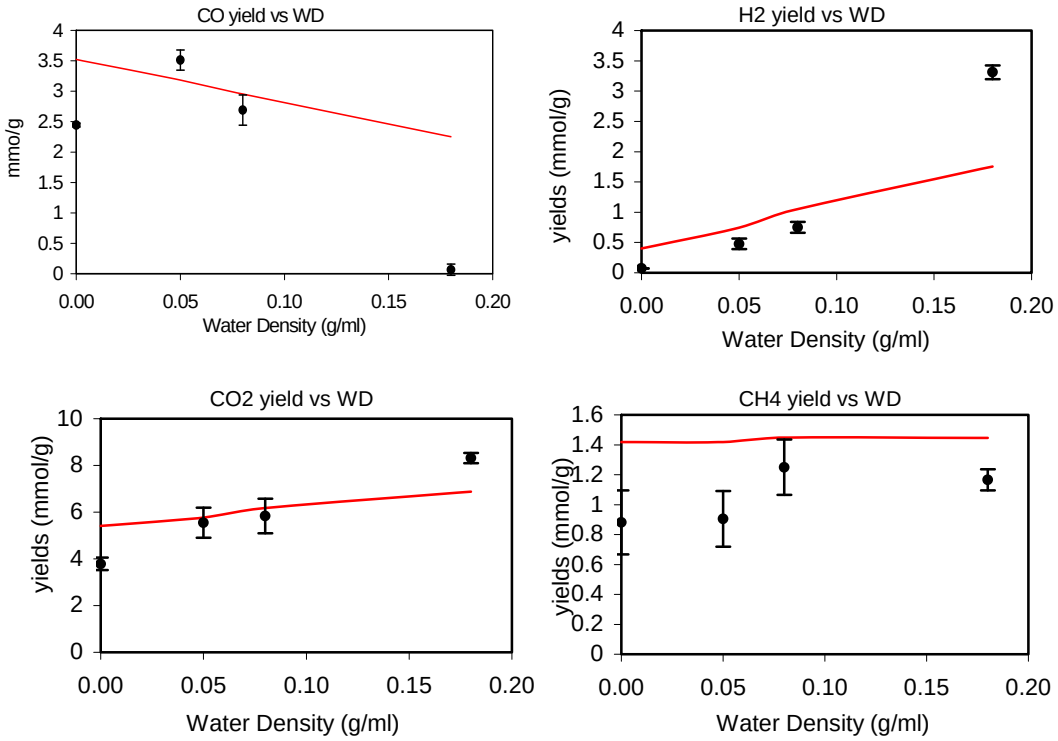

Figure 6.6. Effect of water density for cellulose (7.5 min).

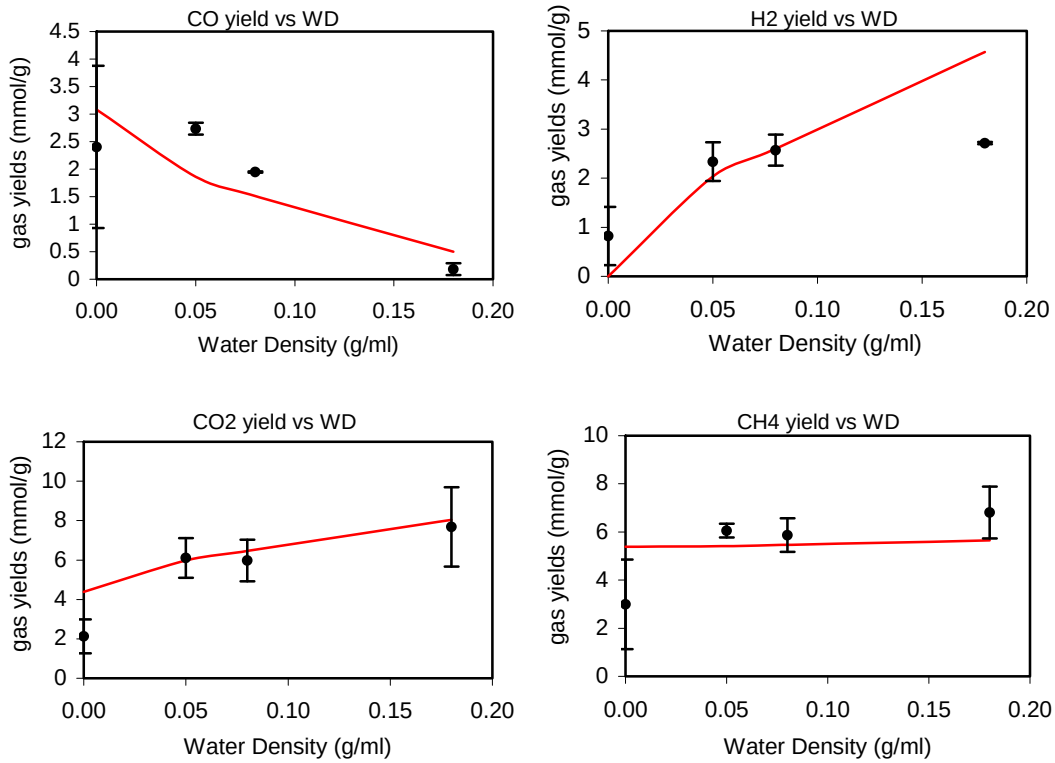

Figure 6.7. Effect of water density for lignin (60 min).

Having tested our model by making predictions at different biomass loadings and water densities, we turn our attention to equilibrium. If the model actually represents the correct chemistry taking place in SCWG, it should be able to provide realistic equilibrium product distributions. We simulated equilibrium SCWG by running the model for long periods of time until the yields stopped changing. This type of approach was only possible for lignin, because for cellulose at 500°C the rate of methanation is very small (fitted as zero), making it impossible to reach equilibrium. For lignin, the yields for all the gas species become constant at about 40,000 minutes (almost 28 days), indicating that at the experimental conditions we worked, we are very far from reaching equilibrium and would certainly need good catalysts for water-gas shift and methanation if we are to achieve this goal.

Once equilibrium is achieved with the kinetic model, we can compare its results with thermodynamic calculations. ASPEN Plus was used for this purpose. We used the RGibbs reactor block in ASPEN. This block calculates equilibrium concentrations without requiring knowledge of reaction stoichiometry, by minimizing the Gibbs free energy. For properties calculation, the UNIQUAC method was used. Neglecting the contribution from the product gases, we estimate the compressibility factor to be 1.0 at these conditions, which means water behaves as an ideal gas. Just as in the kinetic model, our starting monomer from lignin is $C_{10}H_{12}O_4$. The feed contains the monomer and water in the same initial compositions as the corresponding situations in the model. The product can contain the monomer, water, CO, H_2, CO_2 and CH_4. The pressure was set according to the water density (which was one of the variables in the study). Figure 6.8 shows a comparison of model predictions with thermodynamic calculations for lignin at the base case conditions (600°C). Model predictions agree extremely well with thermodynamic equilibrium calculations. H_2 and CO_2 are the major products (35 – 45 % each), with about 25 % of CH_4 and very small molar % of CO. It is important to make a note here about the water-gas shift reaction. Even though under more conventional fuel processing conditions water-gas shift systems at this temperature have a much higher fraction of CO in equilibrium, in SCW systems a large excess of water is present, which pushes the equilibrium in the direction of product formation and consuming CO.

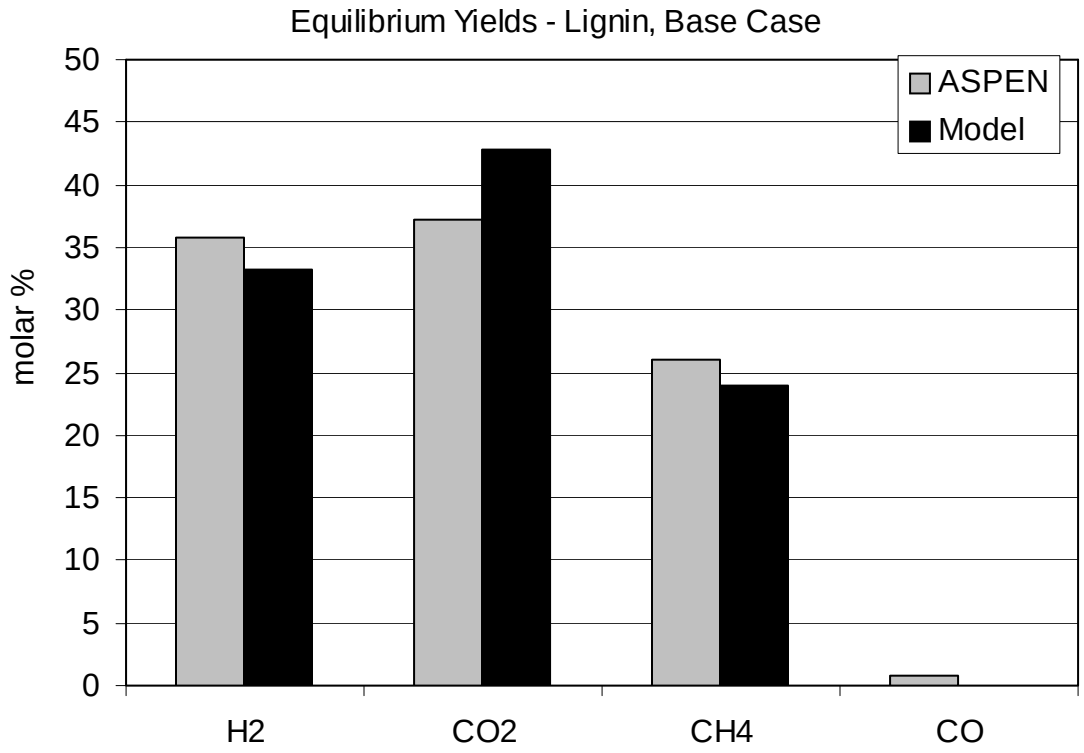

Figure 6.8. Equilibrium Composition for Lignin, Base Case.

It is also important to know if the model predictions for equilibrium respond appropriately to variations in biomass loading and water density. We varied the biomass loading over a wide range (1.0 – 50.0 wt %) to verify the accuracy of model predictions in this range (Figure 6.9). The model and the thermodynamic calculations agree to within a few percent. The CO molar % is less than 2 % up to 50 % lignin loading. The CO_2 molar % slowly increases with loading. The H_2 molar % in equilibrium decreases and the CH_4 molar % increases. The biomass loading is an important tool to control equilibrium selectivities towards H_2 or CH_4.

Figure 6.10 shows the effect of water density on the equilibrium molar %. Once more, the more predictions agree reasonably well with thermodynamic calculations. The water density has a small effect on the equilibrium product composition. CO molar % is close to zero, CO_2 remains at 35- 40 %, H_2 remains at about 30 – 35 %, and CH_4 at about 25-30 %.

We have shown that the kinetic model can successfully predict experimental data for a range of biomass loadings and water densities studied in this work, and that equilibrium predictions also agree with thermodynamic calculations. These successes lead us to believe that the reactions we included in the model and the parameter estimates we obtained are adequate for describing SCWG of lignin and cellulose under the experimental conditions used in this study. Focusing now more specifically on the rate constants, we can establish a few comparisons with work previously reported in the literature. In our model, the intermediate species can be dependent on the type of feedstock used (cellulose or lignin), but the water-gas shift and methanation reactions do not involve the intermediate and therefore do not depend on the type of feedstock used. This means we can compare the rate constants of the water-gas shift and methanation reactions obtained from cellulose and lignin, and we can also compare them with previous work reported in the literature. While the methanation reaction without added catalysts has not yet been studied in SCW, some researchers have studied the kinetics of the water-gas shift in SCW [9, 11]. Table 6.3 shows the rate constants obtained in these studies compared to the water-gas shift rate constants obtained in this work at 500°C (cellulose experiments) and 600°C (lignin experiments).

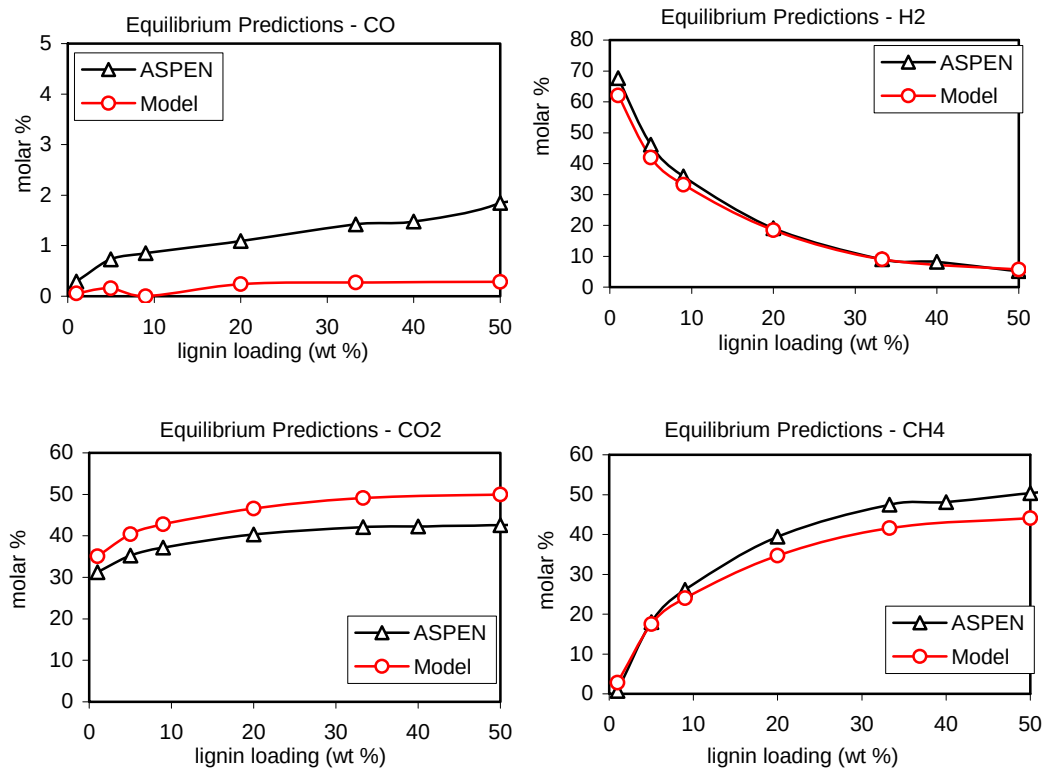

Figure 6.9. Effect of Lignin Loading on Equilibrium Composition.

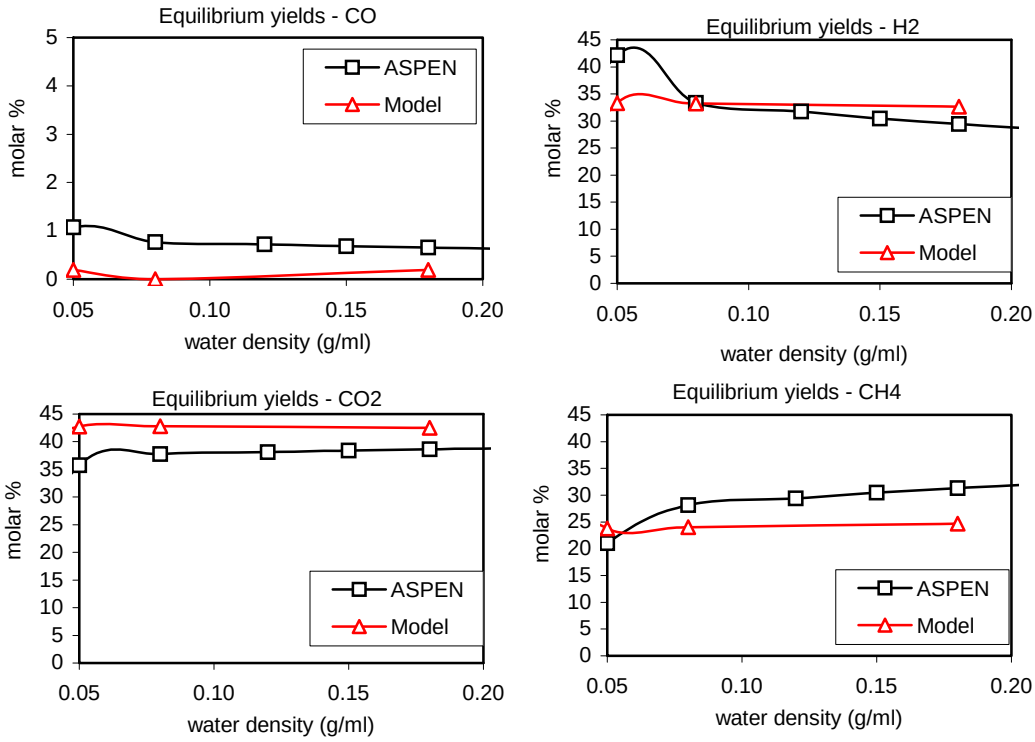

Figure 6.10. Effect of Water Density on Equilibrium Composition (Lignin).

Table 6.3. Rate constants for water-gas shift in SCW.

	T (°C)	Water Density (g/cm^3)	k ($L.mol^{-1}.min^{-1}$)
Rice [9]	480	0.07	$6.00x10^{-3}$
Rice [9]	520	0.06	$2.00x10^{-4}$
Sato [11]	440	0.12	$2.95x10^{-2}$
This Work	500	0.08	$6.09x10^{-3}$
This Work	600	0.08	$2.80x10^{-3}$

From the data set in Table 6.3, the conditions used from Rice (480°C and 0.07 g/cm^3) are the closest ones to experiments in the present work (500 °C and 0.08 g/cm^3). The rate constants agree almost perfectly in this case. When looking at slightly different conditions, the difference between the two works becomes larger. The main point here, though, is to show that these rate constants are in the same order of magnitude. This is true despite the fact we did not isolate the water-gas shift reaction in our study, and studied a much more complex system. Sato obtained a rate constant about 5 times the one we had at 500°C, but his water density was 50 % higher than ours, and we already know this variable can influence rates of reaction. Next, we compare the rates of water-gas shift and methanation, for the two temperatures we have results for (500°C and 600°C). Table 6.4 shows these results.

Table 6.4. Rate constants for water-gas shift and methanation.

k ($L/mol^{-1}.min^{-1}$)	500°C	600°C
Water-Gas Shift	$6.09x10^{-3}$	$2.80x10^{-3}$
Methanation	$0.00x10^{0}$	$7.71x10^{-2}$

We would expect the rates for both reactions to increase as the temperature increases. That does not happen for the water-gas shift reaction. While it is difficult to assure the precise values of these rate constants are exactly correct, it is important to keep in mind that our objective is to focus on finding approximate rate constants. These rate constants allow one to identify the most important routes for gas formation in SCWG, rather than stating exact values. The exact rate constants can only be found by performing

the actual reactions like Sato and Rice did. The rate of methanation at 500°C is very small (fitted as zero), but its rate becomes high at 600°C.

We are now in a position to use the rate equations to quantify how much each individual reaction affects formation and consumption of each gas species, by calculating rates of formation / consumption. For instance, referring back to equation 5, we know the rate of H_2 formation from the forward water-gas shift is $k_{10}C_{CO}C_W$. Figures 6.11 – 6.18 show the rates of formation / consumption for each of the gas species as a function of time, for cellulose and lignin.

Inspection of figures 6.11 – 6.18 allows one to visually determine the reactions leading to formation of each gas species. We can divide the SCWG in two periods: the first 5 minutes, with high rates of formation for all gas species, and after 5 minutes, where the rates are smaller and reactions that change product distribution are dominant. For H_2, the high rates of formation in the first minutes are due to steam-reforming. There are differences concerning cellulose and lignin: steam-reforming I (forming CO) is the dominant type of steam-reforming for cellulose, while steam-reforming II (forming CO_2) is prevalent for lignin. In both cases, the rate of steam-reforming quickly decreases after a few minutes, in such a way that the rate of the forward water-gas shift becomes the largest one for longer periods of time. After reaching a maximum at about 7-8 minutes, the rate of water-gas shift slowly decreases with time. The other gas species seem to originate mostly from the intermediate. Direct formation of CH_4 from the intermediate is the most important reaction for CH_4 formation. For methanation to become significant, a catalyst needs to be used. For CO, the intermediate is also the main source, with smaller contributions from steam-reforming I. The model indicates the water-gas shift is the reaction consuming CO at longer times. CO_2 originates from intermediates during the first minutes, but it can also be formed at much smaller rates from water-gas shift at longer times.

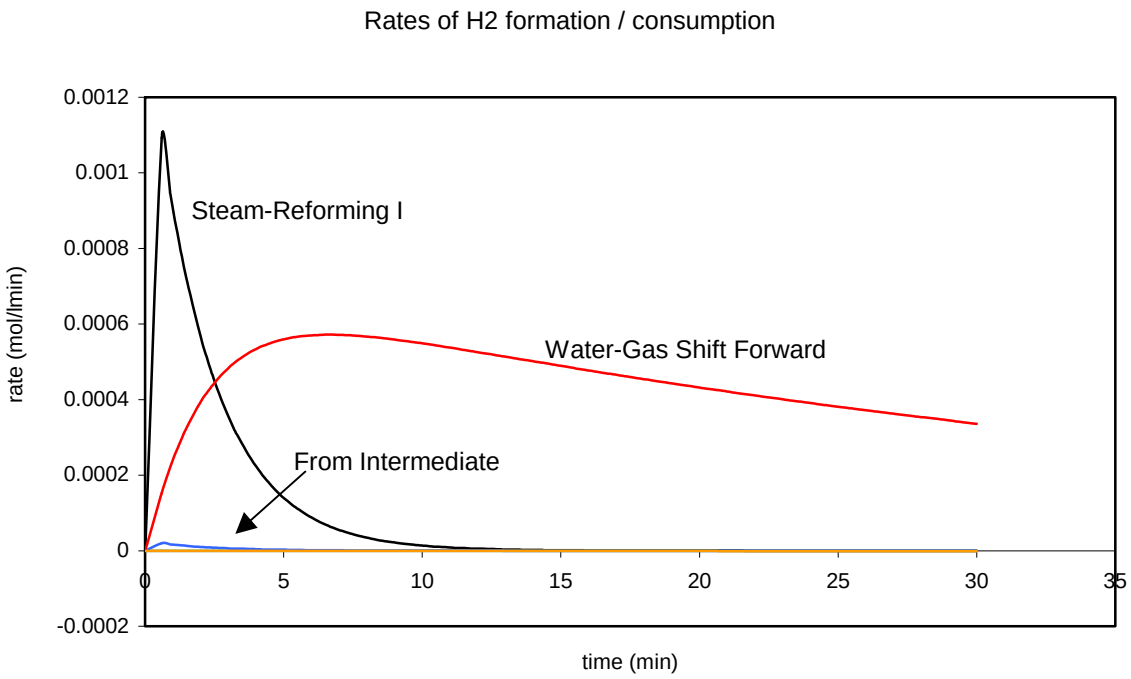

Figure 6.11. Rates of formation / consumption for H_2 (cellulose, 500°C, 9.0 wt % loading, 0.08 g/ml).

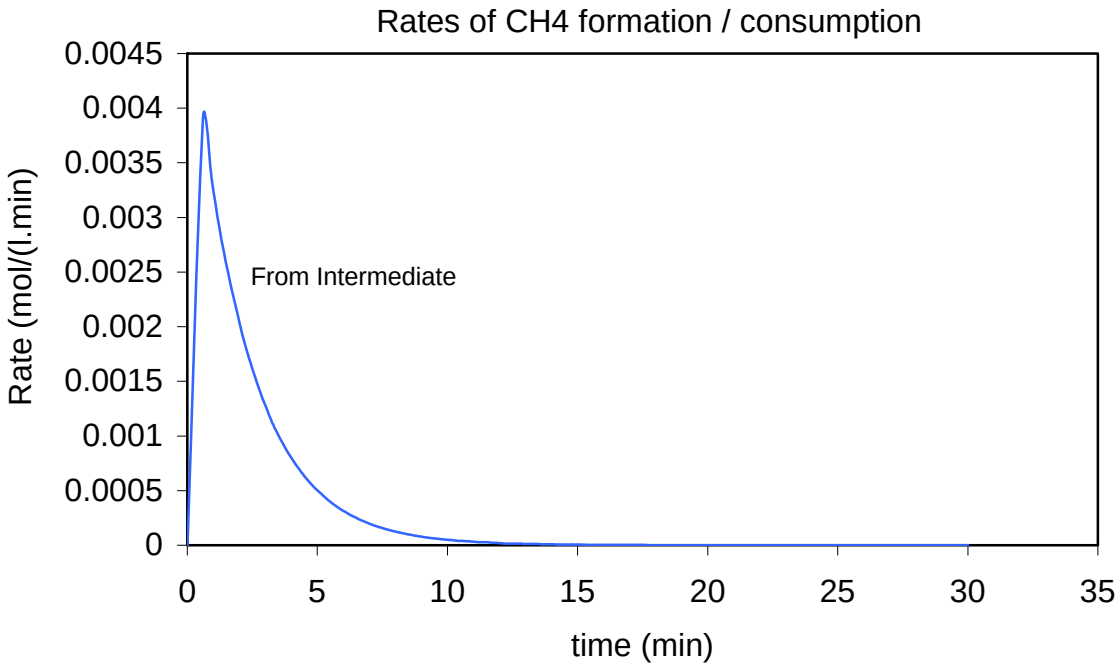

Figure 6.12. Rates of formation / consumption for CH_4 (cellulose, 500°C, 9.0 wt % loading, 0.08 g/ml).

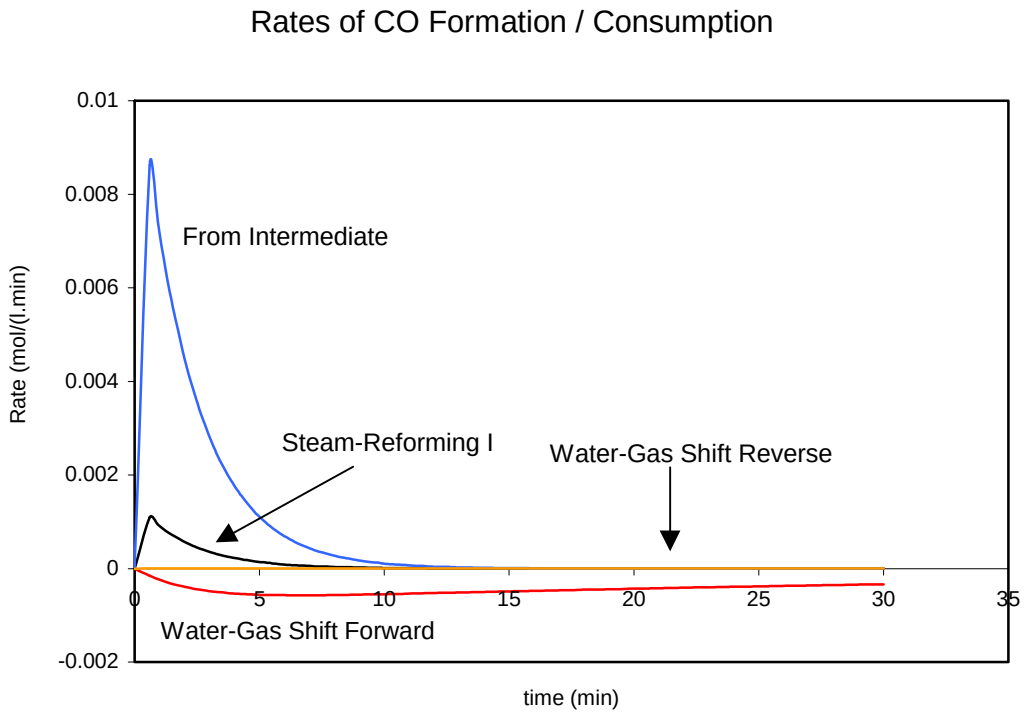

Figure 6.13. Rates of formation / consumption for CO (cellulose, 500°C, 9.0 wt % loading, 0.08 g/ml).

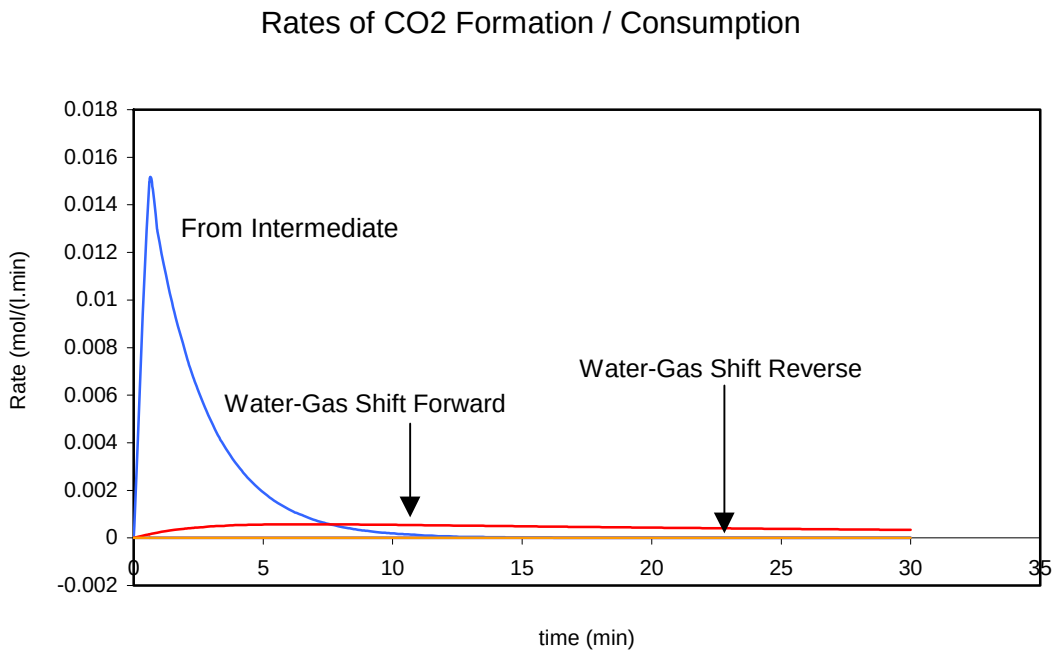

Figure 6.14. Rates of formation / consumption for CO_2 (cellulose, 500°C, 9.0 wt % loading, 0.08 g/ml).

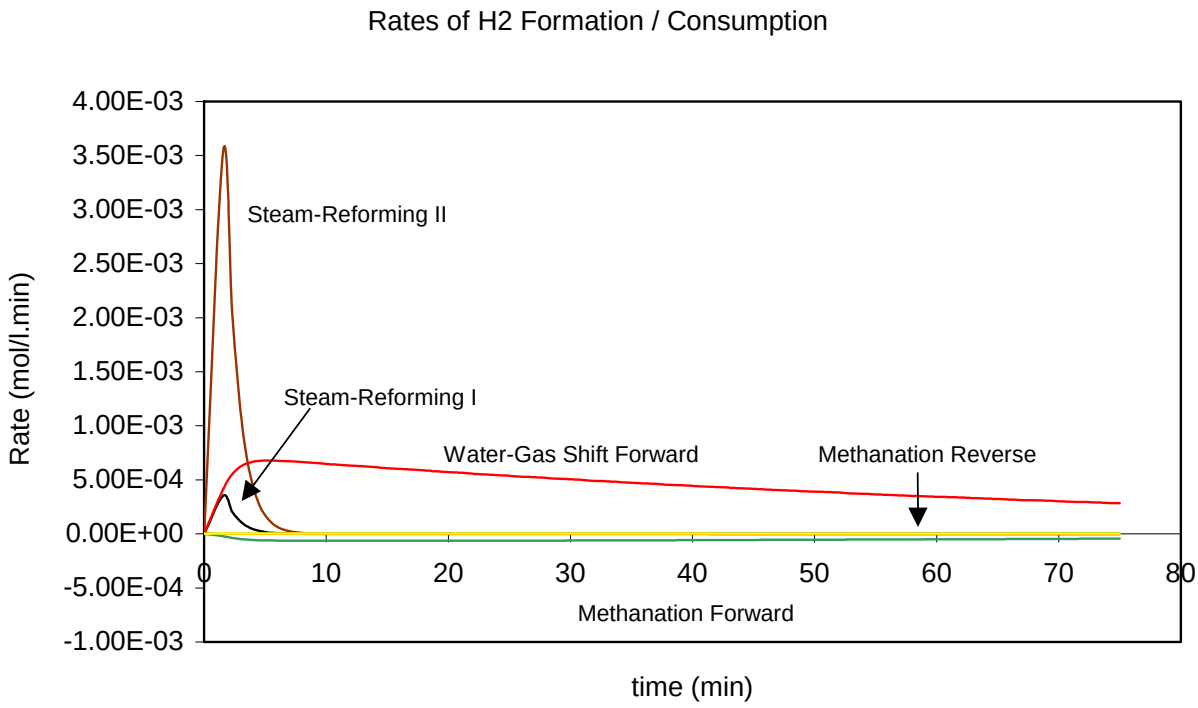

Figure 6.15. Rates of formation / consumption for H_2 (lignin, 600°C, 9.0 wt % loading, 0.08 g/ml).

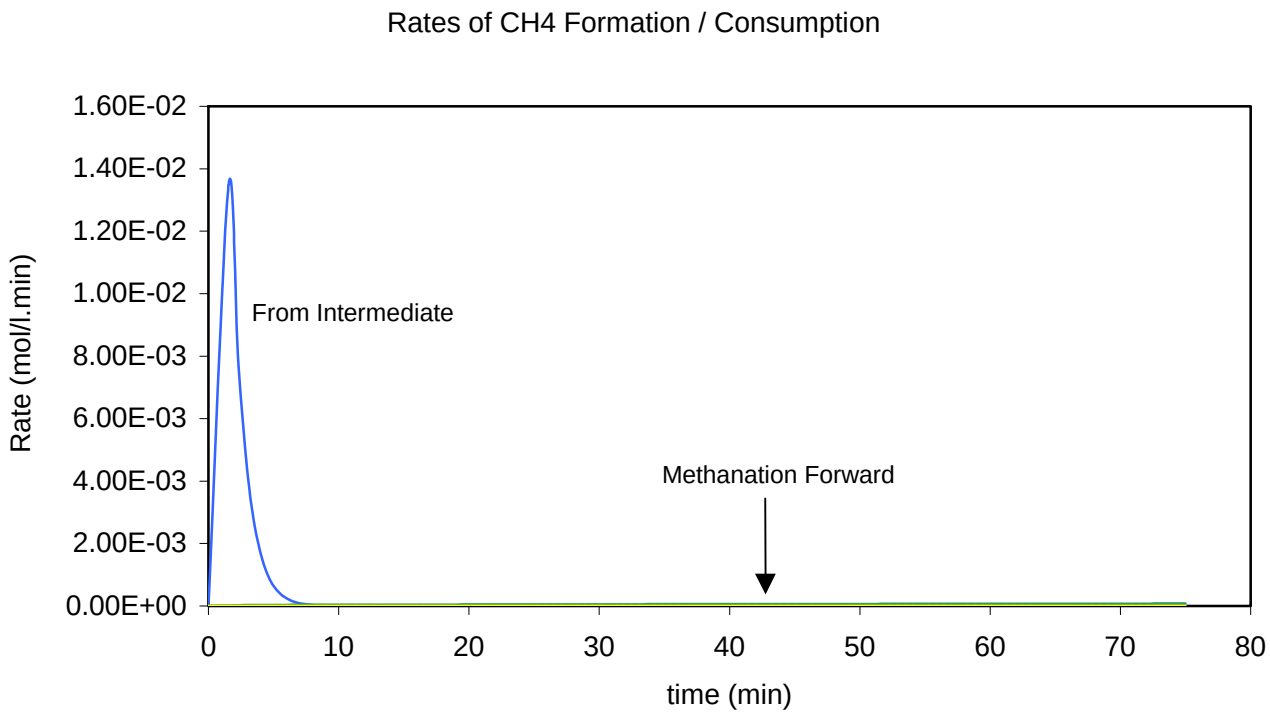

Figure 6.16. Rates of formation / consumption for CH_4 (lignin, 600°C, 9.0 wt % loading, 0.08 g/ml).

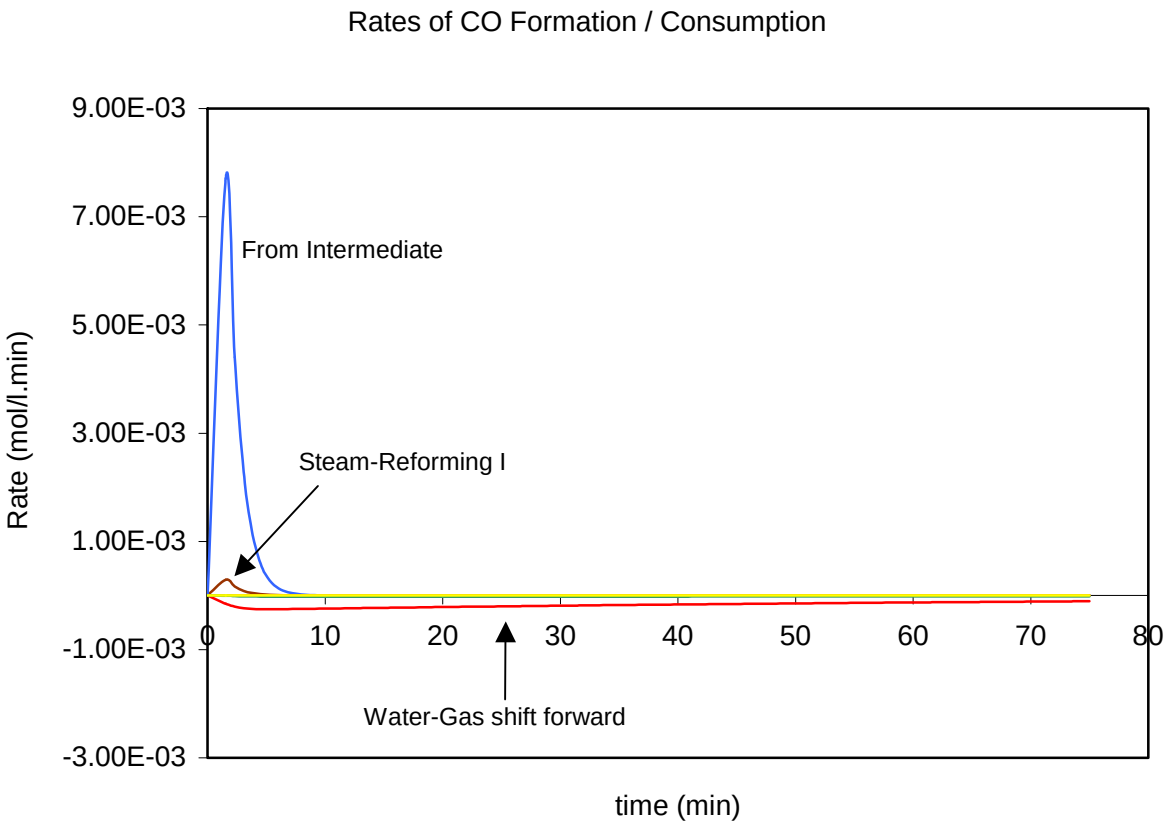

Figure 6.17. Rates of formation / consumption for CO (lignin, 600°C, 9.0 wt % loading, 0.08 g/ml).

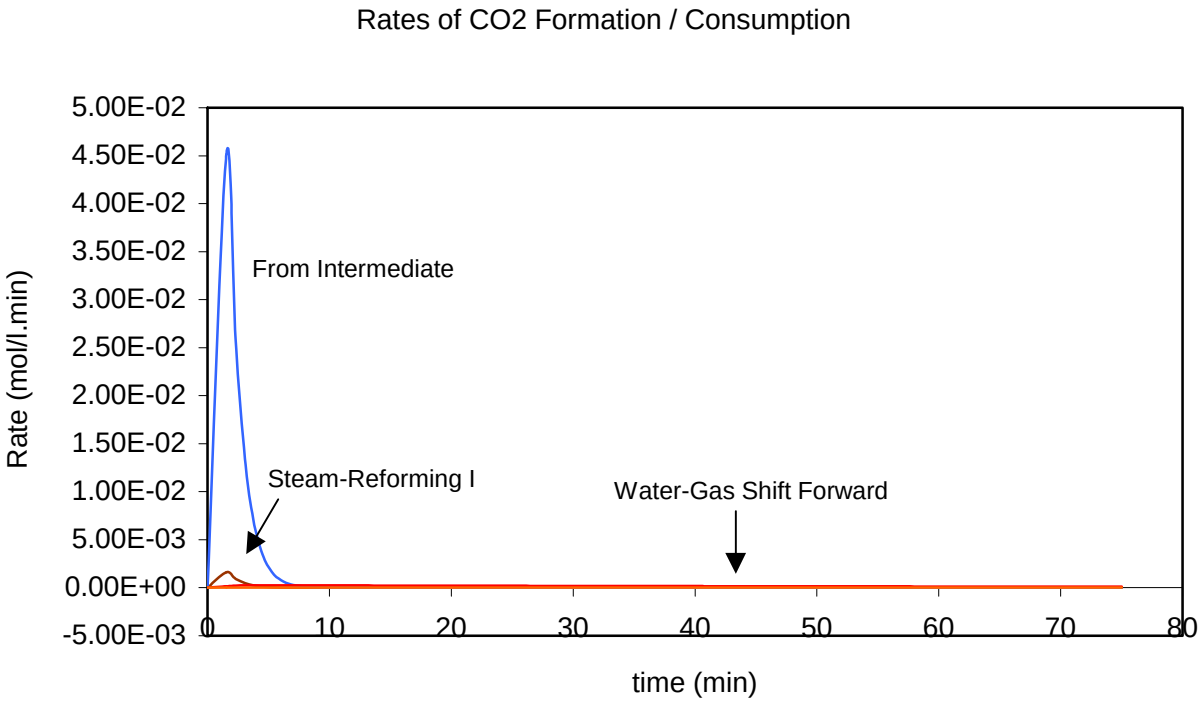

Figure 6.18. Rates of formation / consumption for CO_2 (lignin, 600°C, 9.0 wt % loading, 0.08 g/ml).

To confirm our findings about the key reaction paths, a sensitivity analysis is useful. It can determine responses in the model predictions when the rate constants are varied. The sensitivity coefficient can be defined as in equation 6.16:

$$S_{i,j} = \frac{\partial \ln C_i}{\partial \ln k_j} = \frac{\Delta C_i / C_i}{\Delta k_j / k_j} \tag{6.16}$$

In equation (16), i is one of the gas species and j is one of the reactions. In order to calculate the sensitivity coefficients $S_{i,j}$, model simulations were run applying a positive 5 % variation on each rate constant to calculate ΔC_i. Our analysis of the reaction rates has already shown that we can divide non-catalytic SCWG in two time periods: the first 5 minutes, with high rates of formation for all gases, and after 5 minutes, where the rates become smaller. For this reason, we chose to look at the sensitivities at short times (1 min) and long times (30 min for cellulose and 75 minutes for lignin). Tables 6.5 – 6.8 show the results, and the sensitivity coefficients of at least ± 0.1 are highlighted.

At 1 min, the formation and consumption of intermediate forming char are very sensitive reactions for all the gas species involved. Decomposition from intermediate strongly affects CO, CO_2 and CH_4 formation, while steam-reforming is important for H_2 formation. These findings are in agreement with our reaction rates study. At long times, steam-reforming, char formation and gas formation from intermediate are still important, but the water-gas shift also plays an important role for all gases except CH_4. CO from intermediate becomes an important reaction for CO, CO_2 and H_2 since it provides the CO necessary for the water-gas shift.

Table 6.5. Sensitivity coefficients for cellulose (1 min).

Cellulose	**Sensitivities at 1 min**			
	CO	**CO_2**	**CH_4**	**H_2**
Intermediate Formation	**2.25×10^{-1}**	**2.30×10^{-1}**	**2.28×10^{-1}**	**2.55×10^{-1}**
Steam-Reforming I	**1.77×10^{-1}**	6.67×10^{-2}	6.54×10^{-2}	**9.79×10^{-1}**
Steam-Reforming II	0.00×10^{-0}	0.00×10^{0}	0.00×10^{0}	0.00×10^{0}
CO from Intermediate	**8.87×10^{-1}**	6.62×10^{-3}	5.55×10^{-4}	8.14×10^{-2}
CO_2 from Intermediate	0.00×10^{0}	**9.93×10^{-1}**	5.55×10^{-4}	0.00×10^{0}
CH_4 from Intermediate	0.00×10^{0}	0.00×10^{0}	**1.00×10^{0}**	0.00×10^{0}
H_2 from Intermediate	0.00×10^{0}	0.00×10^{0}	5.55×10^{-4}	1.59×10^{-2}
Char Formation	**-1.31×10^{-1}**	**-1.29×10^{-1}**	**-1.30×10^{-1}**	**-1.19×10^{-1}**
Water-Gas Shift	-1.15×10^{-2}	7.34×10^{-3}	0.00×10^{0}	9.03×10^{-2}
Methanation	0.00×10^{0}	0.00×10^{0}	0.00×10^{0}	0.00×10^{0}

Table 6.6. Sensitivity coefficients for cellulose (30 min).

Cellulose	Sensitivities at 30 min			
	CO	**CO_2**	**CH_4**	**H_2**
Intermediate Formation	-1.52×10^{-2}	-8.38×10^{-4}	2.31×10^{-2}	-4.80×10^{-2}
Steam-Reforming I	8.69×10^{-2}	1.55×10^{-2}	1.26×10^{-2}	$\mathbf{2.14\times10^{-1}}$
Steam-Reforming II	0.00×10^{0}	0.00×10^{0}	0.00×10^{0}	0.00×10^{0}
CO from Intermediate	$\mathbf{8.73\times10^{-1}}$	$\mathbf{2.16\times10^{-1}}$	2.49×10^{-2}	$\mathbf{6.69\times10^{-1}}$
CO_2 from Intermediate	-1.32×10^{-2}	$\mathbf{7.53\times10^{-1}}$	2.31×10^{-2}	-4.95×10^{-2}
CH_4 from Intermediate	-1.40×10^{-2}	-1.13×10^{-3}	$\mathbf{1.02\times10^{0}}$	-4.88×10^{-2}
H_2 from Intermediate	-1.40×10^{-2}	-1.13×10^{-3}	2.31×10^{-2}	-4.56×10^{-2}
Char Formation	$\mathbf{-1.01\times10^{0}}$	$\mathbf{-9.31\times10^{-1}}$	$\mathbf{-9.21\times10^{-1}}$	$\mathbf{-9.44\times10^{-1}}$
Water-Gas Shift	$\mathbf{-6.78\times10^{-1}}$	$\mathbf{1.66\times10^{-1}}$	-9.23×10^{-4}	$\mathbf{5.53\times10^{-1}}$
Methanation	0.00×10^{0}	0.00×10^{0}	0.00×10^{0}	0.00×10^{0}

Table 6.7. Sensitivity coefficients for lignin (1 min).

Lignin	Sensitivities at 1 min			
	CO	**CO_2**	**CH_4**	**H_2**
Intermediate Formation	$\mathbf{4.96\times10^{-1}}$	$\mathbf{5.01\times10^{-1}}$	$\mathbf{4.99\times10^{-1}}$	$\mathbf{5.03\times10^{-1}}$
Steam-Reforming I	1.72×10^{-2}	-1.97×10^{-2}	-1.98×10^{-2}	6.94×10^{-2}
Steam-Reforming II	-2.77×10^{-2}	9.90×10^{-2}	-2.77×10^{-2}	$\mathbf{8.64\times10^{-1}}$
CO from Intermediate	$\mathbf{9.63\times10^{-1}}$	4.93×10^{-3}	8.73×10^{-5}	1.43×10^{-2}
CO_2 from Intermediate	0.00×10^{0}	$\mathbf{8.68\times10^{-1}}$	0.00×10^{0}	0.00×10^{0}
CH_4 from Intermediate	-1.19×10^{-3}	-1.21×10^{-3}	$\mathbf{9.99\times10^{-1}}$	-8.93×10^{-4}
H_2 from Intermediate	0.00×10^{0}	0.00×10^{0}	0.00×10^{0}	0.00×10^{0}
Char Formation	$\mathbf{-6.35\times10^{-1}}$	$\mathbf{-6.37\times10^{-1}}$	$\mathbf{-6.37\times10^{-1}}$	$\mathbf{-6.37\times10^{-1}}$
Water-Gas Shift	-9.34×10^{-3}	3.91×10^{-3}	-1.13×10^{-3}	1.49×10^{-2}
Methanation	-2.96×10^{-4}	-9.30×10^{-5}	8.73×10^{-5}	-1.49×10^{-3}

Table 6.8. Sensitivity coefficients for lignin (75 min).

Lignin	Sensitivities at 75 min			
	CO	**CO_2**	**CH_4**	**H_2**
Intermediate Formation	-7.56×10^{-3}	1.17×10^{-3}	2.46×10^{-4}	1.37×10^{-3}
Steam-Reforming I	2.89×10^{-2}	6.73×10^{-3}	1.28×10^{-3}	5.02×10^{-2}
Steam-Reforming II	-5.59×10^{-2}	7.69×10^{-2}	6.58×10^{-3}	$\mathbf{3.73\times10^{-1}}$
CO from Intermediate	$\mathbf{9.30\times10^{-1}}$	$\mathbf{2.47\times10^{-1}}$	4.12×10^{-2}	$\mathbf{3.55\times10^{-1}}$
CO_2 from Intermediate	3.02×10^{-3}	$\mathbf{6.46\times10^{-1}}$	0.00×10^{0}	-1.47×10^{-3}
CH_4 from Intermediate	5.40×10^{-3}	4.83×10^{-4}	$\mathbf{9.66\times10^{-1}}$	1.25×10^{-2}
H_2 from Intermediate	0.00×10^{0}	0.00×10^{0}	0.00×10^{0}	0.00×10^{0}
Char Formation	$\mathbf{-8.84\times10^{-1}}$	$\mathbf{-9.30\times10^{-1}}$	$\mathbf{-9.66\times10^{-1}}$	$\mathbf{-7.60\times10^{-1}}$
Water-Gas Shift	$\mathbf{-8.44\times10^{-1}}$	$\mathbf{1.60\times10^{-1}}$	-3.34×10^{-3}	$\mathbf{4.10\times10^{-1}}$
Methanation	-7.64×10^{-2}	-7.69×10^{-3}	2.67×10^{-2}	$\mathbf{-1.79\times10^{-1}}$

At 1 min, the formation and consumption of intermediate forming char are very sensitive reactions for all the gas species involved. Decomposition from intermediate strongly affects CO, CO_2 and CH_4 formation, while steam-reforming is important for H_2 formation. These findings are in agreement with our reaction rates study. At long times,

steam-reforming, char formation and gas formation from intermediate are still important, but the water-gas shift also plays an important role for all gases except CH_4. CO from intermediate becomes an important reaction for CO, CO_2 and H_2 since it provides the CO necessary for the water-gas shift.

6.5 Conclusions

1.) We elaborated the first non-catalytic kinetic model for SCWG of biomass. Contrary to previous studies on the field, we used data on gas yields to provide an understanding of the most important routes for gas formation in SCWG.

2.) The proposed set of 11 reactions and the concept of a generic reactive intermediate built a model that can successfully fit the base case experimental data for cellulose and lignin. We verified that the model can predict yields at different biomass loadings and water densities. Its equilibrium predictions agree with thermodynamic calculations, and the rate constants obtained for the water-gas shift are in the same range as reported by previous authors.

3.) High rate constants were obtained for the formation of CO, CO_2 and CH_4 from the intermediate species. This seems to be the major pathway for the formation of these gases at the first minutes in SCWG. H_2 is the only gas that does not appear to originate from intermediates.

4.) H_2 is mostly formed via steam-reforming during the first 5 minutes, and from water water-gas shift after 5 minutes.

5.) According to the model predictions, our experimental data were far from achieving equilibrium for both water-gas shift and methanation. This opens the door for the use of catalysts that can promote these reactions.

6.) Catalysts that can promote formation of gases from intermediates can be also useful, in the sense that they can avoid intermediate decomposition into char.

REFERENCES

[1] M. Sasaki, B. Kabyemela, R. Malaluan, S. Hirose, N. Takeda, T. Adschiri and K. Arai, "Cellulose hydrolysis in subcritical and supercritical water." *Journal of Supercritical Fluids,* vol. 13, pp. 261-268, 1998.

[2] B. M. Kabyemela, T. Adschiri, R. M. Malaluan and K. Arai, "Kinetics of Glucose Epimerization and Decomposition in Subcritical and Supercritical Water." *Ind Eng Chem Res,* vol. 36, pp. 1552-1558, 1997.

[3] Y. Matsumura, M. Sasaki, K. Okuda, S. Takami, S. Ohara, M. Umetsu and T. Adschiri, "Supercritical water treatment of biomass for energy and material recovery." *Combustion Sci. Technol.,* vol. 178, pp. 509-536, 2006.

[4] O. Bobleter, "Hydrothermal degradation of polymers derived from plants." *Progress in Polymer Science,* vol. 19, pp. 797-841, 1994.

[5] A. Kruse, T. Henningsen, A. Sinag and J. Pfeiffer, "Biomass gasification in supercritical water: influence of the dry matter content and the formation of phenols." *Ind Eng Chem Res,* vol. 42, pp. 3711-3717, 2003.

[6] M. Osada, O. Sato, M. Watanabe, K. Arai and M. Shirai, "Water Density Effect on Lignin Gasification over Supported Noble Metal Catalysts in Supercritical Water." *Energy Fuels*, vol. 20, pp. 930-935, 2006.

[7] G.M. Simmons, M. Gentry, “Particle size limitations due to heat transfer in determining pyrolysis kinetics of biomass”, *J. Anal. Appl. Pyrolysis*, vol. 10, pp. 117-127, 1986.

[8] D. Vamvuka, E. Karakas, E. Kastanaki, P. Grammelis, “Pyrolysis characteristics and kinetics of biomass residuals mixtures with lignite”, *Fuel*, vol. 82, pp. 1949-1960, 2003.

[9] S. F. Rice, R. R. Steeper and J. D. Aiken, "Water Density Effects on Homogeneous Water-Gas Shift Reaction Kinetics." *Journal of Physical Chemistry A*, vol. 102, pp. 2673-2678, 1998.

[10] K. Araki, H. Fujiwara, K. Sugimoto, Y. Oshima and S. Koda, "Kinetics of water-gas shift reaction in supercritical water." *J. Chem. Eng. Japan*, vol. 37, pp. 443-448, 2004.

[11] T. Sato, S. Kurosawa, R. L. Smith Jr., T. Adschiri and K. Arai, "Water gas shift reaction kinetics under noncatalytic conditions in supercritical water." *Journal of Supercritical Fluids,* vol. 29, pp. 113-119, 2004.

CHAPTER 7
GASIFICATION OF CELLULOSE AND LIGNIN IN THE PRESENCE OF ADDED METALS

We have concluded our study of non-catalytic SCWG. With this information available, we are in a position to evaluate differences in gas yields when metals are added to quartz reactors. This chapter presents results for the gasification of cellulose and lignin in supercritical water in the presence of metals. The objective of this study is to establish the first comparison of metal-free SCWG data with SCWG data with added metals. The catalytic contribution from the metals can be quantified by this direct comparison. The approach used in this study is very similar to the one in Chapters 4 and 5, starting with the same base case conditions and varying temperature (400 - 725°C), biomass loading (5.0 – 33.3 wt %) and water density (0.08 – 0.18 g/ml). The first part of this chapter shows the effect of these variables in the presence of inexpensive metals such as copper, iron and nickel. This part intends to determine the conditions that maximize catalytic activity within the range studied in this work. In the second part, we attempt to improve catalytic activity over this optimum condition by increasing the catalyst surface area/biomass ratio in our system. For this study we also tested zirconium, zinc, ruthenium and Raney nickel. We have also evaluated the possibility of deactivation by oxidation, exposing the nickel catalyst to supercritical water for 2 hours prior to gasification.

7.1 Introduction

Chapter 2 provides an overview of studies involving catalysts in SCWG. The main catalysts and their effects are summarized in . Researchers have used mostly basic and metal catalysts to promote gas formation in SCWG. This work focuses only on metals. While nickel has been widely studied [1 – 6], there is little mention of other inexpensive metals such as iron and copper [7, 8]. Deactivation of nickel has been

reported [4, 9], and ruthenium appears as a good option for a metal catalyst that can keep catalytic activity over longer periods of time [4].

Table 7.1. Summary of Catalysts used in SCWG.

Catalyst	Reactions promoted	Comments
Basic (NaOH, K_2CO_3)	C-C splitting [10], water-gas shift [10 - 13]	Difficult to recover [14]
Nickel	Tar cracking, water-gas shift, methanation, hydrogenation [1 – 4]	Increases gas yields substantially [1 - 4]
Raney-Nickel	Same as Ni, suppresses methanation [15]	Provides colorless aqueous phase [16]
Zirconia	Decomposes aldehydes and ketones [13 – 14]	Promotes H_2 and CO_2 formation [13 – 14]
Ruthenium	Actively breaks C-C bonds [17]	Maintains activity for long time [4]

One of the issues with the work currently available in the literature is the absence of information on metal-free experiments, because all of them were performed in metallic reactors such as Inconel and Hastelloy. For instance, experiments with added ruthenium in stainless steel reactors also suffer interference from the catalytic effect of nickel in the reactor walls. This unintended catalytic effect makes it difficult to quantify the real effect of ruthenium on SCWG.

The primary contribution of the present chapter is to study the catalytic effect of added metals by comparing these results with the metal-free experiments reported in chapters 4 and 5. This approach allows one to quantify the real effect of each catalyst metal in SCWG, free from external catalytic effects.

7.2 Method

We arbitrarily designate SCWG at 9.0 wt. % biomass, and 0.08 g/cm^3 water density as the base case. For cellulose, the base case temperature is 500°C, and for lignin it is 600°C. From this starting point, we varied one parameter at a time to evaluate its effect on the gas yields and composition. We considered temperatures of 400, 500, 600,

and 725°C, biomass loadings of 5.0, 9.0 and 33.3 wt %, and water densities of 0.05, 0.08 and 0.18 g/cm^3. We used metal wires as catalysts. Copper, nickel, iron, zinc and zirconium were used in wire form. The wires were wiped with 320 grit sand paper (3M Imperial Wetordry 413Q sandpaper 9x11 02004) to reduce the amount of oxides on the wire surface, and loaded into the reactors.

The wires are 16 cm long in order to occupy most of the length of the quartz reactors, and 0.25 mm diameter. The surface area of the wires is 40 mm^2 (or 125 mm^2/g). Ruthenium and Raney nickel are not available in wire form, so ruthenium was used in the form of powder (44 μm particle diameter) and Raney nickel in slurry form (50 wt % in water). In order to keep the total surface area of 40 mm^2, 3.6 mg of Ruthenium powder were used. The Raney-Nickel experiments were designed to study the effect of a high surface area catalyst on the yields, so in this case we simply added the slurry amount needed to reach the same water density as the base case experiments (86 μl). The total surface area of the Raney nickel catalyst was 1.34x10^7 mm^2.

7.3 Results

7.3.1 Effect of Temperature

The effect of copper, iron and nickel as a function of temperature at base case conditions is shown in Figure 7.1 for cellulose, and in Figure 7.2 for lignin. In Figure 7.1, the trends do not change when compared to the metal-free case: the yields for all gases except CO increase with temperature. In most situations, little (if any) catalytic activity is detected as the temperature changes for cellulose and lignin, with the yields in the presence of metals nearly matching the metal-free case. For cellulose, nickel seems to be the catalyst with the largest influence on the yields, especially at 600°C. The H_2 yield increases from 2.6 to 4.7 mmol/g, CO_2 increases from 7.9 to 12.4 mmol/g, and CO decreases from 1.7 to 1.1 mmol/g, with the CH_4 yield being unaffected at about 2.7 mmol/g. For lignin, the catalytic effect is smaller: the largest influence of the metals also appears to take place at 600°C. SCWG with iron for lignin produced 3.3 mmol/g of H_2, 2.3 mmol/g of CO, 6.1 mmol/g of CH_4, and 6.3 mmol/g of CO_2.

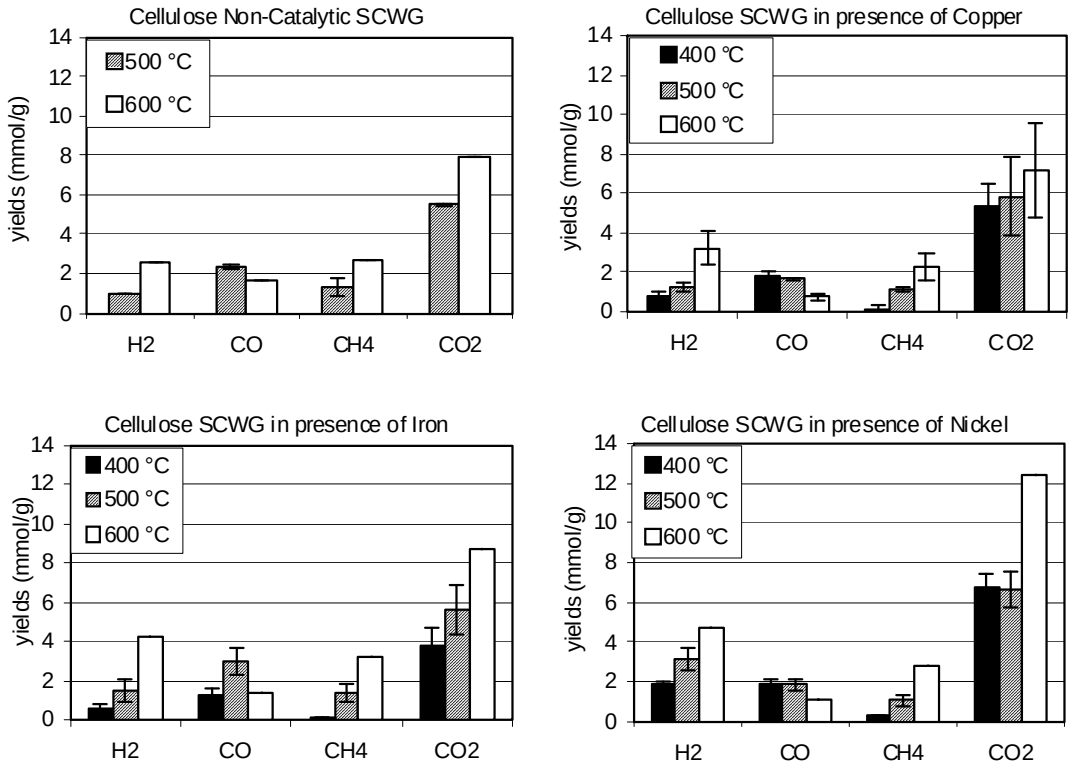

Figure 7.1. Effect of metals presence as a function of temperature (Cellulose), at 10 min.

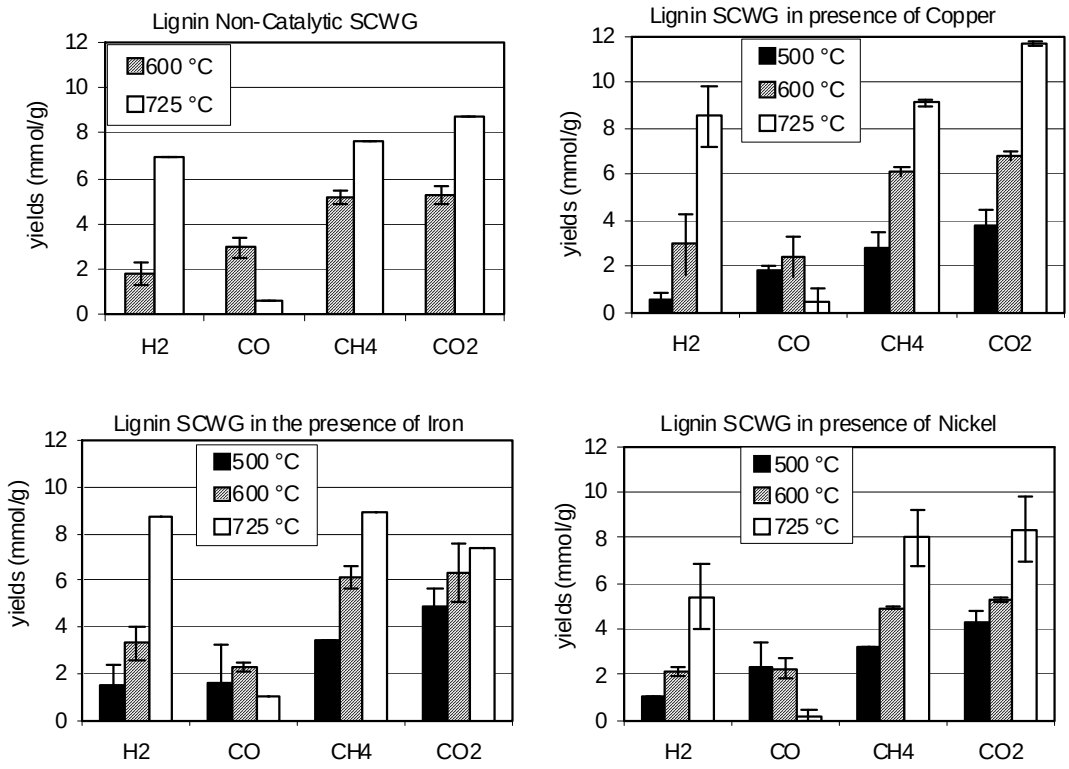

Figure 7.2. Effect of metals presence as a function of temperature (Lignin), at 15 min.

7.3.2 Effect of Water Density

Figures 7.3 and 7.4 show the effect of water density at the base conditions for cellulose and lignin in the presence of metals. The trends are the same as in the absence of metals: the yields at 0.05 and 0.08 g/ml are nearly the same, but at 0.18 g/ml the H_2 and CO_2 yields increase, with the CO yield decreasing. We expect catalysts that promote the water-gas shift reaction, such as nickel, to become more effective as the water density increases. But small catalytic activity is detected as the water density changes. In most situations, the yields in the presence of metals match the yields from the metal-free case. For cellulose, iron and nickel provide a slight increase in H_2 and CO_2 yields at the highest density (0.18 g/cm^3). For lignin, the yields seem to be higher in the presence of the metals at 0.05 g/cm^3. At 0.05 g/cm^3 with iron, the H_2 yield increases from 1.2 to 4.4 mmol/g.

7.3.3 Effect of Biomass Loading

Figures 7.5 and 7.6 show the effect of cellulose and lignin loading at base case conditions on catalytic activity. For the non-catalytic case, the effect of biomass loading on yields is small compared to temperature and water density effects. The yields at 9.0 wt % and 33.3 wt % in the presence and absence of metals are almost the same for cellulose and lignin. At the lowest biomass loading (5.0 wt %), though, the metals make a difference on gas yields and this trend appears to take place for cellulose and lignin. While in the absence of metals there is not a biomass loading that provides higher yields than others, in the presence of metals the 5.0 wt % is clearly the best option in terms of increasing gas yields. The effect is more evident for cellulose, even though it also takes place for lignin. The 5.0 wt % loading is the situation in which catalytic activity is highest within the set of experimental conditions used in this study, and that is valid for the three metals used: nickel, iron and copper.

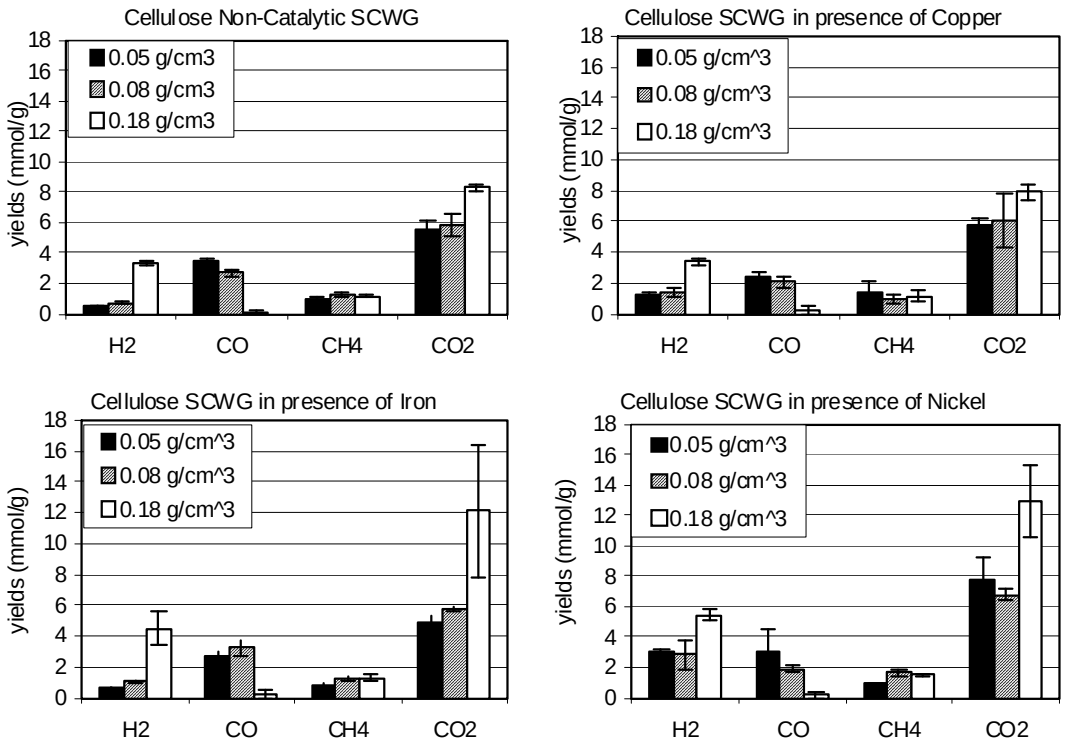

Figure 7.3. Effect of metals presence as a function of water density (cellulose), at 7.5 min.

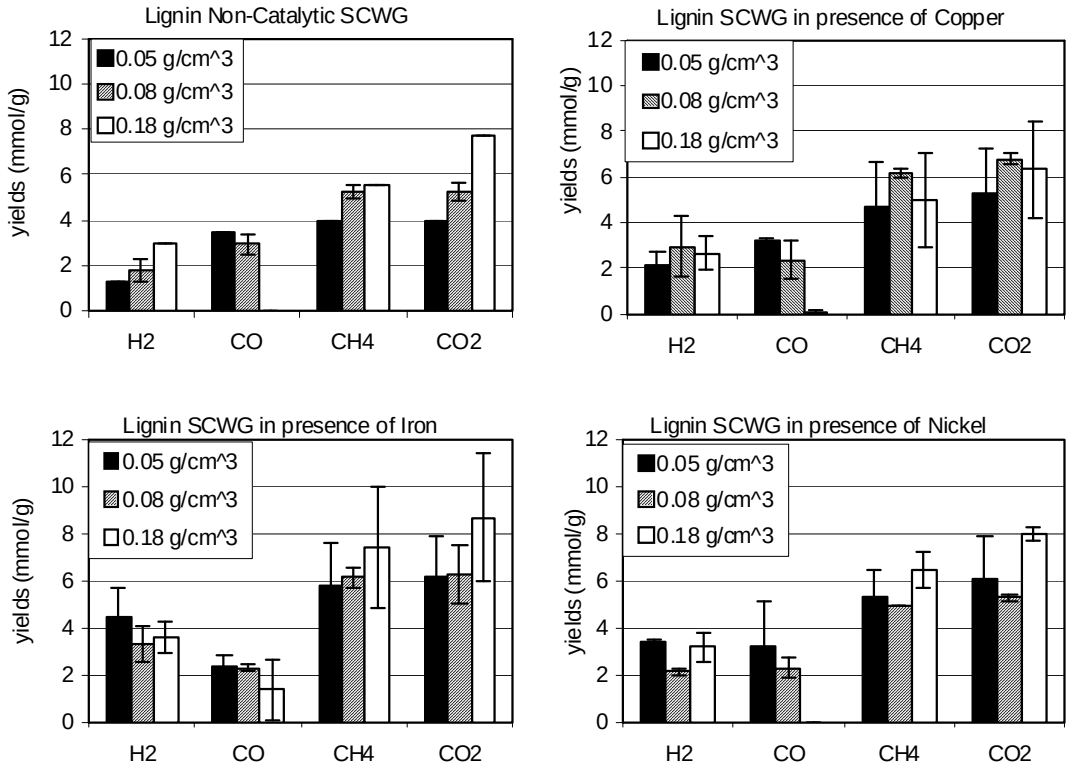

Figure 7.4. Effect of metals presence as a function of water density (lignin), at 15 minutes.

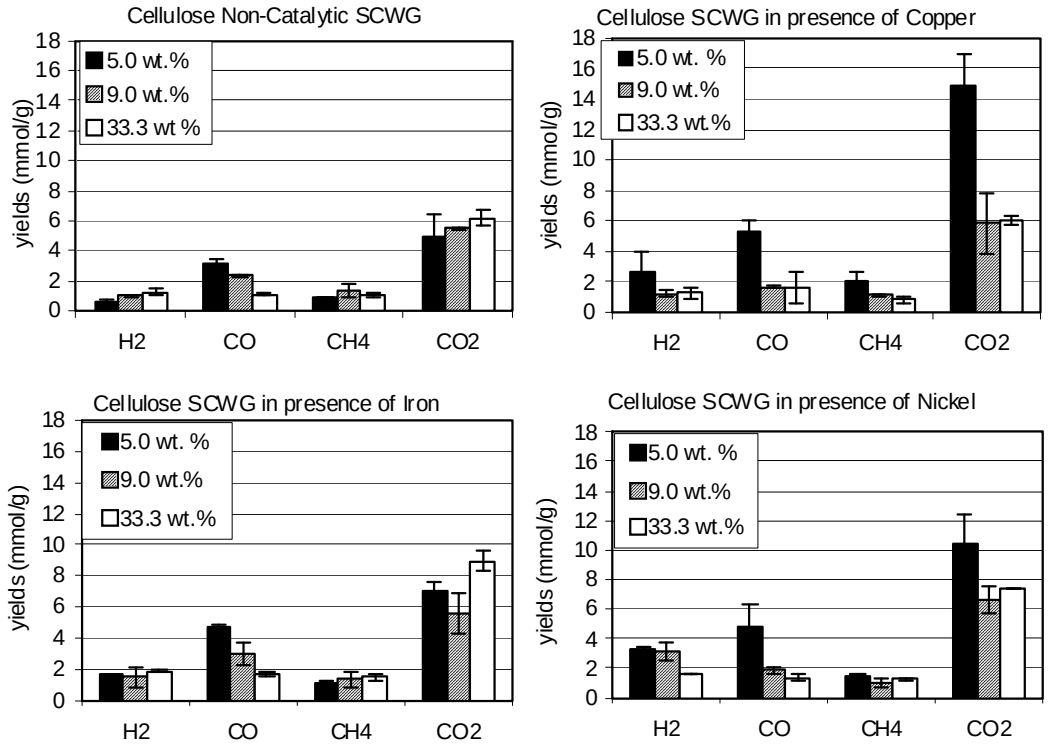

Figure 7.5. Effect of metals presence as a function of cellulose loading, 10 min.

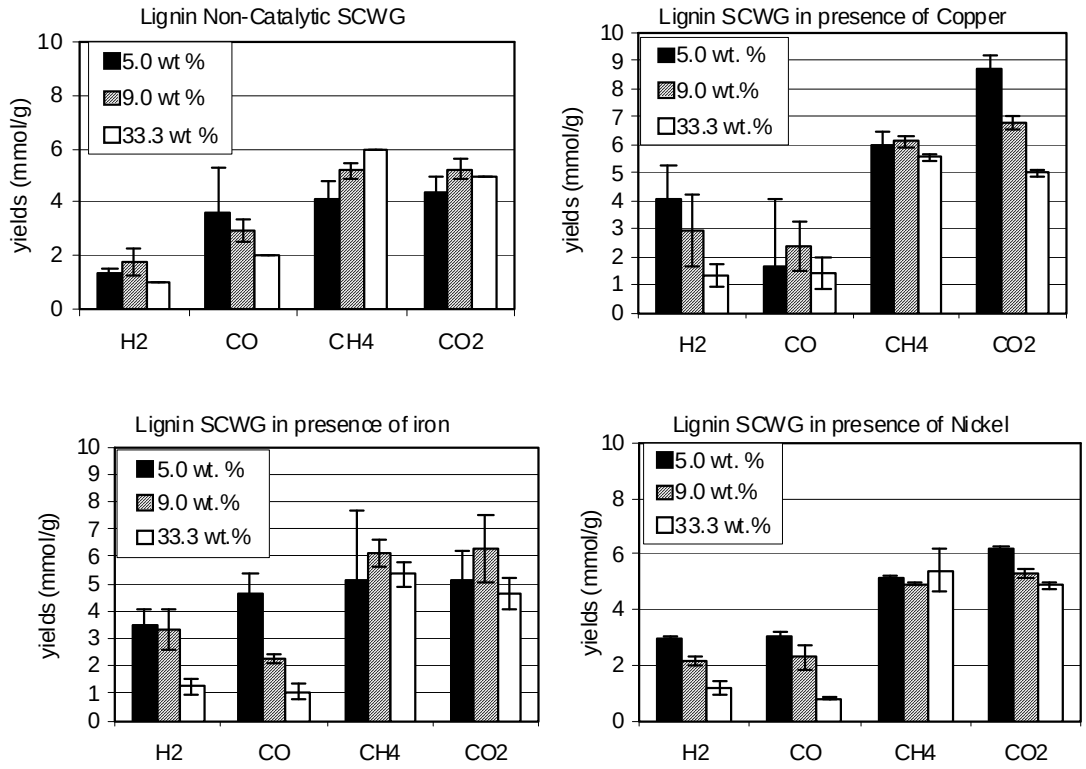

Figure 7.6. Effect of metals presence as a function of lignin loading, 15 min.

Since the 5.0 wt % loading is the situation in which catalytic activity was highest for all the metals, we will focus on this situation. Figure 7.7 compares the non-catalytic data with the experiments with metals added at this loading. For cellulose, without added metals, the H_2 yield is 0.5 mmol/g. In the presence of metals, it is 3.3 mmol/g with nickel, 1.6 mmol/g with iron, and 2.6 mmol/g with copper. The CO yield is 3.1 mmol/g without metals, and it increases to about 5 mmol/g in the presence of any of the metals. The CH_4 yield is not largely affected by the presence of the metals, remaining stable at about 1 mmol/g for all situations except for copper, which increases it to 2 mmol/g. The CO_2 yield is 4.9 mmol/g without metals, and it increases to 10.5 mmol/g with nickel, 7.1 mmol/g with iron and 14.9 mmol/g with copper. The effects of nickel and copper are larger than iron, especially promoting H_2 and CO_2 yields.

For lignin (Figure 7.8), the presence of any of the metals increases the H_2 yield from 1.3 mmol/g to 3-4 mmol/g. Nickel and iron also increase the CO_2 yield from 4.4 to 6.2 and 8.7 mmol/g, respectively. The CH_4 yield increases from 4.1 mmol/g non-catalytic to 5.2 with nickel and iron, and to 6.0 with copper. The effect of the metals on CO yields is small. For comparison, our kinetic model predicts that, in equilibrium, lignin SCWG at 5.0 wt % forms 9.7 mmol/g of H_2, no CO, 4.0 mmol/g of CH_4, and 9.3 mmol/g of CO_2. If the experimental gas yields match equilibrium predictions from our kinetic model (runs for long times), one possible explanation is that the catalyst is promoting water-gas shift and methanation, but it is not interfering with the rates of intermediate decomposition forming gases. In the present situation, the experimental CH_4 yield with copper is about 2.0 mmol/g higher than the equilibrium prediction from the model. One possible explanation is that the catalyst accelerates the rate of CH_4 formation from intermediates, increasing CH_4 yields. Another possibility is shown with the aid of Figure 7.9, where the model predictions for the non-catalytic case at 5.0 wt % are shown as function of time until 5000 min. The CH_4 yield reaches 5.5 mmol/g at 350 minutes, then slowly decreases with time to eventually get to the 4.0 mol/g in equilibrium. If we look at the prediction for 350 min, the CO yield is negligible, the H_2 yield is 4.5 mmol/g, and the CO_2 yield is 7.9 mmol/g. These yields agree exceptionally well with the results shown for copper at Figure 7.8. It could be that copper is promoting water-gas shift and methanation only,

causing the system to achieve yields (in 15 minutes) that would take 350 minutes in its absence. If this is the case, copper would have little or no effect on intermediate decomposition.

Figures 7.10 and 7.11 show the same results from the standpoint of C, H yields and energetic content of the product gas. For cellulose, the non-catalytic C yield is 24.2 %. It increases to 45.3 % with nickel and 60.2 % with copper. The non-catalytic H yield is 7.9 %. It increases to 20.4 % with nickel and 21.4 % with copper. The non-catalytic energetic content is 10.2 %, and it increases to 19.3% with nickel, 15.0 wt % with iron and 21.7 % with copper.

For lignin, the non-catalytic C yield is 21.6 %. The presence of the metals provides a small increase on the C yield, up to 30 wt %. The non-catalytic H yield is 34.1 %, and it increases to 45-55 % in the presence of any of the metals. For lignin, just a slight increase in energetic content of the gas is achieved, from 19.0 wt % to about 25 % with each metal.

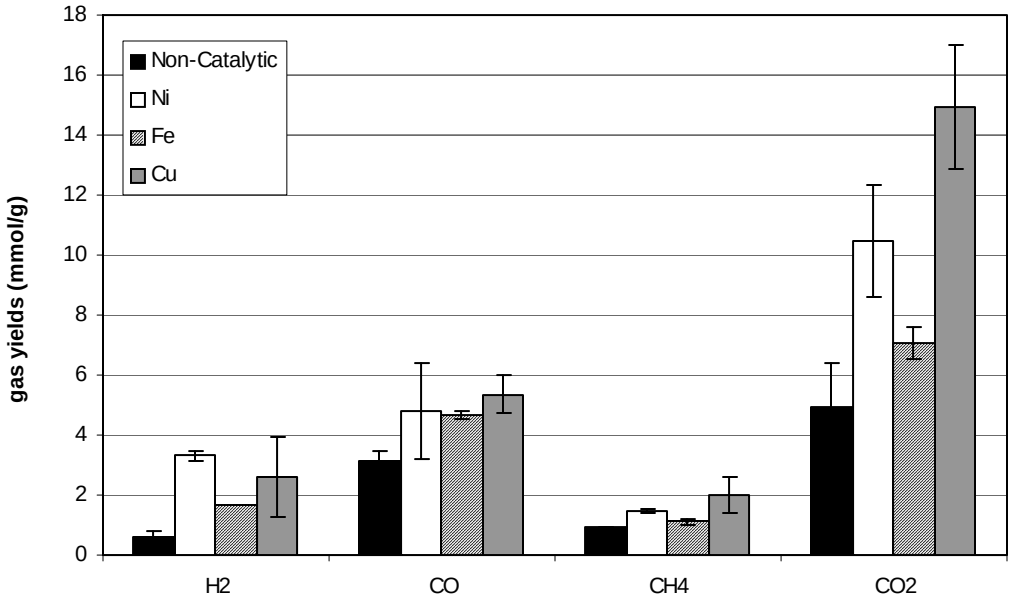

Figure 7.7. Catalysts comparison at 5.0 wt % (cellulose), 10 min.

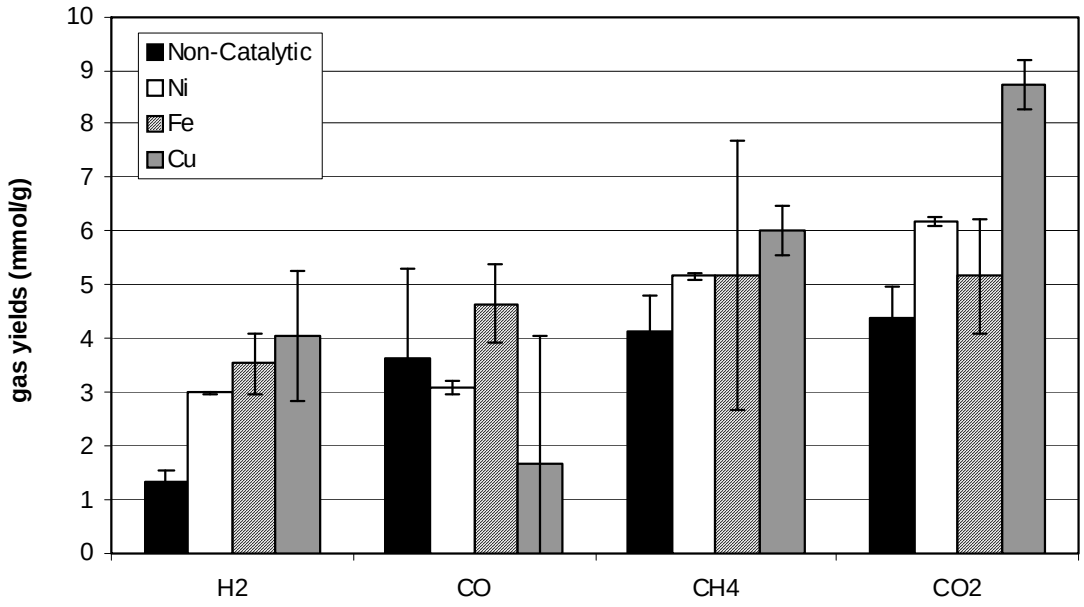

Figure 7.8. Catalysts comparison at 5.0 wt % (Lignin), 15 min.

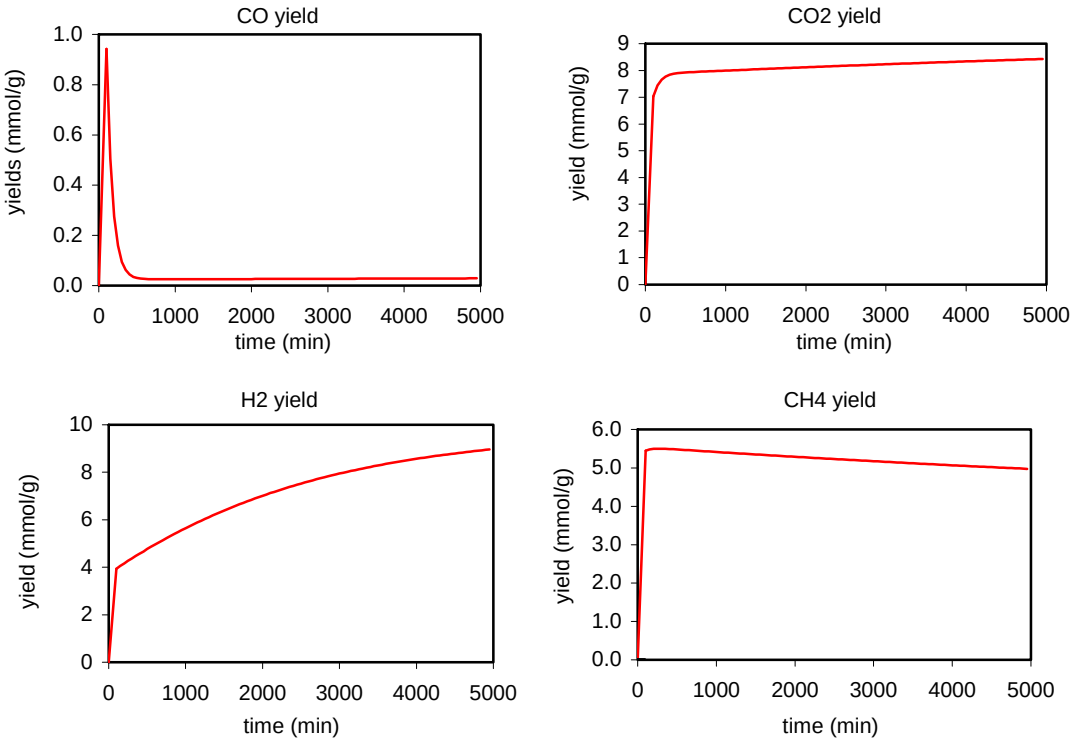

Figure 7.9. Model predictions for 5000 min at 5.0 wt % (lignin, 9.0 wt %, 0.08 g/cm^3).

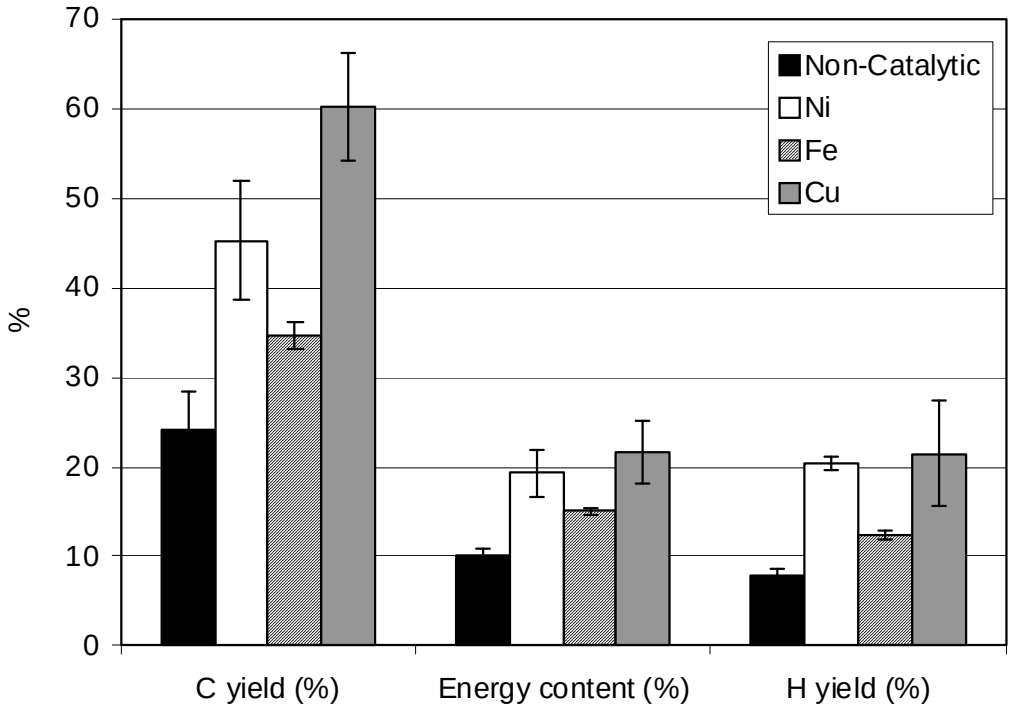

Figure 7.10. Comparison of Efficiencies at 5.0 wt % (cellulose), 10 min.

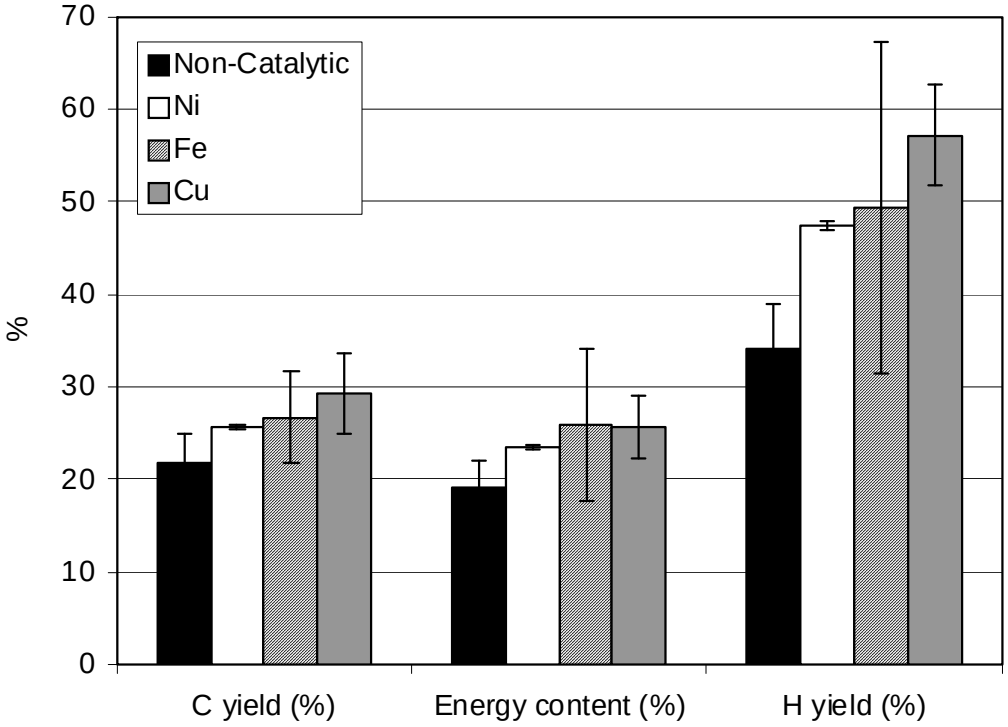

Figure 7.11. Comparison of Efficiencies at 5.0 wt % (Lignin), 15 min.

In general, it seems nickel and copper are better catalysts than iron for cellulose, and they promote H_2 and CO_2 formation to a better extent with cellulose in comparison to lignin. For lignin, the three metals seem to be similar in terms of catalytic effect. At the 5.0 wt % loading, each reactor contains 2.6 mg of biomass exposed to 40 mm^2 of catalyst surface area. That corresponds to a ratio of 15.4 mm^2/mg biomass. Our experiments suggest this ratio might be close to the minimum surface area ratio needed to provide catalytic activity for metals in SCWG. The previous SCWG studies reported in literature with stainless steel reactors had a surface area/biomass ratio of about 18-19 mm^2/mg. This suggests the possibility of catalytic effects from the reactor walls in those studies. In the present work at base case conditions, where small catalytic activity is evident, this ratio is 9.3 mm^2/mg. In order to improve catalytic activity, it is interesting to increase the catalyst surface area per unit biomass weight to verify if higher yields are possible. We can increase the ratio either by increasing the total surface area of the catalyst, or by decreasing the biomass loading. We start by decreasing the biomass loading from 5.0 wt % to 1.0 wt % (0.5 mg). This increases the surface area/biomass ratio to 80.0 mm^2/mg. We ran experiments at 1.0 wt % loading and non-catalytic conditions. We also ran experiments with added nickel, iron, copper and ruthenium. Figures 7.12- 7.15 show the results at 1.0 wt % loading for cellulose and lignin. The uncertainties in the experiments at 1.0 wt % were higher than at other conditions because of the small amount of biomass (0.5 mg) loaded and small GC peaks generated as a result. In general, decreasing the biomass loading did not improve catalytic effects to the extent expected.

For cellulose (Figure 7.12), the non-catalytic H_2 yield is 0.7 mmol/g. Iron and copper increase it to about 2.5 mmol/g, ruthenium increases it to 3.9 mmol/g, and nickel increases it to 8.3 mmol/g. Iron appears to be the only catalyst increasing CO from 2.7 to 5.3 mmol/g. Nickel and iron increase the CH_4 yield from 1.7 mmol/g to 6.3 and 7.7 mmol/g, respectively. Nickel increases CO_2 yield from 6.8 mmol/g to 10.8 mmol/g, and ruthenium increases it to 9.7 mmol/g. Despite promoting increase in H_2 and CO_2 yields, ruthenium as a catalyst was not as effective as reported previously in the literature. We believe the main reason for this discrepancy is due to the physical form of ruthenium: powder instead of wire. The wire form is very appropriate for use in the quartz reactors

because it guarantees any biomass particle will not have to travel any distance higher than the reactor internal diameter in order to interact with the catalyst. When using ruthenium as a powder, there is no guarantee the catalyst is readily available for the biomass particles to interact.

Figure 7.13 compares the catalysts at 1.0 wt % loading at base case conditions for lignin. The non-catalytic H_2 yield is 3.3 mmol/g. Nickel and iron increase it to 6.8 mmol/g. The CO yield is 6.9 mmol/g non-catalytic, and it increases to 10.1 mmol/g with copper. No catalytic effect on CH_4 and CO_2 yields can be noticed. CH_4 remains at about 9.0 mmol/g and CO_2 at 16.9 mmol/g (nickel).

Figure 7.14 shows the effect of the metals at 1.0 wt % loading for cellulose on C, H yield and the energetic content of the gas. The non-catalytic C yield is 30.3 %, which is increased to 50-55 % by nickel and iron. The H yield, 13.3 % at the non-catalytic case, can be increased up to 60-70 % with nickel and iron. The energetic content goes from 13.2 % non-catalytic to about 50 % with nickel and iron. Figure 7.15 shows the effect of metals on the efficiencies for lignin at 1.0 wt %. The H yield increases from 74.7 % to 85-90 % in the presence of nickel and iron. The C yield and energetic content are not influenced by the presence of metals. The C yield remains at about 60 % and the energetic content remains at about 40 %.

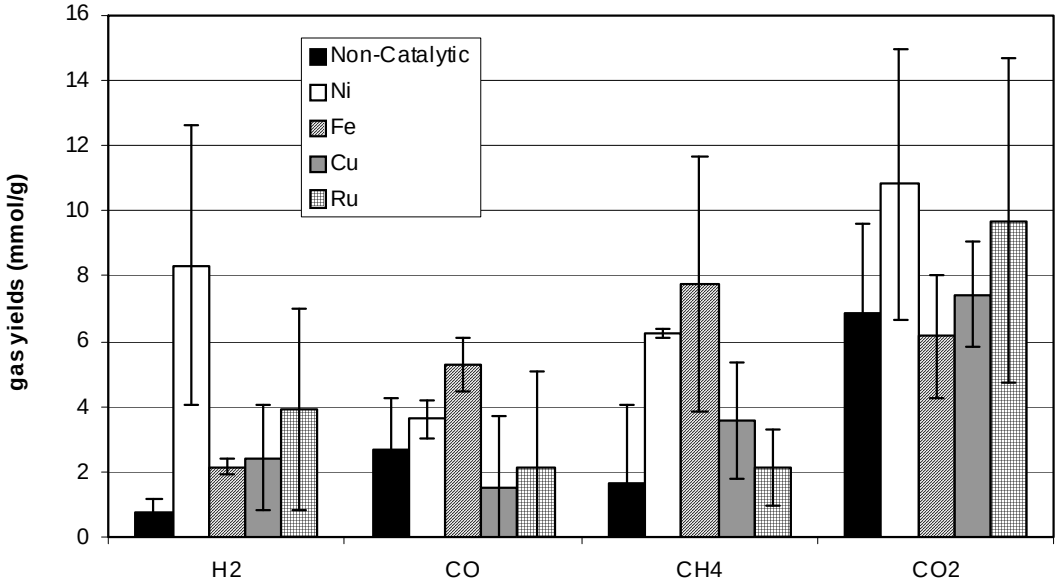

Figure 7.12. Catalysts comparison at 1.0 wt % (cellulose), 10 min.

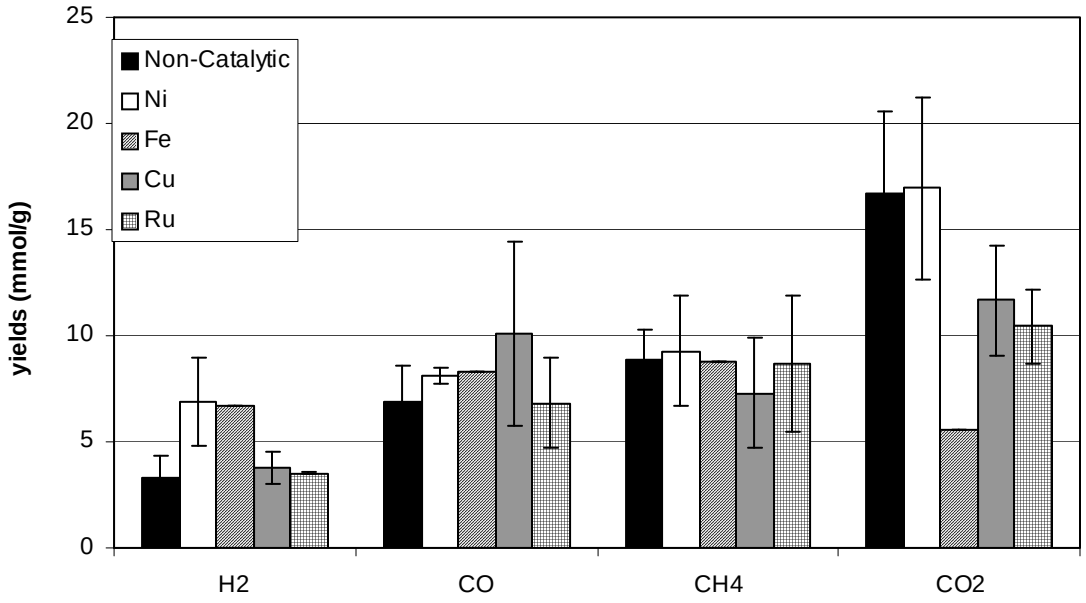

Figure 7.13. Catalysts comparison at 1.0 wt % (lignin), 15 min.

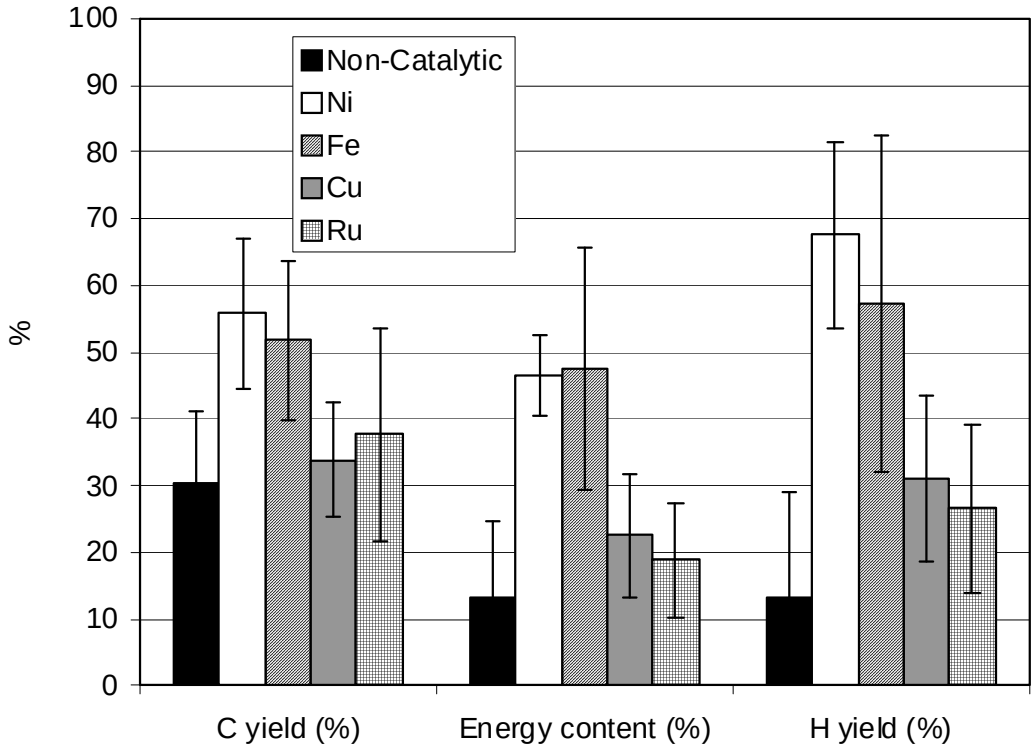

Figure 7.14. Comparison of efficiencies at 1.0 wt % (cellulose), 10 min.

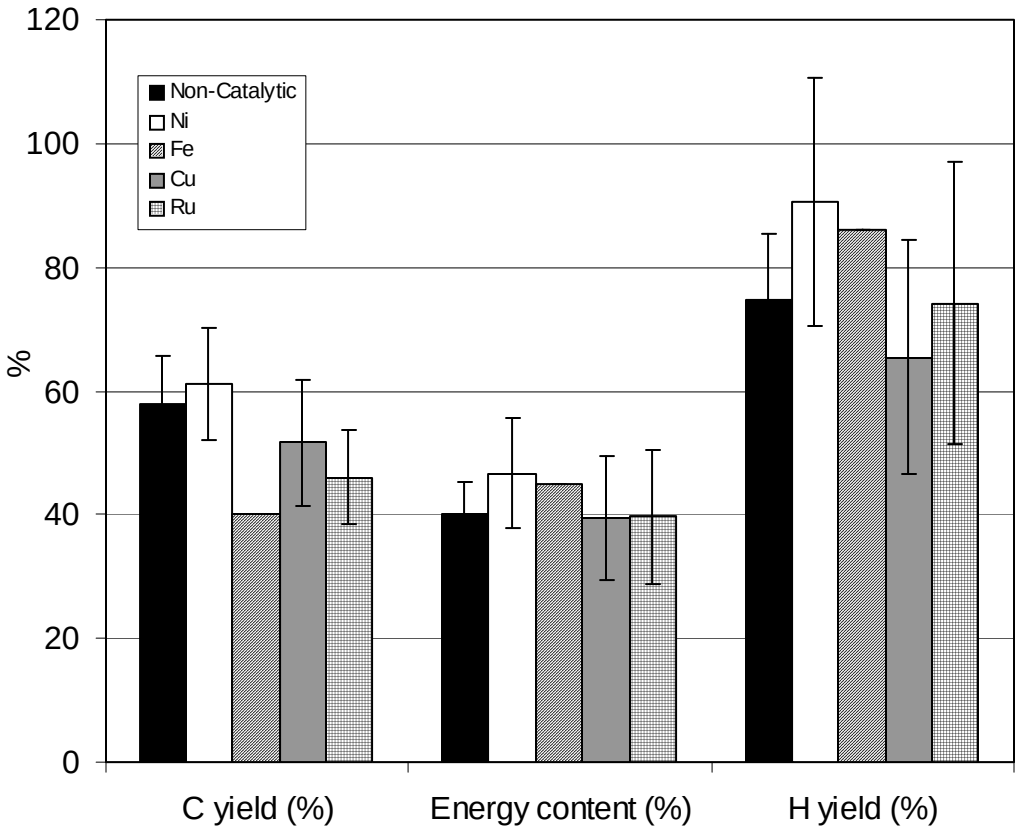

Figure 7.15. Comparison of efficiencies at 1.0 wt % (lignin), 10 min.

Besides nickel, iron, copper and ruthenium, we used zinc, zirconium and Raney-Nickel in our experiments at 1.0 wt % loading. A common result for these three additional metals was the oxidation of the metal, producing large amounts of H_2. This phenomenon was mentioned by Elliott in his recent SCWG review [4]. Oxidation is more evident for zirconium and zinc, where changes in the visual aspect of the material inside the reactors took place. The zinc and zirconium wires disappeared, leaving a solid white powder inside the reactor (which match the descriptions of ZnO and ZrO_2). To verify the possibility of oxidation, we performed sets of experiments with only water and metals added to the reactors, at 500°C and 600°C. For zinc, the 16 cm of wire corresponds to 0.86 mmols. If the zinc completely reacts with water, it would form 0.86 mmols of ZnO and 0.86 mmols of H_2. Experimentally, we observed 650 μmols of H_2 formed at 500°C, suggesting that a large % of the mass of the wire was oxidized in SCW. High H_2 yields were obtained from the zirconium, zinc and Raney nickel reactors. At 500°C, the H_2 yield was 34 μmols from zirconium, and 411 μmols from Raney nickel. At 600°C, the H_2 yield was 561 μmols from zirconium, 609 μmols from zinc and 365 μmols from Raney nickel. Figures 6.16 and 6.17 show the yields obtained when the metals used in this work were exposed to SCW in the absence of biomass. The H_2 yields mentioned above were omitted from the plots for scale purposes. Figures 6.16 and 6.17 reveal that not only H_2 is produced in the interaction of the metals with water. CH_4 is produced from ruthenium at 500° C. At 600° C, CO is produced from the zirconium reactor, CH_4 from Raney nickel, and CO_2 from iron, nickel and ruthenium. While no source of carbon was intentionally added to the reactors, it is possible that some of the metals had carbon impurities contaminating them, generating CO, CO_2 and CH_4 in some cases. This seems to be the only possible reason for the appearance of these gases, since similar experiments carried out with copper and water at 600°C did not show any formation of C-containing gases.

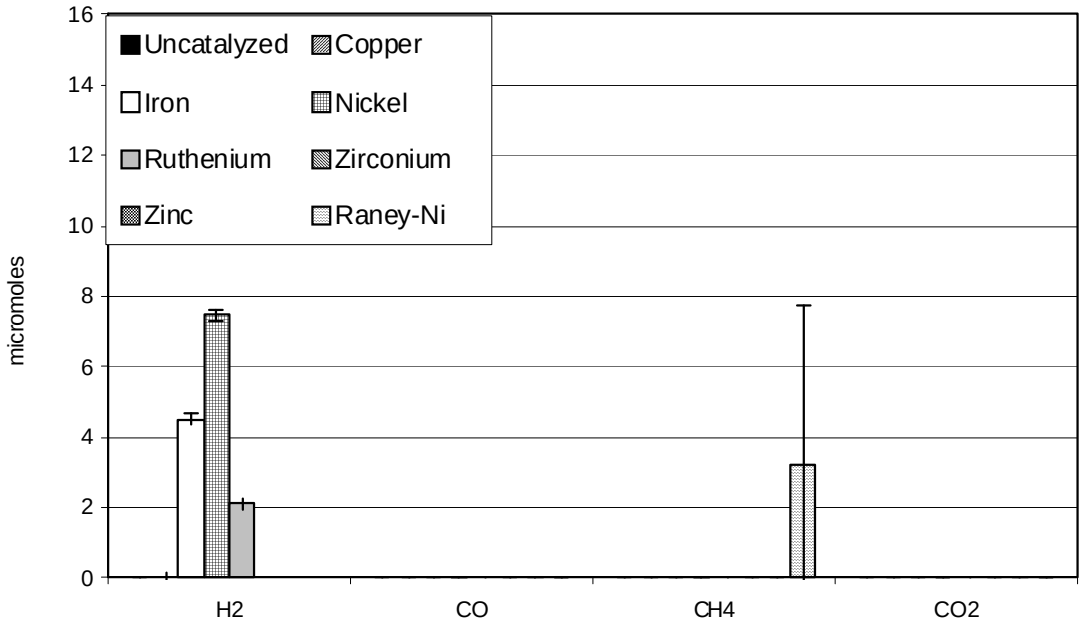

Figure 7.16. Yields of gases with only water and metal (10 min, 500°C, 0.08 g/ml).

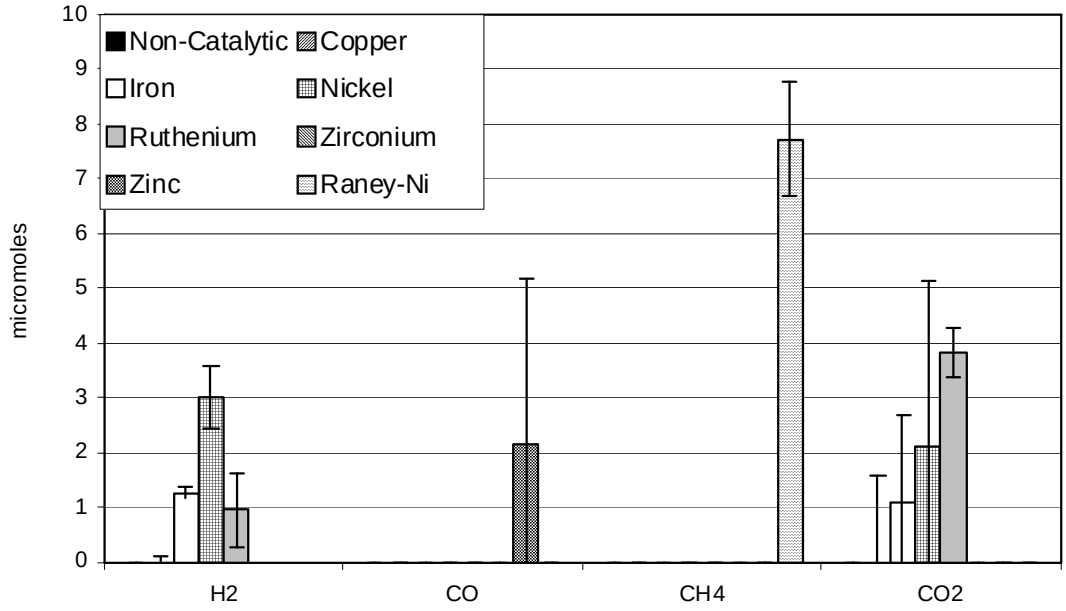

Figure 7.17. Yields of gases with only water and metal (15 min, 600°C, 0.08 g/ml).

The other way to increase the surface area/biomass ratio is to increase the total surface area of the catalyst. We accomplished this by adding multiple wires to the quartz reactor. We chose nickel as the metal to perform this study, since it is an effective catalyst at 1.0 wt % loading. We performed experiments with 2 wires and 3 wires added at this loading. The surface area/biomass ratio is 80 for one wire, 160 mm^2/mg for two wires, and 240 mm^2/mg for 3 wires. Results are shown in Figure 7.18 for cellulose. The non-catalytic H_2 yield is 0.7 mmol/g, and nickel wire increases it to 8.3 mmol/g. With 2 wires, the H_2 yield increases to 15.5 mmol/g, and 3 wires increase it to 23.5 mmol/g. This is the highest H_2 yield from all the conditions studied in this work. The CO yield remains at about 3 mmol/g at most cases, except with 3 wires, where it nearly vanishes. The CO_2 yield increases from 7.0 mmol/g non-catalytic to 11.0 mmol/g with 1 wire, and about 20.0 mmol/g with 2 or 3 wires. The CH_4 yield stays around 2.5 mmol/g with 2 or 3 wires. At 240 mm^2/mg (3 wires), there are great improvements in the H_2 and CO_2 yields, and nearly a CO-free gas, with the CH_4 yield unaffected. The trends are very similar for lignin (Figure 7.19), with high H_2 and CO_2 yields with three nickel wires. The H_2 yield increases from 3.3 non-catalytic to 21.2 mmol/g. The CO yield decreases from 6.9 to 4.9 mmol/g. CH_4 stays around 8.7-8.9 mmol/g, and the CO_2 increases from 16.7 mmol/g to 22.1 mmol/g. At equilibrium, the model predicts 21.7 mmol/g of H_2, 12.3 mmol/g CO_2, 1.0 mmol/g CH_4 and no CO.

While decreasing the biomass loading does not increase catalytic activity substantially, increasing the number of nickel wires effectively increases H_2 and CO_2 yields. Decreasing the biomass loading from 5.0 wt % to 1.0 wt % increases the surface area/biomass weight ratio from 15.4 mm^2/mg to 80.0 mm^2/mg. Increasing the number of wires to 3 increases the ratio to 240.0 mm^2/mg. At 15.4 mm^2/mg we are close to the minimum ratio at which any catalytic activity is observed, so it seems the increase from 80.0 to 240.0 mm^2/mg is much more significant in terms of increasing catalytic activity.

In what concerns gasification efficiencies, the H yield is largely affected by the addition of multiple wires. For cellulose (Figure 7.20), the non-catalytic H yield is 16.2 %, it increases to 60-65 % with 1 or 2 nickel wires, and it increases to 94.2 % when 3 nickel wires are present. The energetic content and the C yield do not significantly

improve with the addition of multiple wires. The reason for this is lack of improvement of CH_4 yields with increase in the catalyst surface area. The C yield remains at about 65 % and the energetic content of the gas is about 45 % with 3 nickel wires. For lignin (Figure 7.21), the H yield is also strongly affected by the addition of multiple nickel wires. It increases from 74.7 % at the non-catalytic case to 137.0 % when 3 wires are present. The C yield stays at around 60 % even with 3 wires, and the energetic content increases from 40.2 to 54.6 %.

Previous studies in the literature have reported deactivation of nickel catalysts in SCWG systems. Elliott [4] mentioned that only nickel in its reduced from can have any type of catalytic activity, and our results suggest oxidation when metals are exposed to SCW. To test for the possibility of deactivation by exposure to SCW at 0.08 g/ml, we defined a pre-treatment in SCWG, consisting of 2 hours of exposure to SCW in quartz reactors at the same temperatures we used for the gasification experiments (500°C and 600°C). We repeated the 1.0 wt % loading experiments with nickel wires after pre-treating them in SCW. The results are shown in Figures 7.22 and 7.23. Different results are observed for cellulose (500° C) and lignin (600° C). For cellulose, only the CH_4 yield is smaller after the SCW pretreatment. H_2 and CO_2 yields, which are the yields strongly promoted by the addition of nickel wires, do not decrease when pretreatment is performed at 500° C. The results suggest that no deactivation takes place in the nickel wire after 2 hours exposure to SCW at 500° C. For lignin, though, all the gas yields decrease compared to the case with no pre-treatment, suggesting that at 600° C, 2 hours of exposure to SCW seems to deactivate nickel. At least in the time frame studied, 500° C would be advisable over 600° C in order to decrease the likelihood of deactivation by oxidation of the nickel.

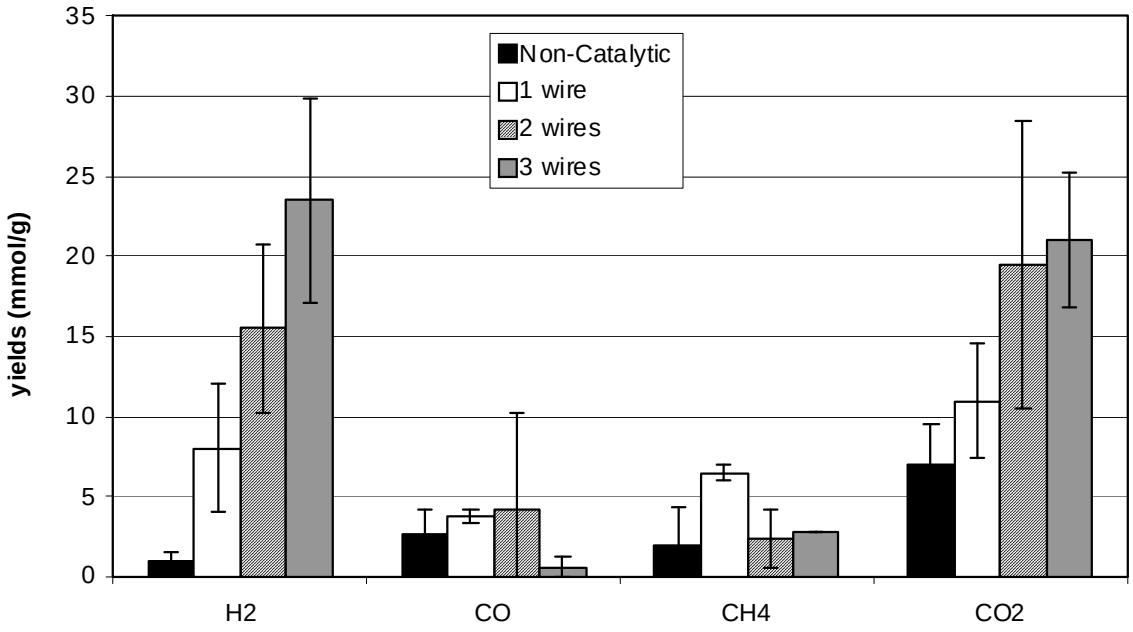

Figure 7.18. Effect of multiple Nickel wires (cellulose, 500°C, 10 min, 1.0 wt %, 0.08 g/ml).

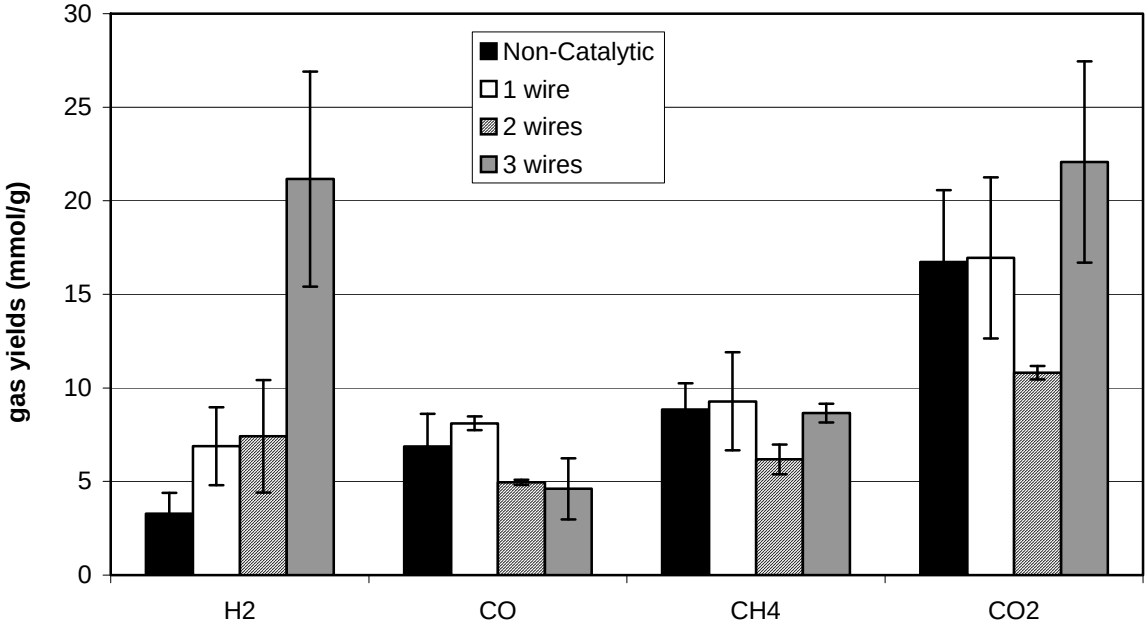

Figure 7.19. Effect of multiple Nickel wires (lignin, 600°C, 15 min, 1.0 wt %, 0.08 g/ml).

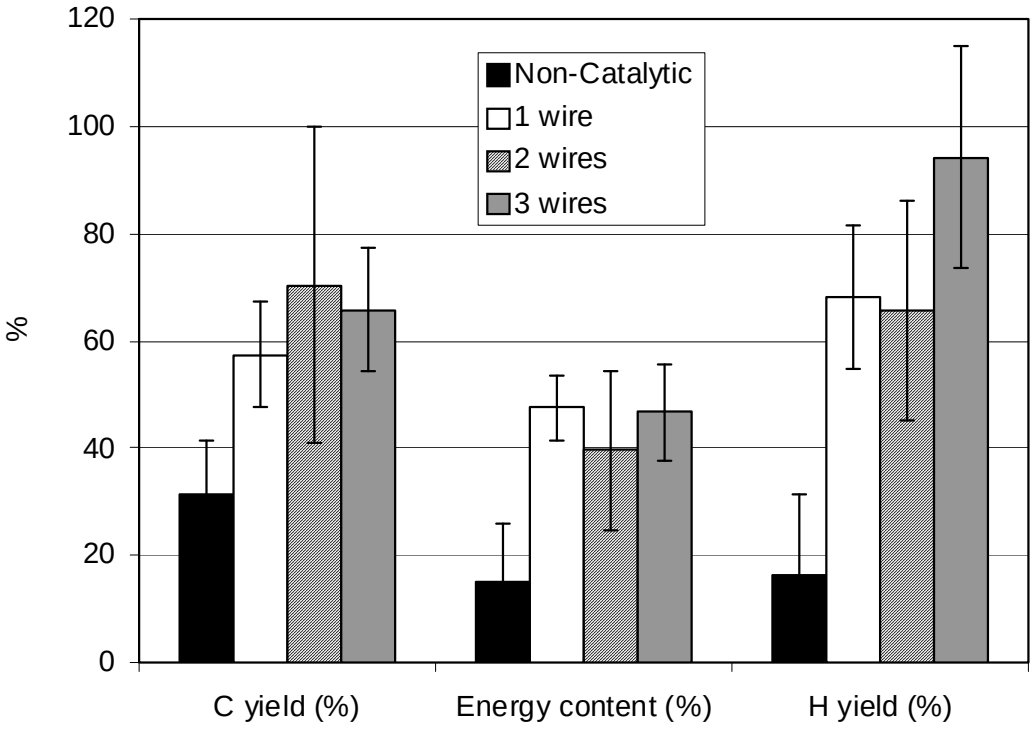

Figure 7.20. Efficiencies for multiple Nickel wires (cellulose, 500°C, 10 min, 1.0 wt %, 0.08 g/ml).

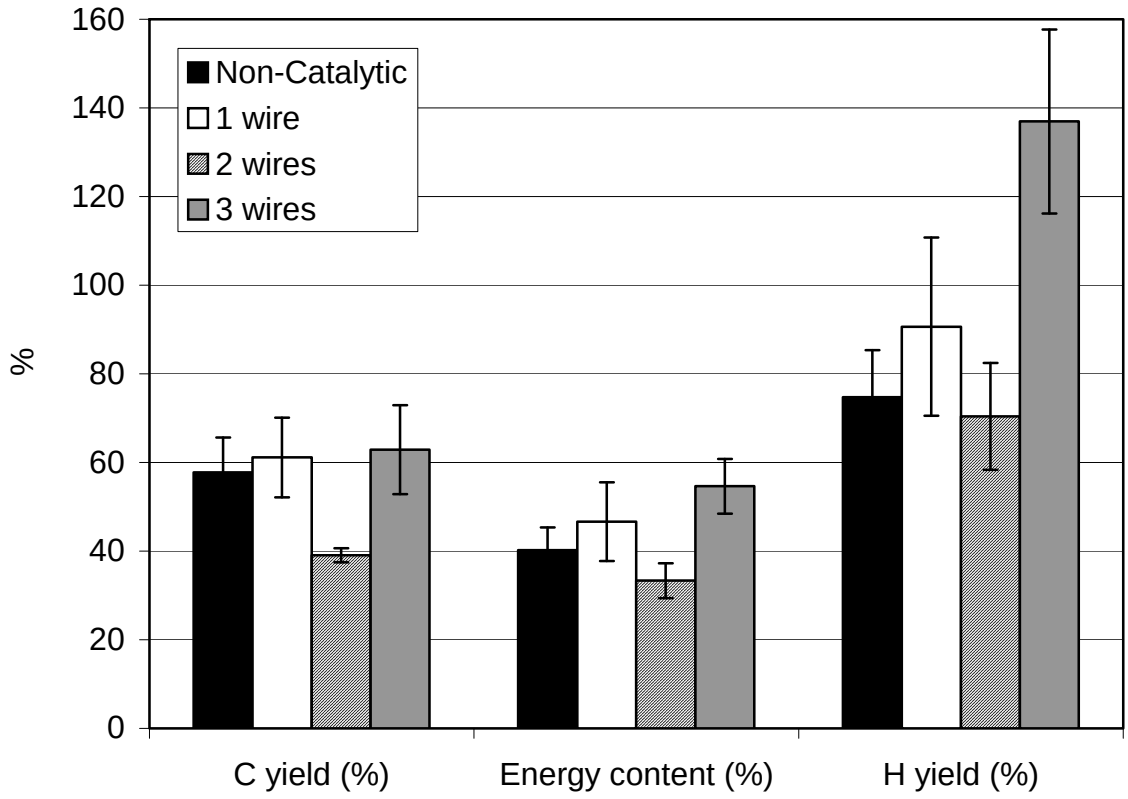

Figure 7.21. Efficiencies for multiple Nickel wires (lignin, 600°C, 15 min, 1.0 wt %, 0.08 g/ml).

.

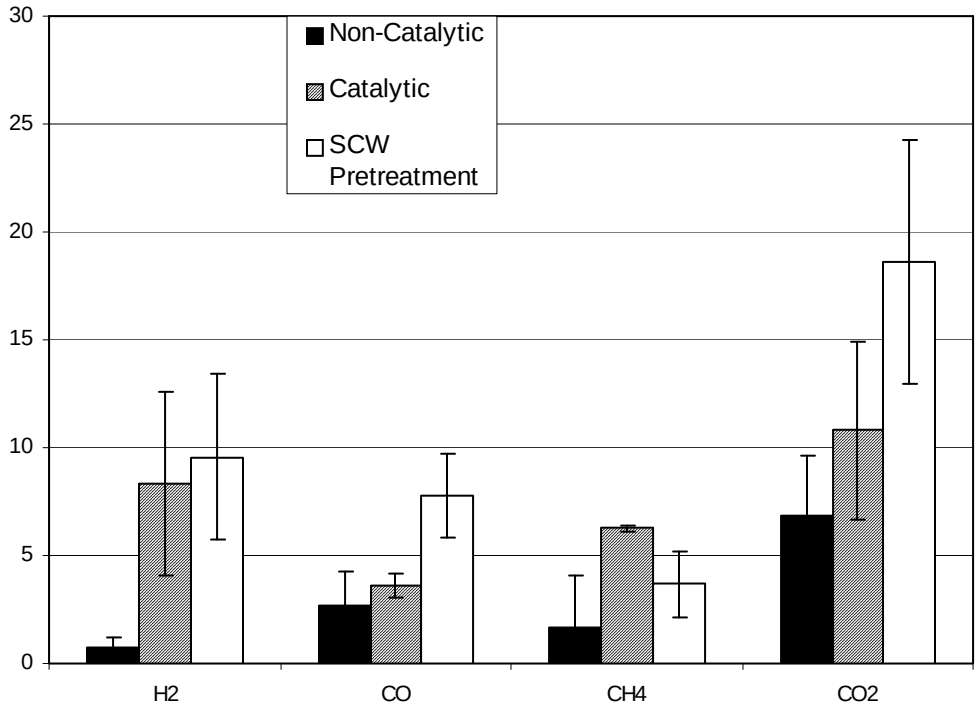

Figure 7.22. Effect of Nickel Exposure to SCW for 2 hours (cellulose, 500°C, 10 min, 1.0 wt %, 0.08 g/ml).

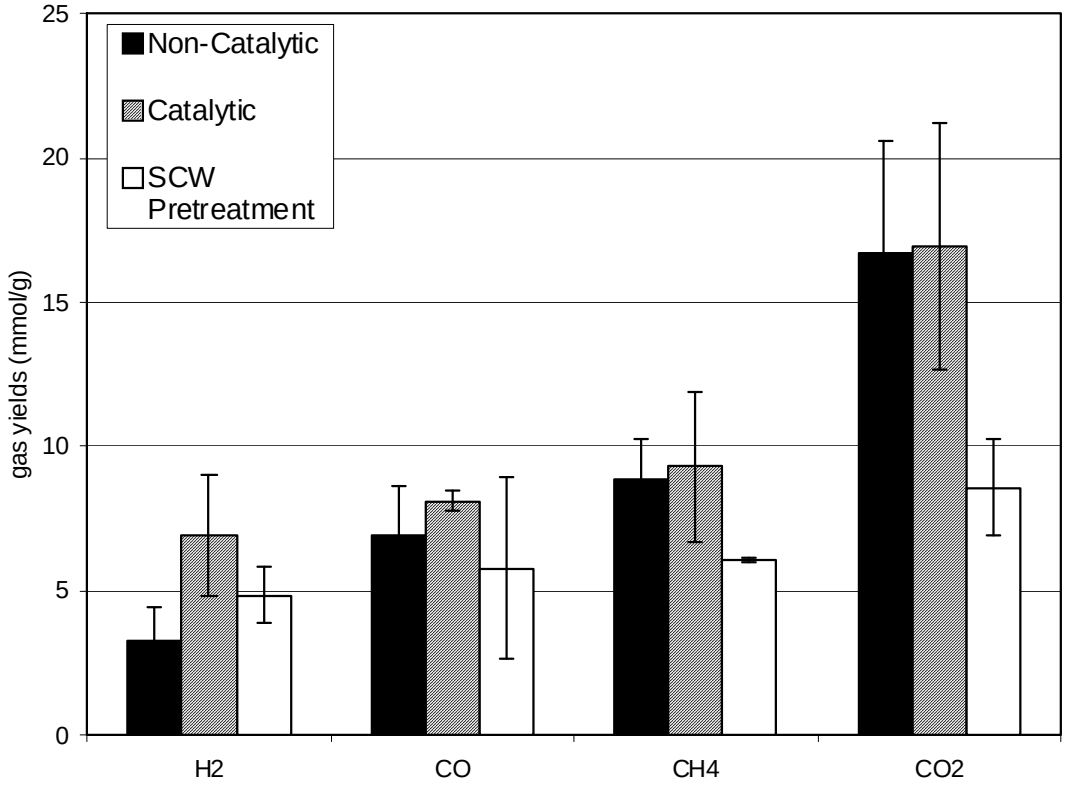

Figure 7.23. Effect of Nickel Exposure to SCW for 2 hours (lignin, 600°C, 15 min, 1.0 wt %, 0.08 g/ml).

7.4 Conclusions

1.) We quantified the catalytic activity of metals in SCWG by performing the first comparison of results in the absence of metal catalysts to results with added metals in quartz reactors.

2.) The highest H_2 yield from all the conditions in this work was 23.5 mmol/g from cellulose, and 21.1 mmol/g from lignin. They were obtained at 1.0 wt % biomass loading in the presence of 3 nickel wires. At these conditions, 94.0 % of the mass of H originally present in the cellulose was recovered in the gases (137.0 % for lignin). This corresponds to a surface area/biomass weight ratio of 240 mm^2/mg.

3.) In order to produce high H_2 yields in SCWG from cellulose, one should use high temperatures, high water densities, low loadings and nickel wire with 240 mm^2/mg surface area/biomass weight ratio. For lignin, water density does not affect yields substantially. In practice, the biomass loading will have to be higher than 1.0 wt % to make SCWG a feasible process, but the catalytic activity might still be kept high at higher biomass loadings if the 240 mm^2/mg ratio is kept. One should keep in mind, though, that equilibrium H_2 yields quickly decrease as the biomass loading increases.

4.) In general, catalysts do not affect the CH_4 yields to a significant extent. This is in agreement with model predictions, in which CH_4 yields are equal or even lower than the experimental ones. Despite the lack of improvement on CH_4 yields, it is possible to generate a gas with almost 50 % energetic content from cellulose at 1.0 wt %, and about 45 % from lignin, using nickel or iron as catalyst. With 3 nickel wires, one can also gasify 66.0 % of the C from cellulose, and 63.0 % from lignin.

5.) Oxidation is a common result for metals exposed to SCW. From the set of metals studied, we observed oxidation for all metals except copper. Strong oxidation takes place for zinc, zirconium, and Raney nickel. Previous studies in the literature have reported Raney-Nickel as an effective catalyst for SCWG [4, 15, 16]. All these studies were performed at milder conditions when compared to our work, so it is unclear whether results reported by those authors may be affected by oxidation of the catalyst.

6.) Previous work in literature reports ruthenium as a catalyst than can actively break C-C bonds, increasing gas yields [11, 18]. In the present work, though, ruthenium had little catalytic activity, especially for lignin SCWG, where it has been previously shown to increase gas yields by preventing recombination of intermediates. We believe this is a result of the physical form of the ruthenium metal (powder), which is not ideal for use in quartz reactors. In quartz reactors, metal wires can increase the likelihood of interactions among the catalyst and the biomass.

REFERENCES

[1] T. Yoshida, Y. Oshima and Y. Matsumura, "Gasification of biomass model compounds and real biomass in supercritical water," *Biomass and Bioenergy,* vol. 26, pp. 71-78, 2004.

[2] T. Yoshida, Y. Oshima and Y. Matsumura, "Partial Oxidative and Catalytic Biomass Gasification in Supercritical Water: A Promising Flow Reactor System", Industrial & Engineering Chemistry Research, vol. 43, pp. 4097-4104.

[3] Y. Matsumura, T. Minowa, B. Potic, S. R. A. Kersten, W. Prins, W. P. M. van Swaaij, B. van de Beld, D. C. Elliott, G. G. Neuenschwander, A. Kruse and M. J. Antal Jr, "Biomass gasification in near- and supercritical water: Status and prospects." *Biomass Bioenergy,* vol. 29, pp. 269-292, 2005.

[4] D. C. Elliott, "Catalytic hydrothermal gasification of biomass." *Biofuels, Bioproducts & Biorefining,* vol. 2, pp. 254-265, 2008.

[5] A. Loppinet-Serani, C. Aymonier and F. Cansell, "Current and foreseeable applications of supercritical water for energy and the environment." *ChemSusChem,* vol. 1, pp. 486-503, 2008.

[6] Z. Fang, T. Minowa, R. L. Smith Jr., T. Ogi and J. A. Kozinski, "Liquefaction and Gasification of Cellulose with Na2CO3 and Ni in Subcritical Water at 350 DegC." *Ind Eng Chem Res,* vol. 43, pp. 2454-2463, 2004.

[7] J. Yanik, S. Ebale, A. Kruse, M. Saglam and M. Yueksel, "Biomass gasification in supercritical water: II. Effect of catalyst." *Int J Hydrogen Energy,* vol. 33, pp. 4520-4526, 2008.

[8] T. Arita, K. Nakahara, K. Nagami and O. Kajimoto, "Hydrogen generation from ethanol in supercritical water without catalyst." *Tetrahedron Lett.,* vol. 44, pp. 1083-1086, 2003.

[9] A. A. Peterson, F. Vogel, R. P. Lachance, M. Froling, M. J. Antal Jr. and J. W. Tester, "Thermochemical biofuel production in hydrothermal media: a review of sub- and supercritical water technologies." *Energy & Environmental Science,* vol. 1, pp. 32-65, 2008.

[10] A. Kruse, T. Henningsen, A. Sinag and J. Pfeiffer, "Biomass gasification in supercritical water: influence of the dry matter content and the formation of phenols." *Ind Eng Chem Res,* vol. 42, pp. 3711-3717, 2003.

[11] M. Osada, T. Sato, M. Watanabe, T. Adschiri and K. Arai, "Low-Temperature Catalytic Gasification of Lignin and Cellulose with a Ruthenium Catalyst in Supercritical Water." *Energy Fuels,* vol. 18, pp. 327-333, 2004.

[12] A. Kruse and A. Gawlik, "Biomass conversion in water at 330-410 DegC and 30-50 MPa. Identification of Key Compounds for Indicating Different Chemical Reaction Pathways." *Ind Eng Chem Res,* vol. 42, pp. 267-279, 2003.

[13] M. Watanabe, H. Inomata, M. Osada, T. Sato, T. Adschiri and K. Arai, "Catalytic effects of NaOH and ZrO2 for partial oxidative gasification of n-hexadecane and lignin in supercritical water." *Fuel,* vol. 82, pp. 545-552, 2003. [13] Watanabe, 2003

[15] G. W. Huber, J. W. Shabaker and J. A. Dumesic, "Raney Ni-Sn Catalyst for H2 Production from Biomass-Derived Hydrocarbons." *Science (Washington, DC, United States),* vol. 300, pp. 2075-2078, 2003.

[16] M. H. Waldner and F. Vogel, "Renewable Production of Methane from Woody Biomass by Catalytic Hydrothermal Gasification." *Ind Eng Chem Res,* vol. 44, pp. 4543-4551, 2005.

[17] M. Osada, O. Sato, M. Watanabe, K. Arai and M. Shirai, "Water Density Effect on Lignin Gasification over Supported Noble Metal Catalysts in Supercritical Water." *Energy Fuels,* vol. 20, pp. 930-935, 2006.

[18] K. C. Park and H. Tomiyasu, "Gasification reaction of organic compounds catalyzed by RuO2 in supercritical water." *Chemical Communications (Cambridge, United Kingdom),* pp. 694-695, 2003.

CHAPTER 8
CONCLUSIONS AND FUTURE WORK

In this chapter, we conclude our study by identifying the main contributions from the present work and their potential impact on the current knowledge about the SCWG process. We also point out some aspects of SCWG that need additional understanding, based on the outcomes of the present work, and outline the research work that can be suggested to generate this knowledge.

Recent reviews by Kruse [1] and Peterson [2] mention the lack of information about non-catalytic SCWG. Without data in the absence of metals, it is very difficult to quantify the effect of added catalysts in SCWG, because the metallic walls in stainless steel reactors also catalyze SCWG reactions. For instance, Hao [3] has reported that addition of 385 m^2 of a Pd/C catalyst increases the H_2 yields from cellulose (500 °C, 20 min, 0.07 g/ml, 9.1 wt % cellulose) from 4.0 to 7.5 mmol/g. In fact, this result is a combined effect of the 385 m^2 of Pd/C catalyst with about 13 cm^2 of stainless steel in the reactor walls. If the walls were built from a different material, or if the total surface area of the reactor was different, the conclusions about the Pd/C catalyst were likely to be different. In the present work, we performed SCWG in quartz at the same conditions and found the H_2 yield to be 1.2 mmol/g. This result suggests the stainless steel wall by itself provides an increase in H_2 yield of 2.8 mmol/g, which is almost as large as the increase provided by the added Pd/C catalyst itself. The increase in H_2 yield due exclusively to the Pd/C catalyst could be different than what is reported by Hao. By confusing the catalytic effects of added catalysts with that of the reactors walls, we might make erroneous conclusions. This lack of proper understanding in catalytic effects may lead to problems in the scale-up of the reactors [2].

The present work marks the first time cellulose and lignin, the main components of biomass, were gasified in supercritical water in the absence of catalytic effects from metallic walls. This information is the basis to quantify the effect of any added catalyst in

SCWG. In the previous example, the true effect of the Pd/C catalyst could be quantified by performing the catalytic experiment in quartz and comparing it to the non-catalytic case. In this sense, every catalyst to be used in SCWG should be evaluated in non-catalytic conditions prior to experiments in metallic reactors, so that its real effect can be seen. The results presented in Chapter 7 are the first step in characterizing the catalytic effect of added metals in SCWG. We found the catalytic effects from nickel, iron and copper to be small when the surface area/biomass weight is below 15 mm^2/mg. In previous studies with stainless steel, the ratio reactor wall surface area/biomass weight is typically 18-19 mm^2/mg, so its catalytic effect is large enough to be significant. In the present work, at high ratios (up to 240 mm^2/mg), nickel appears to be an effective catalyst to promote H_2 and CO_2 formation to over 20 mmol/g. H yields over 100 % and C yields of about 70 % can be obtained at these conditions. The highest energetic contents are about 50 %. In terms of future work, the study of effects of variables for catalytic SCWG could be expanded, by setting a high constant surface area/biomass ratio (such as 240 mm^2/mg) and quantifying the catalytic activity as a function of temperature and water density. At these conditions for cellulose, we also did not observe clear deactivation of the nickel catalyst after 2 hours exposed to SCW.

Further consideration should be given to copper as a catalyst for SCWG. The resistance to oxidation shown by this inexpensive metal when exposed to SCW can potentially overcome deactivation problems that other metals experience. In this work, nickel provided the highest yields at 1.0 wt % loading, but at 5.0 wt % copper is the catalyst that provides yields closer to equilibrium for lignin. It is possible that the use of a higher surface area/biomass weight ratio can lead to higher yields using copper as a catalyst in SCWG. Catalyst deactivation is one of the main issues reported currently for SCWG. Even though oxidation is not the only cause for catalyst deactivation in SCWG, the search for metal catalysts that do not oxidize is important and has been reported recently by Elliott [4]. Another common cause for deactivation is the contamination by deposition of tarry intermediates on the catalyst. Nikolla [5] has shown that the use of alloys such as Ni/Sn can avoid deactivation by carbon deposition for reforming of hydrocarbons. The use of alloys instead of pure metals as catalysts for SCWG could be an option in terms of avoiding deactivation. Also, while in the present work we focused

on identifying the metals which are active catalysts on SCWG, the use of supported metals in quartz is important in evaluating catalysts that can provide long-term stability in SCW.

Another contribution from the present work is the evaluation of the effects of variables on cellulose and lignin non-catalytic SCWG. Researchers have previously reported the effects of variables, as described in Chapter 2. These studies use a number of different model compounds, at different experimental conditions, and at the presence of a number of different catalysts. By performing the systematic study of the effects of variables for cellulose and lignin, we were able to isolate and quantify the effects of these variables for non-catalytic SCWG. In general, we found the yields to increase with the severity of conditions. High yields, and consequently high energetic content of the product gas (up to 50 %), are obtained at high temperature (600-725°C) and water densities (0.18 g/cm^3). Increase in water density increases yields from cellulose, but does not substantially increase yields from lignin in the range up to 0.18 g/cm^3. In other words, the composition of the biomass dictates the water density. Biomass feedstocks with high cellulose content should be gasified at high water densities. If the lignin content is high, though, low water densities should be used to minimize energy consumption without decreasing gas yields. The effect of biomass loading on non-catalytic SCWG is small. The most important effect is the decrease in CO yield with loading. This is an important finding, because we aim to use high biomass loadings to minimize energy consumption as well. Thus, for a feedstock with high lignin content, we can minimize energy consumption by decreasing the water density and increasing biomass loading, without interfering on the yields obtained. In addition, this study demonstrated the exceptional ability of manipulating the product composition in SCWG by changing experimental conditions. With other variables kept at base case conditions, the CO: H_2 ratio for cellulose ranged from 0.0 (at 0.18 g/cm^3) to about 6.5 (at 400°C). The CH_4:H_2 ratio ranged from 0.0 (365°C) to 2.3 (1.0 wt %). This ability to change product composition as function of experimental conditions increases the potential applications of syngas from SCWG.

The kinetic model we developed is the first one to describe gas formation in SCWG. The main contribution from the model is to identify the most important reaction

pathways leading to gas formation. With the aid of the model and ASPEN thermodynamic calculations, we found that we were far from equilibrium conditions in all the non-catalytic experiments described in this work. And, even if methanation and water-gas shift equilibria are achieved, this will not substantially increase the yields in SCWG compared to the highest yields we obtained in this work. The model introduced the concept of a reactive intermediate species, which represents all the intermediates that can be generated from the monomer after cellulose or lignin is attacked by water. Most of the CH_4, CO and CO_2 originate from the intermediates, and the key to increase gas yields seems to be the competition between intermediate decomposition and char formation reactions. Given the importance of these intermediates in gas generation, a more detailed study of these species deserves consideration. Many of the intermediates involved in SCWG are already known, but there are no kinetic models available detailing the pathways for intermediate decomposition forming gases. This type of study could potentially help on selection of catalysts to promote intermediate decomposition, preventing those species from forming char and non-reactive material. For H_2, steam-reforming and water-gas shift are important sources. Catalysts that promote steam-reforming are necessary to increase H_2 yields above the 20 mmol/g observed experimentally in this work.

Cellulose and lignin are the most important compounds in biomass. The study of these two model compounds provides a reasonable picture of the biomass decomposition in SCWG. The next step in this study is to actually gasify real biomass feedstocks. It would be interesting to verify how wet biomass feedstocks such as DDGS (distillers dried grains with solubles) decompose in SCWG. The use of high moisture feedstocks with catalysts in the conditions recommended in this work can potentially provide an interesting alternative to conventional methods of processing these feedstocks.

The value of further studies with quartz reactors could be enhanced if there are also ways to overcome the experimental limitations we found in this work. Experimental work aiming to avoid reactors bursting could be of great value in the sense of allowing experiments to be performed at more severe conditions which in this work led to reactors bursting. At these more severe conditions, H_2 yields are higher.

The findings in the present work bring contributions to the evaluation of catalysts for SCWG, to the search of optimum experimental conditions, and to the understanding of the chemistry involving the product gases. We believe these contributions can play an important role in obtained high gas yields in SCWG, therefore making the process more economically attractive.

REFERENCES

[1] A. Kruse, "Supercritical water gasification." *Biofuels, Bioproducts & Biorefining,* vol. 2, pp. 415-437, 2008.

[2] A. A. Peterson, F. Vogel, R. P. Lachance, M. Froling, M. J. Antal Jr. and J. W. Tester, "Thermochemical biofuel production in hydrothermal media: a review of sub- and supercritical water technologies." *Energy & Environmental Science,* vol. 1, pp. 32-65, 2008.

[3] X. Hao, L. Guo, X. Zhang and Y. Guan, "Hydrogen production from catalytic gasification of cellulose in supercritical water." *Chemical Engineering Journal (Amsterdam, Netherlands),* vol. 110, pp. 57-65, 2005.

[4] D. C. Elliott, "Catalytic hydrothermal gasification of biomass." *Biofuels, Bioproducts & Biorefining,* vol. 2, pp. 254-265, 2008.

[5] E. Nikolla, J. Schwank and S. Linic, "Promotion of the long-term stability of reforming Ni catalysts by surface alloying." *Journal of Catalysis,* vol. 250, pp. 85-93, 2007.